University of Nottingham
UK | CHINA | MALAYSIA

Towards the bioproduction of methacrylate esters: understanding product toxicity in *Escherichia coli*

Laura Martins

Department of Chemical and Environmental Engineering

Thesis submitted to the University of Nottingham

for the degree of Doctor of Philosophy

September 2019

Abstract

Methacrylate esters (MAE) are used as building blocks in the manufacture of Perspex®. A novel pathway for the sustainable bioproduction of MAE in *Escherichia coli* has been previously developed. However, the process is still not economically feasible, as titres are restricted because of product toxicity. Recently, four *E. coli* strains resistant to *n*-butyl methacrylate (BMA) have been isolated. These strains have different combinations of mutations in three different genes, *soxR*, *acrR* and *ybcO*. In this study, the resistance of the *E. coli* mutants to toxic chemicals, particularly BMA, was investigated. The new mutant strains and mutated genes were phenotypically and genotypically characterized, to understand their function in the response to BMA stress.

The *E. coli* strains with mutations in both *soxR* and *acrR* had higher resistance to 20 %(v/v) BMA than the strains with mutations in *soxR* only or *soxR* and *ybcO*. Furthermore, an *E. coli* MG1655 strain with *soxR* and *acrR* mutations had improved tolerance to other commodity chemicals, such as isobutyl methacrylate, n-propyl methacrylate, n-butyl isobutyrate, n-hexane and cyclohexane. Gene deletions and genetic complementation studies of both wildtype (WT) and mutant *E. coli* MG1655 strains confirmed that *soxR* and *acrR* mutations encode genes directly associated with the tolerance to 20 %(v/v) BMA.

The gene expression response to 20 %(v/v) BMA exposure was investigated by transcriptomics and demonstrated a complex network of mechanisms mostly similar in all mutant strains. Transcriptomics and gene deletions data showed that the up-regulation of the oxidative stress response and the genes *acrAB*, part of the multidrug transporter AcrABZ-TolC, was crucial for BMA tolerance. Overall, these findings proved that the novel combination of *soxR* and *acrR* mutations, never reported in literature before, was essential to confer BMA tolerance in *E. coli*. The expression of these genes can be exploited to further solve product toxicity in the bioproduction of MAE or other bio-based processes.

Acknowledgments

Firstly, I would like to thank my supervisors, Professor Gill Stephens, Professor Alex Conradie and Dr. Ian Kerr, for the remarkable guidance, support and all the knowledge passed on that was essential to complete my project. I would also like to thank Dr. Graham Eastham and Dr. David Johnson for all the helpful discussions and ideas. A big thank you to Dr. Luca Rossoni for his tireless patience and for teaching me everything inside and outside the lab.

A big thank you to Dr. Andrew Yiakoumetti, Dr. Charlotte Green, and Russel Menchavez for helping me with excellent ideas and suggestions throughout my project. I would also like to thank Steve, Amy and Rachael for the amazing job in keeping the lab running and helping us to do our work. Finally, a big thank you to everyone from the SPT research group for all the fun times and evenings in the pub.

I would also like to thank my family and friends for the continuous love and support which helped me to get where I am today. Finally, I can not thank Diogo enough for always being there for me throughout this journey. Obrigada.

Table of contents

List of abbreviations

AAT	Alcohol acyl transferase
ACX	Acyl-CoA oxidase
BCKD	Branched chain ketoacid dehydrogenase
BMA	n-Butyl methacrylate
$CaCl_2$	Calcium chloride
carbR	Carbecilinin resistance
cDNA	Complementary deoxyribonucleic acid
chlR	Chloramphenicol resistance
$CoCl_2 \cdot 6H_2O$	Cobalt(II) chloride hexahydrate
$CuSO_4 \cdot 5H_2O$	Copper(II) sulfate pentahydrate
dH_2O	Distilled water
DNA	Deoxyribonucleic acid
dNTPs	Deoxynucleotides triphosphate
EDTA	Ethylenediaminetetraacetic acid
FC	Fold change
$FeSO_4 \cdot 7H_2O$	Ferrous sulfate heptahydrate
FLP	Flippase recombinase
FRT	FLP recognition target sites
gDNA	Genomic deoxyribonucleic acid
GO	Gene ontology
kanR	Kanamicyn resistance
KCl	Potassium chloride
KH_2PO_4	Potassium phosphate monobasic
KI	Knock-in
KO	Knock-out
KOH	Potassium hydroxide
LB	Luria broth
MA	Methacrylate
MAA	Methacrylic acid
MAE	Methacrylate esters
$MgCl_2$	Magnesium chloride
$MgSO_4$	Magnesium sulfate
$MgSO_4 \cdot 7H_2O$	Magnesium sulfate heptahydrate
MMA	Methyl methacrylate
$MnCl_2 \cdot 4H_2O$	Manganese(ii) chloride tetrahydrate
mRNA	Messenger RNA
MSA	Minimal salts medium solution A
MSB	Minimal salts medium solution B
MSX	Minimal salts medium

NaCl	Sodium chloride
NGS	Next generation sequecing
$(NH_4)_6Mo_7O_{24}\cdot 4H_2O$	Ammonium molybdate tetrahydrate
NH_4Cl	Ammonium chloride
OD	Optical density
OSR	Oxidative stress response
PCR	Polymerase chain reaction
PTFE	Polytetrafluoroethylene
RNA	Ribonucleic acid
RNA-seq	RNA sequencing
rpm	Rotations per minute
RT-PCR	Reverse transcription polymerase chain reaction
SE	Standard error
SOC	Super optimal broth with catabolite repression medium
TAE	Tris-acetate EDTA buffer
TCA	Tricarboxylic acid cycle
tetR	Tetracycline resistance
T_m	Melting temperature
tRNA	Transfer RNA
UV	Ultraviolet ligth
WT	Wild type
$ZnSO_4$	Zinc sulfate

List of Figures

List of Tables

1 Introduction

Over time, biotechnological processes have been gaining more relevance in solving different problems in today's society, especially the ones related to sustainable and environmental issues, to reduce the green house effects and the dependency on petrochemical feedstocks[8]. However, product toxicity is a major challenge when it comes to the bio-based production of chemicals[1]. The toxicity towards host microorganisms needs to be tackled in order to improve product titres and, thus, the economic feasibility of bioprocesses, to make the bioprocesses more competitive with current chemical manufacturing processes. One example of a process that can be improved through biotechnology, is the production of methyl methacrylate (MMA)[2]. This process still relies on petrochemicals and efforts are being made to develop a sustainable and environmentally friendly bioprocess.

1.1 Production of methacrylate esters

MAE have a wide variety of applications in manufacturing textiles, coatings and adhesives, resins, packaging, lubricants, automotive equipment, electronics, medical equipment and household goods [9,10]. MMA is the building block for the production of the polymer poly-methyl methacrylate (PMMA), which is commonly known as Perspex® or Plexiglas® and has a wide variety of applications in the plastic industry (Figure 1.1) [11]. Due to this wide variety of applications, MMA has a global annual demand higher than 3 million metric tons [3].

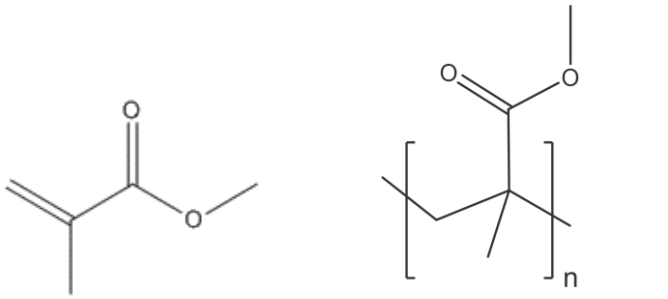

Methyl methacrylate **Poly-methyl methacrylate**

Figure 1.1 - Structures of methyl methacrylate (MMA) and poly-methyl methacrylate (PMMA).

1.1.1 Current manufacturing of methacrylate esters

Since the 1930s, the most widely used process to produce MMA and its derivatives is the one known as the acetone cyanohydrin (ACH) route[12] (Figure 1.2). In the ACH route, dry acetone and hydrogen cyanide are used to form ACH. Then ACH reacts with excess sulfuric acid to form methacrylamide sulphate, which is then treated with water or methanol to form MMA and/or methacrylic acid (MAA). Although the overall MMA production yield starting from ACH is between 80 and 90 %, this process has some disadvantages [11]. The ACH route uses toxic chemicals that are dangerous to handle and transport, namely hydrogen cyanide and sulfuric acid, which increases the cost of the industrial process. Additionally, acetone is also considered an expensive feedstock.

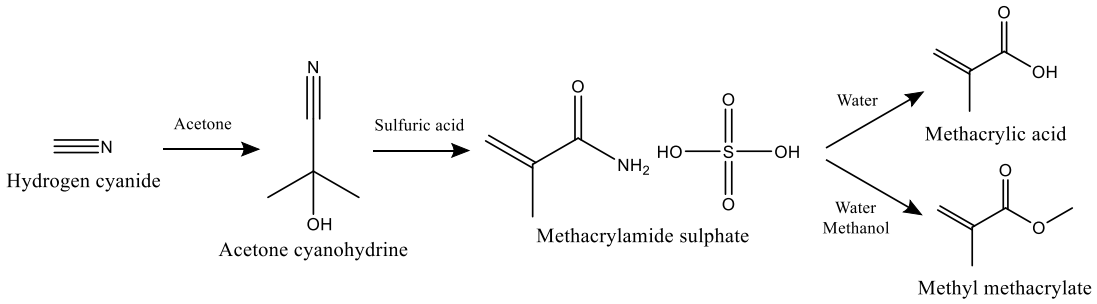

Figure 1.2 - The ACH route for the production of MMA and its derivatives.

In 2008 a new process was implemented, developed by Lucite International, known as the Alpha process[13] (Figure 1.3). The Alpha process is a two-step route to produce MMA from widely available and simple chemicals, ethylene, carbon monoxide and methanol. In the first step, ethylene reacts with carbon monoxide and methanol to form methyl propionate, which then reacts with formaldehyde to form MMA and water in the second step. The Alpha process is about 40 % cheaper and environmental safer than the conventional ACH route process, and, since 2008, it has been operating at 120,000 tonnes per year.

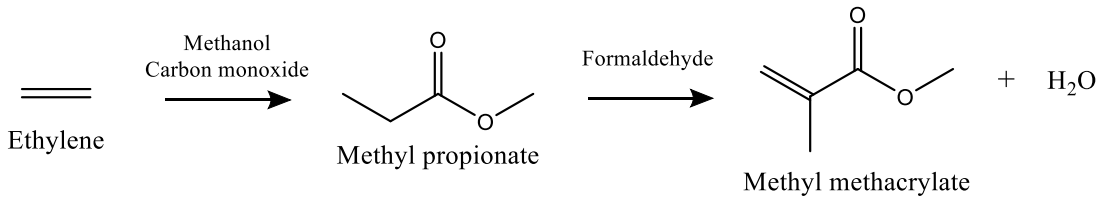

Figure 1.3 - The Alpha process route for the production of MMA.

1.1.2 Towards bioproduction of methacrylate esters

Even though the Alpha process is a greener alternative to the ACH process, it still relies on the use of chemicals from the petrochemical industry[14]. The use of fossil fuels and other fossil derivatives raises questions about its safety, environmental pollution and greenhouse gases emissions, production of toxic by-products, problems with waste disposal and the overall economic uncertainty associated with non-renewable resources[4,5]. By contrast, microorganisms can be used to produce bio-based chemicals in a sustainable way[8]. Although microorganisms have been primarily used for the production of amino acids and antibiotics, many other compounds, such as alcohols, organic acids or terpenoids, have been produced by microbial fermentation[8,15]. Therefore, efforts are being made to develop new bioprocesses to produce MAE using renewable resources [2,14].

A new pathway was developed for the direct bioproduction of MAA using *E. coli* as the host microorganism[6] (Figure 1.4). This pathway starts with 2-ketoisovaleric acid, an intermediate of the natural pathways to produce L-valine or L-leucine from pyruvate. 2-Ketoisovaleric acid is then converted to isobutyryl-CoA, in a reaction catalysed by a branched chain ketoacid dehydrogenase (BCKD), isolated from *Pseudomonas putida* KT2440. Then, a short chain acyl-CoA oxidase (ACX), isolated from the plant *Arabidopsis thaliana*, catalyses the reaction to form methacrylyl-CoA. Finally, a 4-hydroxybenzoyl-CoA thioesterase (4HBT), isolated from *Arthrobacter sp.* strain SU, catalyses the reaction to form MAA.

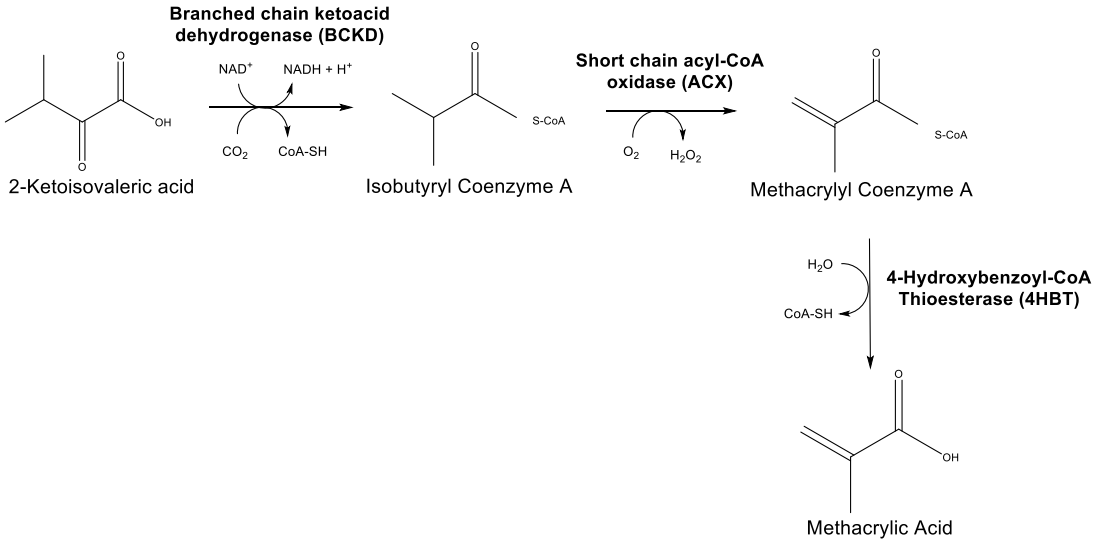

Figure 1.4 - Pathway for the bioproduction of MAA in E. coli.

However, the pathway for the direct production of MAA had low titres, probably due to the toxicity of MAA. The toxicity of a chemical towards a microorganism can be evaluated according to their log P_{ow} value. The log P_{ow} value is known to be the partition coefficient of a chemical in an equimolar mixture of octanol and water [16-20]. The higher the log P_{ow} the more nonpolar and hydrophobic a chemical is [16-20]. Hence, it is thought that with the increase in the log P_{ow} values of chemicals there is a decrease in toxicity. According to literature, in *E. coli*, the limiting log P_{ow} value is 3.8[19]. Thus, chemicals with higher values are not considered toxic to *E. coli* cells[19]. MAA has a log P_{ow} of 0.93, and, therefore, is toxic to *E. coli*.

Alternatively, the pathway could be used for the direct production of MAE, which have higher log P_{ow} values (≥1.38), and thus are less toxic than MAA, but also less polar, which could facilitate the separation process in the downstream process. The pathway used for the production of MAE derived from the pathway for the production of MAA. In the MAE pathway (Figure 1.5), the first two steps with the enzymes BCKD and ACX are the same as in the previous pathway. But in the last step, methacrylyl-CoA is converted into a MAE in a reaction catalysed by an alcohol acyl transferase (AAT; which can be obtained from a variety of fruits), using the corresponding alcohol as substrate.

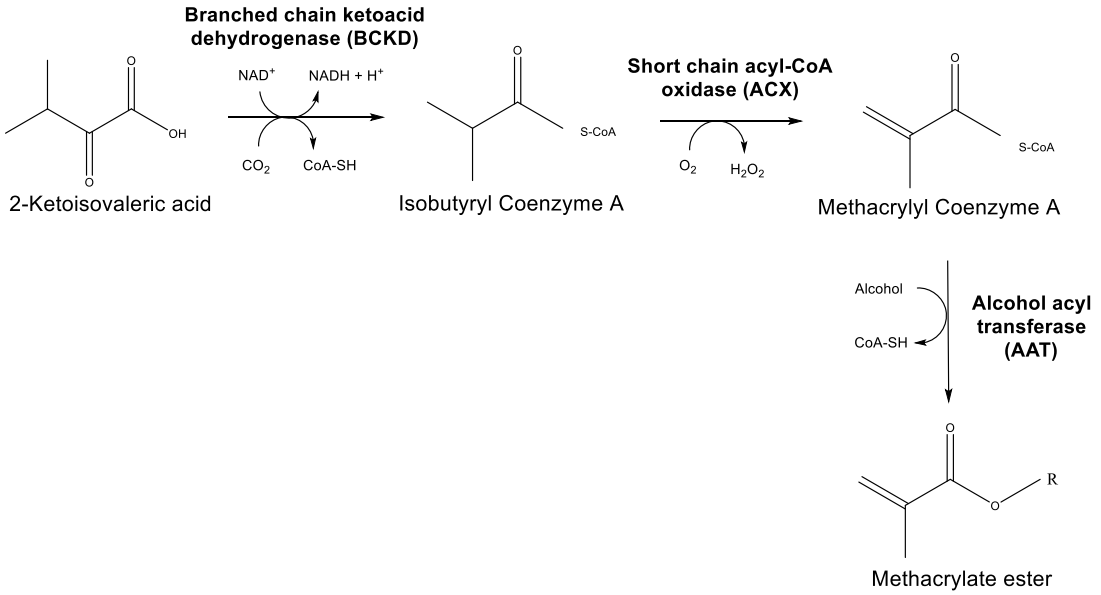

Figure 1.5 - Pathway for the bioproduction of MAE in *E. coli*.

To make this process economically viable, it would be necessary to produce high quantities of MAE, at a productivity of least 2 g/L/h. Yet, the productivities achieved were far from the target. The toxicity of MAE might be limiting product titres. Therefore, it is essential to tackle the toxicity bottleneck and develop *E. coli* strains that are able to tolerate high concentrations of MAE. To achieve this, it is crucial to understand how toxic chemicals affect *E. coli* cells and how *E. coli* responds to counteract chemical-induced stress.

1.2 Biological responses to toxic chemicals

The primary effect of lipophilic chemicals such hydrocarbons, long organic acids or esters, is the disruption of the membrane integrity and fluidity, as they can partition into the cell membrane and intercalate into the lipid bilayer structure[21-27]. This can result in leakage of cofactors and macromolecules, disruption of transport processes, ATP synthesis and energy conservation mechanisms, and dissipation of the proton motive force, ultimately causing cell death[22,26-29]. Depending on the structure or reactivity of the chemical, additional toxicity effects may be observed. Chemicals which are reactive electrophiles, such as aldehydes or epoxides, can also react with DNA, proteins and other resulting in macromolecules extensive cellular

damage[30-32]. Redox active chemicals, such as quinones, phenazines and viologens (*e.g.* paraquat) and other reactive species, act as toxins by entering the cells, where they are readily reduced by a wide range of cellular redox systems, to form reactive species which then react with molecular oxygen to form reactive oxygen species (ROS)[33,34]. ROS are very reactive and can damage a wide range of cellular components, including DNA, RNA, proteins[34-36] and membranes, with the formation of lipid peroxides[37,38]. Some lipophilic, weak organic acids (*e.g*. lactic, acetic, propionic and butyric acids), can cause cellular damage through alteration pH homeostasis[39-46], by causing acidification of the cytoplasm[39], which dissipates the transmembrane pH gradient and decreases the electrochemical potential, interfering with energy synthesis or transport processes[40-42].

Over time, bacteria have evolved to be able to survive in the presence of toxic chemicals and antibiotics[28]. A wide variety of approaches have been used to study the responses of cells exposed to toxic chemicals, including global systems analyses and analysis of membrane composition and structure. Further insights into chemicals tolerance have been obtained by studying bacteria, which have been isolated from natural environments[16,47-53], such as seawater, waste water, sediments and soils, and are resistant to different chemicals such as n-heptane[47], decane[47], pentadecane[47], kerosene[47], benzene[48], p-xylene[48,51], ethylbenzene[48], toluene[16,48,49,51,53], styrene[50], n-butanol[52] and isobutanol[52]. These organisms employ a variety of mechanisms to overcome or prevent the damage caused by toxic chemicals, and the study of these mechanisms has provided many insights into understanding microbial tolerance to chemicals in general.

A wide variety of responses have been identified, which can be broadly divided into three categories: (1) exclusion of the chemical from the cell, (2) modification of the cell envelope, and (3) induction of stress responses. These will be discussed in the chapters below and most of them have also been summarized in Table 11.1 (Appendix 11.1, page 194).

1.2.1 Exclusion of the chemical from the cell

1.2.1.1 Active transporters

Active transporters are membrane proteins that can actively transport chemicals out of the cell through energy-dependent transport processes[54]. Multi drug efflux pumps are amongst the most studied active transporters and were first identified as a first line response to counteract the inhibition caused by a wide range of antibiotics, by pumping the antibiotic out of the cell[55-59]. Since then, these efflux pumps have also been found to export a wide variety of toxic chemicals [60-68]. There are six families of multidrug efflux pumps: the ATP-binding cassette (ABC) family, the major facilitator superfamily (MFS), the small multidrug resistance (SMR) family, the multidrug and toxic compound exporters (MATE) family, the resistance-nodulation-division (RND) family[69] and the proteobacterial antimicrobial compound efflux (PACE) family[59,70].

RND pumps are the most studied multidrug efflux pumps associated with tolerance to toxic chemicals in Gram-negative bacteria[69]. RND pumps transport the substrate across the cell envelope through an H^+-dependent antiporter energy system. In *E. coli,* the best characterized pump is AcrABZ-TolC[60-68], which has been associated with tolerance towards several chemicals, such as ethanol[71], isobutanol[71], n-butanol[71], geraniol[72], n-hexane[73], cyclohexane[73], among others[74,75].

The AcrABZ-TolC complex has an inner-membrane RND pump, AcrB, a periplasmic membrane fusion protein, AcrA, an outer-membrane channel, TolC[60-68], and an additional recently discovered 49 amino acid protein, AcrZ, which binds to AcrB and is thought to affect the preference of AcrB to certain substrates[64]. The crystal structure of the AcrB-AcrZ complex has been also recently solved (RCSB PDB accession code: 4CDI)[76]. This multidrug efflux pump has a ratio of 3:3:6:3 for AcrB:AcrZ:AcrA:TolC. TolC has a transmembrane β-barrel and a periplasmic α-helical domain, and AcrA has an α-helix, a lipoyl, a β-barrel and a membrane-proximal domains. AcrB has a periplasmic docking, porter and transmembrane domains[61,76], and the proton pathway for the antiport system is located in the transmembrane

domain[67]. The α-helical domain of AcrA interacts with the end of the α-helical domain of TolC and the β-barrel and membrane-proximal domains of AcrA interact with the docking and porter domains of AcrB[68,76]. There is no evident interaction between AcrB and TolC, as AcrA binds firstly to AcrB and then to TolC[68,76]. Up to this date, it is still unclear how chemicals enter AcrB[77]. However, it is thought that the substrate enters from the periplasm[62] or outer leaflet of the inner membrane[78].

AcrR is a member of the TetR family of transcriptional repressors[79-81], which represses the expression of the *acrAB* operon, that encodes proteins for the widely studied RND efflux pump AcrABZ-TolC[82]. Yet, *acrZ* is known to be induced by SoxS, MarA and Rob[64], and *tolC* is constitutively highly expressed in *E. coli*, but can be further up-regulated by the regulators SoxS, MarA, Rob, PhoPQ, BaeSR, and EvgAS[83,84]. AcrR is an 215 amino-acid protein, a member of the TetR family of transcriptional repressors and its gene is located 141 bp downstream of the *acrAB* operon[79,80]. AcrR is a homodimer and each unit folds into nine α-helixes and is has an N-terminal DNA-binding domain (α1 to α3) a and a C-terminal ligand-binding domain (α4 to α9; Figure 1.6)[80]. AcrR can bind to different ligands, with preference for neutral or positively charged molecules[80]. It has also been reported that two different ligands can bind to AcrR simultaneously[81]. When the ligand binds to AcrR, the subsequent conformational changes release AcrR from the DNA, ending the repression mechanism[80]. The ligands normally used to study the regulatory action of AcrR are rhodamine 6G, ethidium and proflavin[81,85].

ABC transporters, which are inner membrane pumps that use ATP as the energy source[86,87], have also been shown to be involved in conferring chemicals tolerance in bacteria[88-90]. Remarkably, there are examples of ABC transporters conferring chemical tolerance by controlling the intake of substrates rather than export of chemicals. For example, in *E. coli,* the up-regulation or increased expression of subunits of the OppABCDF uptake system for oligopeptides was shown to be important the tolerance to several chemicals, including toluene[88], n-butanol[88], isobutanol[89] or resveratol, naringenin, and rutin[90]. The inner membrane MATE and MFS transporters, which generally use H^+-dependent antiporters or Na^+-dependent antiporter systems[57,91,92], have also been implicated in resistance to toxic chemicals[88].

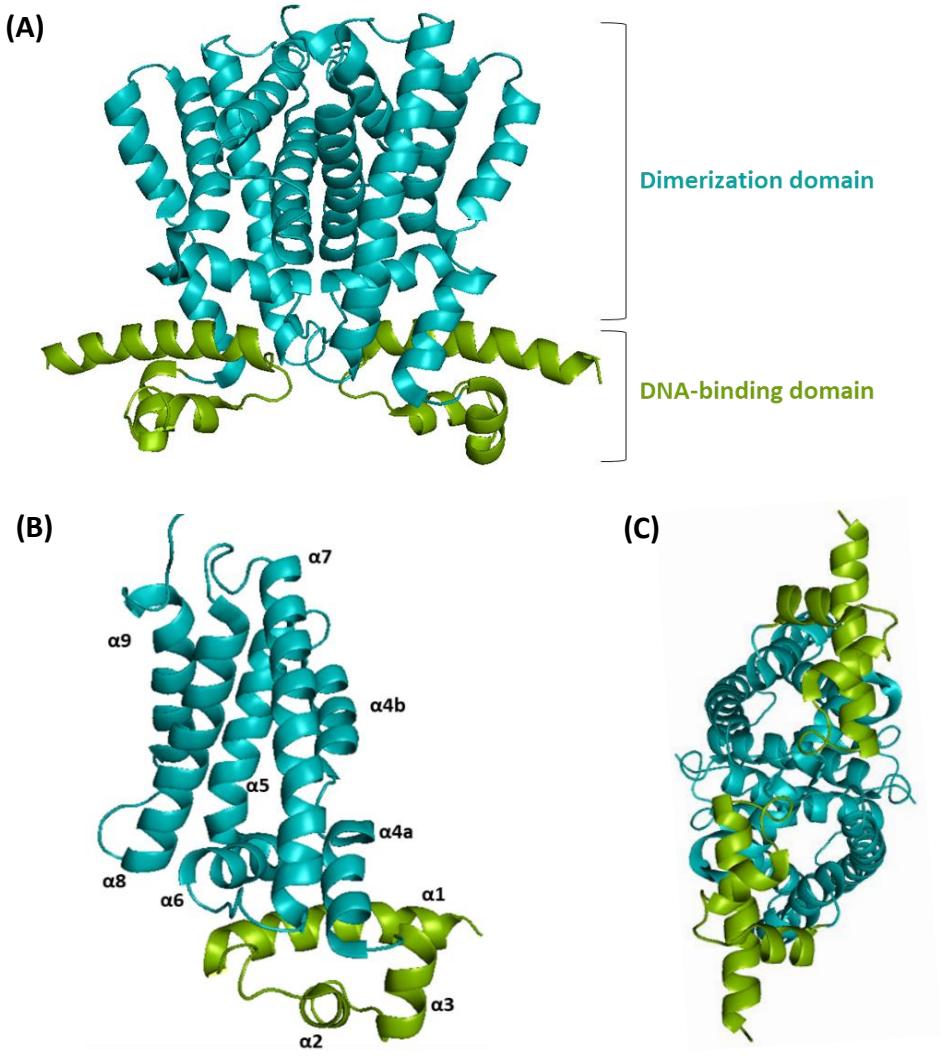

Figure 1.6 - Crystal structure of the AcrR protein. The AcrR homodimer (A), the AcrR monomer (B) and the bottom view of AcrR homodimer (C) are shown (RCSB PDB accession code: 2QOP) [80]. The ligand-binding domain is represented in light blue and the DNA-binding domain in green.

For example, in *E. coli*, The MATE transporters DinF has been up-regulated in the presence of cyclopentanone[88], while the MFS trasnporters EmrB, EmrY and MdtG have been up-regulated in the presence of different chemicals[88]. Moreover, it seems that MFS transporters (*e.g.* EmrAB and EmrKY) can sometimes form, in Gram-negative bacteria, a coordinated system with RND pumps, to pump out chemicals from the cytoplasm into the periplasm and then to the extracellular space[59,93-95].

A number of other active transporters are also up-regulated in response to the presence of toxic chemicals, including sugar and ion transporters[88,96]. For example,

the inorganic ion transporters MgtA, MntH, KefBG and RcnAB were up-regulated in *E. coli* in the presence of several chemicals, including n-butanol and toluene[88], while the sugar transporters, MalE, RbsB, and MglB, were up-regulated in *E. coli* in the presence of ehtanol[96].

1.2.1.2 Passive transporters

Passive transport occurs when chemical compounds can diffuse through membrane based on concentration gradients. Diffusion can often be facilitated by porins, water-filled channels found in the outer membranes of Gram-negative bacteria, involved in the size-selective diffusion of hydrophilic compounds across the outer membrane[97]. Porins can be classified as specific or non-specific/general porins, depending on the pore size and the amino acid composition[98]. Although porins have been implicated in resistance to toxic chemicals, their roles seem to be diverse, since some are up-regulated and others are down-regulated in response to toxic chemicals[89,90,99-102].

For example, the general porin OmpF and the long-chain fatty acid porin FadL were up-regulated when *E. coli* was grown in the presence of the several chemicals such as resveratrol, naringenin or rutin[90]. Similarly, the expression of FadL was induced when *E. coli* was grown in the presence of phenol[99]. However, OmpF is down regulated in the presence of the aliphatic alcohols, isobutanol[89], n-butanol[89,100], ethanol[89], 1,4-butanediol[100] and the aliphatic acid, octanoic acid[101]. This indicates that the expression of porins is differentially regulated according to the structure of the chemical, and may be based on a solute size-selective mechanism[97,103]. In a similar fashion, up or down-regulation of porins (*e.g.* OprH, OprF) in the presence of phenol has been observed in *P. putida KT2440*[102]. Thus, porins appear to play a significant role in resistance to toxic chemicals, but further work is needed to understand their regulation in this context and their mechanisms of action.

1.2.2 Modification of the cell envelope structure

When chemicals disrupt the membrane, microorganisms have the ability to counteract these toxic effects by altering the lipid bilayer composition and structure to maintain its integrity and fluidity[104-107]. This can be either by changing composition of fatty acids and phospholipid head groups or as alterations of the membrane proteins.

1.2.2.1 Changes in the membrane lipid bilayer

As a short-term response, the composition of the lipid bilayer is altered by *cis-trans* isomerization of unsaturated fatty acids, which enables the esterified fatty acids to adopt a denser packing in the membrane[104]. Changes in the ratio of saturated-to-unsaturated fatty acids occurs as a long-term response, together with changes in the abundance of branched, hydroxy, and cyclopropane fatty acids[104,107,108], which allow the membrane to adjust its fluidity[104]. For example, when *E. coli* was exposed to n-butanol increased the production of saturated fatty acids and showed a slight decrease in unsaturated fatty acids; however, the abundance of cyclopropyl fatty acids did not change[109].

Furthermore, the phospholipids found in the cytoplasmic membrane contain several different headgroups. Changes in the proportions of different phospholipid headgroups have been observed in *P. putida* and *E. coli* strains in the presence of toluene[105] and ethanol, respectively[110]. In both strains, the amount of the headgroup phosphatidylethanolamine decreased, and the levels of headgroups cardiolipin and phosphatidylglycerol increased. However, there have been few studies of the effect of toxic chemicals on phospholipid headgroup composition, which suggests that further studies would make a valuable contribution to understanding membrane adaptations.

1.2.2.2 Changes in membrane proteins

Membrane bound proteins form about 50% of the cytoplasmic membrane by weight, and form a bulky, relatively rigid domain of the membrane[28,104,111]. Therefore, proteins make an important contribution to the overall physicochemical properties of the membrane.

An increase in the protein to lipid ratio was observed after exposure of *E. coli*, *Zymomonas mobilis*, and *Oenococcus oeni* to ethanol[112-114], seemingly to enhance the rigidity of the membrane[112-114]. Exposure to chemicals induces various changes in transcripts associated with membrane structure and function in *E. coli*. For example, proteins related to the cell wall biogenesis, LdtB and WzzB were up-regulated in *E. coli* MG1655 in the presence of 1-methyl-2-pyrrolidone[88]. Additionally, Cfa, a cyclopropane fatty acyl phospholipid synthase[115], was also up-regulated in *E. coli* MG1655 in the presence of octanoic acid[101]. Other proteins related to phospholipids accumulation, MlaD and MlaF, are also up regulated in the presence of n-cyclohexyl-pyrrolidone and cyclopentanone[88].

Transcriptomics analysis of *E. coli* has revealed a number of other responses relating to maintenance or composition of the cell envelope[88,96,101]. For example, TolA, TolQ and TolR are up-regulated in the presence of 1-methyl-2-pyrrolidone or n-methyl succinimide[88] . These proteins are components of the Tol-Pal cell envelope system, which is involved in maintaining the cell envelope integrity, resistance to drugs and detergents, formation of outer membrane vesicles and retention of the periplasmic contents[116]. Other proteins related to envelope stress are also affected[96]. For example, in *E. coli* BW21113 and DH5α grown in the presence of ethanol, there is an up-regulation of DegP, a periplasmic serine endoprotease involved in degrading damaged proteins in the periplasm[117,118] and OpgG, a protein involved in the biosynthesis of osmoregulated periplasmic glucans[119].

Proteins involved in biofilm formation are also up-regulated in response to toxic chemicals, suggesting that it would be worthwhile to assess the role of biofilms in chemicals tolerance. YmgA and BhsA, are up-regulated in the presence of octanoic acid, as well as several genes related to colonic acid synthesis, known to be also

associated with biofilm formation, which are up-regulated in the presence of octanoic acid[101], n-butanol, acetate, itaconic acid and succinic acid[100].

1.2.2.3 Phage shock proteins

The phage shock protein response was originally discovered during filamentous phage infection in *E. coli*, hence its designation[120]. However, the phage shock system is now known to maintain the integrity of the membrane under diverse stress conditions[121-125]. Although the mechanism is still not well understood, it is thought that PspA plays an important role by interacting with the inner membrane, thus stabilizing it while maintaining of the proton motive force [126]. In enteric bacteria (*e.g*. *E. coli*), the *pspABCDE* and *pspG* operons are regulated by PspF[126]. In the absence of stress conditions, PspA and PspF form a complex[127,128], which is inactive[129,130]. Under inducing conditions, the inner membrane proteins, PspC and PspB, sense the signals and interact with PspA, resulting in the dissociation of the PspA-PsPF complex allowing PspA to associate with the membrane[127,128].

Several inducing signals have been linked to the phage shock system, including changes in the proton motive force[121-123] or in the redox state of the quinone pool[121,122,131]. Numerous conditions can lead to the induction of these signals, such as filamentous phage infection, osmotic shock, heat shock and chemical exposure[120,122,125]. Indeed, the phage shock system was been reported as induced after exposure to ethanol in different *E. coli* strains [89,132] and *Zymomonas mobilis* ZM4[133]. Moreover, PspA was induced strongly when *E. coli K-12* was exposed to n-hexane and cyclooctane[134], and in *S. lividans,* a *pspA* deletion resulted in an approximately 30 % decrease of dry weight in the presence of ethanol[135].

1.2.3 Induction of stress responses

Microorganisms have regulatory systems in place to respond to various stressful environments that they may encounter, such as nutrient starvation, nitrogen, phosphate, and oxygen limitation, changes in pH and osmolarity, changes in

temperature (heat or cold shock) or oxidative stress[88,100,136-142]. Consequently, responses to stress and toxic chemicals are very complex, involving various transcription factors which regulate the expression of several genes. Hence, cells have a number of stress response mechanisms with different regulatory systems, which can frequently be interconnected.

1.2.3.1 Oxidative stress response

The oxidative stress response (OSR) was first identified as a response to reactive oxygen species (ROS; *e.g.* H_2O_2, $O_2^{-\cdot}$, $OH^{\cdot}$[33-35,143,144]), but is also induced during exposure to redox active chemicals (quinones, phenazines and viologens)[33,34], and reactive species such as furfural[100], all of which generate ROS. The OSR can also be induced by ionizing radiation[145], heat stress and non-redox active chemicals, including n-butanol[100,88], 1,4-butanediol[100], ethanol[96] and cyclopentanone[88]. However, exposure to either heat or toxic chemicals causes disruption of membrane structure in all organisms, and similar disruption of membrane structure in mammalian cells is known to cause generation of ROS, through interference with normal respiration[146-148].

Under normal growth conditions, ROS are produced at low levels as by-products of the oxidative metabolism (*e.g.* aerobic respiration and other oxygen-dependent redox processes) and as intermediates of enzymatic oxidations[34]. Therefore, cells normally produce superoxide dismutases to convert superoxide ($O_2^{-\cdot}$) to O_2 and hydrogen peroxide (H_2O_2), and catalases to inactivate H_2O_2 by conversion to H_2O and O_2[34]. However, direct high exposure to H_2O_2 or redox-active chemicals can overwhelm these systems, and the OSR is induced.

In *E. coli*, OSR is activated by the transcription factors, SoxR, to respond to $O_2^{-\cdot}$ stress, and OxyR, to respond to H_2O_2 stress[33]. SoxR is an iron-sulphur protein and that upon exposure to ROS, becomes oxidized, and activates the expression of several genes, including SoxS, a transcriptional activator responsible for the regulation of dozens of other oxidative stress genes. SoxR can also be directly oxidized by toxic, redox-active chemicals, even under anaerobic growth conditions when $O_2^{-\cdot}$ and/or

H_2O_2 cannot be generated[149]. The SoxRS transcription factors regulate the expression of the SoxRS regulon[150-159], estimated to comprise over 100 genes[158,160].

SoxR is a 154 amino-acid protein, member of the MerR family of proteins, and a homodimer, where each monomer has a DNA-binding domain (α1-α4 and β1 and β2), a dimerization helix (α5) and an iron-sulphur ($[2Fe\text{-}2S]^+$) cluster-binding domain (Figure 1.7)[161]. Each $[2Fe\text{-}2S]^+$ cluster is coordinated by four cysteine residues and further stabilized by interactions with other helixes (α3' and α5')[161]. Upon binding to DNA, the DNA-binding domain rotates outward leading to an outward rotation of the cluster-binding domain as well. This allows an easy electron transfer to redox-cycling compounds with different sizes and conformations, during the oxidation process[149,161].

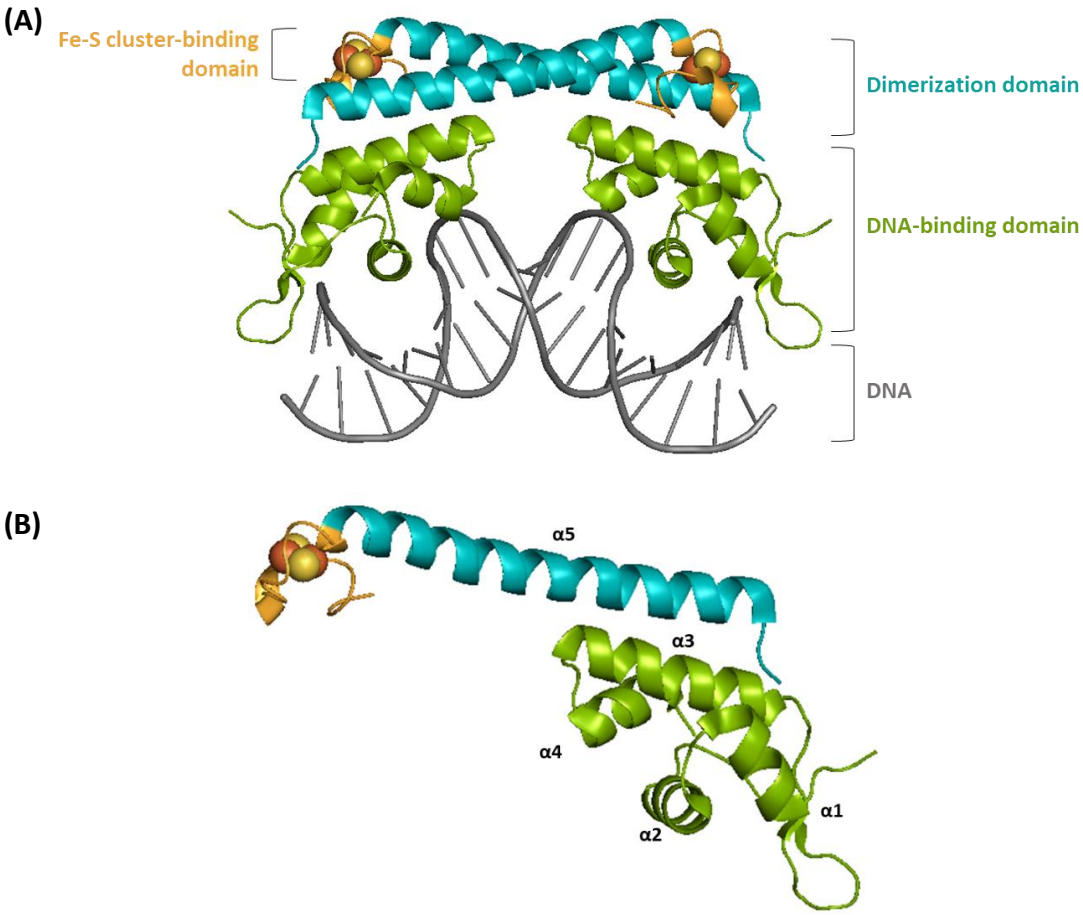

Figure 1.7 - Crystal structure of the SoxR homodimer. SoxR is shown as a dimer bound to DNA (A) and as a monomer (B) (RCSB PDB accession code: 2ZHG)[161]. The dimerization domain is represented in light blue, the DNA-binding domain in green, the Fe-S cluster domains in yellow and the DNA in grey.

The reduced form of SoxR can bind to DNA, however only the oxidized form is able to activate the transcription of other genes, such as *soxS*[161]. When the cluster is oxidized, subsequent conformational changes in the cluster-binding domain and then in the DNA-binding domain lead to a distortion of the DNA, so that the RNA polymerase can bind. In addition, when the oxidative stress stops, SoxR returns to its reduced state and remains in that state until further induction[161].

On the other hand, OxyR is activated by oxidation of Cys199 and Cys208 to form a disulphide bond, which is reduced again in the absence of the ROS[158]. In its oxidized form, OxyR binds to DNA and activates the expression of over 30 genes[160,162], including *oxyS*[158,163]. OxyS is a small RNA which, upon interaction with Hfq (RNA chaperone), affects the regulation of several genes by affecting mRNA stability or translation efficiency[158,163].

Although the OSR has been studied in detail during exposure to ROS and viologens, typically paraquat, there is much less information about the effect of non-redox active industrial chemicals on the induction of the OSR. Nevertheless, such chemicals are known to induce genes related to oxidative stress in *E. coli*, including n-butanol, n-cyclohexyl-pyrrolidone, cyclopentanone, dimethyl sulphide, toluene, ethanol, octanoic acid and 1,4-butanediol[88,96,100,101]. For example, several genes that are activated by SoxRS[160], are also up-regulated in the presence of different chemicals, including *sodA* (manganese containing superoxide dismutase)[100,96], *marA* (transcriptional regulator)[101], *acnA* (aconitate hydratase A)[96], *fumC* (fumarase C)[96], nuoA-N (NADH:quinone oxidoreductase subunits)[96] and *pqiAB* (intermembrane transport, unknown substrate)[88]. Additionally, *dsbG* (disulphide chaperone-isomerase), which is up-regulated by OxyR[162], is also up-regulated in the presence of ethanol [96]. Yet, the ORS is a complex mechanism often associated with another stress response mechanism, namely the homeostatic regulation of iron[164-166].

1.2.3.2 Iron homeostasis

Iron is normally taken up into cells as ferrous (Fe^{2+}) and ferric (Fe^{3+}) ions and is essential for cellular survival, as it is involved in many biological redox processes[164-

[166]. However, excess iron can be damaging to cells when ROS are present, as a result of the Fenton[164-166] and the Haber-Weiss reactions[165,167]. In the Fenton reaction, Fe^{2+} is oxidized to Fe^{3+} by hydrogen peroxide (1). This generates highly reactive hydroxyl radicals, capable of extensive cellular damage, plus hydroxide ions. Furthermore, the reaction is a dismutation, in which the Fe^{3+} is reduced back to Fe^{2+}, generating equally reactive hydroperoxide radicals (2).

$$Fe^{2+} + H_2O_2 \rightarrow Fe^{3+} + \bullet OH + OH^- \quad (1)$$

$$Fe^{3+} + H_2O_2 \rightarrow Fe^{2+} + HOO\bullet + H^+ \quad (2)$$

Net reaction:

$$2\ H_2O_2 \rightarrow HO\bullet + HOO\bullet + H_2O \quad (3)$$

Similarly, Fe^{3+} can be reduced to Fe^{2+} by superoxide in the Haber-Weiss reaction (4)[165,167]. The Fe^{2+} is then reoxidized to Fe^{3+} by the Fenton reaction (1), generating hydroxyl radicals.

$$Fe^{3+} + \bullet O_2^- \rightarrow Fe^{2+} + O_2 \quad (4)$$

$$Fe^{2+} + H_2O_2 \rightarrow Fe^{3+} + \bullet OH + OH^- \quad (1)$$

Net reaction:

$$\bullet O_2^- + H_2O_2 \rightarrow \bullet OH + OH^- + O_2 \quad (5)$$

Additionally, ROS can also damage the Fe-S clusters present in many proteins, resulting in the release of free iron ions in the cell[167], showing how iron homeostasis and the OSR are closely related[164,165,167,168].

Fur is the central iron-dependent regulator that controls iron homeostasis, but it is only activated when associated with its co-repressor, Fe^{2+}, and a structural Zn^{2+} [165,167,169,170]. Under iron excess, of either ferrous or ferric ions, the Fur-Fe^{2+} complex represses the expression of dozens of genes by binding to a sequence in their promoters known as the Fur box. Several of these down-regulated genes are related to iron uptake[165,166,171,172], either the outer membrane porins and inner membrane transport systems involved in Fe^{2+} uptake (*e.g.* EfeUOB, FeoABC, YfeABCD or FutABC)[166], or the siderophore or hemophore (mediated with outer membrane receptors, with energy provided by TonB-ExbB-ExbD protein complex) and the inner membrane ABC transport systems involved in Fe^{3+} uptake (*e.g*. FhuDC or FecCDE)[165,166]. On the other hand, Fur-Fe^{2+} induces the expression of proteins related

to iron storage (*e.g*. ferritin, FtnA; and the mini-ferritins, Dps proteins)[165,173], Fe^{2+} efflux (*e.g*. P-type ATPases)[173] and several proteins containing Fe-S clusters (*e.g.* AcnA, FumA, FumB, SdhCDAB)[165,173], which are part of central metabolism and closely related to oxidative stress[158,160] and regulated by the aerobic/anaerobic regulators, Fnr and ArcA[174-178]. Fur is also linked to the respiratory chain[171]. In an *E. coli* MC4100 *fur* deletant, several iron containing proteins involved in the respiratory chain were down-regulated, including the cytochromes bo3 and bd-I (CyoA-E and CyaAB, respectively), the nitrate reductases A (NarGHJI) and Z (NarZYWV), and the NADH dehydrogenases NuoA-N (NADH DH-I) and Nhd (NADH DH-I)[171]. Additionally, both OxyR and SoxRS induce the expression of Fur[157], showing the significant cross-talk between the OSR, the iron homeostasis system and the central metabolism.

In *E. coli*, transcriptomic studies showed that the iron homeostasis system is associated with responses to several toxic chemicals, including n-butanol, isobutanol, cyclopentanone, ethanol, toluene and 1,4-butanediol[88,89,96,99,100,102]. For example, genes responsible for assembly of Fe-S clusters, namely the *isc* and *suf* operons, are up-regulated in the presence of different chemicals[88,96,100]. Moreover, several genes are down-regulated, including ferric iron transporters (*e.g*. *fhuA, fhuC*), ferric ion reductase (*fhuF*) and the sigma factor (*fecI*) that regulates the ferric citrate ABC transporter (*fecCDE*), in the presence of isobutanol, n-butanol and ethanol[89]. Additionally, in *P. putida KT2440*, a proteomics study also showed that the addition phenol down-regulated the expression of proteins involved in siderophore-mediated ferric iron uptake (*e.g*. FpvA and CirA)[102].

However, other studies show contradictory results. For example, the regulation of other iron uptake-related proteins (*e.g*. EfeO and ExbBD) appears to be dependent on the concentration of the toxic chemical, since the corresponding genes were down-regulated when *E. coli* was exposed to 5.9 g/L n-butanol[100], but up-regulated when exposed to 1.0 g/L n-butanol[88], despite the regulation of *fur* not being affected in either case[88,100]. Other proteins related to ferrous iron uptake (e.g. FeoA, FeoB and EfeO) and siderophore-mediated ferric iron uptake (e.g. ExbBD, YncD, TonB and FepBD) were also up-regulated in *E. coli* in the presence of several chemicals, including n-butanol, cyclopentanone, N,N-dimethylacetamide and toluene[88,100].

Additionally, in a proteomics study, Dps down regulated in *E. coli* K-12 K99+ grown in the presence of phenol[99]. Thus, further work is needed to analyse the complex interplay between iron homeostasis systems, other microbial stress responses, and responses to different classes and concentrations of chemicals.

1.2.3.3 Heat shock response

The heat shock response enables living organisms to respond to increases in temperature or other perturbations that cause protein denaturation or thermally-induced damage to other cellular components (*e.g.* membranes and nucleic acids)[156-160]. Organic compounds may also induce the heat shock response, by entering the cell through diffusion[106,179] and affecting the structure and function of proteins[104,180]. As a stress response, heat shock proteins protect against protein aggregation, help in refolding/unfolding of damaged proteins, repair damaged proteins, reactivate inactivated proteins, or help degrade irreparably denatured proteins[28,104,105,181-185]. Additionally, heat shock proteins are also involved in RNA and DNA repair, metabolism, regulation, cell structure maintenance, and restoration of membrane stability[182,186,187].

In *E. coli*, transcriptomics analysis revealed that different chaperones, such as DnaKJ, GroES, HtpG, ClpB and Spy, are up-regulated under the stress of several chemicals, including n-butanol, cyclopentanone, ethanol, isobutanol and 1,4-butanediol [88,89,96,100,188]. The chaperones IbpA and IbpB, which belong to a family of widely conserved small heat-shock proteins, have also been associated with the response to n-butanol[189] and isopentenol[190] in *E. coli.* Various heat shock proteins were also induced, together with proteins associated with carbon starvation, when *E. coli* is exposed to ethanol, ether and benzene[191]. Thus, induction of heat shock proteins seems to play an important part in the stress response to various organic chemicals in a range of different organisms[88,89,96,100,188,192-196]. However, it should be noted that a range of other genes are also up-regulated or down-regulated in all of these studies, and further work is needed to confirm the relative importance of the heat shock proteins compared with other responses.

1.2.3.4 Stringent response

The stringent response was first identified as a response to amino acid starvation[197], but is also triggered by other nutritional limitations (*e.g*. carbon sources, fatty acids, iron or phosphate starvation)[198-202], heat shock[198,203,204], and it has also been linked to chemical tolerance[96,205-207]. The stringent response ensures cellular survival in stressful conditions by preventing unbalanced metabolism, which can lead to growth inhibition[198-202]. In bacteria, the stringent response is mediated by the intracellular levels of the small nucleotides, guanosine pentaphosphate (pppGpp) and guanosine tetraphosphate (ppGpp), collectively referred to as (p)ppGpp[198-202,208]. The RelA–SpoT homologues family of enzymes are the key regulators of the concentration of (p)ppGpp, as reviewed previously[198,209]. When (p)ppGpp accumulates in the cell, the stringent response is triggered. The primary mechanism of action of (p)ppGpp is to bind to the RNA polymerase, which causes inhibition of transcription from the promoters of rRNA, tRNA and ribosomal genes, resulting in a strong down-regulation of the translational machinery in the cell[198-200,202]. The change in the activity of the RNA polymerase also activates transcription of amino acid biosynthesis genes and indirectly activates sigma factors[199-202,208]. (p)ppGpp further affects translation, by inhibiting the activity of initiation factors, elongation factors and small GTPases[199,200,208], and DNA replication, by inhibiting the DNA primase, DnaG[199,202].

The role of the stringent response in chemicals tolerance has been identified through the analysis of alcohol-tolerant *E. coli* strains[96,205-207]. Different mutations in *relA*, among other genes, were detected in *E. coli* strains that were independently evolved under selection in the presence of ethanol[206] or isopropanol[207], through adaptive evolution in serial subcultures. Other omics studies also show that other toxic chemicals might also induce the stringent response[89,99,102,210], although the evidence is less clear and sometimes contradictory. In *E. coli* BW25113, transcriptomics showed that several 50S ribosomal subunits (*rplCDWB, rplV, rplP*) are down-regulated in the presence of isobutanol. However, proteomic analysis of *E. coli* K-12 K99+ grown in the presence of phenol showed that expression of TufA (translation elongation factor EF-Tu 1) is induced[99], even though it is normally

repressed by the stringent response[208,211]. However, the exact relationship between the stringent response and chemical tolerance still needs to be clarified further.

1.2.3.5 Osmotic stress response

In bacteria, the osmotic stress response involves a complex set of mechanisms that work together to accumulate or release small organic solutes and water[212]. Osmosensing proteins play an important role in responding to changes in osmotic pressure[212,213]. While aquaporins regulate the inflow and outflow of water, bacteria also use, for example, osmoprotectant transporters and potassium transporters, or mechanosensitive channels to counteract high osmolarity environments[212,213].

In Gram-negative bacteria, OmpR and EnvZ constitute the two-component signal transduction system that responds to osmotic stress[212,214,215]. EnvZ is a transmembrane sensory histidine kinase/phosphatase located in the inner membrane which, in the presence of osmotic stress, regulates the phosphorylation of OmpR, the transcriptional regulator[215-217]. In *Escherichia coli* K-12 MG1655, over 30 genes are part of the OmpR regulon[218], including the outer membrane porins, OmpF (activated[218]), OmpC (activated[218]), FadL (repressed[219]) and NmpC (repressed[218]), the curli assembly related proteins, CsgDFEG (activated[218]), the two transcription regulators of flagella production, FlhDC (repressed[220]), or the sugar transporters MalEFGK (repressed[218]) and GalP (repressed[218]).

Studies showed that OmpR was up-regulated in *E. coli* in the presence of octanoic acid[101], ethanol[96] and isobutanol[89]. Furthermore, genes that are also regulated by OmpR are also differentially expressed[88-90,96,101]. For example, the porins OmpF and NmpC are down-regulated in the presence of octanoic acid[101] and isobutanol[89], but OmpC is up-regulated in the presence of ethanol[96] and octanoic acid[101]. OmpF and FadL are also up-regulated in the presence of resveratrol, naringenin or rutin[90]. MicF, a small RNA that represses the translation of OmpF, is up-regulated in the presence octanoic acid[101] and isobutanol[89]. In addition, the curli and flagella related proteins CsgDF and FlhDC are down-regulated in *E. coli* BW25113 in the presence of isobutanol[89], and FlhDC is also down-regulated in the presence of toluene and

n-butanol[88]. Additionally, MalE and MalK, part of the maltose ABC transporter MalEFGK, are also up-regulated in *E. coli* in the presence of ethanol[96], resveratrol, naringenin or rutin[90] although MalE is known to be repressed by OmpR[218].

In the same studies with isobutanol[89], ethanol[96], octanoic acid[101] or toluene[88], among others[88], other proteins known to be osmosensitive but not part of the OmpR regulon are also up-regulated. These proteins included ProVWX (glycine betaine ABC transporter) and ProP (MFS transporter), both involved in the uptake of glycine betaine and proline betaine in high osmolarity environments[213], OsmY, a periplasmic chaperone[221,222], OsmB, an outer membrane lipoprotein, and OsmC a peroxiredoxin associated with the reduction of organic hydroperoxides[223,224]. Additionally, an analysis of the metabolome of *E. coli* Trans10 exposed to n-butanol and isobutanol revealed that genes associated with production of the osmoprotectant, trehalose, are up-regulated[225].

1.2.3.6 Acid stress responses

A number of systems involved in the acid stress response are up-regulated in response to toxic chemicals in *E. coli*, even when the chemicals do not contain acidic hydrogen atoms[89,96,100,101]. In *E. coli*, there are a total of over 10 genes that contribute to acid resistance[46,226]. The global regulators, RpoS (sigma factor S), Fur (iron homeostasis transcriptional regulator), PhoPQ (two component transcriptional regulator) and OmpR (osmotic stress response transcriptional regulator) also induce the response to acidic environments[227,228]. Consequently, there is a complex linkage and overlap between the different stress responses.

One of the best characterised mechanisms for the acid stress response is the glutamate decarboxylase system, known as the Gad system, as reviewed by several authors[46,226,228,229]. At low pH, intracellular glutamate is decarboxylated to form gamma-aminobutyric acid, by GadAB (glutamate decarboxylases A and B), consuming one proton, and thus raising the intracellular pH. The antiporter, GadC, exports gamma-aminobutyric acid and imports another glutamate molecule. The expression

of GadA and GadB is positively regulated by GadX[46] and GadE, together with the major regulator RcsB[228].

The Gad system has been reported as up-regulated in *E. coli* under ethanol[96] and octanoic acid[101] stress. Additionally, the acid shock-associated periplasmic chaperones, HdeA and HdeB, are also reported as up-regulated in *E. coli* K-12 MG1655 in the presence of octanoic acid[101]. Additionally, Asr, an acid shock protein, strongly induced at low pH[230], is also up-regulated under the stress of different chemicals such as isobutanol, n-butanol and ethanol[89,96,100]. The significance of these changes related to acid stress and the cross-talk with other stress responses is still not well understood and requires further studies.

1.2.3.7 Flagella-dependent cell motility

Bacterial flagella are complex organelles normally associated with cell motility and chemotaxis [231-237]. The number and position of the flagella on the cell membrane varies from species to species, with each flagellum being composed of over 30 different proteins. Due to the complexity of this organelle, there is a high energy requirement for synthesis and assembly, and, of course, to drive rotation of the flagella[233,236]. Therefore, this process is regulated at several levels, where, in enteric bacteria, FlhD and FlhC are the master regulators that control the production of flagella, as reviewed previously [231,233,237]. These proteins activate the expression of flagellar proteins involved in the hook and basal body synthesis and the expression of the sigma factor, σ^{28} (FliA), which up regulates the filament related genes, and the anti-sigma factor, σ^{28} (FlgM). Additionally, the expression of FlhDC can be repressed by the transcription regulators, OmpR and RcsAB, and activated by CsrA[236].

Flagellar proteins have been widely associated with bacterial stress responses to toxic chemicals. Most flagellar genes are down-regulated in *E. coli* in response to several chemicals, including among others, toluene, n-butanol and ethanol[88,96,101]. In some of these studies, flagellar transcriptional activators are also down-regulated, including FlhDC[88], FliZ[88,101] and FliA[88]. However, the methyl-accepting chemotaxis sensor proteins, Aer, Tsr, Tap and Tar, are up-regulated in *E. coli* DH5α and in *E. coli*

BW25113 in the presence of lower concentrations of ethanol, whereas the genes related to flagella regulation, production or assembly were not detected as differentially expressed[96]. Consequently, there is some uncertainty about the precise role of flagellar shutdown in response to toxic chemicals, although it has been suggested that this response might be related to energy saving[141], firstly during biosynthesis of the flagellar components and during operation of the flagella to drive cell motility. It is also possible that flagellar shut down could be a consequence of the up-regulation of other transcription factors that repress flagellar gene expression, such as the osmotic stress transcription factor, OmpR[100]. However, OmpR is only up-regulated in half of the studies where flagella genes are down-regulated[88,96,101].

1.2.3.8 Changes in metabolism

As noted above, ROS and the iron homeostasis system are activated upon exposure to toxic chemicals and affect the expression of a number of enzymes involved in energy metabolism. However, exposure to toxic chemicals appears to cause significant changes in energy metabolism both within and beyond these two regulons [88,89,96,99,100,102,141,210,238,239].

The main metabolic effects of toxic chemicals seem to concern the expression of genes related to the TCA cycle and/or the respiratory chain[88,89,96,99,100,102,141,210,238,239]. Most prokaryotes have diverse and branched respiratory chains that allow the cells to adapt to the availability of oxygen or other electron acceptors[240-242]. The respiratory chain is composed of dehydrogenases and terminal reductases/oxidases which are linked with a quinone pool[240-242]. The dehydrogenases include the NADH dehydrogenases NuoA-N (NADH DH-I; oxic or anoxic conditions) and Ndh (NADH DH-I; anoxic conditions) with the redox pair NAD^+/NADH; HyaABCDEF and HybABCDEFG, hydrogenases 1 and 2 (anoxic conditions), respectively, with the redox pair H^+/H_2; and the succinate dehydrogenase (SdhCDAB; oxic or anoxic conditions) with the redox pair fumarate/succinate[240]. Under aerobic conditions, *E. coli* uses the heme containing terminal reductase, cytochromes bo3 (CyoABCDE), bd-I (CydABX) or bd-II (CbdABX, also known as AppBCX), all with the redox pair O_2/H_2O[240,242]. Under

anaerobic conditions, the terminal reductases include the nitrate reductases A (NarGHJI) and Z (NarZYWV), with the reducing pair NO_3^-/NO_2^-; the fumarate reductase, FrdABCD, with the redox pair fumarate/succinate; or the trimethylamine N-oxide reductase (TorCAD) with the redox pair trimethylamine N-oxide/trimethylamine[240].

Genes related to the respiratory chain are regulated by two major regulators, Fnr and ArcA (part the two-component system ArcAB[240,242]), which together regulate the expression of hundreds of genes[240,242-244]. Moreover, Fnr is thought to co-regulate a number of genes with other transcription factors, namely CRP (cAMP receptor protein), NarLP (nitrate-responsive regulators), Fur (iron homeostasis regulator) or OxyR (oxidative stress regulator)[244]. This also shows how the respiratory chain is also strongly linked to iron homeostasis and oxidative stress, as quinones can generate reactive oxygen species as superoxide or hydrogen peroxide[241].

Various transcriptomics studies revealed that several genes related to energy metabolism are affected by exposure to chemicals in *E. coli*[89,96,100]. Genes related to the respiratory chain (NuoA-N, NADH dehydrogenase; CyoABCDE, cytochrome *bo₃* ubiquinol oxidase subunits; HyaABCD, hydrogenase 1 subunits) are down-regulated in *E. coli* BW25113 grown in the presence of ethanol[96]. Additionally, CyoABCDE are also down-regulated in *E. coli* BW25113 in the presence of isobutanol, n-butanol, and ethanol, while CydAB, the cytochrome bd-I ubiquinol oxidase subunits I and II, are up-regulated[89]. However, NuoA-N and CyoABCDE are up-regulated in *E. coli* DH5α in the presence of different concentrations of ethanol, and furthermore, CydAB, the cytochrome bd-I ubiquinol oxidase subunits I and II, are up-regulated *E. coli* DH5α in the presence of higher concentrations of ethanol but down-regulated at lower concentrations[96]. Anaerobic oxidoreductases are also up-regulated in the presence of ethanol, including FrdABCD (anaerobic fumarate reductase) and TorAC (trimethylamine N-oxide reductase I)[96]. Moreover, enzymes responsible for the anaerobic β-oxidation of fatty acids (FadI and FadK) are not affected in *E. coli* DH5α, but are up-regulated in *E. coli* BW21113 in the presence of ethanol, while FadD, involved in the aerobic β-oxidation of fatty acids, is down-regulated also, but only in *E. coli* BW25113 in the presence of ethanol[96]. Additionally, fermentation related

enzymes are also up-regulated in *E. coli* BW25113 in the presence of ethanol (*e.g*. PflB, formate C-acetyltransferase 1/pyruvate formate-lyase 1; Pta, phosphate acetyltransferase; AckA, acetate kinase A; Ppc, phosphoenolpyruvate carboxylase)[96]. However, Ppc, Pta and AckA are down-regulated in *E. coli* DH5α in the presence of ethanol[96]. Additionally, in another study, genes involved in the TCA cycle, succinyl-CoA synthesis (*sucABCD*) and succinate dehydrogenase (*SdhCDAB*), are down-regulated in *E. coli* BW25113 in the presence of isobutanol, n-butanol and ethanol, while the NADH:quinone oxidoreductase II (*ndh*) are up-regulated[89]. In this study, transcriptional regulator Fnr is up-regulated in *E. coli* BW25113 in the presence of isobutanol and n-butanol, but not in the presence of ethanol, whereas the expression of the regulator ArcA is not affected by any of the chemicals tested[89].

Similarly, in another transcriptomic analysis also showed changes related to metabolism in *E. coli* K-12 MG1655[100]. Fnr is up-regulated in the presence of n-butanol, whereas ArcA is up-regulated in the presence of (S)-beta-hydroxy-gamma-butyrolactone, furfural, 1,4-butanediol and acetate[100]. Consistent with these observations, several genes related to fermentation, anaerobic respiration and both the aerobic/anaerobic electron transport chains are up-regulated after exposure to n-butanol, (S)-beta-hydroxy-gamma-butyrolactone or furfural[100]. Furthermore, in the presence of 1,4-butanediol or acetate, genes related to anaerobic respiration, fermentation and both aerobic/anaerobic electron transport chain are also up-regulated, but with a lower number of genes compared with the cells exposed to n-butanol, (S)-beta-hydroxy-gamma-butyrolactone or furfural[100]. Additionally, glycolysis and pentose phosphate pathway genes are up-regulated[100]. Interestingly, different sets of sugar transporters are down-regulated in the presence of different chemicals, even though other glycolysis and pentose phosphate pathway genes are up-regulated. The presence of (S)-beta-hydroxy-gamma-butyrolactone leads to the down-regulation of the highest number of sugar transporters, namely glucose, mannose, galactose, galactitol and maltose transporters[100].

There is much less information about changes in the proteome or metabolome associated with the energy metabolism. The expression of AceA (isocitrate lyase) and AtpB (ATP synthase Fo complex subunit) are induced when *E. coli* K-12 K99+ is grown

in the presence of phenol[99]. In minimal media, ^{13}C-NMR was used to analyse the effect of octanoic acid on metabolic flux in *E. coli* MG1655 growing on a mixture of labelled and unlabelled glucose[239]. Octanoic acid stress decreases the carbon flux *via* pyruvate dehydrogenase (pyruvate to acetyl-CoA) and the TCA cycle, reduces the net production of CO_2, and activates the pyruvate oxidative pathway (acetate synthesis from pyruvate, mediated by the pyruvate oxidase PoxB) and the extracellular acetate production pathway[239]. Yet, further studies are still necessary to fully understand the complex network of regulators and stress response mechanisms that affect the central metabolism of bacteria.

In summary, the changes in gene expression described in the sections above provide information about responses to industrially relevant chemicals and focus on well characterised genes and stress responses, where it is possible to make some interpretation of the data available, however limited or contradictory. Many different tolerance mechanisms can be induced or repressed upon exposure to different toxic chemicals, and are greatly interconnected, forming a complex network of responses. Yet, it becomes difficult to compare different studies when the culture conditions and techniques greatly vary from study to study. It should be noted that there is a need to standardize the culture conditions used for global “omics” analysis and to ensure that experiments are designed to prevent loss of volatile chemicals from the culture systems. Nonetheless, previous studies provide a good foundation knowledge to further comprehend the toxic effects of chemicals in bacteria. Understanding the biological responses induced by toxic chemicals is essential to further know how methacrylate esters can possibly affect *E. coli* cells. Since MAE are more non-polar chemicals, it could be hypothesised that the main toxic effect would be the disruption of the membrane fluidity and integrity, by intercalating into the lipid bilayer, which can then lead do the disruption of many other essential biological processes.

1.3 Isolation of *E. coli* mutants tolerant to BMA

BMA (Figure 1.8), is a MAE that is a flammable and irritant colourless liquid, insoluble in water[12]. Generally, BMA is used in decorative paints, wood finishes and automotive and textiles industries [10], or can be transesterified into MMA.

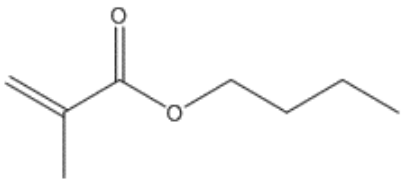

n-Butyl methacrylate

Figure 1.8 – Chemical structure of n-butyl methacrylate (BMA).

Four E*. coli* mutant strains, which can grow in the presence of 20 %(v/v) BMA, have been isolated and sequenced previously[7]. Whole genome sequencing showed that all mutant strains have different sets of mutations for three different genes; *soxR*, an oxidative stress response regulator[33], *acrR, a* repressor of AcrAB multidrug efflux pump proteins[82], and *ybcO,* an uncharacterized protein. All four strains have the same *soxR* mutation, and one strain has an additional *ybcO* mutation, one has an additional *acrR* missense mutation and the third has an additional deletion in *acrR* which lead to a frameshift. The strains were named *E. coli* MG1655 *soxR*(R20H), *E. coli* MG1655 *soxR*(R20H)*ybcO*(I87M), *E. coli* MG1655 *soxR*(R20H)*acrR*(V29G) and *E. coli* MG1655 *soxR*(R20H)*acrR*(T32fs).

All four BMA-resistant strains that have been isolated have the same mutation in *soxR*, which may suggest that it was the first gene to mutate in the presence of BMA, thus might be essential for the phenotype observed. This is a missense mutation, where an arginine in position 20 is substituted by a histidine (R20H). The mutation is located in helix α1 of the DNA binding domain (Figure 1.9) and may affect the capability of the protein to bind to DNA and the interaction between subunits[245]. The mutation is close to Arg55, which drives the conformational changes needed for DNA

binding, together with the Fe-S cluster and another residue, Gly123', from the other subunit. These conformational changes occur upon oxidation of the Fe-S cluster[161].

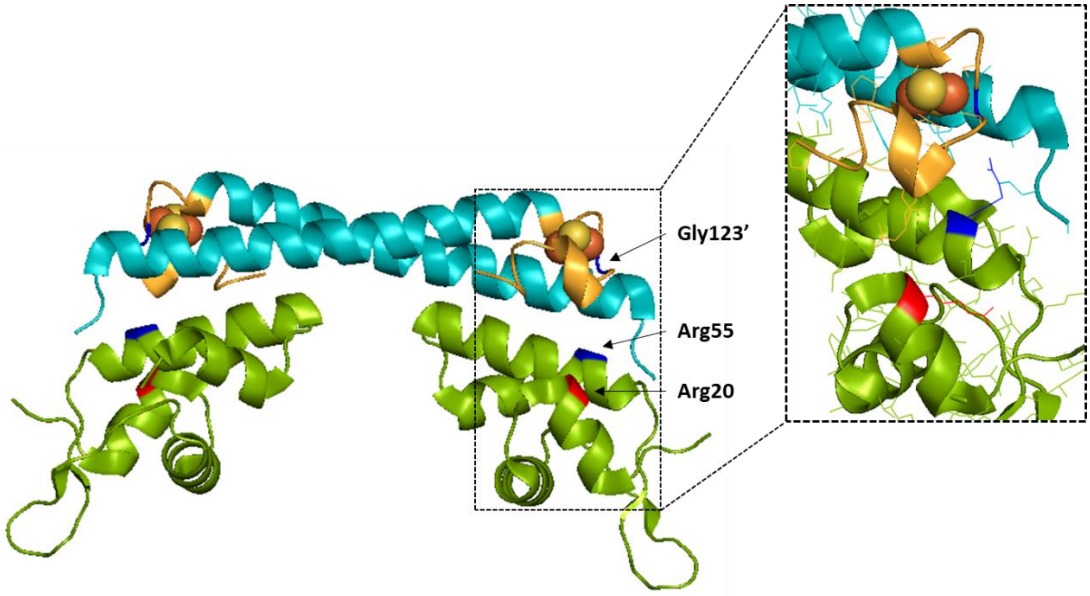

Figure 1.9 - Crystal structure of the SoxR homodimer, with the mutated residue shown. The dimerization domain is represented in light blue, the DNA-binding domain in green and the Fe-S cluster domains in yellow. Arg20, the mutated residue found in *soxR*(R20H) is coloured in red and Arg55 and Gly123, the residues related to conformational changes in SoxR, are coloured in dark blue (RCSB PDB accession code: 2ZHG).

In another study, an *soxR*(R20H) mutation was also found in a fluoroquinolone tolerant *E. coli* strain[246]. This strain also has a mutation in *gyrA* (a DNA gyrase, also known as topoisomerase II) and is tolerant to chloramphenicol, nalidixic acid, ciprofloxacin and paraquat. Since the mechanism of action of fluoroquinolone is inhibiting topoisomerase II[247], the mutation in *gyrA* may be more relevant for the resulting phenotype. However, the individual effect of *soxR*(R20H) was not investigated[246]. In another study, a nalidixic acid and ciprofloxacin-resistant isolate of *Salmonella enterica* serovar Enteritidis had a *soxR*(R20H) mutation, with two additional mutations in *gyrA*, and also one mutation in *soxS* (E52K)[248]. Additionally, increases in expression of *acrB*, *soxS* and *marA* were observed, with fold changes of 6, 26 and 9, respectively.

Other mutations found in *E. coli* in the DNA binding domain (Y31H, L36V, I62V, I62N and I73F) were reported to decrease the ability of SoxR to bind DNA and to lead to unstable $[2Fe\text{-}2S]^{+}$ clusters [249,250]. This suggests that the R20H mutation could have a similar effect. The effect of other mutations in the dimerization domain (I106T, L94P

and S95P) has also been investigated previously, suggesting to interfere with the interaction between the SoxR monomers and to lead to an activation-defective SoxR[249,250].

By contrast, two different *acrR* mutations were found in two of the strains isolated. The strain named *E. coli* MG1655 *soxR*(R20H)*acrR*(T32fs) has a deletion of a nucleobase at position 94. This deletion leads to a frameshift starting at threonine 32, changing the subsequent sequence of amino acids and culminating with a truncated protein, with a stop codon at position 73 (Figure 1.10). Even if the first 31 amino acids have the right sequence, it is uncertain how this truncated AcrR of 72 amino acids will fold, or if folds at all, and how it may interact with DNA.

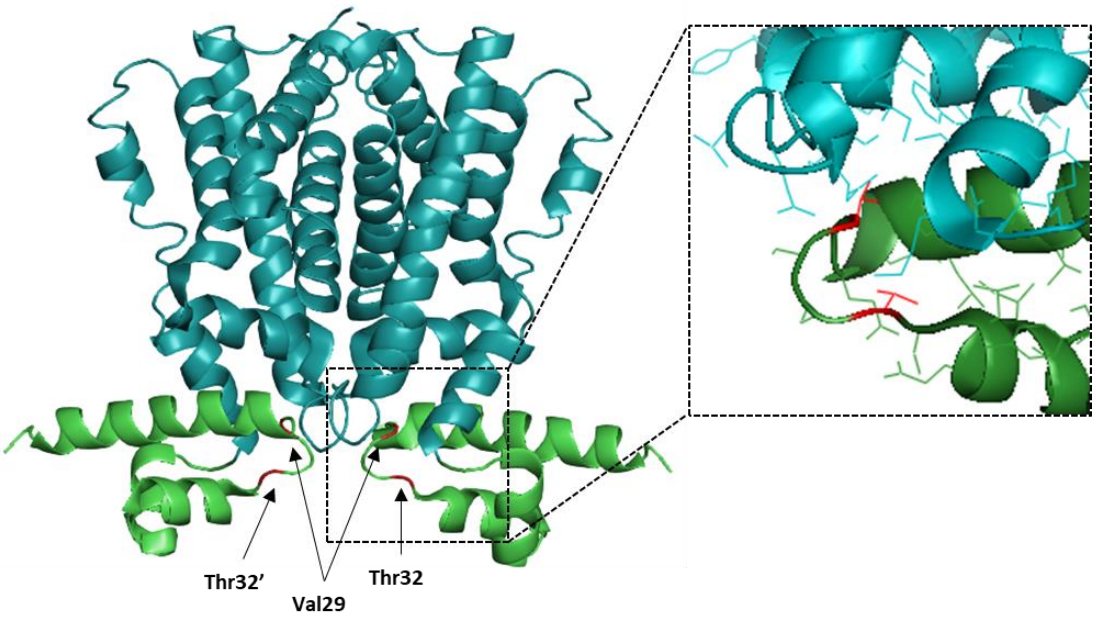

Figure 1.10 - Crystal structure of an AcrR homodimer, with the mutated residues shown. The ligand-binding domain is represented in light blue and the DNA-binding domain in green (RCSB PDB accession code: 2QOP)[80]. The residues coloured in red represent the Val29 residue that is mutated in *acrR*(V29G), and the Thr32 residue that is mutated in *acrR*(T32fs).

No similar mutation has been reported previously, but *E. coli* JA300 mutant strains previously reported as tolerant to cyclohexane and/or a mixture (7:3) of cyclohexane and *p*-xylene have different mutations in *acrR* and *marR* (multiple antibiotic resistance transcriptional repressor)[251]. There are three strains with three different mutations in *acrR*, missense mutations A41D and M1I, and a 1195 bp insertion sequence (IS5) element at residue 74. The strains with the *acrR*(A41D) and the IS5

element mutations, also have additional mutations in *marR*. Yet, these strains still have improved tolerance to cyclohexane and a mixture (7:3) of cyclohexane and *p*-xylene, compared to other mutant strains with only *marR* mutations[251]. This suggests that the insertion sequence in AcrR and the missense mutation M1I, which would not have the start codon, could result in non-functional protein, which is not able to bind to DNA and therefore is not capable of repressing *acrAB* transcription. Likewise, the deletion found in *acrR*(T32fs), that will be investigated in this work, may have the same effect.

The second *acrR* mutation found in the BMA-tolerant strains is the substitution of valine 29 with glycine (Figure 1.10). The strain was named *E. coli* MG1655 *soxR*(R20H)*acrR*(V29G). This mutation is located in the DNA-binding domain (α1, α2, α3 and α4a), more specifically in the loop between helixes α1 and α2 (Figure 2.6 and Figure 1.10). This loop is suggested to be essential for the communication between the ligand-binding domain and the DNA-binding domains [80]. When AcrR binds to DNA, the loop shifts upward and consequently, the α6 helix moves toward the ligand-binding pocket, which makes helix α4 move as well, decreasing the volume of the pocket. Therefore, the location of the V29G mutation may have an effect on this mechanism.

Recently, two *E. coli* strains with the same *acrR*(V29G) mutation were isolated after being exposed to the antibiotics ertapenem and meropenem[252]. One of these strains also has mutations in *envZ* (regulator of two membrane porins, OmpF and OmpC), *ftsI* (peptidoglycan synthesis) and *lon* (protease), and the other had mutations in *envZ*, *mrdA* (peptidoglycan synthetises), *spoT* (stringent response regulator) and *nanC* (membrane porin). In another study, an *E. coli* mutant tolerant to norfloxacin was also isolated and has an *acrR*(V29G) mutation and additional mutations in *gyrA* (topoisomerase II), *parE* (topoisomerase IV subunit), *deoA* (thymidine and uracil phosphorylase) and *ompR* (regulator of two membrane porins, OmpF and OmpC) [95]. Another study also reported that three levofloxacin-tolerant clinical isolates from urine samples have the same V29G mutation in *acrR*[253]. One of the isolates has extra mutations in *marR* and in the topoisomerases *gyrA*, *parE* and *parC*. Yet, the other two isolates, which have the exact same mutations, also have

additional mutations in *acrR*, namely T213I and N214T, both in the ligand-binding domain, and in *soxR*, specifically T38S and G74R, part of the DNA-binding domain. This indicates that the mutated gene *acrR*(V29G) is frequently observed in *E. coli* strains tolerant to different antibiotics.

The third gene involved in BMA tolerance, *ybcO*, encodes for an uncharacterized protein. Although no studies have been reported regarding the definite function of this protein, a crystal structure is available without a published reference (RCSB PDB accession code: 3G27; Figure 1.11). According to the crystal structure, YbcO is a homodimer, and each monomer has two α-helixes, two β-sheets and Zn^{2+} and Ca^{2+} ligands. Nevertheless, YbcO has been predicted to be a possible nuclease, due to structure similarities to a family of His-Me nucleases[254], and has also been reported, among other genes, as up-regulated in *E. coli* MG1655 wild type biofilms[255].

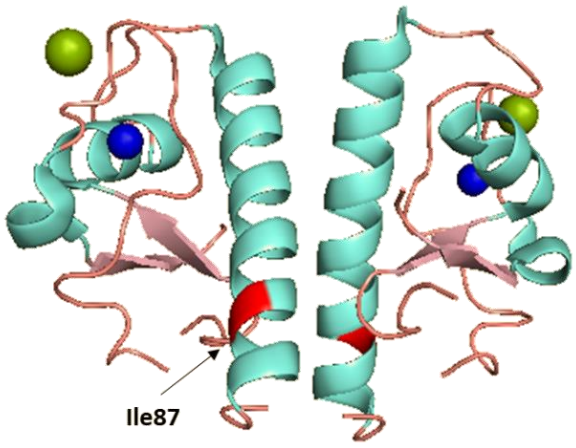

Figure 1.11 - Crystal structure of the YbcO homodimer. The residues coloured in red represent the Ile87 residue that is mutated in *ybcO*(I87M) (RCSB PDB accession code: 3G27).

E. coli MG1655 *soxR*(R20H)*ybcO*(I87M) has a missense mutation in *ybcO,* where isoleucine 87 is substituted by a methionine. As this is an uncharacterized protein, it is still uncertain how a mutation in *ybcO* can affect the tolerance of *E. coli* towards BMA and other chemicals.

2 Aims and objectives

To the best of my knowledge, no strains have been previously found with the sets of *ybcO*(I87M), *acrR*(V29G) or *acrR*(T32fs) mutations together with a *soxR*(R20H) mutation. The main goal of this project was to understand *E. coli* resistance to toxic chemicals, by studying these new mutant strains and their mutated genes, using BMA as the target molecule. Three main objectives were set:

i) Characterize genotypically and phenotypically each of the mutated genes, to understand their function and effect on BMA tolerance.

ii) Determine which stress response mechanisms are involved in BMA tolerance in *E. coli* and further evaluate their importance.

iii) Analyse the toxicity effects of other commodity chemicals, including other methacrylate esters, alcohols, alkanes and alkenes, to determine if the strains are cross-tolerant to other types of chemicals relevant to industry.

3 Materials and methods

3.1 Materials and reagents

The following reagents were purchased from Sigma-Aldrich: isopropanol, isobutanol, styrene, cyclohexane, cyclohexene, ethylcyclohexane, vinylcyclohexane, agarose, tris-acetate salt, Calcium chloride ($CaCl_2$), cobalt(II) chloride hexahydrate ($CoCl_2 \cdot 6H_2O$), potassium phosphate monobasic (KH_2PO_4), potassium hydroxide (KOH), sodium chloride (NaCl), ammonium molybdate tetrahydrate ($(NH_4)_6Mo_7O_{24} \cdot 4H_2O$), ammonium chloride ($NH_4Cl$), ethylenediaminetetraacetic acid (EDTA), D-(+)-glucose, L-arabinose, glycerol, chloramphenicol and tetracycline. The following reagents were purchased from Thermo-Fisher: n-butanol, toluene, isohexane, n-heptane, Luria broth (LB) Miller, potassium chloride (KCl), magnesium sulphate heptahydrate ($MgSO_4 \cdot 7H_2O$), manganese(II) chloride tetrahydrate ($MnCl_2 \cdot 4H_2O$), ethidium bromide.

The chemicals ethyl methacrylate, isopropyl methacrylate, 2-ethylhexyl methacrylate and n-hexyl methacrylate were purchased from TCI. Methyl methacrylate, n-propyl methacrylate, n-butyl methacrylate, isobutyl methacrylate, n-pentyl methacrylate, n-heptyl methacrylate and n-octyl methacrylate were kindly donated by Lucite International. The esters n-butyl acetate, n-butyl isovalerate and n-butyl isobutyrate were purchased from Sigma-Aldrich. All esters were >99 % pure, expect for hexyl methacrylate (>98 %), isopropyl methacrylate (>98 %), n-propyl methacrylate (>97 %), n-octyl methacrylate (>98 %), n-butyl isovalerate (>98 %) and n-butyl isobutyrate (>98 %). All MAE were stabilized with 30 to 100 ppm monomethyl ether hydroquinone (MEHQ) as inhibitor, except for ethyl methacrylate which was stabilized with hydroquinone (HQ). The carbenicillin disodium salt and kanamycin monosulphate were purchased from Melford. n-Hexane and yeast extract were purchased from Fluka. Magnesium chloride ($MgCl_2$) and zinc sulphate ($ZnSO_4$) were purchased from BDH. Ethanol, cyclooctane, copper(II) sulphate pentahydrate ($CuSO_4 \cdot 5H_2O$), ferrous sulphate heptahydrate ($FeSO_4 \cdot 7H_2O$), agar, trypticase pentone

were purchased from Honeywell Riedel-de Haën, Alfa Aesar, Acros, VWR, Oxoid, BD, respectively. All chemicals had purity between 96 % and >99 %.

Molecular biology kits were purchased either from Sigma-Aldrich (GenElute™ Bacterial Genomic DNA Kit, GenElute™ Gel Extraction Kit, GenElute™ PCR Clean-Up Kit, GenElute™ Plasmid Midiprep Kit), Qiagen (RNeasy Protect Bacteria Mini Kit) or New England Biolabs (NEBuilder® HiFi DNA Assembly Cloning Kit). Other molecular biology related reagents were purchased from Qiagen (RNAprotect Bacteria Reagent, RNaseZAP), Thermo-Fisher (Gene Ruler™ 1 Kb DNA Ladder), or New England Biolabs (Purple Gel Loading Dye - 6X). Enzymes were purchased from New England Biolabs (Q5® High-Fidelity DNA Polymerase), Sigma-Aldrich (REDTaq® ReadyMix™ PCR Reaction Mix), Thermo Scientific (RevertAid H Minus Reverse Transcriptase, RiboLock™ RNase Inhibitor) or Qiagen (RNase-Free DNase I Set).

3.1.1 Strains, plasmids and synthetic oligonucleotides

All *E. coli* MG1655 and *E. coli* BW25113 wild type (WT) or mutant strains, plasmids and synthetic oligonucleotides used in this study are listed in Table 3.1, Table 3.2 and Table 3.3, respectively. All synthetic oligonucleotides used in this work were synthesized by Integrated DNA Technologies.

Table 3.1 - Bacterial strains used in this study.

***E. coli* strains**	**Relevant genotype and Source**
E. coli MG1655 WT	Internal collection
E. coli MG1655 *soxR*(R20H)	Previous work in the lab [7]
E. coli MG1655 *soxR*(R20H)*ybcO*(I87M)	Previous work in the lab [7]
E. coli MG1655 *soxR*(R20H)*acrR*(V29G)	Previous work in the lab [7]
E. coli MG1655 *soxR*(R20H)*acrR*(T32fs)	Previous work in the lab [7]
E. coli BW25113 WT	Internal collection
E. coli BW25113 *ΔybcO::kan* (JW0537)	Keio collection [256]
E. coli BW25113 *ΔsoxR::kan* (JW4024)	Keio collection [256]
E. coli BW25113 *ΔacrR::kan* (JW0453)	Keio collection [256]
E. coli BW25113 *ΔybcO::kan*	kanR; this study
E. coli BW25113 *ΔsoxRΔacrR::kan*	kanR; this study
E. coli BW25113 *ΔsoxRΔybcO::kan*	kanR; this study
E. coli MG1655 *ΔsoxR*	Cured; this study
E. coli MG1655 *ΔsoxR::kan*	kanR; this study
E. coli MG1655 *ΔsoxR::chl*	chlR; this study

E. coli MG1655 *ΔacrR*	Cured; this study
E. coli MG1655 *ΔacrR::kan*	kanR; this study
E. coli MG1655 *ΔacrR::chl*	chlR; this study
E. coli MG1655 *ΔybcO*	kanR; this study
E. coli MG1655 *ΔsoxRΔacrR*	Cured; this study
E. coli MG1655 *ΔsoxR::kanΔacrR*	kanR; this study
E. coli MG1655 *ΔsoxRΔacrR::kan*	kanR; this study
E. coli MG1655 *ΔsoxR::kanΔacrR::chl*	kanR, chlR; this study
E. coli MG1655 *ΔsoxR::chlΔacrR::kan*	kanR, chlR; this study
E. coli MG1655 *ΔsoxRΔybcO*	Cured; this study
E. coli MG1655 *soxR(R20H)ΔacrR*	Cured; this study
E. coli MG1655 *soxR(R20H)ΔybcO*	Cured; this study
E. coli MG1655 *acrR(V29G)*	Cured; this study
E. coli MG1655 *acrR(T32fs)*	Cured; this study
E. coli MG1655 *ybcO(I87M)*	Cured; this study
E. coli MG1655 Δ*soxS*	Cured; this study
E. coli MG1655 *soxR*(R20H)-Δ*soxS*	Cured; this study
E. coli MG1655 *soxR*(R20H)*acrR*(T32fs)-Δ*soxS*	Cured; this study
E. coli MG1655 Δ*acrA*	Cured; this study
E. coli MG1655 Δ*acrB*	Cured; this study
E. coli MG1655 Δ*acrAB*	Cured; this study
E. coli MG1655 *soxR*(R20H)*acrR*(T32fs)-Δ*acrA*	Cured; this study
E. coli MG1655 *soxR*(R20H)*acrR*(T32fs)-Δ*acrB*	Cured; this study
E. coli MG1655 *soxR*(R20H)*acrR*(T32fs)-Δ*acrAB*	Cured; this study
E. coli MG1655 *ΔyjiY*	Cured; this study
E. coli MG1655 *soxR(R20H)-ΔyjiY*	Cured; this study
E. coli MG1655 *soxR(R20H)acrR(V29G)-ΔyjiY*	Cured; this study

kanR, kanamycin resistance; chlR, chloramphenicol resistance.

Table 3.2 – Plasmids used in this study.

Plasmids	**Relevant genotype and source**
pKD4	carbR, kanR [257]
pKD3	carbR, chlR [257]
pKD46	carbR [257]
pCP20	carbR [257]
pSC101	tetR; purchased from DSMZ
pSC101_*acrR*(WT)	tetR; this study
pSC101_*soxR*(WT)	tetR; this study
pSC101_*acrR*(WT)_*soxR*(WT)	tetR; this study
pSC101_*acrR*(V29G)	tetR; this study
pSC101_*acrR*(T32fs)	tetR; this study
pSC101_*soxR*(R20H)	tetR; this study
pSC101_*soxR*(R20H)_*acrR*(V29G)	tetR; this study
pSC101_*soxR*(R20H)_*acrR*(T32fs)	tetR; this study

kanR, kanamycin resistance; chlR, chloramphenicol resistance; carbR, carbenicillin resistance; tetR, tetracycline resistance.

Table 3.3 - Synthetic oligonucleotides used in this study.

Primer Name	Primer Sequence	Assay
AcrR 50bp F	5′-ACATTCACAAATGTATGTAAATCTAACGCCTGTAAATTCACGAACATATGGTGTAGGCTGGAGCTGCTTC-3′	Gene KO/KI
AcrR 50bp R	5′-CAGGAAAAATCCTGGAGTCAGATTCAGGGTTATTCGTTAGTGGCAGGATTCATATGAATATCCTCCTTAG-3′	
YbcO 50bp F	5′-TGGTTGATAAAAAATGGTTGCGACTGGCAGCAAGGAGGAGTCATGGCTGAGTGTAGGCTGGAGCTGCTTC-3′	
YbcO 50bp R	5′-AGGCCAGGGTAATGTGATGCTGTAGGTATTCACGCCTTAATAACCCCCTCCATATGAATATCCTCCTTAG-3′	
SoxR 50bp R	5′-ATTCCTCAAGTTAACTTGAGGTAAAGCGATTTATGGTGTAGGCTGGAGCTGCTTC-3′	Gene KO
SoxR 50bp R	5′-CCCTTGTGGCGCTTTAGTTTTGTTCATCTTCCAGCATATGAATATCCTCCTTAG-3′	
YjiY 50bp F	5′-TCGGCCAACTATTAATCAATACATGCCAGGTTTTACTATGGTGTAGGCTGGAGCTGCTTC-3′	
YjiY 50bp R	5′-GAAGCGGGGCTAAACACGGTTAGTGGTGCGAAGAGATCTTCATATGAATATCCTCCTTAG-3′	
AcrR knockin F	5′-GTGCTATGGTACATACATTCACAAATGTATGTAAATCTAACGCCTGTAAATTCACGAACATATGGCACG-3′	Gene KI
AcrR cass rv	5′-CTTCGAAGCAGCTCCAGCCTACACTTATTCGTTAGTGGCAGGATTAC-3′	
AcrR cass F	5′-TAATCCTGCCACTAACGAATAAGTGTAGGCTGGAGCTGCTTCG-3′	
YbcO knockin F	5′-GGTTGATAAAAAATGGTTGCGACTGGCAGCAAGGAGGAGTCATGGCTGATTTG-3′	
YbcO cass rv	5′-CGAAGCAGCTCCAGCCTACACTCACGCCTTAATAACCCCCTC-3′	
YbcO cass F	5′-GAGGGGGTTATTAAGGCGTGAGTGTAGGCTGGAGCTGCTTCGAAG-3′	
AcrR 500bp F	5′-GATTCACCGTCAATTGCGCGATATTGG-3′	Gene KO/KI validation
AcrR 500bp R	5′-ACAGCGTGCTCAGAATTTTGCGC-3′	
SoxR 500bp F	5′-GGTTCTTTGCGAAGGCGATGC-3′	
SoxR 500bp R	5′-GTCAAGATGCGTGGCGGACAATC-3′	
YbcO 500bp F	5′-GCTTTCGCATGGTGCTTAAACCG-3′	
YbcO 500bp R	5′-CCTGCTCCTGTCAGGGTTTTG G-3′	
YjiY 500bp F	5′-GATTGCTGCTGGCGAATGGTTTG-3′	
YjiY 500bp R	5′-TATTGCCCTTGTCGAGATTGTCCAGC-3′	
K1	5′-CAGTCATAGCCGAATAGCCTC-3′	
K2	5′-CGGTGCCCTGAATGAACTGC-3′	
C1	5′-TTATACGCAAGGCGACAAGG-3′	
C2	5′-GATCTTCCGTCACAGGTAGG-3′	
A1	5′-GAGCGGATTTGAACGTTTAAACCTCGAGTGTCCG-3′	Plasmid construction
A2	5′-GCAGTTCCCTACTCTCGGAGTCAGATTCAGGGTTATTC-3′	
P1	5′-CAGTTCCCTACTCTCCAGTTCATCGTGACAGAGC-3′	
P2	5′-CGGATTTGAACGTTTAGCTGATTGCCATCAACGC-3′	
T1	5′-GCTCTGTCACGATGAACTGGAG-3′	
T2	5′-GACACTCGAGGTTTAAACGTTCAAATCCGCTCCC-3′	
T3	5′-GAATCTGACTCCGAGAGTAGGGAACTGCCAGG-3′	
T4	5′-CGTTGATGGCAATCAGCTAAACG-3′	
T5	5′-CTGAAAAGAGGCAGATTTAACGTTCAAATCCGCTCCC-3′	
T6	5′-CAAAACTAAAGCGAGAGTAGGGAACTGCCAGGC-3′	
S1	5′-CGGATTTGAACGTTAAATCTGCCTCTTTTCAGTGTTCAGTTCG-3′	
S2	5′-CGCTTTAGTTTTGTTCATCTTC-3′	
S1 seq	5′-CACAGAAAAATCAGGGCAGCC-3′	Plasmid validation
S2 seq	5′-CGCAGCTTCGCTTCCTTTG-3′	
SSoxR1	5′-CGAAGGGCATACGTTAAGTGCG-3′	
SSoxR2	5′-GCAACACGCCAAACGCTTC-3′	
SAcrR1	5′-GTCACCGTGGATTCAAGAACATG-3′	
SAcrR2	5′-ACGGCGTCGATTATTGATGGAG-3′	
pykF F	5′-TCATGGTGACTATGCAGAACACGG-3′	RNA purity confirmation
pykF R	5′-CAGGACGTGAACAGATGCGGTG-3′	

3.2 General culture growth and maintenance

Depending on the purpose of the experiments, *E. coli* strains were grown in either LB medium[258] or minimal salts (MSX) medium[259]. LB medium was prepared using granulated LB Miller's broth (25g/L) dissolved in distilled water (dH_2O), which was then autoclaved or filter (0.22 µm) sterilised. MSX medium was comprised of three solutions, MSA, MSB and Vishniac trace elements[260], with a reduced concentration of $ZnSO_4$. Vishniac trace elements solution was prepared by dissolving EDTA disodium salt (50 g/L) in 800 mL dH_2O, by adding KOH pellets, then adding $ZnSO_4$ (2.2 g/L), $CaCl_2$ (5.54 g/L), $MnCl_2{\cdot}4H_2O$ (5.06 g/L), $FeSO_4{\cdot}7H_2O$ (5 g/L), $(NH_4)_6Mo_7O_{24}{\cdot}4H_2O$ (1.1 g/L), $CuSO_4{\cdot}5H_2O$ (1.57 g/L) and $CoCl_2{\cdot}6H_2O$ (1.61 g/L). The pH of the trace elements solution was then adjusted to 6 using KOH and made up to 1 L. MSA was prepared with KH_2PO_4 (6g; 6 g/L) and Vishniac trace elements solution (2 mL; 2mL/L), adjusted to pH 7 using KOH and made up to 760 mL with dH_2O. MSB was prepared by dissolving NH_4Cl (3 g; 3 g/L) and $MgSO_4{\cdot}7H_2O$ (0.4 g; 0.4 g/L) in 200 mL dH_2O. MSA and MSB were autoclaved separately and combined once cooled down. Finally, 40 mL D-glucose (from pre-sterilised stock solution) was added to a final concentration of 5 g/L, making the MSX medium made up to 1 L. To prepare LB or MSX agar plates, agar (15 g/L) was added to the media before autoclaving. Once the media was cooled down to approximately 50°C, it was poured into sterile Petri dishes, solidified and dried in a biological safety cabinet, then stored at 4°C until further use.

If necessary, antibiotics were added to either liquid or solid media, after autoclaving and cooling down. Chloramphenicol (34 µg/mL), carbenicillin (50 µg/mL), kanamycin (50 µg/mL) or tetracycline (12.5 µg/mL) were added from filter sterilised stock solutions of chloramphenicol (34 mg/mL in 100% ethanol), carbenicillin (100 mg/mL in dH_2O), kanamycin (50 mg/mL in dH_2O) and tetracycline (12 mg/mL in 100% ethanol), respectively. Aliquots of 1.5 mL antibiotics stocks were prepared and stored at -20°C.

For long-term storage of a strain, a single colony was selected from a solid LB agar plate, picked with a sterile loop and inoculated in liquid LB medium (10 mL) in 50 mL sterilized Flacon tubes. Strains were incubated at 37°C and 250 rpm, until the

exponential growth phase was reached. Samples (850 µL) were then mixed with sterile 80% (v/v) glycerol (150 µL), to a final concentration of 12 % (v/v) glycerol, and stored in cryovials at -80°C. When required, strains were streaked from the glycerol cryostocks into fresh LB or MSX agar plates and incubated overnight at 37°C.

Super optimal broth with catabolite repression (SOC) medium was used as the outgrowth media following the transformation of bacterial cells (see section 3.3.7), SOC medium was composed of yeast extract (5 g/L), trypticase peptone (20 g/L), NaCl (0.584 g/L), KCl (0.186 g/L), $MgCl_2$ (0.952 g/L), $MgSO_4$ (1.204 g/L) and glucose (3.603 g/L). The SOC medium was then sterilized and store in -20 °C until further use.

In order to perform all growth tests, in either vials, flasks or 96-well plates, inocula were firstly prepared by inoculating single colonies isolated from MSX plates into MSX medium (10 mL) in 50 mL Falcon tubes, which were then incubated overnight at 37 °C and 250 rpm.

The overnight cultures were used to inoculate 7 mL or 50 mL of MSX medium, in either 30 mL vials sealed with polypropylene screw cap with PTFE/silicone septa or 250 mL Quickfit® conical flasks sealed with sterile Suba-seals® stoppers, respectively. The initial optical density at 600nm (OD_{600nm}) of all cultures was normalised to approximately 0.05. When needed, 0.1 to 20 % (v/v) of different chemicals were added to the cultures immediately after inoculation or during mid exponential phase (OD_{600nm} of approximately 0.3). Cultures were subsequently incubated at 37 °C with 250 rpm shaking for 24 to 48 h. Samples were collected at several time points using a sterile syringe and needle after first swabbing the Suba-seals® or vial caps with 70 % isopropanol. The OD_{600nm} was determined at each time point. OD_{600nm} measurements were made with a Shimadzu UVmini-1240 spectrophotometer. When the reading was outside of a 0-0.8 range, samples were diluted in water 5 or 10 times. When possible to calculate, the specific growth rate was equivalent to the linear regression slope between time and $\ln(OD_{600nm})$ values, during the phase of maximum exponential growth, with the highest coefficient of determination.

For microplate assays, the overnight cultures were used to inoculate MSX medium (120 µL), in sterile flat-bottom polypropylene 96 well microplates (Greiner Bio-One).

The initial OD_{600nm} of all cultures was normalised to approximately 0.1. When required, 0.1 to 20 % (v/v) of different chemicals were added to the cultures immediately after inoculation. All cultures were done with 6 replicates, including blank controls with only MSX or MSX plus the chemical. The plates were sealed with polypropylene ThermalSeal A™ sealing films (Sigma-Aldrich). Cultures were then incubated for 24 h at 37 °C and 600 rpm, in a Thermo-Shaker PHMP-4 (Grant Bio). Growth curves were followed using the microplate nephelometer NEPHELOstar® (BMG Labtech). Nephelometry measurements were taken at different time points with a laser intensity of 50 % and a beam focus of 2.5 mm, with measurement time of 0.1 s per well and position delay of 0.5 s. The optical densities of the cultures was calculated using calibration curves of OD_{600nm} as a function of nephelometry units (Figure 11.7, Appendix 11.4.1, page 210).

3.3 Molecular biology methods

3.3.1 DNA extraction

To extract gDNA, *E. coli* strains were grown overnight in 10mL LB medium, in 50 mL Falcon tubes, at 37 °C and 250 rpm. Culture samples (1.5 mL) were collected and the extraction and isolation of genomic DNA (gDNA) was done using the GenElute™ Bacterial Genomic DNA Kit, according to the manufacturer's guidelines. Briefly, the cells were lysed and ethanol was added to facilitate DNA binding to the spin column, gDNA was then eluted and stored at -20°C until further use.

To extract plasmid DNA, single isolated colonies of the strains of interest were selected and were grown overnight in 250 mL shake flasks, in 100 mL LB medium supplemented with the appropriate antibiotic, at 37 °C and 250 rpm. Plasmid DNA was then extracted using the GenElute™ Plasmid Midiprep Kit, according to the manufacturer's guidelines. Briefly, the entire culture was centrifuged, the pellet resuspended, and the cells lysed. A binding solution was added to the lysate and the plasmid DNA was purified using a spin column. The eluted samples containing the plasmids were then stored at -20 °C until further use.

3.3.2 RNA extraction

E. coli cultures were grown in MSX medium (120 mL) in 250 mL Quickfit® conical flasks sealed with sterile Suba-seals® stoppers, at 37°C and 250 rpm. The first sample (50 mL) for RNA extraction was collected when an OD_{600nm} of approximately 0.3 was reached, *i.e.* mid exponential phase. Immediately after, 20 %(v/v) BMA was added to the culture and 1 h later the second sample (50 mL) for RNA extraction was collected. Cultures and subsequent total RNA extraction were done in three biological replicates. Immediately after collection, each sample was kept on ice and centrifuged for 10 min at 4 °C and 5000×g. The supernatant was discarded, the pellet was resuspended in RNAprotect Bacteria Reagent (10 mL), which provides immediate stabilization of RNA prior to extraction, and centrifuged again for 10 min at 4 °C and 5000×g. The supernatant was discarded and the pellets were stored at -80 °C until further used for the subsequent extraction process. The pellets were thawed on ice, and the RNA was then extracted with the RNeasy Protect Bacteria Mini Kit, according to the manufacturer's guidelines on the protocol for enzymatic lysis of bacteria. Briefly, cells were disrupted by enzymatic lysis, then ethanol was added to the lysate to allow binding of DNA to the spin column. After a centrifugation cycle spin column with the sample, a DNase digestion was done using the RNase-Free DNase Set, in order to avoid gDNA contamination. Samples were then washed and the eluted RNA was stored in 3 aliquots at -80 °C, until further use. Thus, all three biological replicates of a time point sample, had three aliquots of RNA extracted, to a total of 9 aliquots per time point sample. The entire procedure for the RNA extraction was done as much as possible in an RNase free environment, by cleaning all surfaces and equipment with the RNase cleaning agent RNaseZAP, and using RNase-free pipette tips, Eppendorf tubes and Falcon tubes.

One aliquot was used for subsequent polymerase chains reactions (PCR) and reverse transcription PCR (RT-PCR) reactions (see section 3.3.5), and to determine concentration and purity. To confirm that no gDNA contamination was present in the RNA samples, the house keeping gene pykF (pyruvate kinase I) was amplified from RNA, cDNA and gDNA (control sample from the respective strain) and then analysed by agarose gel electrophoresis (see section 3.3.3). If the house keeping gene, which

would be present if there was a gDNA contamination, could not be amplified from RNA samples, but could be amplified from cDNA samples, it would mean that the RNA samples were free of gDNA. Only the remaining aliquots were used for RNA sequencing, to avoid RNA degradation from thawing and freezing cycles.

3.3.3 Analysis and quantification of RNA and DNA

After extraction and purification, the concentration of plasmid DNA, gDNA or RNA was determined using a BioDrop µLite (BioDrop). The ratios of absorbance A260/280nm and A260/230nm were also analysed.

The concentration of PCR products was estimated by agarose gel electrophoresis. Agarose gels were prepared by dissolving 1 %(w/v) agarose in tris-acetate EDTA (TAE) buffer (40 mM Tris-acetate, 1 mM EDTA), using a microwave. The gel was cooled down and 1 %(v/v) ethidium bromide was added to the still warm agarose gel solution, which was then poured into the electrophoresis tank with the comb in place (Bio-Rad). After the gel was solidified, the comb was taken out and the samples (8 to 30 µL) were loaded into the wells. GeneRuler™ 1 kb Plus DNA Ladder was used as a standard. Separation was typically performed at 85 mV for 30 min using Mini-Sub® Cell GT and PowerPac™ electrophoresis systems (Bio-Rad). Gel photographs were obtained using the uGenius3 Gel Documentation System (Syngene).

3.3.4 DNA gel extraction and purification

When necessary, PCR products were purified with a gel extraction using the GenElute™ Gel Extraction Kit. Unwanted DNA fragments were separated by agarose gel electrophoresis and, as quickly as possible, the target DNA fragment was carefully excised from the agarose gel under UV light with a clean scalpel. The gel portion weight was determined, and the DNA was then extracted and purified according to the manufacturer's guidelines. Briefly, agarose gel slices were dissolved, isopropanol was added to the solubilized gel solution and the DNA was then purified using a spin

column. The concentration of the eluted DNA was determined by agarose gel electrophoresis and the DNA was then stored at -20 °C until further use.

If the PCR product was determined to be free of any other unwanted fragments, after an analysis on an agarose gel electrophoresis, the sample would purified with the GenElute™ PCR Clean-Up Kit, according to the manufacturer's guidelines. Briefly, a binding solution was added to the PCR samples, which were then then purified using a spin column. The concentration of the eluted DNA was determined using a BioDrop µLite, and the DNA was then stored at -20 °C until further use.

3.3.5 Polymerase chain reactions

To amplify genes of interest, high fidelity PCRs were performed with Q5® High-Fidelity polymerase. Reactions mixtures (50 µL) were prepared, containing dNTPs (200 µM each), forward and reverse primers (0.5 µM each), 5× Q5® reaction buffer (1×), Q5® polymerase (0.02 U/µL), DNA template (gDNA or plasmid DNA) and nuclease-free water (made up to 50 µL). Total amount of DNA for the 50 µL reaction varied between 1 ng to 1 µg for gDNA or 1 pg to 1 ng for plasmid DNA. Generally, the following thermocycling conditions were used: initial denaturation for 5 min at 98 °C, 30 cycles with 3 steps of denaturation at 98 °C for 10 s, annealing at 50–72 °C, with lowest primer melting temperature (T_m), for 30 s, and extension at 70 °C for 30 s/kb, followed by a final extension at 72 °C for 5 min.

A two step RT-PCR was performed in order to amplify housekeeping gene *pykF*, pyruvate kinase I, from total RNA samples. The first step, *i.e.* reverse transcription, was done using the RevertAid H Minus Reverse Transcriptase, which lacks RNase H activity. In a nuclease-free Eppendorf tube, and using nuclease-free tips, the reaction components were added in the following order: gene-specific primer (20 pmol), nuclease-free water (to 12.5 µL), 5X Reaction Buffer (4 µL), RiboLock™ RNase Inhibitor (1 U/µL), dNTPs (1 mM each), and RevertAid H Minus Reverse Transcriptase (10 U/µL), with a total reaction volume of 20 µL. The reaction was mixed gently, briefly centrifuged and incubated at 42 °C for 60 min. The enzymes were then inactivated by incubating the mixture at 70 °C for 10 min. Reverse transcription

reaction product was then the first strand of cDNA, which was directly used for the second step of the process, a PCR. This PCR was done with Q5® High-Fidelity polymerase, according to the protocol described previously, with 2 µL of cDNA used as the template.

To confirm the successful transformation of *E. coli* strains with either linear DNA or plasmid DNA, colony PCRs were performed with a lower fidelity DNA polymerase. The reaction mixtures (20 µL) contained REDTaq® ReadyMix™ PCR Reaction Mix (10 µL), a single colony of the transformed strain (incubated overnight in LB agar, plus antibiotic if necessary, at 30 °C or 37 °C) was resuspended in sterile dH_2O (2 µL), primers (0.75 µM each) and nuclease-free water (made up to 20 µL). The thermocycling conditions typically started with an initial denaturation at 94 °C for 5 min, 30 cycles with 3 steps of denaturation at 94 °C for 30 s, annealing at 55 °C for 30 s and extension at 72 °C for 1 min/kb, followed by a final extension at 72 °C for 5 min.

3.3.6 Plasmid construction

All plasmids were constructed using the NEBuilder® HiFi DNA Assembly Cloning Kit. With this method it was possible to, in one step, clone up to four DNA fragments with overlapping regions (20 to 35 bp) between them. All DNA fragments used for the assembly were firstly purified by agarose gel electrophoresis (see section 3.3.3), to guarantee high purity. Additionally, when the DNA fragments used for the assembly were amplified from plasmid templates, samples were digested with DpnI (10 U/µL), to digest any plasmid template left, and incubated at 37 °C for 1 h. The optimal amount for each DNA fragment was calculated according to the number and size of fragments used for each assembly, as recommended by the guidelines of the cloning kit. NEBuilder HiFi DNA Assembly Master Mix (10 µL) and nuclease-free water (made up to 20 µL) were then also added to the reaction mix. Immediately after, the mixtures were incubated at 50 °C for 1 h and then stored at -20 °C until further use.

3.3.7 Transformation of bacterial cells

E. coli strains were transformed by electroporation with either linear DNA, for the homologous recombination method (see section 3.3.8), or plasmid DNA. To prepare *E. coli* electrocompetent cells, strains were grown to an OD_{600nm} of 0.6-0.8 in 100 mL LB medium, in 250 mL shake flasks, supplemented with an antibiotic if necessary, at 250 rpm and either 30 °C or 37 °C, depending if temperature sensitive plasmids were used or not. The cultures were then transferred into ice cold sterile 50 mL Falcon tubes and centrifuged at 4000 rpm for 10 min at 4 °C. The supernatant was carefully discarded, and the pellet was resuspended and washed with ice could sterile water in 3 cycles of centrifugation at 4000 rpm for 10 min at 4 °C. The last wash was done with sterile 20 % (v/v) glycerol (10 mL) and centrifugation at 4000 rpm for 10 min at 4 °C. The obtained loose pellet was then dispensed into 50 µL aliquots and kept on ice or stored at -20 °C until further use.

To transform electrocompetent competent cells, a plasmid sample (approximately 50 ng) or linear DNA fragment (approximately 500 ng) was added to the electrocompetent cells (50 µL) in a pre-chilled 2 mm electroporation cuvette, and electroporation was performed at 2.5 kV, 200 Ω and 25 µF, using a GenePulser Xcell™ electroporation system (Bio-Rad). Immediately after, sterilised SOC medium (950 µL) was added to the electroporation cuvette. The samples were then transferred into sterile Eppendorf tubes and incubated at for 45 min or 120 min, for plasmid or linear DNA transformations, respectively, at 250 rpm and 37 °C or 30 °C, depending if temperature sensitive plasmids were used or not. Subsequently, the samples were plated in LB agar plates, supplemented with an antibiotic if necessary, and incubated overnight at 37 °C or 30 °C. Positive colonies were then confirmed by colony PCR (see section 3.3.5) and the region of interest sequenced (see section 3.4.1). Cryostocks were prepared and stored at -80 °C, until further use.

When plasmids were constructed using the NEBuilder® HiFi DNA Assembly Cloning Kit, before they were transformed into the strain of interest, they had to first be transformed into high efficiency NEB 5-alpha competent *E. coli* cells, provided in the NEBuilder® HiFi DNA Assembly Cloning Kit. The chemically-competent cells were

thawed on ice for 5 min and the assembled plasmid was added. The sample was gently mixed by pipetting up and down, incubated on ice for 30 min, then heated at 42 °C for 30 s and again incubated on ice for 2 min. Afterwards, SOC medium (950 µL) was added and the samples were incubated for 1 h at 37 °C and 250 rpm. Cells were then spread onto LB agar plates supplemented with the appropriate antibiotic and incubated overnight at 37 °C. Positive colonies were then confirmed by colony PCR (see section 3.3.5). The obtained plasmids were then extracted from *E. coli* NEB 5-alpha, sequenced and reintroduced in the strain of interest by electroporation. Cryostocks were prepared and stored at -80°C, until further use.

3.3.8 Homologous recombination

Homologous recombination was performed to delete (knock-out, KO) or insert (knock-in, KI) genes using the system known as the λ red recombination[257]. In this method, the λ red proteins required for the homologous recombination are regulated by an arabinose promoter (P_{BAD}) and encoded in the plasmid pKD46, which is temperature sensitive and has ampicillin resistance. The plasmids pKD3 and pKD4, which have ampicillin resistance but also the chloramphenicol and kanamycin resistance cassettes, respectively, were used has the source of antibiotic resistance cassettes. To do the KO, the antibiotic resistance cassettes were amplified using plasmids with flanking regions (25-35 bp) homologous to the flanking region of the gene to be deleted. To prepare the linear DNA for the KI, an overlap extension PCR was used to combine a fragment containing the gene of interest together with an antibiotic resistance cassette. This longer fragment was amplified with a flanking region homologous to the chromosome region where it would be inserted. All DNA fragments used for homologous recombination were gel purified (see section 3.3.3) and stored at -20 °C until further use.

As the first step of homologous recombination, pKD46 was transformed by electroporation into the strain where a gene was to be deleted or inserted. A single colony was selected and grown overnight in 50 mL Falcon tubes, in 10 mL LB medium supplemented with carbenicillin (50 µg/mL), at 30 °C with 250 rpm shaking. This

culture was then used to inoculate a larger culture of 100 mL LB medium supplemented with carbenicillin (50 µg/mL) and arabinose (10 mg/mL), where the λ red proteins were expressed. The culture was grown in 250 mL shake flasks and incubated at 30 °C and 120 rpm, until an OD_{600nm} of 0.6 to 0.8 was reached. This culture, which had the λ red proteins expressed, was then used to prepare electrocompetent cells, where the linear DNA necessary for the KO or KI was transformed into, by electroporation. Positive colonies, grown in LB plates supplemented with kanamycin or chloramphenicol, were then selected by colony PCR (see section 3.3.5) and sequenced. If required, the antibiotic resistance cassette was then cured. This was possible because the resistance cassettes are flanked by flippase (FLP) recombinase recognition target sites (FRT), which allow the cassettes to be removed with the FLP recombinase, encoded by the temperature sensitive plasmid pCP20, which also has ampicillin resistance. Thus, KO or KI strains were transformed by electroporation with pCP20. Positive colonies with the eliminated cassettes were selected on agar plates containing only LB medium and confirmed by colony PCR. For each step of the homologous recombination method, cryostocks were prepared and stored at -80 °C until further use.

3.4 Nucleotide sequencing

3.4.1 DNA sequencing

Plasmid and linear DNA sequencing was performed by Eurofins Genomics. Purified DNA samples (15 µL) were used at a concentration of 5-10 ng/µL or 50-100 ng/µL for linear or plasmid DNA, respectively. Primers (1.2 µM) were added to the samples to make up a total volume of 17 µL.

3.4.2 RNA sequencing

RNA sequencing was performed at the Next Generation Sequencing (NGS) Facility, located at the University of Nottingham. Sample preparation was done by Dr. Sunir

Malla. At the NGS Facility, total RNA quality was assessed using the Agilent RNA 6000 Nano Kit (Agilent Tecnologies, 5067-1511) on the Agilent 2100 Bioanalyzer. Total RNA concentration was measured using Qubit RNA BR assay kit (Life technologies, Q10210). 1µg of Total RNA was used for rRNA depletion using Ribo-Zero rRNA Removal Kit (Illumina, MRZMB126). Illumina stranded whole transcriptome sequencing libraries were prepared using NEBNext Ultra Directional RNA library prep kit for Illumina (NEB, E7420S). Dual Index Primers Set 1 was used to generate barcoded multiplex libraries (NEB, E7600S). Library QC was performed using bioanalyser HS kit (Agilent biotechnologies, 5067-4626). Libraries were quantified using qPCR (Kapa Biosystems, KK4824). Equimolar library pool was loaded for sequencing according to manufacturer's instructions. Lastly, sequencing was performed on the Illumina NextSeq500 sequencing platform to generate 2 x 75bp paired end reads.

3.4.3 Bioinformatics

The key bioinformatic analysis to determine differentially expressed genes was done at NGS Facility, by Dr. Daniel Zadik. The raw fastq files for each sample for each direction, but different lanes were concatenated, which were then adaptor trimmed using Trimmomatic. The trimmed reads were assessed using the FastQC read analysis tool. To filter tRNA and rRNA, reads were mapped to the tRNA and rRNA only FASTA file using TopHat. These unmapped reads were then mapped against the reference genome, using the mRNA GTF file to limit initial mapping to those genes, using TopHat. Reads that mapped to multiple positions in the genome and those which did not map to correct positions relative to their partner read were then filtered out using AWK based on the mapping flags assigned by TopHat. The number of reads with a mapping quality of ≥ 20 mapped to each gene from the filtered BAM file was counted using SAMtools. Reads Per Kilobase of transcript per Million mapped reads (RPKMs) were generated from the counts file with a bespoke Perl script. The read count files for all samples were merged into matrix using a bespoke Perl script. Differential expression analysis was done in R, using DESeq2.

3.4.3.1 Gene Ontology analysis

After obtaining the raw bioinformatics date, I did a functional enrichment analysis of gene ontology (GO) terms for Biological Processes, using the CytoScape v3.7.1 pluggin ClueGO v2.5.4[261]. Over-represented Biological Process terms were determined based on a two-sided hypergeometric statistical test, with a Bonferroni step-down p-value correction and a kappa score of 0.4. Only GO terms with p-values < 0.05 were considered as statistically significant.

Heatmaps were generated using the web-based software Morpheus (https://software.broadinstitute.org/morpheus/). Venn diagrams were generated using the InteractiVenn tool[262].

4 Characterization of *E. coli* mutants tolerant to BMA

Before the start of this project, four different *E. coli* MG1655 mutant strains, which were able to grow in the presence of 20 %(v/v) BMA, were isolated[7]. It was essential to characterize these new strains and understand how the level of tolerance of *E. coli* MG1655 *soxR*(R20H), *E. coli* MG1655 *soxR*(R20H)*ybcO*(I87M), *E. coli* MG1655 *soxR*(R20H)*acrR*(V29G) and *E. coli* MG1655 *soxR*(R20H)*acrR*(T32fs) was compared to the wild type (WT) strain and analyse the differences in growth profiles between each combination of mutations. Most importantly, it was also crucial to establish if these strains could potentially be used as robust hosts for a viable bioproduction of MAE.

4.1 Effect of BMA on the growth behaviour of *E. coli* mutants

To investigate the effect of the mutations in conferring tolerance to BMA, mutant and wild type strains were grown in the presence or absence of 20 %(v/v) BMA and compared. BMA was either added immediately after inoculation or during the exponential phase.

4.1.1 Addition of BMA immediately after inoculation

Firstly, *E. coli* MG1655 WT, *E. coli* MG1655 *soxR*(R20H), *E. coli* MG1655 *soxR*(R20H)*ybcO*(I87M), *E. coli* MG1655 *soxR*(R20H)*acrR*(V29G) and *E. coli* MG1655 *soxR*(R20H)*acrR*(T32fs) were grown in the absence or presence of 20 %(v/v) BMA added immediately after inoculation (Figure 4.1 and Table 4.1). Without the addition of BMA, all mutant strains had similar growth rates as the WT, which had a growth rate of 0.65 ± 0.02 h^{-1}. However, in the absence of BMA *E. coli* MG1655 *soxR*(R20H)*acrR*(V29G) had a lower maximum OD and an apparent slower initial growth (Figure 4.1 C and Table 4.1). In the presence of 20 %(v/v) BMA, the different strains tested showed different levels of tolerance. As expected, the WT strain did not grow at all (Figure 4.1 E), even after 28h of culture, whereas all four mutant strains grew. This confirms that the mutations contribute to the resistance to BMA

and that the normal resistance mechanisms induced upon exposure to chemicals stress are not enough for wild type *E. coli* to survive.

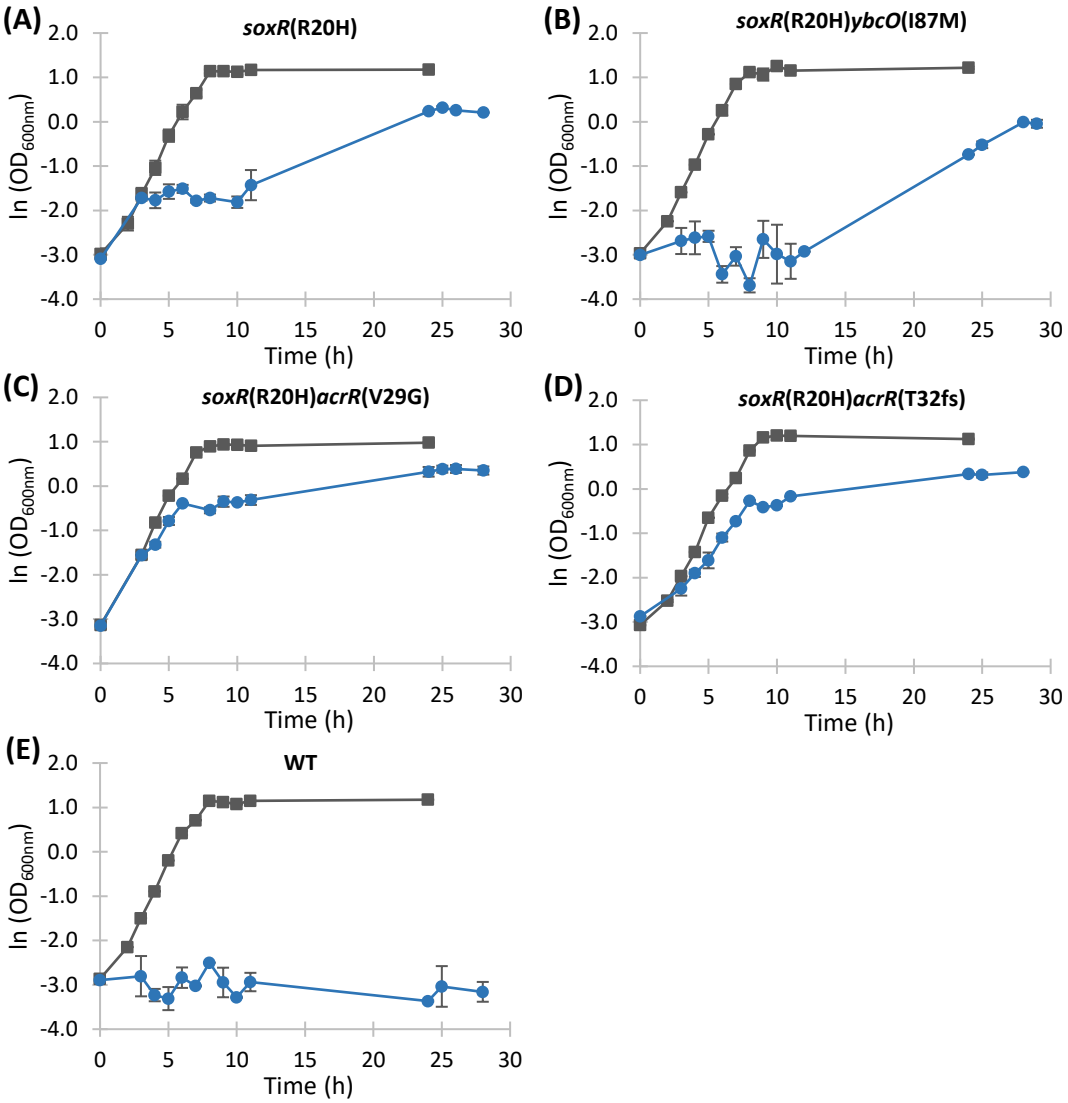

Figure 4.1 - Effect of BMA, added immediately after inoculation, on the growth of *E. coli* MG1655 strains. *E. coli* MG1655 *soxR*(R20H) (A), *E. coli* MG1655 *soxR*(R20H)*ybcO*(I87M) (B), *E. coli* MG1655 *soxR*(R20H)*acrR*(V29G) (C), *E. coli* MG1655 *soxR*(R20H)*acrR*(T32fs) (D) and *E. coli* MG1655 WT (E) were grown in MSX medium in the absence [■] or presence [●] of 20 %(v/v) BMA, in 250 mL shake flasks at 37°C and 250 rpm shaking. BMA was added immediately after inoculation. Means of two replicates are shown and error bars represent standard deviations.

In the presence of 20 %(v/v) BMA, the strains without *acrR* mutations, *E. coli* MG1655 *soxR*(R20H) (Figure 4.1 A) and *E. coli* MG1655 *soxR*(R20H)*ybcO*(I87M) (Figure 4.1 B) took a longer time to reach an high OD_{600nm}, with lag phases of at least 11 h. While *E. coli* MG1655 *soxR*(R20H)*acrR*(V29G) (Figure 4.1 C) and *E. coli* MG1655 *soxR*(R20H)*acrR*(T32fs) (Figure 4.1 D) had no lag phase when grown in the presence

of BMA and were able to reach growth rates of 0.46 ± 0.05 h^{-1} and 0.42 ± 0.04 h^{-1}, respectively. Nevertheless, it must be noted that although all mutant strains were able to grow in the presence of BMA, the maximum OD_{600nm} was decreased by at least 45 %, compared to when the same strains were grown in the absence of BMA, and the specific growth rate was up to one third lower (Table 4.1).

Table 4.1 - Effect of BMA on maximum OD_{600nm} and specific growth rate of *E. coli* MG1655 strains. All strains were grown in MSX medium in the absence or presence of 20 %(v/v) BMA, in 250 mL shake flasks at 37°C and 250 rpm. BMA was added immediately after inoculation. Means of three replicates and standard deviations are shown. All specific growth rates had p-values lower than 0.05. Values with n/a were not possible to determine, due to slow growth. NG: no growth.

	0 %(v/v) BMA		**20 %(v/v) BMA**	
***E. coli* MG1655 strains**	**Max OD_{600nm}**	**μ (h^{-1})**	**Max OD_{600nm}**	**μ (h^{-1})**
WT	3.24 ± 0.03	0.65 ± 0.02	NG	
soxR(R20H)	3.24 ± 0.03	0.64 ± 0.03	1.38 ± 0.04	n/a
soxR(R20H)*ybcO*(I87M)	3.51 ± 0.04	0.62 ± 0.03	0.99 ± 0.00	n/a
soxR(R20H)*acrR*(V29G)	2.66 ± 0.03	0.56 ± 0.04	1.47 ± 0.12	0.46 ± 0.05
soxR(R20H)*acrR*(T32fs)	3.33 ± 0.08	0.61 ± 0.05	1.46 ± 0.02	0.42 ± 0.04

The final concentration of BMA present in the shake flasks was not analytically quantified to confirm that the BMA did not evaporate, *i.e.* that the concentration of BMA was maintained constant at 20 %(v/v) throughout the experiments. However, it should be noted that after 24 h of incubation, a clear BMA phase was still observed in the shake flasks, whether the strains grew (Figure 4.2 B) or not (Figure 4.2 A). This suggests that the BMA concentration was always high and possibly maintained at 20 %(v/v), assuring that the toxic effects were induced on the cells until the end of the experiments.

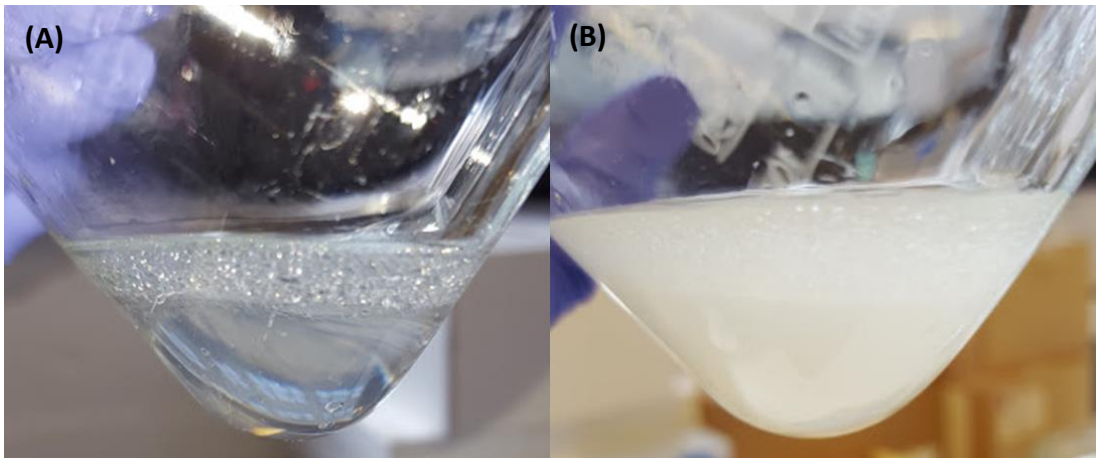

Figure 4.2 – Appearance of *E. coli* MG1655 cultures incubated in the presence of BMA for 24 h. *E. coli* MG1655 WT (A) and an *E. coli* MG1655 mutant strain (B) were grown in MSX medium in presence of 20 %(v/v) BMA, in 250 mL shake flasks, at 37 °C and 250 rpm shaking. BMA was added immediately inoculation and pictures were taken after 24 h of incubation.

Nevertheless, the combination of both *soxR* and *acrR* mutations improved tolerance to 20 %(v/v) BMA compared to the *soxR* mutation alone, or *soxR* plus *ybcO* mutations. In addition, since both strains with *soxR* and *acrR* mutations had similar growth rates and maximum OD_{600nm} in the presence of BMA, it is possible that the truncated AcrR may help to improve tolerance to BMA at the same level as the missense mutated AcrR, whether these proteins are functional or not.

4.1.2 Addition of BMA during exponential phase

Following the initial tests, a different strategy was used to characterize the growth behaviour the mutant strains, where 20 %(v/v) BMA was added during mid exponential phase. In this case, the concentration of BMA per cell would be much lower than when added immediately after inoculation, potentially allowing the cells to easily adapt to the new environment. Therefore, it would be possible to know if the different mutants would still show different levels of BMA resistance. *E. coli* MG1655 WT, *E. coli* MG1655 *soxR*(R20H), *E. coli* MG1655 *soxR*(R20H)*ybcO*(I87M), *E. coli* MG1655 *soxR*(R20H)*acrR*(V29G) and *E. coli* MG1655 *soxR*(R20H)*acrR*(T32fs) were grown in MSX medium and 20 %(v/v) BMA was added at an OD_{600nm} of approximately 0.3 (Figure 4.3 and Table 4.2).

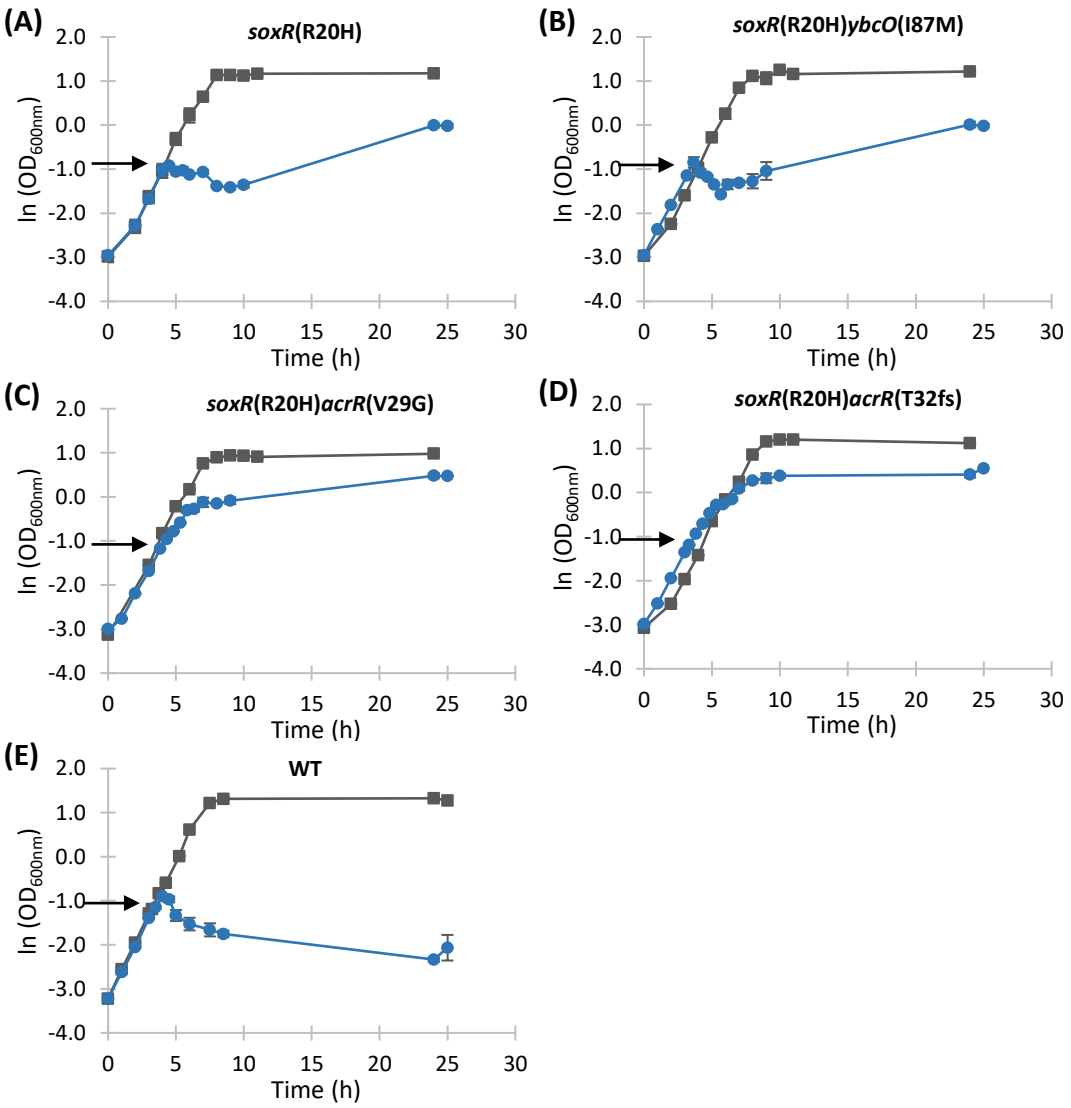

Figure 4.3 - Effect of BMA, added during mid exponential phase, on the growth of *E. coli* MG1655 mutant strains. *E. coli* MG1655 *soxR*(R20H) (A), *E. coli* MG1655 *soxR*(R20H)*ybcO*(I87M) (B), *E. coli* MG1655 *soxR*(R20H)*acrR*(V29G) (C), *E. coli* MG1655 *soxR*(R20H)*acrR*(T32fs) (D) and *E. coli* MG1655 WT (E) were grown in MSX medium in the absence [■] or presence [●] of 20 %(v/v) BMA, in 250 mL shake flasks at 37°C and 250 rpm. BMA was added after reaching an OD_{600nm} of approximately 0.3 (arrows). Means of three replicates are shown and error bars represent standard deviations.

Before the BMA addition, all strains were able to grow, having similar growth rates (Figure 4.3), comparable with the previous tests done in the absence of BMA (Figure 4.1). However, after the BMA addition during mid exponential phase, the strains tested had different behaviours. BMA inhibited the growth of *E. coli* MG1655 WT, as the OD_{600nm} started to decrease after its addition (Figure 4.3 E). When WT cells were observed under the microscope, after the addition of BMA there was a loss of cell motility, compared to before the addition. This showed once more that the WT strain

was not resistant to 20 %(v/v) BMA. On the other hand, *E. coli* MG1655 *soxR*(R20H) (Figure 4.3 A) and *E. coli* MG1655 *soxR*(R20H)*ybcO*(I87M) (Figure 4.3 B) had growth inhibition after BMA addition and stopped growing for at least 5 h, also showing a loss of motility under the microscope However, both *E. coli* MG1655 *soxR*(R20H) and *E. coli* MG1655 *soxR*(R20H)*ybcO*(I87M) were eventually able to adapt and grow, reaching a final OD_{600nm} of 0.98 ± 0.06 and 0.98 ± 0.04, respectively.

Table 4.2 - Effect of the addition of BMA during mid-exponential phase on growth rate and OD_{600nm} of *E. coli* strains. Strains were grown in MSX medium in in 250 mL shake flasks, at 37°C and 250 rpm. 20 %(v/v) BMA was added after reaching an OD_{600nm} of approximately 0.3. Means of three replicates and standard deviations are shown. All specific growth rates had p-values lower than 0.05. Values with n/a were not possible to determine, due to slow growth.

***E. coli* MG1655 strain**	**μ (h^{-1}) before addition**	**μ (h^{-1}) after addition**	**OD (9 h)**	**OD (25 h)**
WT	0.61 ± 0.03	n/a	0.17 ± 0.01	0.13 ± 0.04
soxR(R20H)	0.63 ± 0.03	n/a	0.24 ± 0.01	0.98 ± 0.05
soxR(R20H)*ybcO*(I87M)	0.57 ± 0.01	n/a	0.35 ± 0.07	0.98 ± 0.03
soxR(R20H)*acrR*(V29G)	0.56 ± 0.04	0.42 ± 0.05	0.92 ± 0.07	1.61 ± 0.01
soxR(R20H)*acrR*(T32fs)	0.55 ± 0.03	0.28 ± 0.05	1.38 ± 0.15	1.73 ± 0.16

By contrast, *E. coli* MG1655 *soxR*(R20H)*acrR*(V29G) (Figure 4.3 C) and *E. coli* MG1655 *soxR*(R20H)*acrR*(T32fs) (Figure 4.3 D), were able to continue to grow after addition of 20 %(v/v) BMA. Yet, after the addition of BMA, *E. coli* MG1655 *soxR*(R20H)*acrR*(V29) and *E. coli* MG1655 *soxR*(R20H)*acrR*(T32fs) had growth rates of 0.42 ± 0.05 h^{-1} and 0.28 ± 0.05 h^{-1}, respectively. This corresponded to a decrease of 25 to 50 % on the growth rate, compared to the growth rates obtained before the addition of BMA. Furthermore, the strains with both *soxR* and *acrR* mutations, *E. coli* MG1655 *soxR*(R20H)*acrR*(V29) and *E. coli* MG1655 *soxR*(R20H)*acrR*(T32fs), reached a final OD_{600nm} of 1.61 ± 0.01 and 1.73 ± 0.16, respectively, at least 1.6-fold higher than the other mutant strains, *E. coli* MG1655 *soxR*(R20H) (Figure 4.3 A) and *E. coli* MG1655 *soxR*(R20H)*ybcO*(I87M). These results illustrated, once again, that the mutated genes *acrR*(V29G) and *acrR*(T32fs) in combination with *soxR*(R20H) improved the adaptation of the cells and conferred further tolerance to BMA than the *soxR*(R20H) mutation alone. Moreover, *ybcO*(I87M) did not seem to confer any

additional tolerance to BMA in *E. coli*, above and beyond the tolerance already observed in the mutant strain with just the mutated gene *soxR*(R20H).

4.2 Toxicity of other commodity chemicals towards *E. coli*

The mutant strains found had improved tolerance to 20 %(v/v) BMA, compared to the WT strain. However, different MAE can be used as precursors for a sustainable production of PMMA. Even though BMA already proved to be a good candidate, the mutant strains might also have resistance to other relevant MAE, which might be more suitable for bio-based production of PMMA. Furthermore, the toxicity of the alcohols which are used as substrates for converting methacrylyl-CoA into a MAE by an alcohol acyl transferase, is also a crucial factor to take into consideration, as well as the toxicity of the other esters generated as co-products during the fermentation process. In addition, *E. coli* strains were also tested against other groups of chemicals, namely alkanes and alkenes, to determine if there was further cross-tolerance between different commodity chemicals.

The mutant strains with *acrR* and *soxR* mutations, *E. coli* MG1655 *soxR*(R20H)*acrR*(V29) and *E. coli* MG1655 *soxR*(R20H)*acrR*(T32fs), had higher tolerance to BMA than the other mutant strains (see Figure 4.1 and Figure 4.3). Hence, one of these strains, *E. coli* MG1655 *soxR*(R20H)*acrR*(T32fs), was used for the following assays, alongside with the WT as a control.

A high-throughput method was developed to carry out the toxicity tests in 96-well microplates (see Appendix 11.4.1, page 207). Instead of the standard polystyrene 96-well microplates, polypropylene microplates where used to ensure the chemicals tested would not react with the plastic material. Furthermore, polypropylene microplates the sealed with polypropylene ThermalSeal A™ sealing films, to avoid evaporation and possible cross-contamination of chemical gas phases between wells, compared to the commonly used polystyrene lids.

4.2.1 Esters

4.2.1.1 Methacrylate esters

In addition to BMA, ten other MAE were tested for their toxicity towards *E. coli*, namely methyl methacrylate, ethyl methacrylate, n-propyl methacrylate, isopropyl methacrylate, isobutyl methacrylate, n-pentyl methacrylate, 2-ethylhexyl methacrylate, n-hexyl methacrylate, n-heptyl methacrylate and n-octyl methacrylate (Figure 4.4). Both *E. coli* MG1655 WT and *E. coli* MG1655 *soxR*(R20H)*acrR*(T32fs) were grown in the presence of MAE at concentrations ranging from 0.1 to 20 %(v/v), added immediately after inoculation (Figure 4.5 and Figure 4.6; and Table 11.2, in Appendix 11.4, page 203).

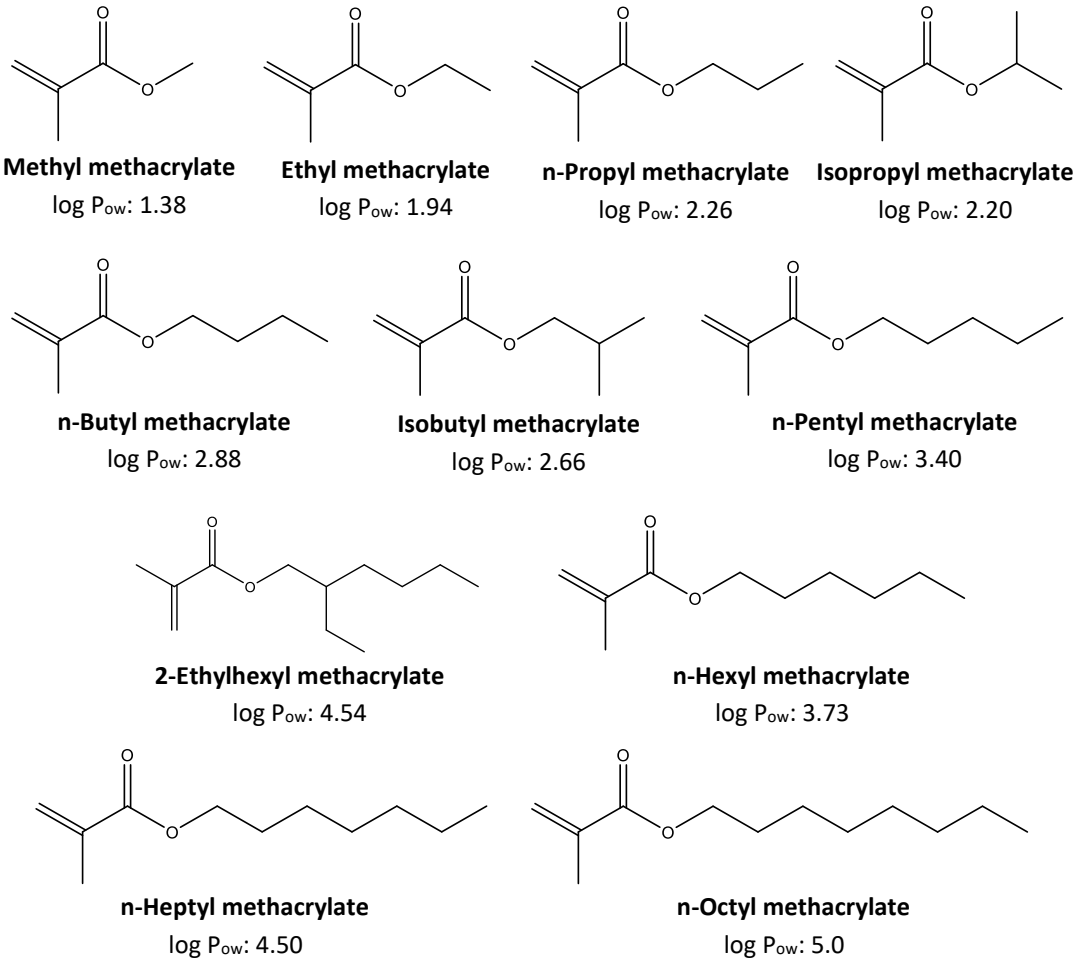

Figure 4.4 - Chemical structure and respective log P_{ow} values of several methacrylate esters.

Both *E. coli* MG1655 WT and *E. coli* MG1655 *soxR*(R20H)*acrR*(T32fs), could grow in the presence of 20 %(v/v) n-pentyl methacrylate , 2-ethylhexyl methacrylate, n-hexyl methacrylate , n-heptyl methacrylate and n-octyl methacrylate , with similar growth profiles as the control with no added chemical (Figure 4.5). Thus, these five MAE did not have toxic effects towards either the WT strain or the mutant strain, when added extracellularly. For this reason, these esters were not tested at lower concentrations.

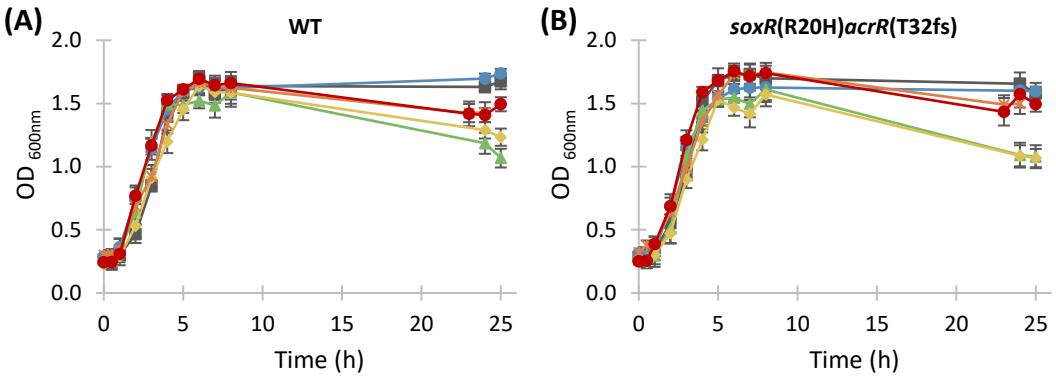

Figure 4.5 - Effect of higher MAE on the growth of *E. coli* MG1655 strains. *E. coli* MG1655 WT (A) and *E. coli* MG1655 *soxR*(R20H)*acrR*(T32fs) (B) were grown in MSX medium in the absence [■] or presence of 20 %(v/v) n-pentyl methacrylate [●], 2-ethylhexyl methacrylate [▲], n-hexyl methacrylate [◆], n-heptyl methacrylate [*] and n-octyl methacrylate [●], added immediately after inoculation. All strains were grown in 96-well microplates at 37°C and 600 rpm. Means of six replicates are shown and error bars represent standard deviations. Growth parameters are shown in Appendix 11.4, Table 11.2, page 203.

In contrast, methyl methacrylate, ethyl methacrylate, n-propyl methacrylate, isopropyl methacrylate, BMA and isobutyl methacrylate showed largely different toxicity effects on the cells (Figure 4.6 and Figure 4.7; and Table 11.2 in Appendix 11.4, page 203). In the presence of ethyl methacrylate and methyl methacrylate, the most toxic of the MAE tested, the WT strain proved to be slightly more resistant than the mutant strain *E. coli* MG1655 *soxR*(R20H)*acrR*(T32fs) (Figure 4.6 A, B, C and D). Still, both strains did not grow in the presence of 1 and 20 %(v/v) methyl methacrylate (Figure 4.6 A and B) or 20 %(v/v) ethyl methacrylate (Figure 4.6 C and D).

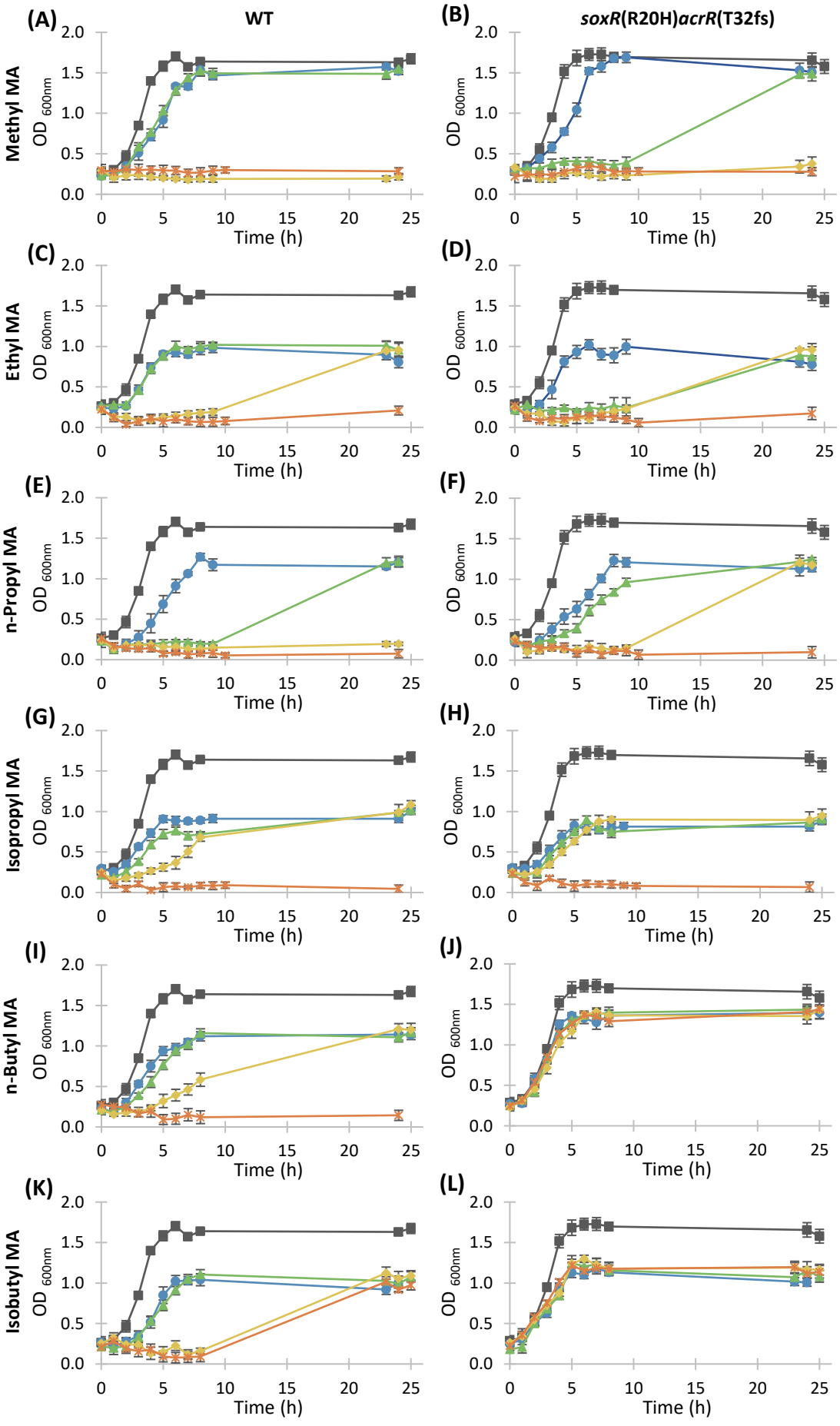
(A)
WT
(B)
soxR(R20H)acrR(T32fs)
Methyl MA
Ethyl MA
n-Propyl MA
Isopropyl MA
n-Butyl MA
Isobutyl MA
OD 600nm
Time (h)
(C)
(D)
(E)
(F)
(G)
(H)
(I)
(J)
(K)
(L)

Figure 4.6 - Effect of lower MAE on the growth of *E. coli* MG1655 strains. *E. coli* MG1655 WT (A, C, E, G, I and K) and *E. coli* MG1655 *soxR*(R20H)*acrR*(T32fs) (B, D, F, H, J and L) were grown in MSX medium in the absence [■] or presence of methyl methacrylate (A and B), ethyl methacrylate (C and D), n-propyl methacrylate (E and F), isopropyl methacrylate (G and H), BMA (I and J) and isobutyl methacrylate (K and L), added immediately after inoculation, at concentrations of 0.1 %(v/v) [●], 0.5 %(v/v) [▲], 1 %(v/v) [◆] and 20 %(v/v) [*]. All strains were grown in 96-well microplates at 37°C and 600 rpm. Means of six replicates are shown and error bars represent standard deviations. Growth parameters are shown in Appendix 11.4, Table 11.2, page 203.

E. coli MG1655 WT and *E. coli* MG1655 *soxR*(R20H)*acrR*(T32fs) did grow in the presence of up to 0.5 %(v/v) methyl methacrylate, reaching similar maximum OD_{600nm} as the control with no chemical addition (Figure 4.6 A and B), although *E. coli* MG1655 *soxR*(R20H)*acrR*(T32fs) could only grow after a lag phase of at least 9 h. By contrast, *E. coli* MG1655 WT and *E. coli* MG1655 *soxR*(R20H)*acrR*(T32fs) did grow in the presence of up to 1 %(v/v) ethyl methacrylate, though in some cases with long lag phases, but had similar maximum OD_{600nm} at all concentrations (Figure 4.6 C and D).

E. coli MG1655 *soxR*(R20H)*acrR*(T32fs) was able to survive in up to 20 %(v/v) BMA (Figure 4.6 J), as expected, but also in up to 20 %(v/v) isobutyl methacrylate (Figure 4.6 L), with similar maximum OD_{600nm} reached at all concentrations tested of each ester (Figure 4.7 J and L). Still, *E. coli* MG1655 *soxR*(R20H)*acrR*(T32fs) had higher growth rates and maximum OD_{600nm} in the presence of BMA than in the presence of isobutyl methacrylate, at all concentrations tested. However, there was a slight decrease in growth rates of *E. coli* MG1655 *soxR*(R20H)*acrR*(T32fs) with the increase of concentration of BMA (Figure 4.7 K). On the other hand, *E. coli* MG1655 WT could grow in the presence of up to 1 %(v/v) BMA (Figure 4.6 I), with a significant decrease in growth rates with the increasing concentration of BMA (Figure 4.7 K). Additionally, *E. coli* MG1655 WT could grow in the presence of up to 20 %(v/v) isobutyl methacrylate, although with lag phases of at least 8 h in the presence of 1 and 20 %(v/v) isobutyl methacrylate (Figure 4.6 K).

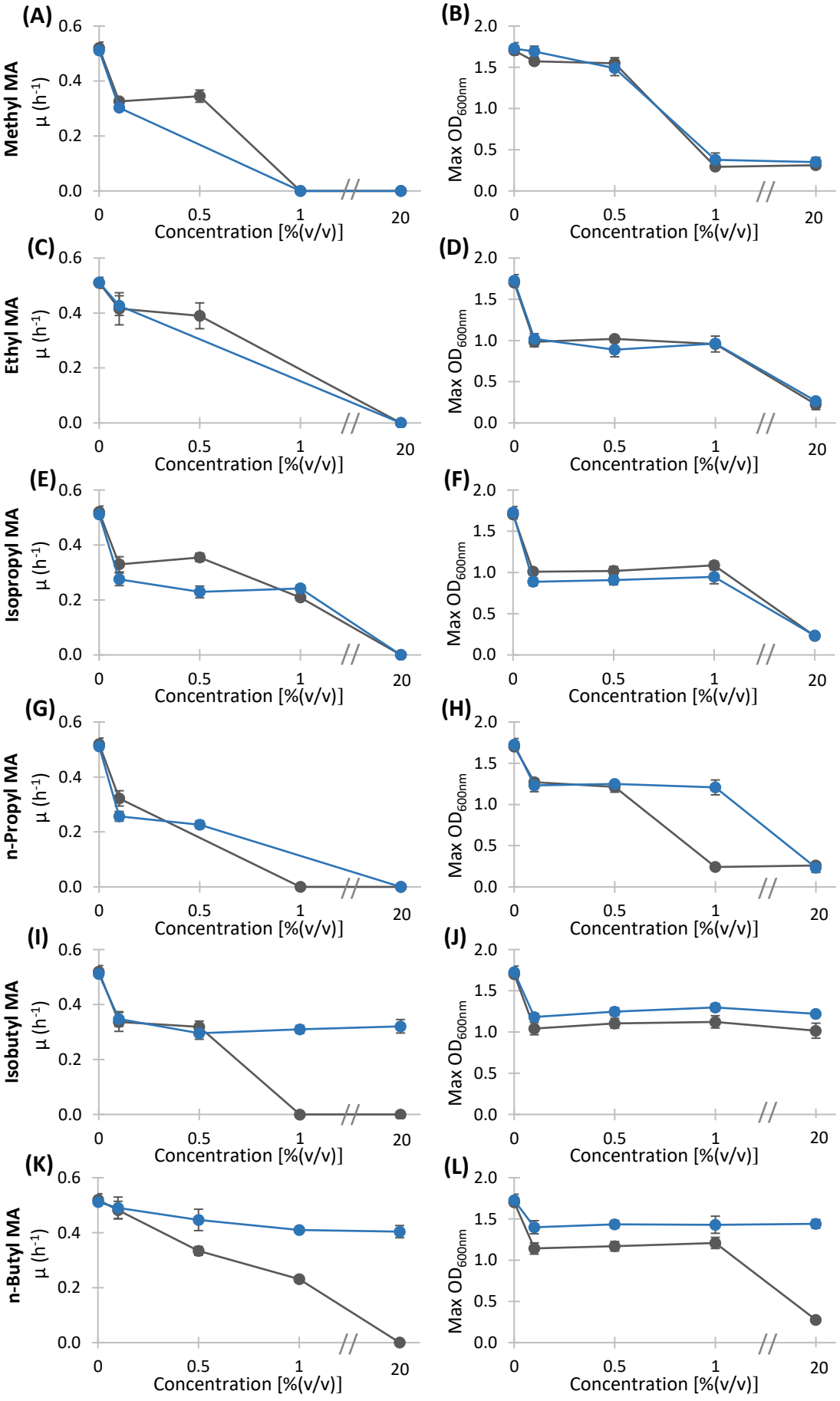
(A)
Methyl MA
μ (h-1)
0.6
0.4
0.2
0.0
0
0.5
1
20
Concentration [%(v/v)]
(B)
Max OD600nm
2.0
1.5
1.0
0.5
0.0
0
0.5
1
20
Concentration [%(v/v)]
(C)
Ethyl MA
μ (h-1)
0.6
0.4
0.2
0.0
0
0.5
1
20
Concentration [%(v/v)]
(D)
Max OD600nm
2.0
1.5
1.0
0.5
0.0
0
0.5
1
20
Concentration [%(v/v)]
(E)
Isopropyl MA
μ (h-1)
0.6
0.4
0.2
0.0
0
0.5
1
20
Concentration [%(v/v)]
(F)
Max OD600nm
2.0
1.5
1.0
0.5
0.0
0
0.5
1
20
Concentration [%(v/v)]
(G)
n-Propyl MA
μ (h-1)
0.6
0.4
0.2
0.0
0
0.5
1
20
Concentration [%(v/v)]
(H)
Max OD600nm
2.0
1.5
1.0
0.5
0.0
0
0.5
1
20
Concentration [%(v/v)]
(I)
Isobutyl MA
μ (h-1)
0.6
0.4
0.2
0.0
0
0.5
1
20
Concentration [%(v/v)]
(J)
Max OD600nm
2.0
1.5
1.0
0.5
0.0
0
0.5
1
20
Concentration [%(v/v)]
(K)
n-Butyl MA
μ (h-1)
0.6
0.4
0.2
0.0
0
0.5
1
20
Concentration [%(v/v)]
(L)
Max OD600nm
2.0
1.5
1.0
0.5
0.0
0
0.5
1
20
Concentration [%(v/v)]

Figure 4.7 - Growth parameters of *E. coli* MG1655 strains when grown at different concentrations of lower esters. *E. coli* MG1655 WT [■] and *E. coli* MG1655 *soxR*(R20H)*acrR*(T32fs) [●] were grown in MSX medium in the presence of methyl methacrylate (A and B), ethyl methacrylate (C and D), isopropyl methacrylate (E and F), n-propyl methacrylate (G and H), isobutyl methacrylate (I and J) and BMA (K and L) added immediately after inoculation at different concentrations. All strains were grown in 96-well microplates at 37°C and 600 rpm. Means of six replicates are shown and error bars represent standard deviations. Growth parameters are shown in Appendix 11.4, Table 11.2, page 203.

E. coli MG1655 WT and *E. coli* MG1655 *soxR*(R20H)*acrR*(T32fs) could grow in the presence of up to 1 %(v/v) isopropyl methacrylate (Figure 4.6 G and H), but *E. coli* MG1655 *soxR*(R20H)*acrR*(T32fs) always had a slightly lower maximum OD_{600nm} than the WT strain (Figure 4.7 F). Additionally, *E. coli* MG1655 WT had higher growth rates than *E. coli* MG1655 *soxR*(R20H)*acrR*(T32fs) when grown in the presence of 0.1 and 0.5 %(v/v) isopropyl methacrylate (Figure 4.7 E).

By contrast, *E. coli* MG1655 *soxR*(R20H)*acrR*(T32fs) was able to grow in the presence of up to 1 %(v/v) n-propyl methacrylate (Figure 4.6 E and F), with a decrease in growth rates with the increase in concentration of n-propyl methacrylate (Figure 4.7 G and Figure 4.6 F). On the other hand, *E. coli* MG1655 WT was only able to grow in the presence of up to 0.5 %(v/v) n-propyl methacrylate, and after a lag phase of at least 9 h, at a concentration of 0.5 %(v/v) (Figure 4.7 G and Figure 4.6 E). Yet, the WT strain reached similar maximum ODs compared to the ones obtained with *E. coli* MG1655 *soxR*(R20H)*acrR*(T32fs).

The log P_{ow} value is an indicator of the toxicity of a chemical towards a microorganism, as with the increase in the log P_{ow} values of chemicals there is a decrease in toxicity[16-20] (see section 1.1.2). However, in this work there was not an exact correlation between the log P_{ow} and the levels of toxicity observed for the esters at any of the concentrations tested (Figure 4.8 and Figure 4.9).

Overall, there was a higher variability of the levels of toxicity of each MAE at lower concentrations, 0.1 and 0.5 %(v/v) (Figure 4.8). At a concentration of 1 %(v/v) most of the growth rates and maximum OD of either *E. coli* MG1655 WT or *E. coli* MG1655 *soxR*(R20H)*acrR*(T32fs), increased with the increase of the log P_{ow}, except for n-propyl methacrylate (Figure 4.8 E and F). The variability observed could be due to the low concentrations and the low volumes used, associated with the volatility of the

chemicals. However, when the boiling points and vapour pressures of these chemicals were analysed there was not a clear correlation between the volatility properties of the chemicals and their levels of toxicity, that could explain the oscillations in the growth rates and maximum ODs obtained (Table 11.4, in Appendix 11.4, page 205).

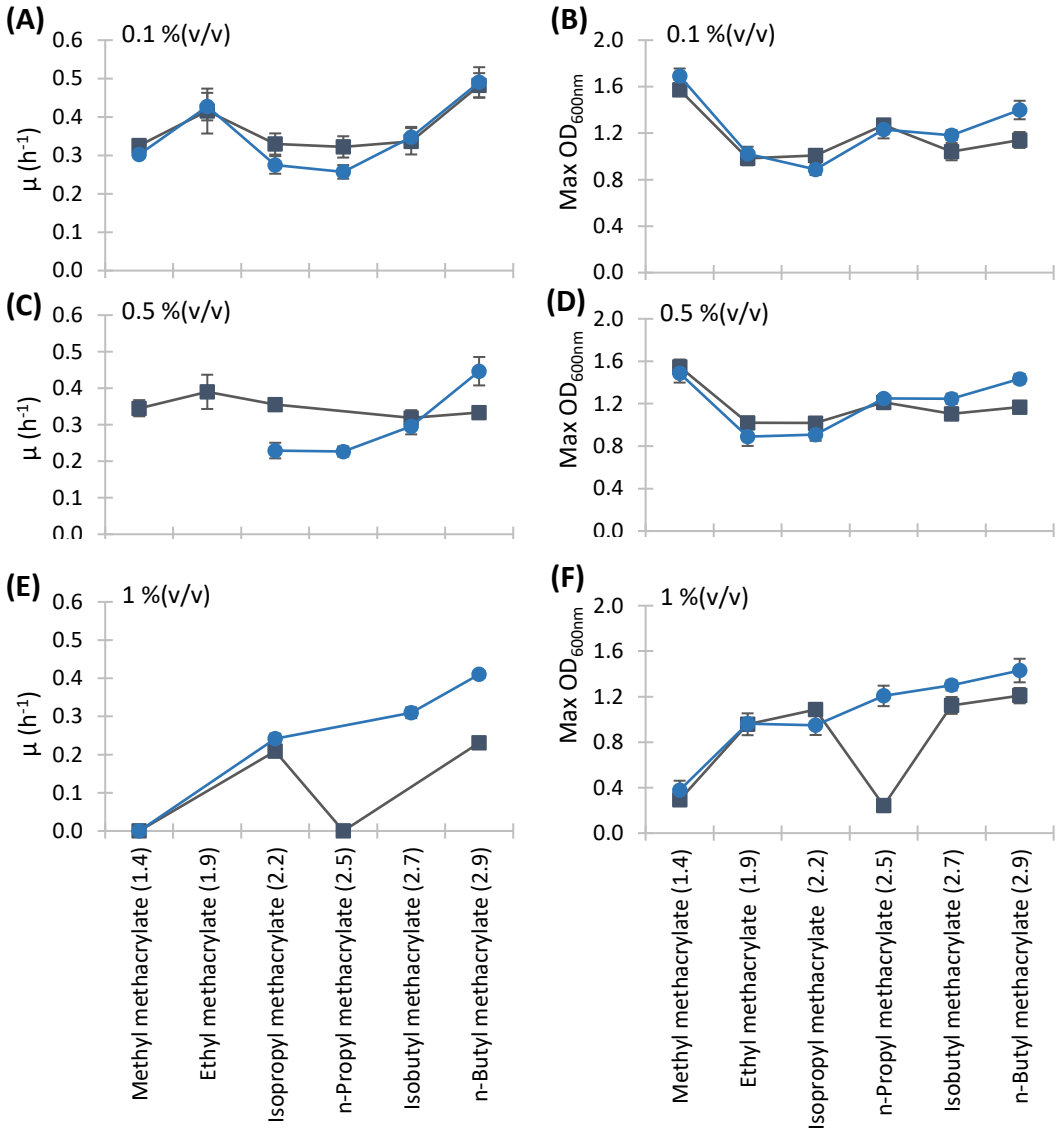

Figure 4.8 - Correlation between the growth parameters of *E. coli* MG1655 strains and the log P_{ow} of MAE at different concentrations. *E. coli* MG1655 WT [■] and *E. coli* MG1655 *soxR*(R20H)*acrR*(T32fs) [●] were grown in MSX medium, in the presence of different chemicals added immediately after inoculation at 0.1 %(v/v) (A and B), 0.5 %(v/v) (C and D) and 1 %(v/v) (E and F). All strains were grown in 96-well microplates at 37°C and 600 rpm. Means of six replicates are shown and the error bars represent standard deviations. Growth parameters are shown in Appendix 11.4, Table 11.2, page 203.

However, at a concentration of 20 %(v/v), the growth rates and maximum OD of *E. coli* MG1655 WT and *E. coli* MG1655 *soxR*(R20H)*acrR*(T32fs) increased with the increase of the log P_{ow} values of the MAE, except for BMA, in which *E. coli* MG1655 WT did not grow (Figure 4.9).

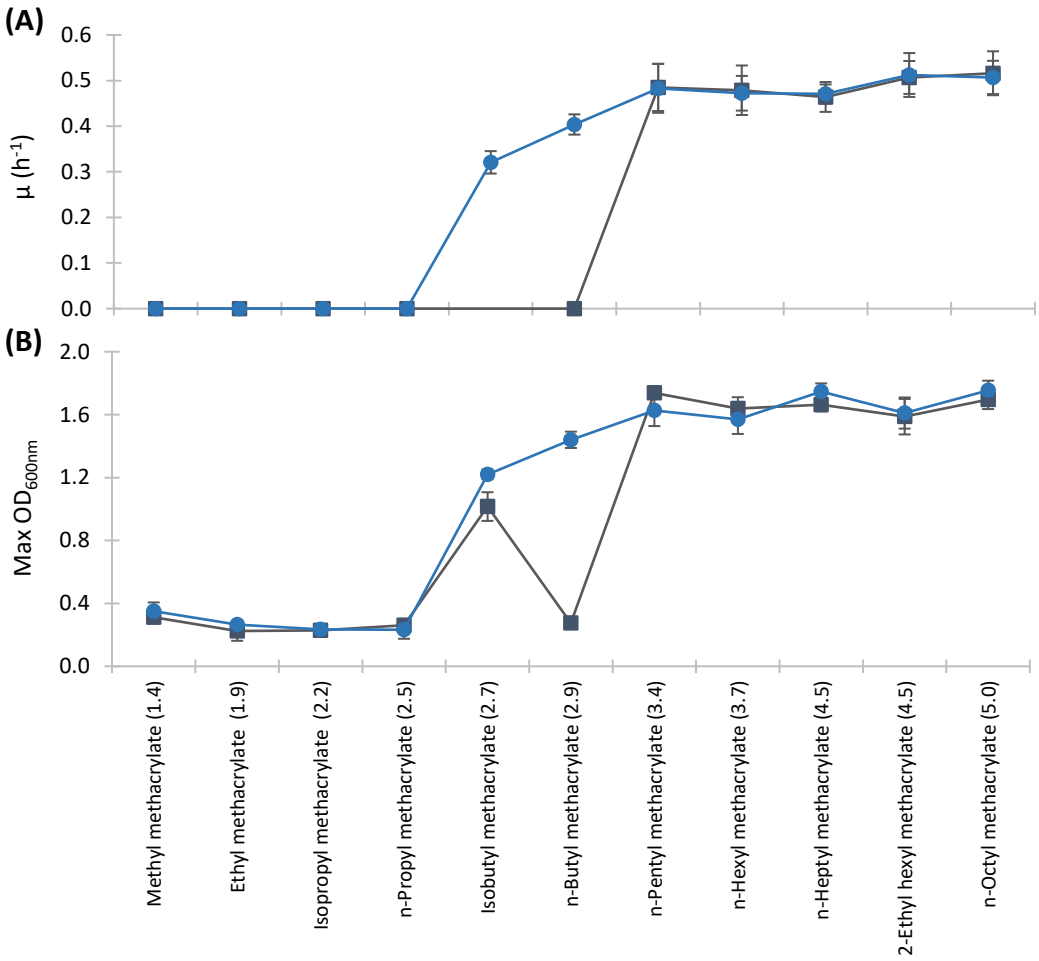

Figure 4.9 - Correlation between the growth parameters of *E. coli* MG1655 strains and the log P_{ow} of MAE immediately after inoculation at 20 %(v/v). *E. coli* MG1655 WT [■] and *E. coli* MG1655 *soxR*(R20H)*acrR*(T32fs) [●] were grown in MSX medium, in 96-well microplates at 37°C and 600 rpm. Growth rates (A) and maximum OD (B) are shown, with means of six replicates and error bars that represent standard deviations. Growth parameters are shown in Appendix 11.4, Table 11.2, page 203.

In this study, both *E. coli* MG1655 WT and *E. coli* MG1655 *soxR*(R20H)*acrR*(T32fs) did not grow in the presence of 20 %(v/v) of MAE with log P_{ow} value equal or lower than 2.5. Moreover, both *E. coli* MG1655 WT and *E. coli* MG1655 *soxR*(R20H)*acrR*(T32fs) grew in the presence of 20 %(v/v) of MAE with log P_{ow} values equal or higher than 3.4, showing that at least for this group of chemicals, the limiting log P_{ow} of *E. coli* was lower than the previously reported limiting log P_{ow} value of 3.8[19].

In summary, the native mechanisms of resistance in the WT strain were still useful to counteract relatively high concentrations of these extremely toxic MAE, though the mutations in *soxR* and *acrR* offered an additional benefit. However, the mutant strain *E. coli* MG1655 soxR(R20H)acrR(T32fs) displayed overall improved tolerance to n-propyl methacrylate, BMA and isobutyl methacrylate, when compared to the WT strain. Furthermore, *E. coli* MG1655 *soxR*(R20H)*acrR*(T32fs) could grow in the presence of 20 %(v/v) BMA and isobutyl methacrylate with no apparent lag phase, whereas the WT strains did not. Therefore, it seems that the mutations in *soxR* and *acrR* induce mechanism of tolerance that are rather specific to a small range of chemicals.

4.2.1.2 Esters generated as co-products

Apart from MAE, co-product toxicity can also be a bottleneck when it comes to developing a feasible bioprocess for the production of PMMA. In this case, when BMA is the target final product, several possibly problematic co-products can be formed during fermentation, namely n-butyl isobutyrate, n-butyl isovalerate and n-butyl acetate (Luca Rossoni and Clemency Tilley, University of Nottingham; Unpublished data; Figure 4.10). These co-product esters were tested for their toxicity effects towards *E. coli* MG1655 WT and *E. coli* MG1655 *soxR*(R20H)*acrR*(T32fs), at concentrations from 0.1 to 20 %(v/v) (Figure 4.11 and Figure 4.12; Table 11.2 in Appendix 11.4, page 203).

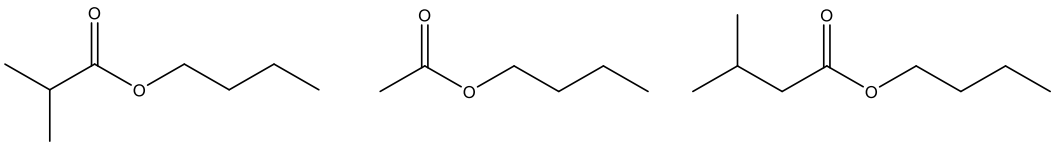

n-Butyl Isobutyrate log P_{ow}: 2.40 | **n-Butyl acetate** log P_{ow}: 1.78 | **n-Butyl isovalerate** log P_{ow}: 2.60

Figure 4.10 - Chemical structure and respective log P_{ow} values of the esters n-butyl isobutyrate, n-butyl acetate and n-butyl isovalerate.

E. coli MG1655 WT and *E. coli* MG1655 *soxR*(R20H)*acrR*(T32fs) had different responses to the different esters (Figure 4.11). *E. coli* MG1655 *soxR*(R20H)*acrR*(T32fs) could grow in the presence of up to 20 %(v/v) n-butyl isobutyrate, with similar growth

rates at the different concentrations of n-butyl isobutyrate tested (Figure 4.12 B; Figure 4.11 A and B). Whereas, even though *E. coli* MG1655 WT could also grow in the presence of up to 20 %(v/v) n-butyl isobutyrate, it had long lag phases at 1 and 20 %(v/v) (Figure 4.11 A and Figure 4.12 A).

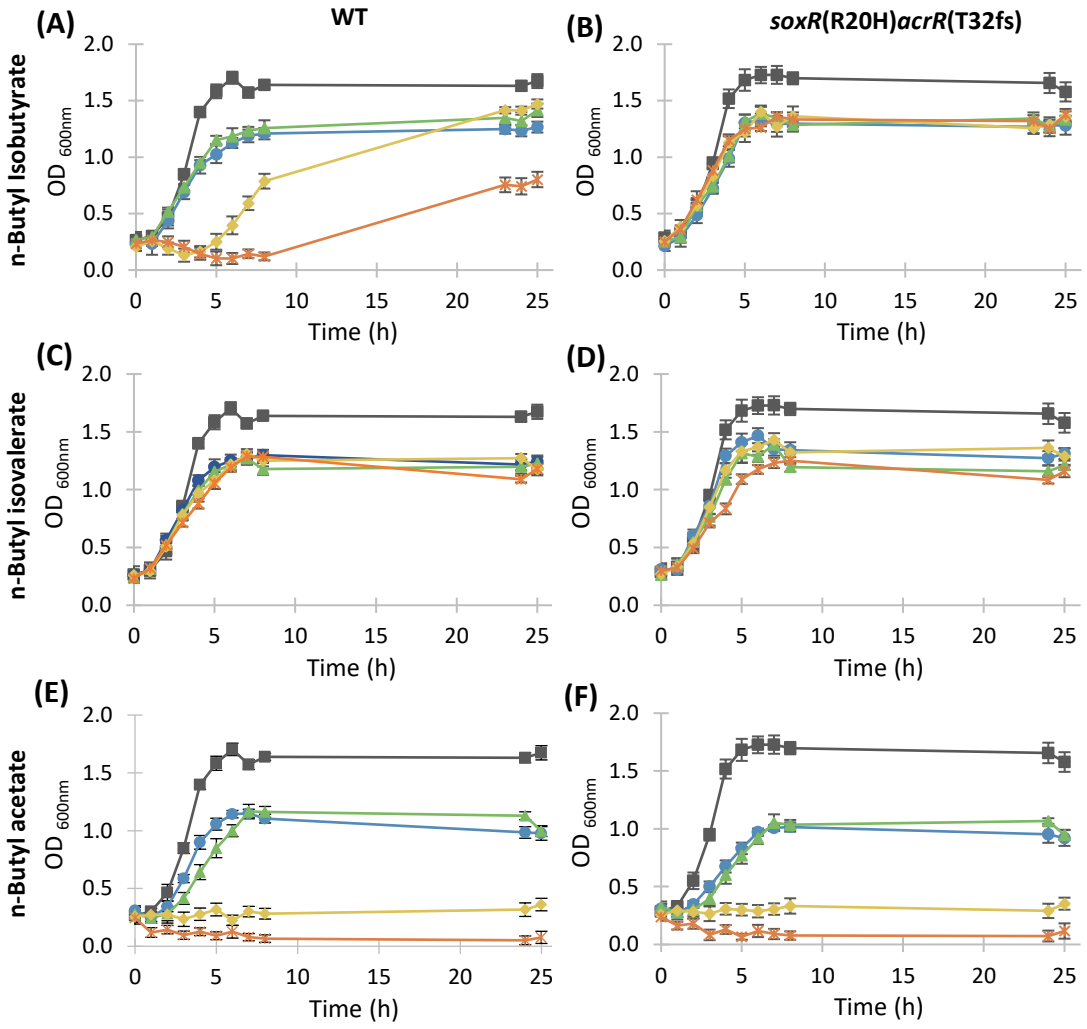

Figure 4.11 - Effect of co-product esters on the growth of *E. coli* MG1655 strains. *E. coli* MG1655 WT (A, C and E) and *E. coli* MG1655 *soxR*(R20H)*acrR*(T32fs) (B, D and F) were grown in MSX medium in the absence [■] or presence of n-butyl isobutyrate (A and B), n-butyl isovalerate (C and D) and n-butyl acetate (E and F) added immediately after inoculation at concentrations of 0.1 %(v/v) [●], 0.5 %(v/v) [▲], 1 %(v/v) [◆] and 20 %(v/v) [*]. All strains were grown in 96-well microplates at 37°C and 600 rpm. Means of six replicates are shown and error bars represent standard deviations. Growth parameters are shown in Appendix 11.4, Table 11.2, page 203.

By contrast, in the presence of n-butyl acetate and n-butyl isovalerate, *E. coli* MG1655 *soxR*(R20H)*acrR*(T32fs) and *E. coli* MG1655 WT had very similar results (Figure 4.11 and Figure 4.12). Both strains could grow in up to 20 %(v/v) butyl isovalerate, but *E. coli* MG1655 *soxR*(R20H)*acrR*(T32fs) had a slight decrease in the

growth rates and maximum OD_{600nm} with the increase in concertation of n-butyl isovalerate (Figure 4.12 C and D). On the other hand, *E. coli* MG1655 WT (Figure 4.11 E) and *E. coli* MG1655 *soxR*(R20H)*acrR*(T32fs) (Figure 4.11 F) were only able to grow in the presence of up to 0.5 %(v/v) n-butyl acetate, but the WT had higher growth rates and slightly higher maximum OD_{600nm} than the mutant strain (Figure 4.12 E).

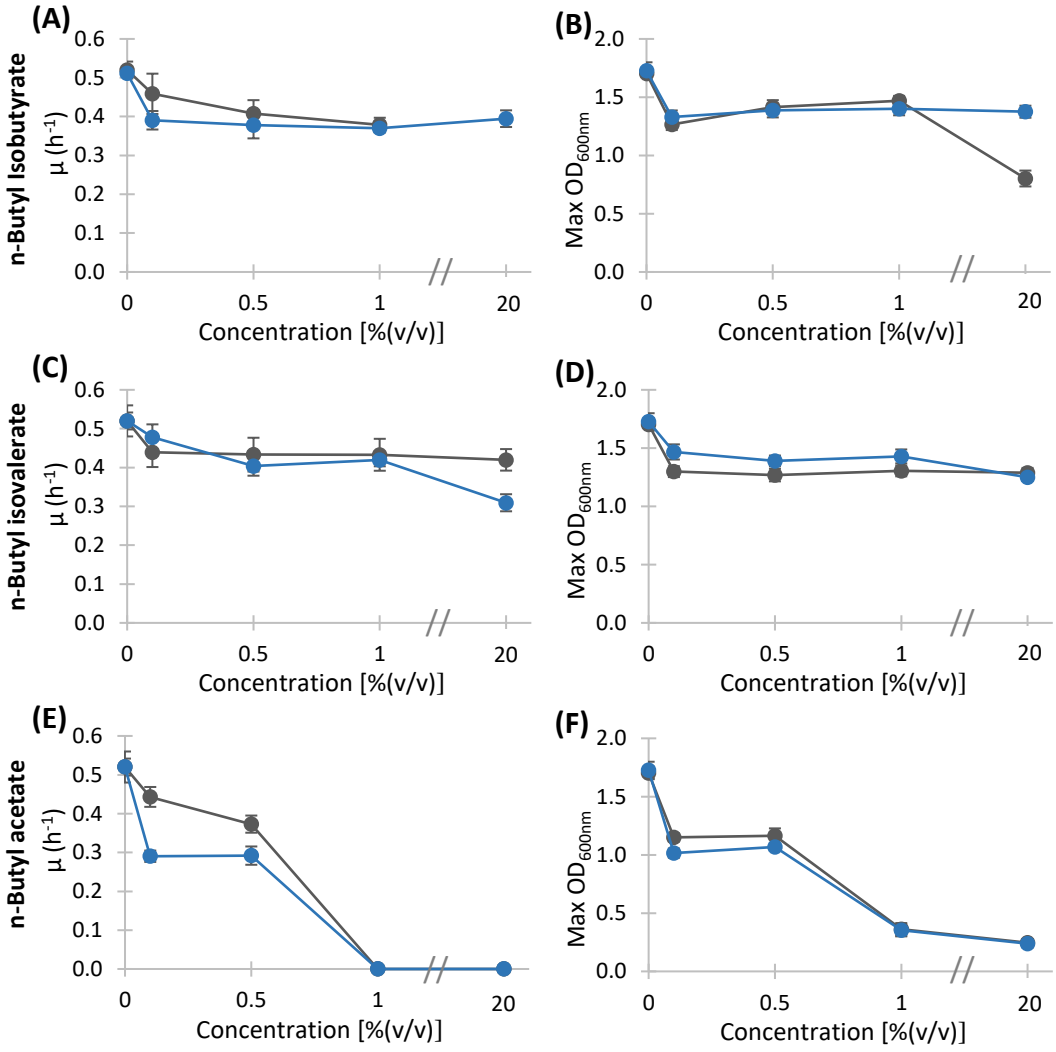

Figure 4.12 - Growth parameters of *E. coli* MG1655 strains when grown at different concentrations of co-product esters. *E. coli* MG1655 WT [■] and *E. coli* MG1655 *soxR*(R20H)*acrR*(T32fs) [●] were grown in MSX medium, in the presence of n-butyl isobutyrate (A and B), n-butyl isovalerate (C and D) and n-butyl acetate (E and F) added immediately after inoculation at different concentrations. All strains were grown in 96-well microplates at 37°C and 600 rpm. Means of six replicates are shown and error bars represent standard deviations. Growth parameters are shown in Appendix 11.4, Table 11.2, page 203.

Overall, with the esters generated as co-products, there was a decrease in chemical toxicity towards *E. coli* MG1655 WT and *E. coli* MG1655 *soxR*(R20H)*acrR*(T32fs) with the increase in the P_{ow} value (Figure 4.13). There was only on exception to this trend,

as at a concentration of 20 %(v/v), *E. coli* MG1655 *soxR*(R20H)*acrR*(T32fs) was more tolerant to n-butyl isobutyrate than n-butyl isovalerate, which have a log P_{ow} value of 2.4 and 2.6, respectively.

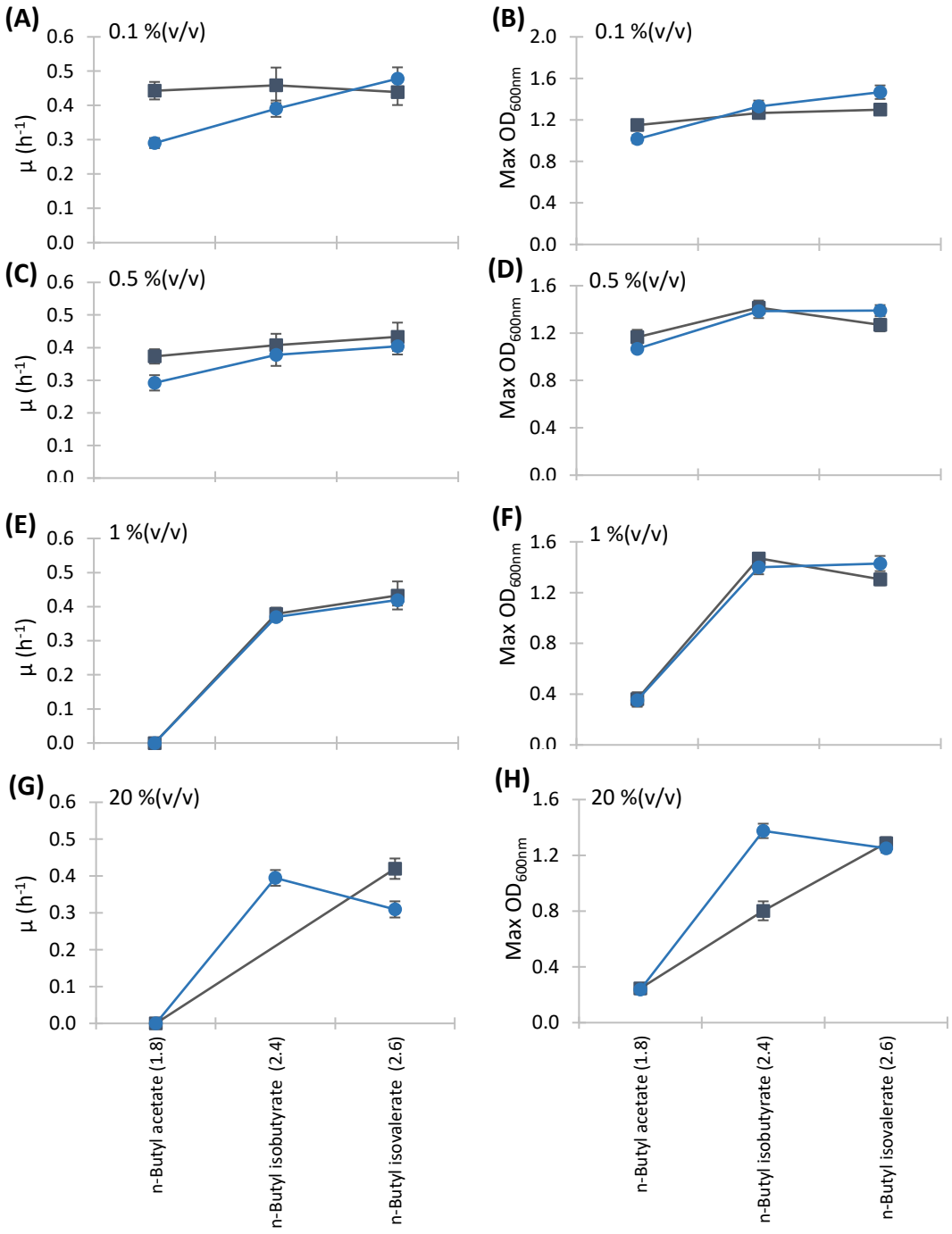

Figure 4.13 - Correlation between the growth parameters of *E. coli* MG1655 strains and the log P_{ow} of esters generated as co-products, at different concentrations. *E. coli* MG1655 WT [■] and *E. coli* MG1655 *soxR*(R20H)*acrR*(T32fs) [●] were grown in MSX medium, in the presence of different chemicals added immediately after inoculation at 0.1 %(v/v) (A and B), 0.5 %(v/v) (C and D), 1 %(v/v) (E and F) and 20 %(v/v) (G and H). All strains were grown in 96-well microplates at 37°C and 600 rpm. Means of six replicates are shown and the error bars represent standard deviations. Growth parameters are shown in Appendix 11.4, Table 11.2, page 203.

In summary, compared to the WT strain, *E. coli* MG1655 *soxR*(R20H)*acrR*(T32fs) had improved tolerance only towards n-butyl isobutyrate. Furthermore, n-butyl acetate seems to be the most toxic of the three co-product esters tested, whereas the external addition of n-butyl isovalerate had no significant toxic effects in *E. coli*.

4.2.1 Alcohols

Alcohols are commodity chemicals mainly used as solvents, paint diluents, fuels or fuels additives[263], and are also used for the production of PMMA, as substrates for converting methacrylyl-CoA into a MAE. *E. coli* MG1655 WT and *E. coli* MG1655 *soxR*(R20H)*acrR*(T32fs) were then tested for their resistance to n-butanol, isobutanol, ethanol and isopropanol (Figure 4.14), to find out whether or not the mutations in *soxR* and *acrR* would improve tolerance to these alcohols.

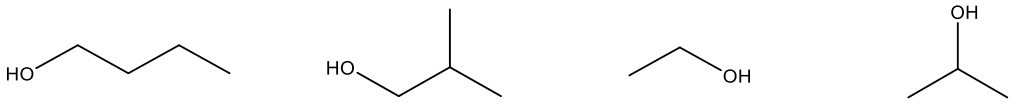

n-Butanol log P_{ow}: 0.88 | **Isobutanol** log P_{ow}: 0.76 | **Ethanol** log P_{ow}: -0.31 | **Isopropanol** log P_{ow}: 0.05

Figure 4.14 - Chemical structure and respective log P_{ow} values of C2-C4 alcohols.

E. coli MG1655 WT and *E. coli* MG1655 *soxR*(R20H)*acrR*(T32fs) were grown in the presence of 0.5 and 1 %(v/v) n-butanol, 0.5 and 1 %(v/v) isobutanol, 1, 5 and 10 %(v/v) ethanol and 1 and 5 %(v/v) isopropanol, added immediately after inoculation (Figure 4.15; Table 11.2 in Appendix 11.4, page 203). The growth profiles obtained were very similar between the strains (Figure 4.15). *E. coli* MG1655 WT and *E. coli* MG1655 *soxR*(R20H)*acrR*(T32fs) could grow in the presence of 0.5 %(v/v) n-butanol (Figure 4.15 A and B), 0.5 %(v/v) isobutanol (Figure 4.15 C and D), 5 %(v/v) ethanol (Figure 4.15 E and F) and 1 %(v/v) isopropanol (Figure 4.15 G and H), but did not survive when the concentrations were increased to 1 %(v/v) n-butanol, 1 %(v/v) isobutanol, 10 %(v/v) ethanol and 5 %(v/v) isopropanol. n-Butanol and isobutanol had the highest toxic effects towards *E. coli*, whereas ethanol was the least toxic alcohol.

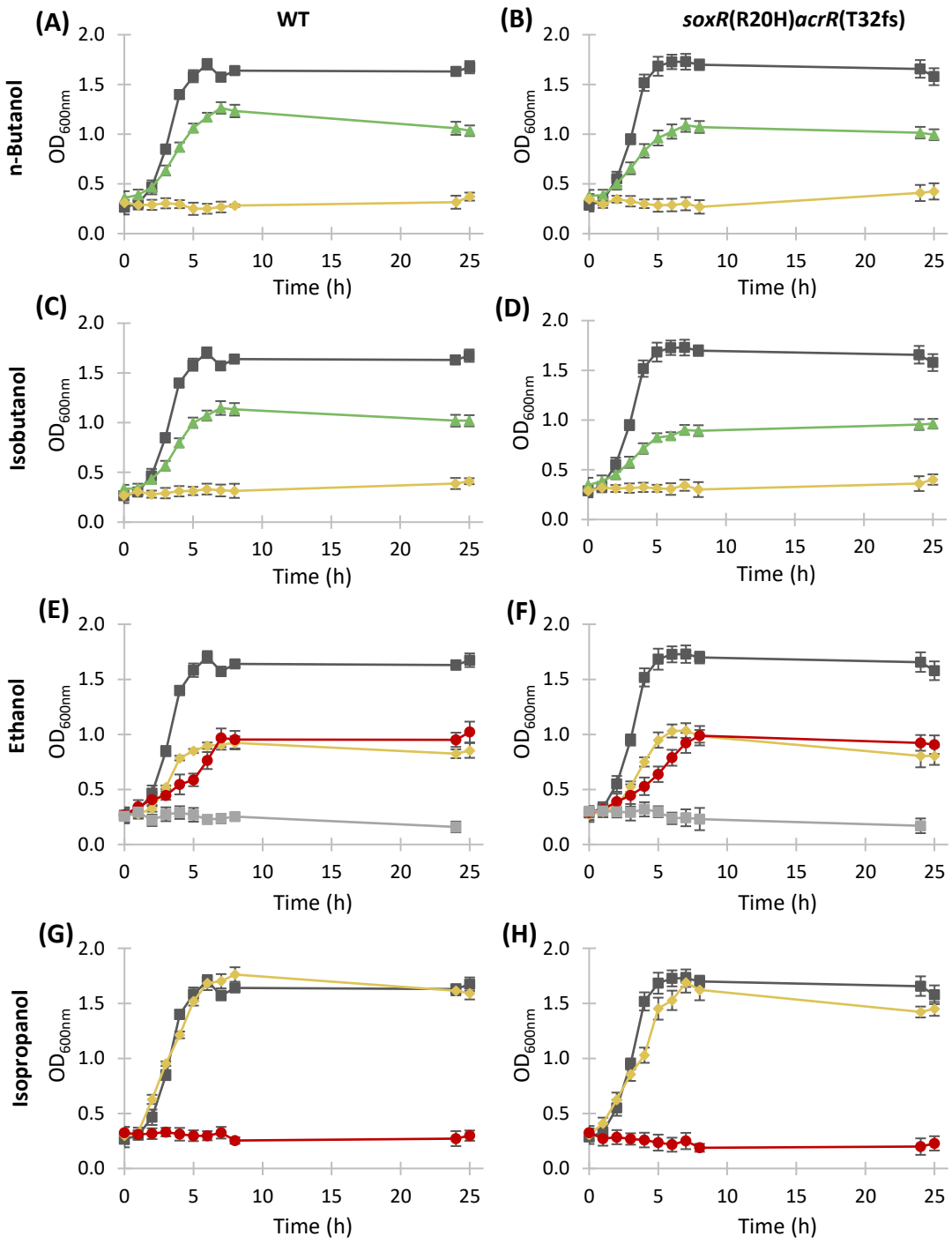

Figure 4.15 - Effect of n-butanol and isobutanol on the growth of *E. coli* MG1655 strains. *E. coli* MG1655 WT (A and C) and *E. coli* MG1655 *soxR*(R20H)*acrR*(T32fs) (B and D) were grown in MSX medium in the absence [■] or presence of n-butanol (A and B), isobutanol (C and D), ethanol (E and F) and isopropanol (G and H), added immediately after inoculation at concentrations of 0.5 %(v/v) [▲], 1 %(v/v) [◆], 5 %(v/v) [●] and 10 %(v/v) [■]. All strains were grown in 96-well microplates at 37°C and 600 rpm. Means of six replicates are shown and error bars represent standard deviations. Growth parameters are shown in Appendix 11.4, Table 11.2, page 203.

Overall, there was a decrease in the growth rates and maximum OD_{600nm} of *E. coli* MG1655 WT and *E. coli* MG1655 *soxR*(R20H)*acrR*(T32fs) with the increase in

concentration of alcohols (Figure 4.16). Furthermore, in general, in the presence of lower concentrations of alcohols, *E. coli* MG1655 *soxR*(R20H)*acrR*(T32fs) had slightly lower growth rates and maximum OD_{600nm} compared to the WT strain (Figure 4.16).

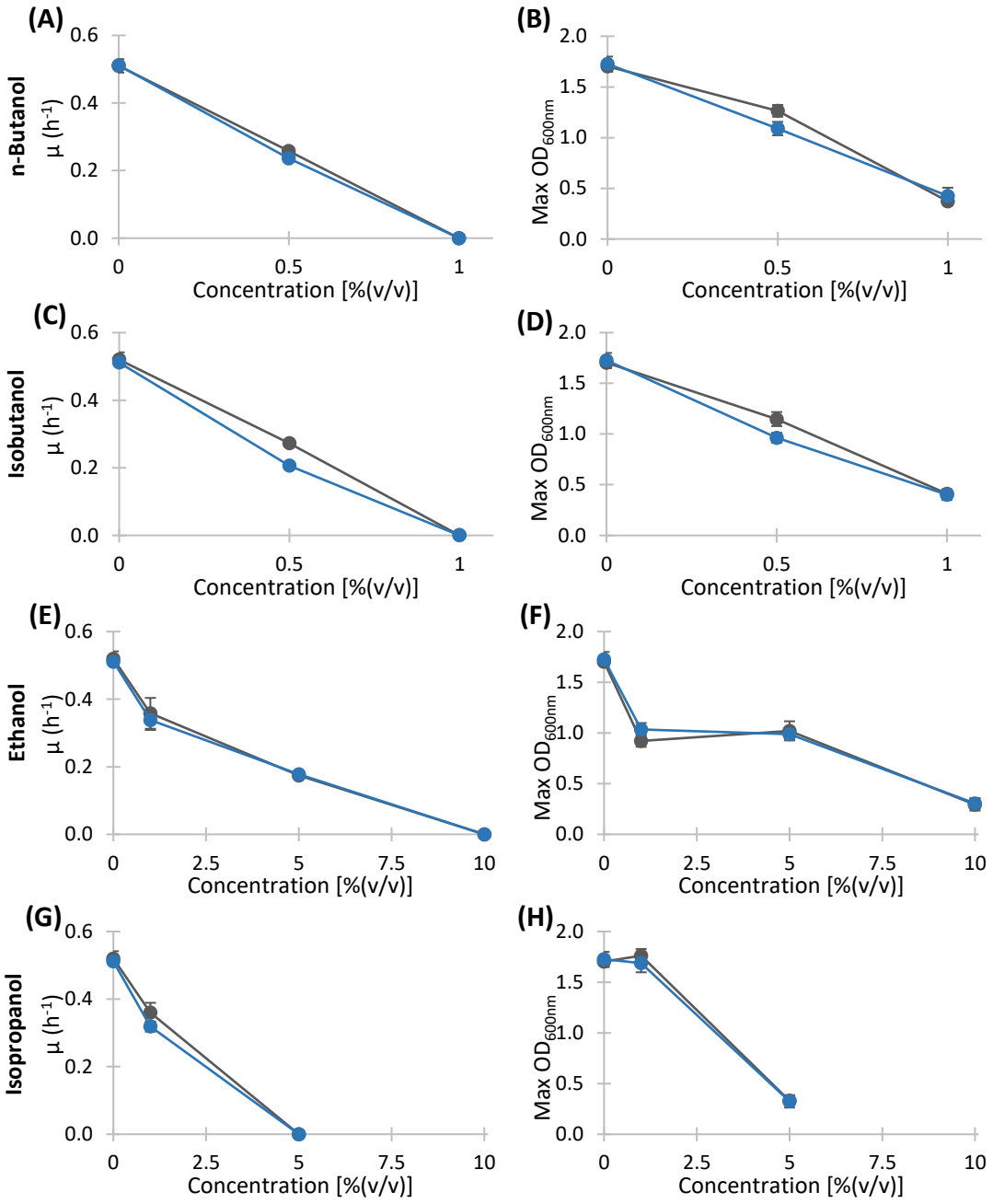

Figure 4.16 - Growth parameters of *E. coli* MG1655 strains when grown at different concentrations of n-butanol and isobutanol. *E. coli* MG1655 WT [■] and *E. coli* MG1655 *soxR*(R20H)*acrR*(T32fs) [●] were grown in MSX medium, in the presence of n-butanol (A and B), isobutanol (C and D), ethanol (E and F) and isopropanol (G and H), added immediately after inoculation at different concentrations. All strains were grown in 96-well microplates at 37°C and 600 rpm. Means of six replicates are shown and error bars represent standard deviations. Growth parameters are shown in Appendix 11.4, Table 11.2, page 203.

In the presence of 0.5 %(v/v) n-butanol (Figure 4.16 A), 0.5 %(v/v) isobutanol (Figure 4.16 C), 5 %(v/v) ethanol (Figure 4.16 E) and 1 %(v/v) isopropanol (Figure 4.16 G), the lowest concentrations of alcohols tested, *E. coli* MG1655 WT and *E. coli* MG1655 *soxR*(R20H)*acrR*(T32fs) had a decrease in the growth rates of 30 to 60 %, when compared to the control with no chemical added.

Moreover, the toxicity of alcohols towards *E. coli* did not decrease with the increase of their log P_{ow} values (Figure 4.17). *E. coli* MG1655 WT and *E. coli* MG1655 *soxR*(R20H)*acrR*(T32fs) had similar growth rates in the presence of 1 %(v/v) ethanol and isopropanol, with the log P_{ow} values of -0.31 and 0.05, respectively, but an increased maximum OD_{600nm} in the presence of 1 %(v/v) isopropanol. Yet, both strains could not grow in the presence of 1 %(v/v) isobutanol and n-butanol, which have higher log P_{ow} values of 0.76 and 0.88 (Figure 4.17).

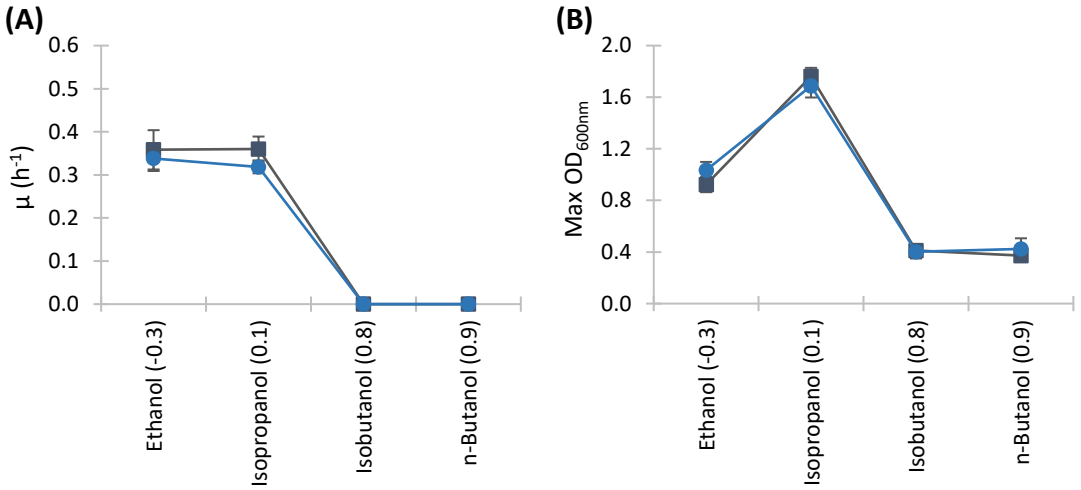

Figure 4.17 - Correlation between the growth parameters of *E. coli* MG1655 strains and the log P_{ow} of alcohols. *E. coli* MG1655 WT [■] and *E. coli* MG1655 *soxR*(R20H)*acrR*(T32fs) [●] were grown in MSX medium, in the presence 1 %(v/v) of different alcohols added immediately after inoculation. All strains were grown in 96-well microplates at 37°C and 600 rpm. Means of six replicates are shown and the error bars represent standard deviations. Growth parameters are shown in Appendix 11.4, Table 11.2, page 203.

The fact that the toxicity of alcohols did not decrease with the increase in the log P_{ow}, could possibly be explained by the volatility of these chemicals (Table 4.3). Ethanol and isopropanol have lower boiling points and higher vapour pressures than isobutanol and n-butanol, and, consequently, are more volatile. Thus, at a low concentration of 1 %(v/v), ethanol and isopropanol were apparently less toxic, but this could be due to their higher volatility and a possible decrease in the

concentration of alcohols in direct contact with the cells. Yet, *E. coli* MG1655 WT and *E. coli* MG1655 *soxR*(R20H)*acrR*(T32fs) could also grow in the presence of 5 %(v/v) ethanol (Figure 4.15 E and F). Further studies would be necessary to fully understand the effect of volatility on the toxicity tests performed.

Nonetheless, the presence of the mutations in the genes *soxR* and *acrR* found in *E. coli* MG1655 *soxR*(R20H)*acrR*(T32fs) did not improve resistance the C2 to C4 alcohols tested, n-butanol, isobutanol, ethanol and isopropanol, compared to the WT. Thus, there was no cross-tolerance between the two groups of chemicals tested, esters and alcohols.

Table 4.3 - Chemical properties of alcohols and their toxicity towards *E. coli* MG1655 strains. *E. coli* MG1655 WT and *E. coli* MG1655 *soxR*(R20H)*acrR*(T32fs) were grown in MSX medium, in the presence 1 %(v/v) of different alcohols added immediately after inoculation. All strains were grown in 96-well microplates at 37°C and 600 rpm.

Chemical	Log P_{ow}	Boiling point (°C)	Vapour pressure (mmHg)	*E. coli* MG1655 strains	
				WT	*soxR*(R20H)*acrR*(T32fs)
Ethanol	-0.3	78	59	+	+
Isopropanol	0.1	82	45	++	++
Isobutanol	0.8	108	10	-	-
n-Butanol	0.9	118	7	-	-

Caption: ++, growth similar to control; + growth worse than the control; -, no growth.

4.2.2 Alkanes and alkenes

Alkanes and alkenes are commodity chemicals generally used as fuels, lubricants and platform chemicals[264]. Different alkanes and alkenes (Figure 4.18) were tested for their toxicity against *E. coli* MG1655 WT and the mutant *E. coli* MG1655 *soxR*(R20H)*acrR*(T32fs). Both strains were grown in the presence of the cyclohexane, n-hexane, cyclooctane, ethylcyclohexane, vinylcyclohexane, n-heptane, isohexane and cyclohexene, added immediately after inoculation at different concentrations, 0.5, 1, 5, 10 and/or 20 %(v/v) (Figure 4.19 and Figure 4.20; Table 11.2 in Appendix 11.4, page 203).

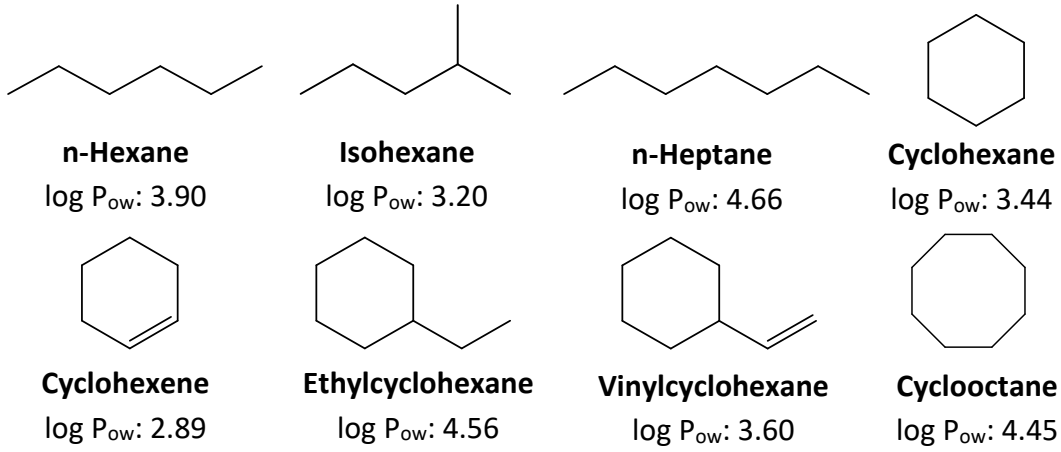

Figure 4.18 - Chemical structure and respective log P_{ow} values of different alkanes and alkenes.

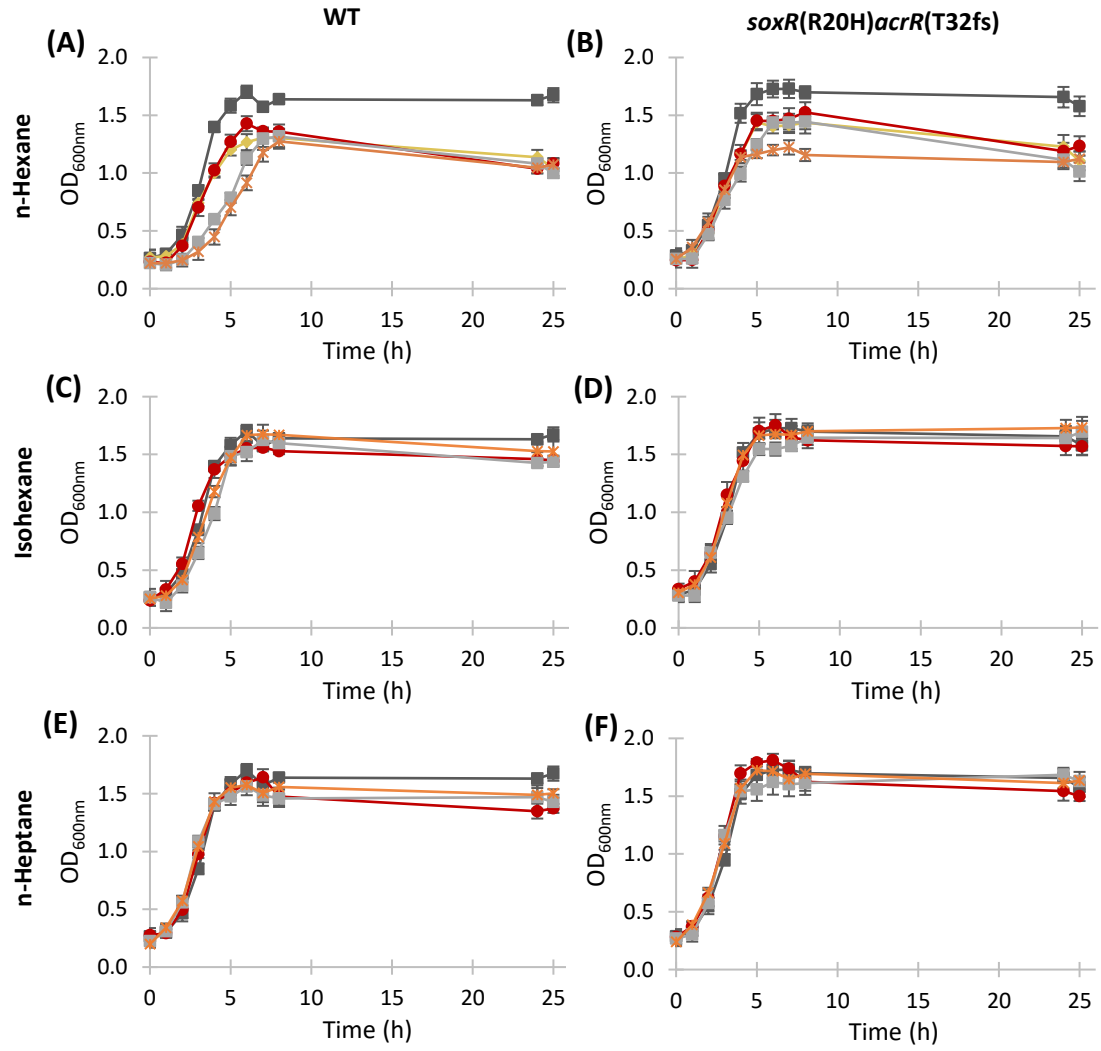

Figure 4.19 - Effect of the presence of alkanes on the growth of *E. coli* MG1655 strains. *E. coli* MG1655 WT (A, C and E) and *E. coli* MG1655 *soxR*(R20H)*acrR*(T32fs) (B, D and F) were grown in MSX medium in the absence [■] or presence of n-hexane (A and B), isohexane (C and D) and n-heptane (E and F) added immediately after inoculation at concentrations of 1 %(v/v) [♦], 5 %(v/v) [●], 10 %(v/v) [■] and 20 %(v/v) [✳]. All strains were grown in 96-well microplates at 37°C and 600 rpm. Means of six replicates are shown and error bars represent standard deviations. Growth parameters are shown in Appendix 11.4, Table 11.2, page 203.

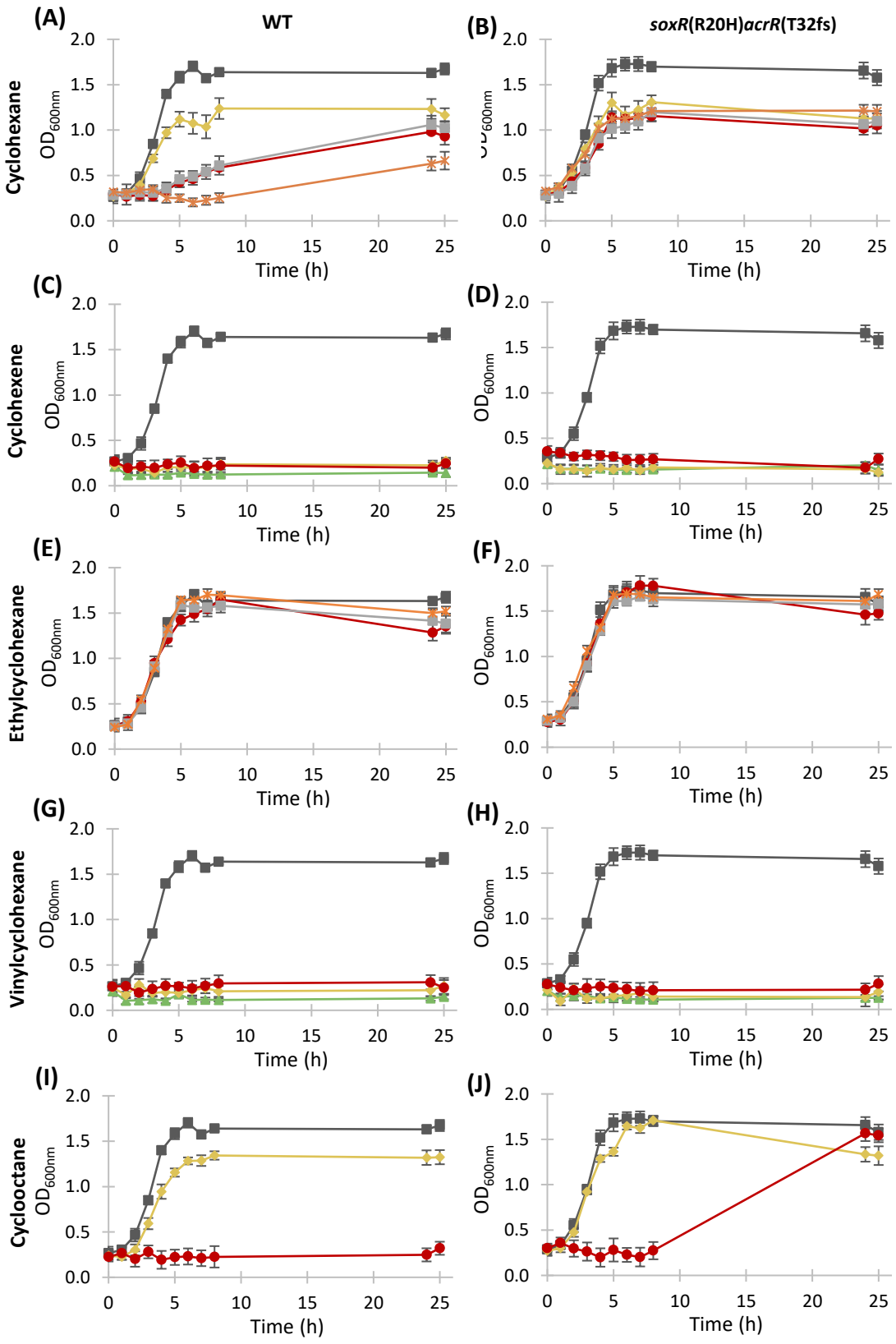

Figure 4.20 - Effect of the presence of cycloalkanes and cycloalkenes on the growth of *E. coli* MG1655 strains *E. coli* MG1655 WT (A, C, E, G, I) and *E. coli* MG1655 *soxR*(R20H)*acrR*(T32fs) (B, D, F, H and J) were grown in in MSX medium in the absence [■] or presence of cyclohexane (A and B), cyclohexene (C and D), ethylcyclohexane (E and F), vinylcyclohexane (G and H) and cyclooctane (I and J) added immediately after inoculation at concentrations of 0.5 %(v/v) [▲], 1 %(v/v) [◆], 5 %(v/v) [●], 10 %(v/v) [■] and 20 %(v/v) [*]. All strains were grown, in 96-well

microplates at 37°C and 600 rpm. Means of six replicates are shown and error bars represent standard deviations. Growth parameters are shown in Appendix 11.4, Table 11.2, page 203.

E. coli MG1655 WT and the mutant *E. coli* MG1655 *soxR*(R20H)*acrR*(T32fs) could grow in the presence of up to 20 % (v/v) n-hexane (Figure 4.19 A and B), isohexane (Figure 4.19 C and D), n-heptane (Figure 4.19 E and F) and ethylcyclohexane (Figure 4.20 E and F). By contrast, the WT and the mutant strain *E. coli* MG1655 *soxR*(R20H)*acrR*(T32fs) could not grow in the presence of cyclohexene (Figure 4.20 C and D) and vinylcyclohexane (Figure 4.20 G and H), even at concentrations as low as 0.5 %(v/v).

However, there were clear differences in the growth profiles of *E. coli* MG1655 WT and *E. coli* MG1655 *soxR*(R20H)*acrR*(T32fs) when these strains were grown in the presence of the cyclic alkanes cyclohexane (Figure 4.20 A and B) and cyclooctane (Figure 4.20 I and J). *E. coli* MG1655 *soxR*(R20H)*acrR*(T32fs) was able to grow in the presence of up to 20 %(v/v) cyclohexane (Figure 4.20 B). However, *E. coli* MG1655 WT could only grow with a high specific growth rate in the presence of 1 % (v/v) cyclohexane (Figure 4.20 A). At higher concentrations of cyclohexane, 5, 10 and 20 %(v/v), the WT strain had lag phases of at least 3 h and low growth rates. In the presence of 1 % (v/v) cyclooctane, both strains were able to grow (Figure 4.20 I and J). Yet, in the presence of 5 % (v/v) cyclooctane, *E. coli* MG1655 WT was not able to grow after 25 h (Figure 4.20 I), but *E. coli* MG1655 *soxR*(R20H)*acrR*(T32fs) was able to grow, after a lag phase of at least 8 h (Figure 4.20 J).

With the analysis of the growth rates and maximum OD_{600nm} values plotted against the concentration of chemicals used, it was possible to draw further conclusions (Figure 4.21). Without the addition of any chemical, the growth rate of *E. coli* MG1655 WT was 0.51 ± 0.02 h^{-1}, but in the presence of 1% (v/v) and 10 % (v/v) cyclohexane, the growth rate decreased by a 20 % and 75 %, respectively (Figure 4.21 A). Thus, with the increase in the concentration of cyclohexane, there was a significant decrease in the specific growth rate of the WT strain.

In a concentration of 1 to 20 %(v/v) cyclohexane, *E. coli* MG1655 *soxR*(R20H)*acrR*(T32fs) had always similar growth rates, between 0.33 and 0.36 h^{-1}

(Figure 4.21 A). A similar profile was observed for the maximum OD_{600nm}, which decreased in the WT with the increase in the cyclohexane concentration, but in *E. coli* MG1655 *soxR*(R20H)*acrR*(T32fs) was maintained at similar values in the presence of 1 to 20 %(v/v) cyclohexane (Figure 4.21 B).

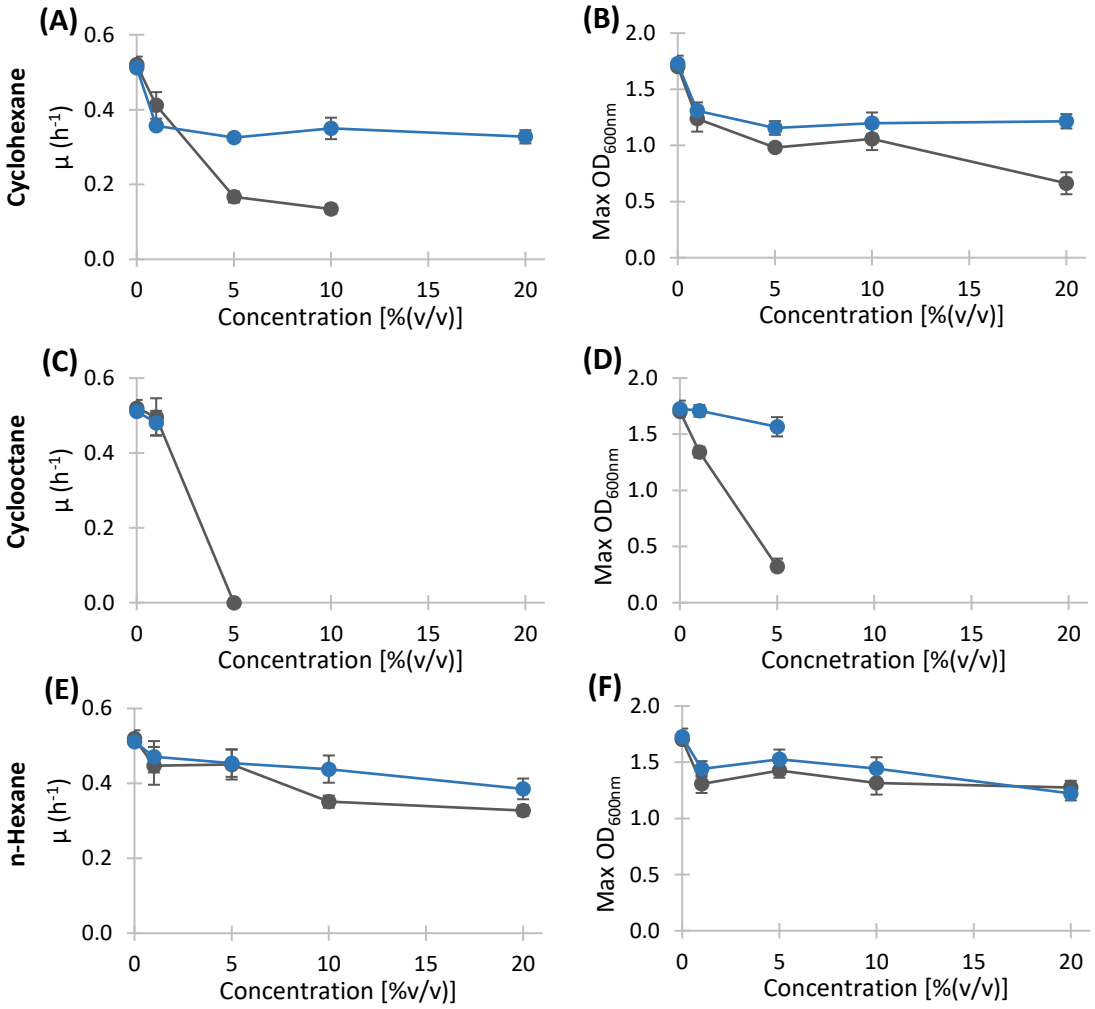

Figure 4.21 - Growth parameters of *E. coli* MG1655 strains when grown at different concentrations of alkanes. *E. coli* MG1655 WT [■] and *E. coli* MG1655 *soxR*(R20H)*acrR*(T32fs) [●] were grown in in MSX medium in the presence of cyclohexane (A and B), cyclooctane (C and D) and n-hexane (E and F) added immediately after inoculation at different concentrations. All strains were grown, in 96-well microplates at 37°C and 600 rpm. Means of six replicates are shown and error bars represent standard deviations. Growth parameters are shown in Appendix 11.4, Table 11.2, page 203.

In the presence of 1 %(v/v) cyclooctane, *E. coli* MG1655 WT and *E. coli* MG1655 *soxR*(R20H)*acrR*(T32fs) could grow, with similar growth rates but different maximum OD_{600nm}, 1.34 ± 0.05 and 1.71 ± 0.05, respectively (Figure 4.21 D). However, when the concentration of cyclooctane was increased to 5 %(v/v), the WT did not grow and *E. coli* MG1655 *soxR*(R20H)*acrR*(T32fs) had a lag phase of at least 8 h. In addition, *E. coli*

MG1655 WT and *E. coli* MG1655 *soxR*(R20H)*acrR*(T32fs) were able to grow in the presence of up to 20 %(v/v) n-hexane (Figure 4.19 A and B), yet in the presence of 10 and 20 % (v/v) n-hexane, *E. coli* MG1655 WT had a decrease in the growth rate of 20 % and 15 %, respectively, when compared to *E. coli* MG1655 *soxR*(R20H)*acrR*(T32fs). Thus, the *soxR* and *acrR* mutations found in *E. coli* MG1655 *soxR*(R20H)*acrR*(T32fs) seem to improve the levels of tolerance of *E. coli* towards cyclohexane, n-hexane and cyclooctane.

The results obtained when the cells were tested in 96 well microplates were further confirmed at larger scale, by growing *E. coli* MG1655 and/or *E. coli* MG1655 *soxR*(R20H)*acrR*(T32fs) in the presence of 20 %(v/v) n-hexane, 20 %(v/v) isohexane, 20 %(v/v) n-heptane, 20 %(v/v) cyclohexane, 5 %(v/v) cyclooctane and 20 %(v/v) ethylcyclohexane, using 30 mL glass vials. The glass vials were sealed with polypropylene screw cap with PTFE/silicone septa. It was confirmed that *E. coli* MG1655 WT could grow in the presence of 20 %(v/v) isohexane, n-heptane and ethylcyclohexane (Figure 11.5; Table 11.3 in Appendix 11.4, page 207).

Moreover, tests done in the 30 mL vials showed once again that *E. coli* MG1655 *soxR*(R20H)*acrR*(T32fs) had improved tolerance to 20 %(v/v) n-hexane (Figure 4.22 A and B) and 20 %(v/v) cyclohexane (Figure 4.22 C and D), compared to the WT strain. Yet, in the presence of 5 %(v/v) cyclooctane, neither *E. coli* MG1655 WT nor *E. coli* MG1655 *soxR*(R20H)*acrR*(T32fs) could grow (Figure 4.22 E and F). Although, in microplates *E. coli* MG1655 *soxR*(R20H)*acrR*(T32fs) could grow in the presence of up to 5 %(v/v) cyclooctane after a lag phase of at least 8 h, it did not grow in the presence of 5 %(v/v) cyclooctane when grown in 30 mL vials. Further studies would be necessary to understand the observed difference.

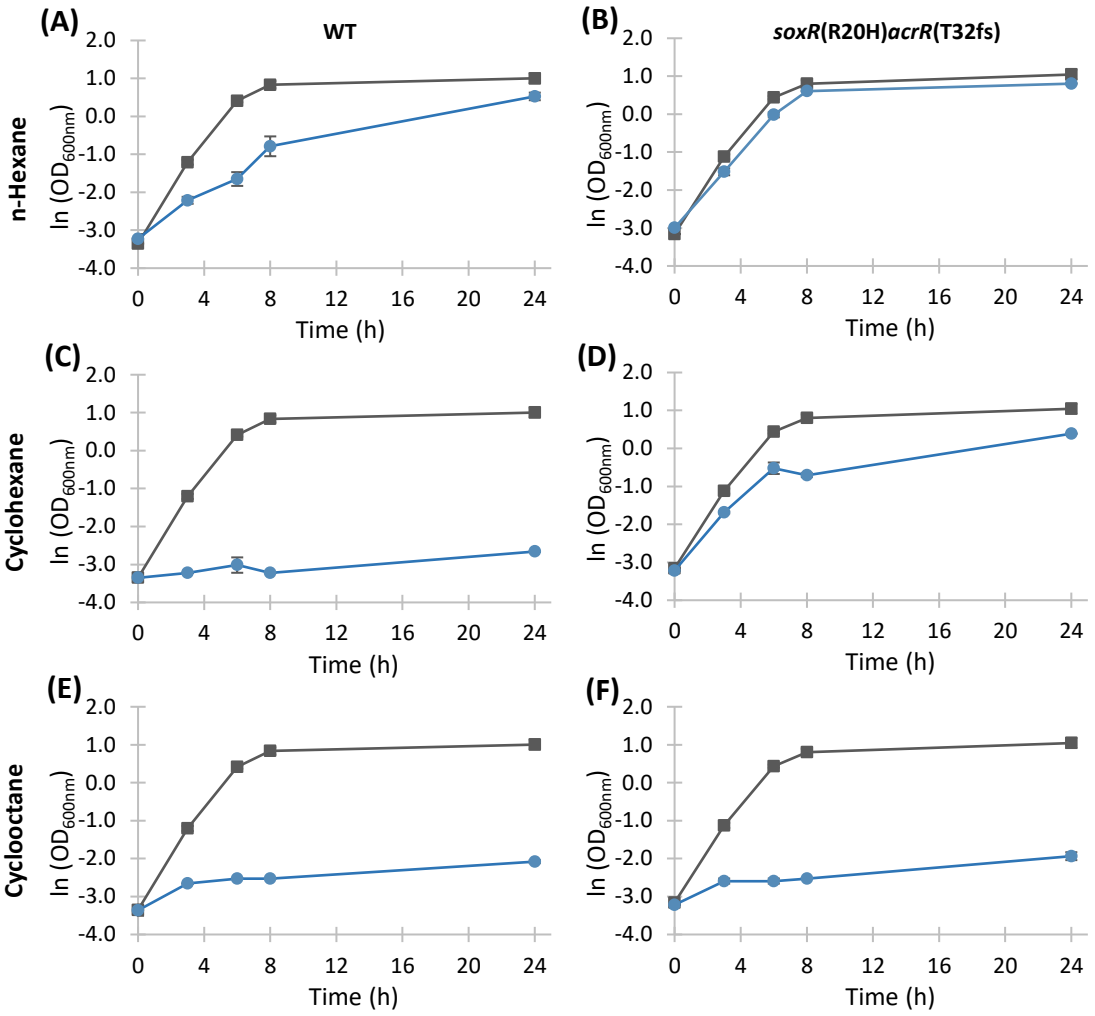

Figure 4.22 - Effect of alkanes on the growth of *E. coli* MG1655 stains. *E. coli* MG1655 WT (A, C and D) and *E. coli* MG1655*soxR*(R20H)*acrR*(T32fs) (B, D and F) were grown in MSX medium in the absence [■] or presence [●] of 20 %(v/v) n-hexane (A and B), 20 %(v/v) cyclohexane (C and D) and 5 %(v/v) cyclooctane (E and F) added immediately after inoculation. All strains were grown in 30 mL vials, at 37°C and 250 rpm shaking. Means of two replicates are shown and error bars represent standard deviations. Growth parameters are shown in Appendix 11.4, Table 11.3, page 205.

The correlation between the log P_{ow} of each chemical and the growth parameters was also analysed (Figure 4.23). Overall, there was not a distinct increase of growth rates and maximum OD_{600nm} with the increase of the log P_{ow} of each chemical. Although *E. coli* MG1655 WT and *E. coli* MG1655 *soxR*(R20H)*acrR*(T32fs) had constant growth rates and OD_{600nm} in the presence of 5, 10 and 20 %(v/v) of the linear and branched alkanes, isohexane, n-hexane and n-heptane, the cyclic compounds had oscillating results with the increase of log P_{ow} values.

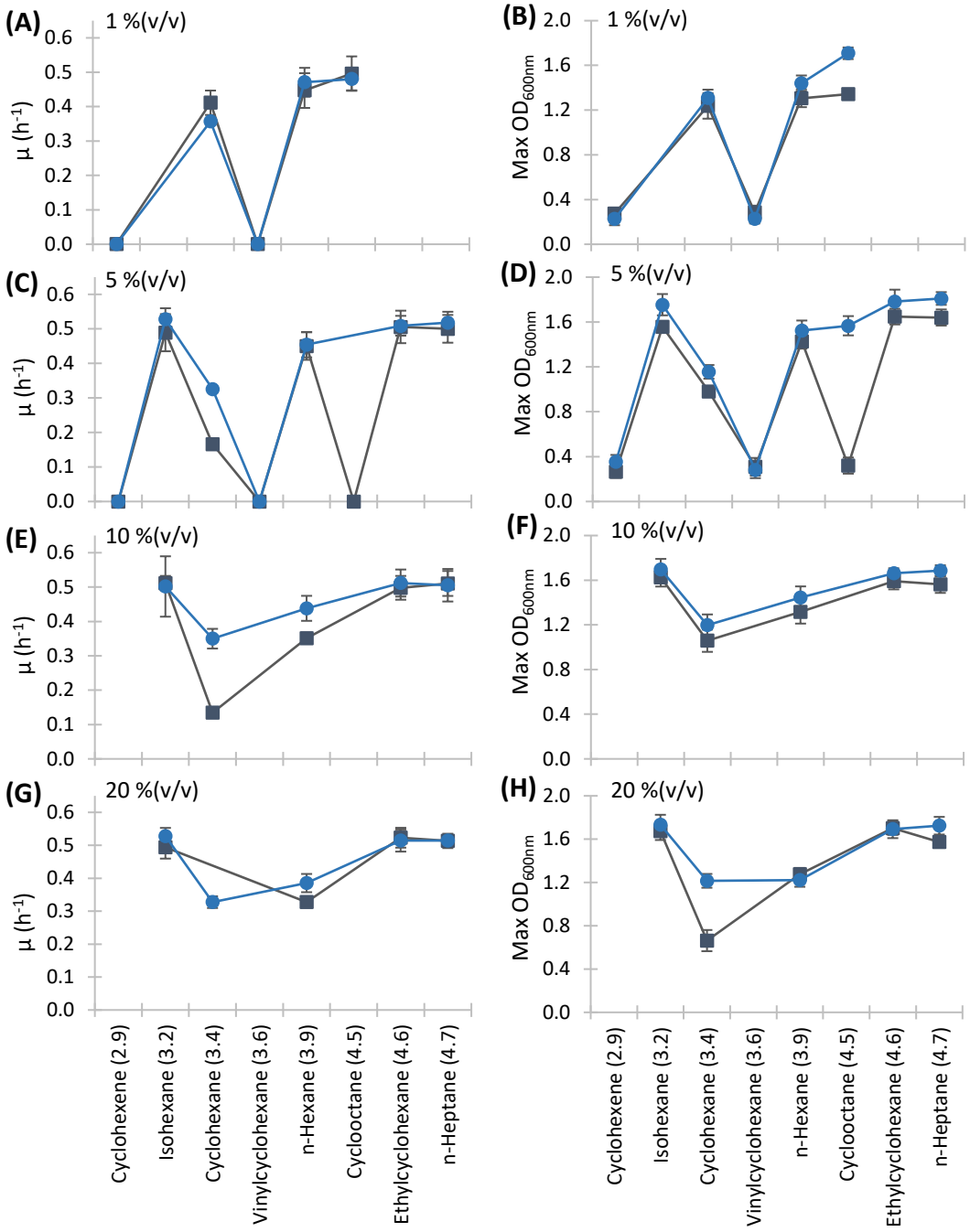

Figure 4.23 - Correlation between the growth parameters of *E. coli* MG1655 strains and the log P_{ow} of alkanes and alkenes at different concentrations. *E. coli* MG1655 WT [■] and *E. coli* MG1655 *soxR*(R20H)*acrR*(T32fs) [●] were grown in MSX medium, in the presence of different chemicals added immediately after inoculation at 0.1 %(v/v) (A and B), 0.5 %(v/v) (C and D), 1 %(v/v) (E and F) and 0.5 %(v/v) (G and H). All strains were grown in 96-well microplates at 37°C and 600 rpm. Means of six replicates are shown and the error bars represent standard deviations. Growth parameters are shown in Appendix 11.4, Table 11.2, page 203.

For example, at a concentration of 5 %(v/v), the strains *E. coli* MG1655 WT and *E. coli* MG1655 *soxR*(R20H)*acrR*(T32fs) could grow in the presence of cyclohexane and ethylcyclohexane, which have log P_{ow} values of 3.4 and 4.6, respectively, but did not grow in the presence of cyclohexene and vinylcyclohexane, which have log P_{ow}

values of 2.9 and 3.6, respectively (Figure 4.23). Furthermore, *E. coli* MG1655 WT also could not grow in the presence of 5 %(v/v) cyclooctane, which has a log P_{ow} of 4.5, and *E. coli* MG1655 *soxR*(R20H)*acrR*(T32fs) only grew after a lag phase of at least 8 h. Although higher concentrations of 10 and 20 %(v/v) of cyclohexene, vinylcyclohexane and cyclooctane were not tested, it would be safe to say that *E. coli* would not grow at these concentrations. Hence, the variability of toxicity levels with the increase of log P_{ow} values would most likely still happen at higher concentrations, even though it was not directly observed in Figure 4.23.

Once again, the variability in the toxic effects of chemicals with different log P_{ow} values could be due to the volatility of the chemicals (Table 4.4). Vinylcyclohexane and cyclooctane have higher boiling points and lower vapour pressures, and consequently, are less volatile than n-hexane, cyclohexane and isohexane. This could explain why vinylcyclohexane and cyclooctane were more toxic towards *E. coli* than other chemicals with lower log P_{ow} values. However, further studies would be needed to confirm this hypothesis.

Table 4.4 - Chemical properties of alkanes and alkenes and their toxicity towards *E. coli* MG1655 strains. *E. coli* MG1655 WT and *E. coli* MG1655 *soxR*(R20H)*acrR*(T32fs) were grown in MSX medium, in the presence 1, 5, 10 and/or 20 %(v/v) of different chemicals added immediately after inoculation. All strains were grown in 96-well microplates at 37°C and 600 rpm.

Chemical	Log P_{ow}	Boiling point (°C)	Vapour pressure (mmHg)	WT Concentration [%(v/v)]				*soxR*(R20H)*acrR*(T32fs) Concentration [%(v/v)]			
				1	5	10	20	1	5	10	20
Cyclohexene	2.89	83	89	-	-			-	-		
Isohexane	3.2	60	211		++	++	++		++	++	++
Cyclohexane	3.44	81	97	++	+	+	+	++	++	++	++
Vinylcyclohexane	3.6	128	14	-	-			-	-		
n-Hexane	3.9	69	151	++	++	+	+	++	++	++	+
Cyclooctane	4.45	149	6	++	-			++	+		
Ethylcyclohexane	4.56	132	13		++	++	++		++	++	++
n-Heptane	4.66	98	46		++	++	++		++	++	++

Caption: ++, good growth ; + worse growth; -, no growth.

In summary, the initial characterization of the new mutant strains found was important to have a better understanding of how the mutated genes *soxR*(R20H), *acrR*(V29G), *acrR*(T32fs) and *ybcO*(I87M) might affect BMA resistance in *E. coli*. The mutant strains with mutations in both *soxR* and *acrR* had higher levels of tolerance to BMA. It seems that the *soxR* mutation may have to be present to assure cell

survival but that either mutations in AcrR may provide additional benefits. Nevertheless, SoxR and AcrR may be strictly related to stress response mechanisms in *E. coli*, possibly affecting regulations of other genes. Furthermore, the combination of the mutated genes *soxR*(R20H) and *acrR*(T32fs), never found in the literature before, improved tolerance to not only BMA, but also isobutyl methacrylate, n-propyl methacrylate, n-butyl isobutyrate, n-hexane and cyclohexane, when added externally and compared to the WT strain.

Yet, further understanding the resistance mechanisms in *E. coli*, which are affected and/or regulated by these mutations found in *soxR*, *acrR* and *ybcO*, will be a crucial step forward towards the industrial bioproduction of BMA and possibly other commodity chemicals.

5 Evaluation of the importance of each mutation on BMA tolerance

5.1 Effect of the mutated genes on BMA tolerance

The BMA resistant *E. coli* isolates contained mutations in the genes *soxR, acrR* or *ybcO*. Although, *E. coli* MG1655 *soxR*(R20H)*ybcO*(I87M), *E. coli* MG1655 *soxR*(R20H)*acrR*(V29G) and *E. coli* MG1655 *soxR*(R20H)*acrR*(T32fs) could tolerate high levels of BMA, all these strains have different combinations of mutations. With *E. coli* MG1655 *soxR*(R20H) it was possible to observe that the *soxR*(R20H) mutation was able to confer tolerance to BMA by itself, but the effect of the remaining individual mutations is not known. Hence, *E. coli* knock-in (KI) *s*trains with single mutations were prepared to understand the effect of the mutated genes *ybcO*(I87M), a*crR*(V29G) and ac*rR*(T32fs) on BMA tolerance and, therefore, if they encode functional or non-functional proteins. Furthermore, to understand whether the BMA tolerance observed in the mutant strains was due to the loss of function of the encoded proteins, new *E. coli* knock-out (KO) strains with single gene deletions of *soxR*, *acrR* or *ybcO* were tested. Additionally, strains with double gene deletions of the combinations of *soxR* plus *acrR* and *soxR* plus *ybcO,* were also prepared.

The KI strains were prepared using the homologous recombination λ red system, where the WT genes were replaced with the mutated gene plus an antibiotic resistance cassette downstream of the gene (Figure 5.1 A). The antibiotic resistance cassette was then eliminated, leaving a scar sequence of 99 bp. The KO strains were developed with the same method, where the gene of interest was replaced with an antibiotic resistance cassette, which had sequences homologous to the upstream and downstream regions of the gene[257] (Figure 5.1 B). The antibiotic resistance cassette was then eliminated, leaving a scar sequence of 102 bp, which included the start codon and the last 6 codons of the C-terminal of the gene of interest. This sequence encodes a translatable peptide known as the scar peptide[256,257]. For *ybcO* deletants, the scar peptide was encoded by a sequence of 107 bp, to avoid the deletion of last 5 bp of the gene *ninE*, located upstream of *ybcO.*

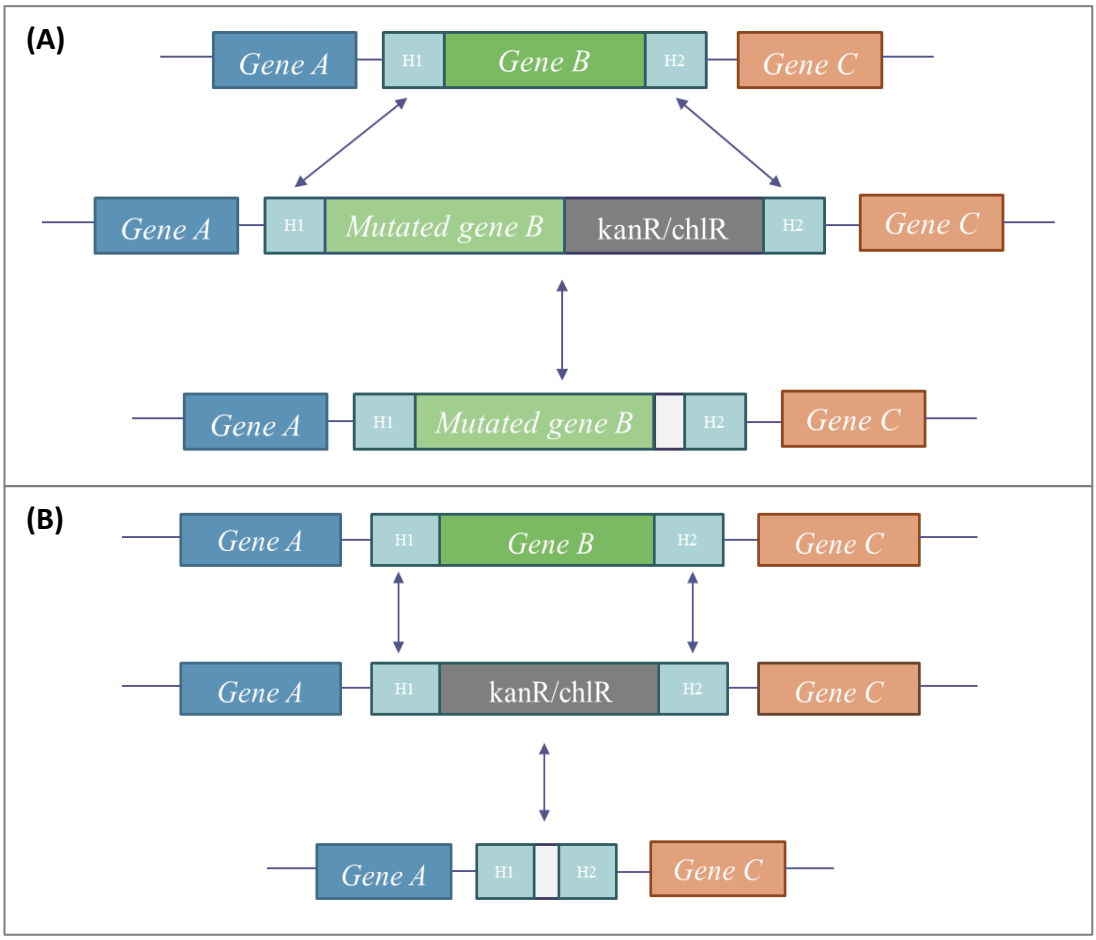

Figure 5.1 – Schematic overview of the λ red recombination method. Gene knock-ins (A) or gene knock-outs (B) are prepared using this method[257]. Homologous upstream (H1) and downstream (H2) regions are represented in light blue, while the scar sequence left after eliminating the antibiotic resistance cassette is represented in white. KanR and chlR indicate the kanamycin and chloramphenicol resistance cassettes, respectively.

Additionally, genetic complementation assays were also done where the genes of interest were expressed in a recombinant plasmid. Plasmid-based genetic complementation is a useful method to evaluate the function of a gene by assessing their ability to restore a given phenotype. Either the WT genes *acrR* and *soxR* or the mutated genes a*crR*(V29G), a*crR*(T32fs) and *soxR*(R20H) were inserted in pSC101, individually or in different sets of combinations. pSC101 is a low copy plasmid, with about 5 copies per cell and a tetracycline resistance cassette, and it was the first cloning vector developed[265,266]. With pSC101 the number of copies of the genes could be maintained as low as possible, comparable to the native chromosomal genes. In addition, the native promoters of each gene were used to further minimize the metabolic burden.

5.1.1 *soxR* mutants

5.1.1.1 Effect of gene deletions

SoxR is a transcription factor that activates the expression of several genes related to the oxidative stress response mechanism[158,160]. The mutated gene *soxR*(R20H) conferred tolerance to BMA in *E.coli* (Figure 4.1 and Figure 4.3, section 4.1). Yet, further studies were performed to understand if *soxR*(R20H) encodes a functional transcriptional factor.

A new KO strain, *E. coli* MG1655 Δ*soxR,* was developed and the presence of the KO was confirmed by colony PCR (Figure 5.2). All the engineered strains that were prepared during this project were tested with the same method (data not shown).

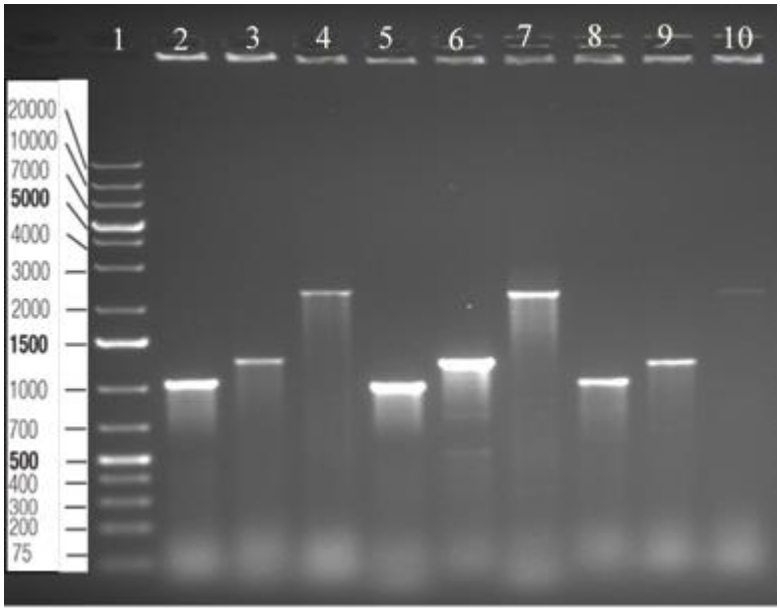

Figure 5.2 – Example of a DNA agarose gel electrophoresis of PCR fragments confirming the deletion of *soxR* and other genes in *E. coli* MG1655 mutants. For each gene, the deletion was confirmed by using 3 different set of primers. For example, for the deletion of *soxR*, the following primers were used: "SoxR 500bp F" and "K1" (lane 5; ~1000bp), "SoxR 500bp R" and "K2" (lane 6; ~1350bp), and "SoxR 500bp F" and "SoxR 500bp R" (lane 7; ~2500bp) (see Table 3.3, in section 3.1.1, for detailed primer information). In this gel, PCR fragments for the confirmation of the *acrR* (lanes 1-3) and *ybcO* (lane 8-10) deletions are also shown.

E. coli MG1655 Δ*soxR* was tested in the absence and presence of 20 %(v/v) BMA added immediately after inoculation, and its growth profile was compared to the WT strain (Figure 5.3). *E. coli* MG1655 WT and *E. coli* MG1655 Δ*soxR* could grow in the

absence of 20 %(v/v) BMA, reaching similar OD_{600nm}. In in the presence of 20 %(v/v) BMA, the WT strain (Figure 5.3 A) and *E. coli* MG1655 Δ*soxR* (Figure 5.3 B) did not grow.

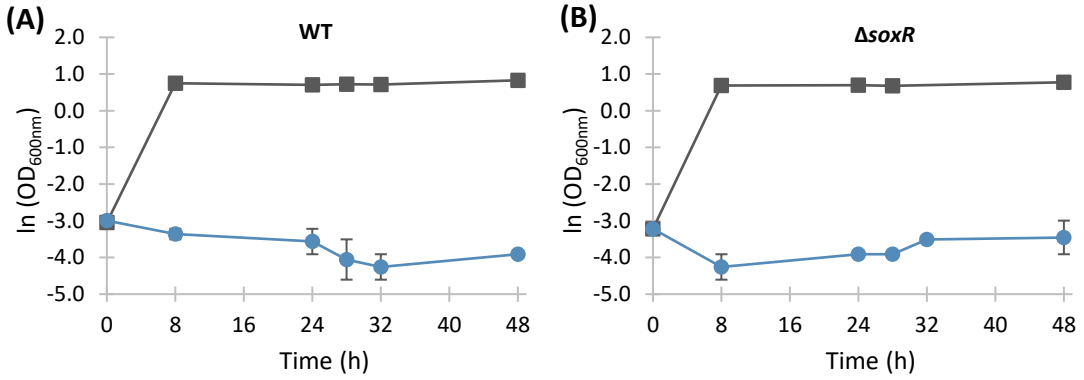

Figure 5.3 - Effect of BMA on the growth of *E. coli* MG1655 *soxR* mutants. *E. coli* MG1655 WT (A) and *E. coli* MG1655 Δ*soxR* (B) were grown in MSX medium in the absence [■] or presence [●] of 20 %(v/v) BMA, in 30 mL vials at 37°C and 250 rpm shaking. BMA was added immediately after inoculation. Means of two replicates are shown and error bars represent standard deviations. Growth data shown in Table 5.1, page 102.

As an additional control, a KO strain purchased from the Keio collection[256] was also tested in the absence and presence of 20 %(v/v) BMA, added immediately after inoculation (Appendix 11.5, Table 11.5, page 210). The deletions on these commercially available strains are done with the same homologous recombination method as the one used in this study, but still have the antibiotic resistance cassette present, more specifically kanamycin resistance cassette[256,257]. Additionally, the Keio collection strains are in an *E. coli* BW25113 background, which is an *E. coli* K-12 derivative similar to *E. coli* MG1655. Yet, the results obtained were the same, *E. coli* BW25113 Δ*soxR::kan* (*E. coli* JW4024) could grow when no BMA was added, but in the presence of 20 %(v/v) BMA, did not grow for the 24 h period that it was tested.

The loss of function of the transcriptional activator SoxR was not beneficial for BMA tolerance. Therefore, *soxR*(R20H) might encode a functional protein. Yet, further tests would be necessary to confirm that the protein encoded by *soxR*(R20H) can bind to the DNA and, consequently, up-regulate the expression of other genes, including *soxS*.

5.1.1.2 Effect of genetic complementations

Plasmid-based genetic complementations were also done to test if the resistance to BMA could be restored in *E. coli* MG1655 Δ*soxR* or *E. coli* MG1655 WT, which did not grow in the presence of 20 %(v/v) BMA. A pSC101 plasmid containing the *soxR* mutated gene, pSC101_*soxR*(R20H), was then transformed into the strains. The resulting strains, *E. coli* MG1655 Δ*soxR* pSC101_*soxR*(R20H) and *E. coli* MG1655 WT pSC101_*soxR*(R20H) were tested in the absence and presence of 20 %(v/v) BMA. In addition, other control strains were also tested, namely *E. coli* MG1655 WT pSC101 and *E. coli* MG1655 WT pSC101_*soxR*(WT), which had an empty pSC101 plasmid and a pSC101 plasmid with the WT *soxR*, respectively (Figure 5.4 and Table 5.1).

In the absence of BMA, all strains, *E. coli* MG1655 Δ*soxR* pSC101_*soxR*(R20H), *E. coli* MG1655 WT pSC101_*soxR*(R20H), *E. coli* MG1655 WT pSC101_soxR(WT) and *E. coli* MG1655 WT pSC101, were able to grow, reaching a similar maximum OD_{600nm}, showing that the presence of the either the empty plasmid or the recombinant plasmids did not affect the normal growth of the cells (Figure 5.4 A). By contrast, in the presence of 20 %(v/v) BMA, *E. coli* MG1655 WT pSC101_*soxR*(WT) and *E. coli* MG1655 WT pSC101 could not grow (Figure 5.4 B). However, both *E. coli* MG1655 Δ*soxR* pSC101_*soxR*(R20H) and *E. coli* MG1655 WT pSC101_*soxR*(R20H) could grow in the presence of 20 %(v/v) BMA, with similar growth profiles (Figure 5.4 B).

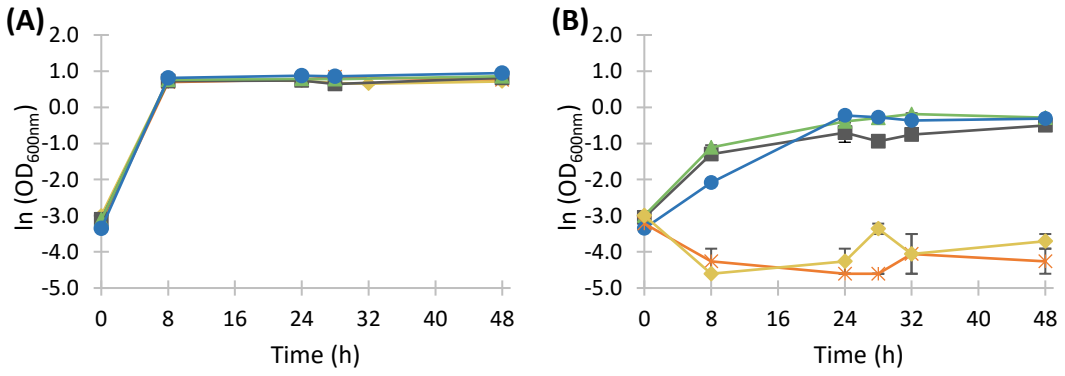

Figure 5.4 - Effect of BMA on the growth of *E. coli* MG1655 strains with chromosomal or plasmid-based *soxR* mutations. *E. coli* MG1655 *soxR*(R20H) **[●]**, *E. coli* MG1655 Δ*soxR* pSC101_*soxR*(R20H) **[■],** *E. coli* MG1655 WT pSC101_*soxR*(R20H) [▲], *E. coli* MG1655 WT pSC101_soxR(WT) [◆] and *E. coli* MG1655 WT pSC101 [*] were grown in MSX medium with tetracycline (12.5 µg/mL), in the absence (A) or presence (B) of 20 %(v/v) BMA, in 30 mL vials at 37°C and 250 rpm. BMA was added immediately after inoculation. Means of two replicates are shown and error bars represent standard deviations. Growth data shown in Table 5.1, page 102.

In the presence of BMA, *E. coli* MG1655 Δ*soxR* pSC101_ *soxR*(R20H) reached an OD_{600nm} of 0.28 ± 0.02 after 8 h and a maximum OD_{600nm} of 0.61 ± 0.01, while *E. coli* MG1655 WT pSC101_*soxR*(WT) reached an OD_{600nm} of 0.33 ± 0.02 after 8 h and a maximum OD_{600nm} of 0.83 ± 0.02 (Figure 5.4 B). Furthermore, both *E. coli* MG1655 Δ*soxR* pSC101_ *soxR*(R20H) and *E. coli* MG1655 WT pSC101_*soxR*(WT) had faster growth in the presence of BMA than the original mutant *E. coli* MG1655 *soxR*(R20H). Although *E. coli* MG1655 *soxR*(R20H) reached a maximum OD_{600nm} of 0.80 ± 0.07, after 8 h, it only had an OD_{600nm} of 0.13 ± 0.01, at least two times lower than *E. coli* MG1655 Δ*soxR* pSC101_ *soxR*(R20H) or *E. coli* MG1655 WT pSC101_*soxR*(WT).

Thus, the introduction of pSC101_*soxR*(R20H) did confer BMA tolerance in strains that would not otherwise grow in the presence of 20 %(v/v) BMA, such as the WT strain and the *soxR* KO strain. Furthermore, the presence of the WT *soxR* in the chromosome of *E. coli* MG1655 WT did not seem to affect the mechanism of tolerance when the mutated *soxR*(R20H) was expressed in a plasmid.

Table 5.1 - Effect of BMA on the OD_{600nm} of *E. coli* MG1655 *soxR* mutant strains. All strains were grown in MSX medium in the absence or presence of 20 %(v/v) BMA, in 30 mL vials at 37°C and 250 rpm. BMA was added immediately after inoculation. Means of two replicates and standard deviations are shown. NG indicates no growth.

	0 %(v/v) BMA		**20 %(v/v) BMA**	
***E. coli* MG1655 strains**	**OD_{600nm} after 8 h**	**Max OD_{600nm}**	**OD_{600nm} after 8 h**	**Max OD_{600nm}**
WT	2.12 ± 0.08	2.29 ± 0.01	NG	
WT pSC101	2.01 ± 0.08	2.31 ± 0.10	NG	
soxR(R20H)	2.25 ± 0.06	2.58 ± 0.03	0.13 ± 0.01	0.80 ± 0.07
Δ*soxR*	1.99 ± 0.01	2.17 ± 0.01	NG	
Δ*soxR* pSC101_*soxR*(R20H)	2.07 ± 0.05	2.26 ± 0.03	0.28 ± 0.02	0.61 ± 0.01
WT pSC101_*soxR*(R20H)	2.14 ± 0.09	2.36 ± 0.01	0.33 ± 0.02	0.83 ± 0.02
WT pSC101_*soxR*(WT)	2.14 ± 0.01	2.14 ± 0.01	NG	

In summary, the R20H mutation found in the DNA binding domain of SoxR did confer tolerance to 20 %(v/v) BMA, while the deletion of *soxR* did not. Furthermore, the genetic complementation of the WT strain or *E. coli* MG1655 Δ*soxR* with the plasmid pSC101_*soxR*(R20H) also restored the tolerance to 20 %(v/v) BMA. Hence, the loss of function of *soxR* or the expression of just the native *soxR* was not beneficial

for the desired phenotype and, therefore, *soxR*(R20H) most likely encodes a functional transcriptional factor capable of activating the necessary mechanism of resistance.

5.1.2 *acrR* mutants

5.1.2.1 Effect of gene insertions and deletions

AcrR is a transcription factor that represses the expression of AcrA and AcrB, which are part of the membrane transporter AcrABZ-TolC[60-68]. The importance of AcrR towards BMA tolerance was evaluated by preparing KI and KO strains. *E. coli* MG1655 *acrR*(V29G), *E. coli* MG1655 *acrR*(T32fs), *E. coli* MG1655 Δ*acrR* and *E. coli* MG1655 WT, were grown in the absence or presence of 20 %(v/v) BMA, added immediately after inoculation (Figure 5.5).

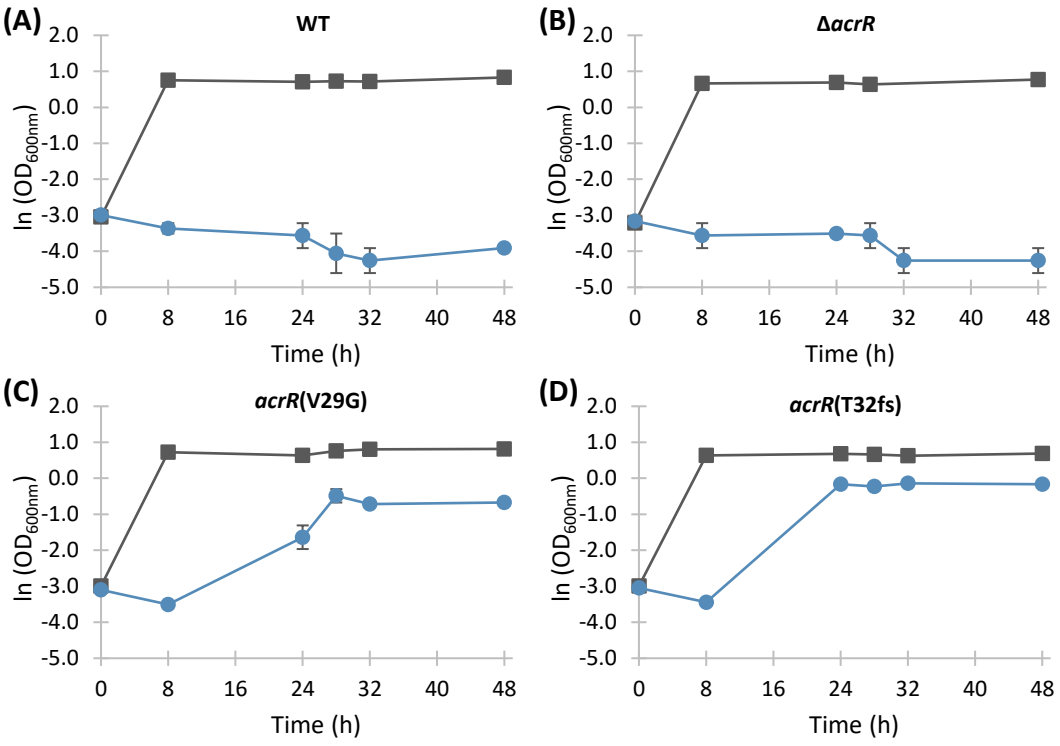

Figure 5.5 - Effect of BMA on the growth of *E. coli* MG1655 *acrR* mutants. *E. coli* MG1655 WT (A), *E. coli* MG1655 Δ*acrR* (B), *E. coli* MG1655 *acrR*(V29G) (C) and *E. coli* MG1655 *acrR*(T32fs) (D) were grown in MSX medium in the absence [■] or presence [●] of 20 %(v/v) BMA, in 30 mL vials at 37°C and 250 rpm shaking. BMA was added immediately after inoculation. Means of two replicates are shown and error bars represent standard deviations. Growth data shown in Table 5.2, page 107.

In the absence of BMA, all strains, *E. coli* MG1655 *acrR*(V29G), *E. coli* MG1655 *acrR*(T32fs), *E. coli* MG1655 Δ*acrR* and *E. coli* MG1655 WT, were able to grow with similar growth profiles, showing that the neither the absence of *acrR* nor the presence of the *acrR*(V29G) or *acrR*(T32fs) affected growth under non-toxic conditions (Figure 5.5). However, in the presence of 20 %(v/v) BMA, the *E. coli* strains tested showed different levels of tolerance. Both *E. coli* MG1655 WT and *E. coli* MG1655 Δ*acrR* were not able to grow in the presence of 20 %(v/v) BMA (Figure 5.5 A and B). This indicated that the loss of function of *acrR* was not beneficial for BMA resistance.

Although *E. coli* MG1655 *acrR*(V29G) (Figure 5.5 C) and *E. coli* MG1655 *acrR*(T32fs) (Figure 5.5 D) had a lag phase of at least 8 h, they were eventually able to grow in the presence of 20 %(v/v) BMA. Still, there were differences between the strains, as *E. coli* MG1655 *acrR*(V29G) and *E. coli* MG1655 *acrR*(T32fs) reached a maximum OD_{600nm} of 0.63 ± 0.12 and 0.87 ± 0.05, respectively. Furthermore, after 24 h, *E. coli* MG1655 *acrR*(V29G) had an OD_{600nm} 10 times lower than *E. coli* MG1655 *acrR*(T32fs). Hence, even though both strains with single *acrR* mutations behaved similarly, the strain with the truncated AcrR, *E. coli* MG1655 *acrR*(T32fs), had a shorter lag phase and reached higher OD_{600nm} than *E. coli* MG1655 *acrR*(V29G). Encoding a truncated AcrR, which most likely leads to a non-functional protein incapable of repressing the expression of *acrAB*, improved tolerance to BMA. Hence, these *acrR* KO and KI tests showed results that are difficult to reconcile. Further studies would be necessary to understand whether the mutated *acrR* genes encode a functional or non-functional AcrR.

Additionally, the *acrR* KO strain purchased from the Keio collection[256], *E. coli* BW25113 Δ*acrR::kan* (*E. coli* JW0453), was also tested in the absence and presence of 20 %(v/v) BMA, as an extra control. The results obtained were comparable to *E. coli* MG1655 Δ*acrR. E. coli* BW25113 Δ*acrR::kan* was able to grow in the absence of BMA, but in the presence of BMA, it did not grow even after 24 h (Appendix 11.5, Table 11.5, page 210).

5.1.2.2 Effect of genetic complementations

Since neither the *acrR* KO strain with the eliminated antibiotic cassette, *E. coli* MG1655 Δ*acrR*, nor *E. coli* MG1655 WT were able to grow in the presence of 20 %(v/v) BMA, the mutated genes *acrR*(V29G) or *acrR*(T32fs) were supplemented in a recombinant plasmid to know whether the BMA resistance would be restored. *E. coli* MG1655 Δ*acrR* pSC101_*acrR*(V29G), *E. coli* MG1655 WT pSC101_*acrR*(V29G), *E. coli* MG1655 Δ*acrR* pSC101_*acrR*(T32fs) and *E. coli* MG1655 WT pSC101_*acrR*(T32fs) were grown in the absence or presence of 20 %(v/v) BMA, and compared to the KI strains *E. coli* MG1655 *acrR*(V29G) and *E. coli* MG1655 *acrR*(T32fs) (Figure 5.6, Figure 5.7 and Table 5.2). In addition, other control strains were tested in the same way, namely *E. coli* MG1655 WT pSC101, *E. coli* MG1655 WT pSC101_*acrR*(WT) (Figure 5.6, Figure 5.7 and Table 5.2).

In the absence of BMA, all the new strains with the plasmids pSC101_*acrR*(V29G), pSC101_*acrR*(T32fs), pSC101_*acrR*(WT) or the empty pSC101 were able to grow (Figure 5.6 A and Figure 5.7), showing that the presence of the plasmids brought no extra burden on the normal growth of the cells. In accordance with the previous data, the control strains *E. coli* MG1655 WT pSC101 and *E. coli* MG1655 WT pSC101_*acrR*(WT) could not grow in the presence of 20 %(v/v) BMA (Figure 5.6 B).

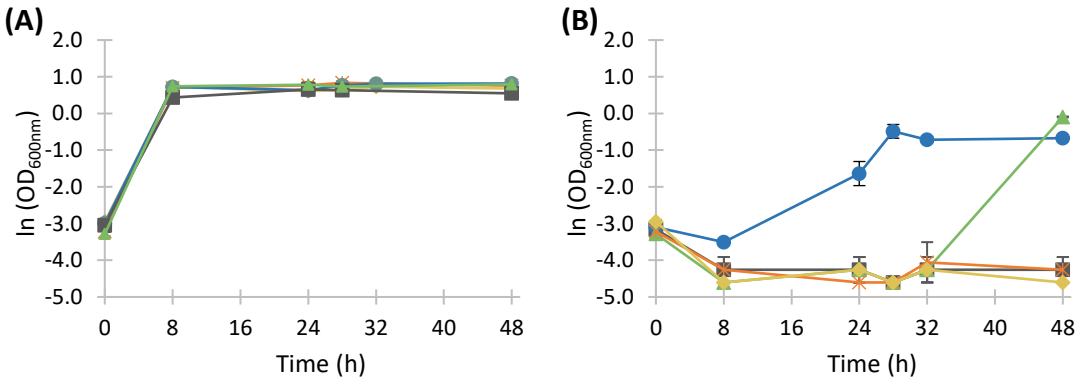

Figure 5.6 - Effect of BMA on the growth of *E. coli* MG1655 strains with the chromosomal or plasmid-based *acrR*(V29G) mutation. *E. coli* MG1655 *acrR*(V29G) **[●]**, *E. coli* MG1655 Δ*acrR* pSC101_*acrR*(V29G) **[■],** *E. coli* MG1655 WT pSC101_*acrR*(V29G) [▲], *E. coli* MG1655 WT pSC101_*acrR*(WT) [◆] and *E. coli* MG1655 WT pSC101 [✳] were grown in MSX medium with tetracycline (12.5 µg/mL), in the absence (A) and presence (B) of 20 %(v/v) BMA, in 30 mL vials at 37°C and 250 rpm. BMA was added immediately after inoculation. Means of two replicates are shown and error bars represent standard deviations. Growth data shown in Table 5.2, page 107.

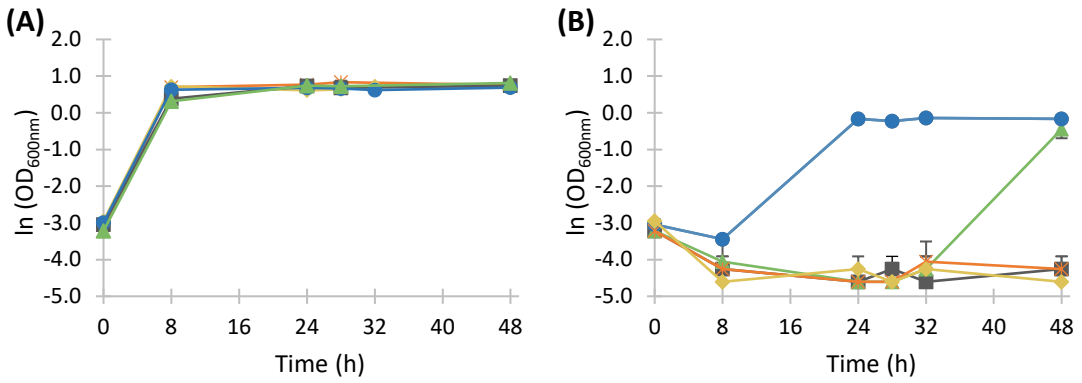

Figure 5.7 - Effect of BMA on the growth of *E. coli* MG1655 strains with the chromosomal or plasmid-based *acrR*(T32fs) mutation. *E. coli* MG1655 *acrR*(T32fs) **[●]**, *E. coli* MG1655 Δ*acrR* pSC101_*acrR*(T32fs) **[■],** *E. coli* MG1655 WT pSC101_*acrR*(T32fs) [▲], *E. coli* MG1655 WT pSC101_*acrR*(WT) [◆] and *E. coli* MG1655 WT pSC101 [*] were grown in MSX medium with tetracycline (12.5 µg/mL), in the absence (A) and presence (B) of 20 %(v/v) BMA, in 30 mL vials at 37°C and 250 rpm. BMA was added immediately after inoculation. Means of two replicates are shown and error bars represent standard deviations. Growth data shown in Table 5.2, page 107.

However, *E. coli* MG1655 Δ*acrR* pSC101_*acrR*(V29G) (Figure 5.6 B) and *E. coli* MG1655 Δ*acrR* pSC101_*acrR*(T32fs) (Figure 5.7 B) could not grow in the presence of 20 %(v/v) BMA, even after 48 h. Yet, as shown before, the KI mutants *E. coli* MG1655 *acrR*(V29G) (Figure 5.6 B) and *E. coli* MG1655 *acrR*(T32fs) (Figure 5.7 B) were able to reach maximum OD_{600nm} of 0.63 ± 0.12 and 0.87 ± 0.05, respectively. Thus, the addition of the plasmids pSC101_*acrR*(V29G) and pSC101_*acrR*(T32fs) to the *acrR* KO strains made no difference in terms of ability to tolerate BMA. *E. coli* MG1655 Δ*acrR* could not grow in the presence of BMA and the addition of pSC101_*acrR*(V29G) or pSC101_*acrR*(T32fs) gave the same results.

By contrast, *E. coli* MG1655 WT pSC101_*acrR*(V29G) (Figure 5.6 B) and *E. coli* MG1655 WT pSC101_*acrR*(T32fs) (Figure 5.7 B) were able to reach maximum OD_{600nm} of 0.91 ± 0.01 and 0.66 ± 0.16, respectively, yet they both had a lag phase of at least 32 h. Even though the mutated *acrR* genes were being expressed, the presence of the WT *acrR* possibly had a negative effect, still repressing the expression of *acrAB*. Thus, the addition of pSC101_*acrR*(V29G) or pSC101_*acrR*(T32fs) did not fully restore tolerance to BMA in the WT strain.

Table 5.2 - Effect of BMA on the OD_{600nm} of *E. coli* MG1655 *acrR* mutant strains. All strains were grown in MSX medium in the absence or presence of 20 %(v/v) BMA, in 30 mL vials at 37°C and 250 rpm. BMA was added immediately after inoculation. Means of two replicates and standard deviations are shown. NG indicates no growth.

	0 %(v/v) BMA		20 %(v/v) BMA	
***E. coli* MG1655 strains**	**OD_{600nm} after 8 h**	**Max OD_{600nm}**	**OD_{600nm} after 8 h**	**Max OD_{600nm}**
WT	2.12 ± 0.08	2.29 ± 0.01	NG	
WT pSC101	2.01 ± 0.08	2.31 ± 0.10	NG	
acrR(V29G)	2.07 ± 0.16	2.26 ± 0.02	0.03 ± 0.00	0.63 ± 0.12
acrR(T32fs)	1.88 ± 0.04	1.99 ± 0.07	0.03 ± 0.00	0.87 ± 0.05
Δ*acrR*	1.95 ± 0.01	2.17 ± 0.19	NG	
Δ*acrR* pSC101_*acrR*(V29G)	1.54 ± 0.03	1.93 ± 0.05	NG	
Δ*acrR* pSC101_*acrR* (T32fs)	1.47 ± 0.01	2.10 ± 0.12	NG	
WT pSC101_*acrR* (V29G)	2.09 ± 0.05	2.22 ± 0.12	0.01 ± 0.00	0.91 ± 0.01
WT pSC101_*acrR* (T32fs)	1.37 ± 0.03	2.26 ± 0.11	0.02 ± 0.01	0.66 ± 0.16
WT pSC101_*acrR*(WT)	2.07 ± 0.02	2.07 ± 0.04	NG	

In summary, with the new KI strains *E. coli* MG1655 *acrR*(V29G) and *E. coli* MG1655 *acrR*(T32fs) it was established that the mutated genes *acrR*(V29G) and *acrR*(T32fs) can confer tolerance to BMA by themselves, without the extra *soxR*(R20H) mutation. Yet, in the presence of BMA, both *E. coli* MG1655 *acrR*(V29G) and *E. coli* MG1655 *acrR*(T32fs) had a lag phase of at least 8 h and a slower growth compared to *E. coli* MG1655 *soxR*(R20H), which after 8 h reached an OD_{600nm} of 0.13 ± 0.01 (Table 5.1). However, *E. coli* MG1655 ΔacrR was not able to grow in the presence of BMA. As AcrR is a transcription factor that represses the expression of the membrane transporter proteins AcrAB, the experiments showed contradictory results. As the *acrR*(T32fs) gene most likely encodes a non-functional truncated protein, and the presence of both *acrR*(T32fs) or *acrR*(V29G) mutations gave the same level of BMA resistance, it could be concluded that the possible effect of the *acrR* mutations is the loss of function of AcrR. However, since the *acrR* KO did not confer tolerance to BMA, it seems that the mutated genes need to be present, *i.e.* a region encoded within the *acrR* gene could be essential to control the transcription of *acrAB* or other genes. This could be explained by the presence of a regulatory small RNA in the *acrR* sequence. However, to the best of my knowledge, no small RNA has been identified in that region of the DNA in *E. coli* MG1655. Further tests would be necessary to know if the

mutations found in *acrR* lead to a functional or non-functional protein and how the mutations possibly affect the regulation of *acrAB*. Moreover, the genetic complementations with the plasmids pSC101_*acrR*(V29G) or pSC101_*acrR*(T32fs) did not confer a high tolerance to BMA, such as the tolerance levels seen with *E. coli* MG1655 *acrR*(V29G) and *E. coli* MG1655 *acrR*(T32fs).

5.1.3 *ybcO* mutants

New KI and KO strains were also prepared to evaluate the impact of the uncharacterized protein YbcO towards BMA resistance. *E. coli* MG1655 Δ*ybcO* and *E. coli* MG1655 *ybcO*(I87M) were tested in the absence and presence of 20 %(v/v) BMA, added immediately after inoculation (Figure 5.8). In the absence of BMA, both *E. coli* MG1655 Δ*ybcO* (Figure 5.8 B) and *E. coli* MG1655 *ybcO*(I87M) (Figure 5.8 C) were able to grow similarly to the WT strain. However, in the presence of 20 %(v/v) BMA, both *E. coli* MG1655 Δ*ybcO* (Figure 5.8 B) and *E. coli* MG1655 *ybcO*(I87M) (Figure 5.8 C) did not grow, even after 48 h.

E. coli BW25113 Δ*ybcO::kan* (*E. coli* JW0537), purchased from the Keio collection[256] was also tested in the presence of 20 %(v/v) BMA, added immediately after inoculation (Appendix 11.5, Table 11.5, page 210). *E. coli* BW25113 Δ*ybcO::kan* (*E. coli* JW0537) had the same results as *E. coli* MG1655 Δ*ybcO*, it was able to grow normally when no BMA as added, but in the presence of 20 %(v/v) BMA did not grow for the 24 h period that was tested. It is also worth mentioning that the gene deletion in the Keio collection strain *E. coli* BW25113 Δ*ybcO::kan* (*E. coli* JW0537) affects the upstream gene of *ybcO*, named *ninE*, also an uncharacterized protein part of the DLP12 prophage, as is *ybcO*[267]. The gene *ninE* is partially overlapping with *ybcO*, so the PCR primers used in the Keio collection also delete the last 5 bp of *ninE*, including the stop condon. Hence, as an extra control, a new strain with the *ybcO* deletion in the same BW25113 background was also prepared in this study, yet the results obtained were the same. The new *E. coli* BW25113 Δ*ybcO::kan* was also able to grow in the absence of BMA but not in its presence (Appendix 11.5, Table 11.5, page 210).

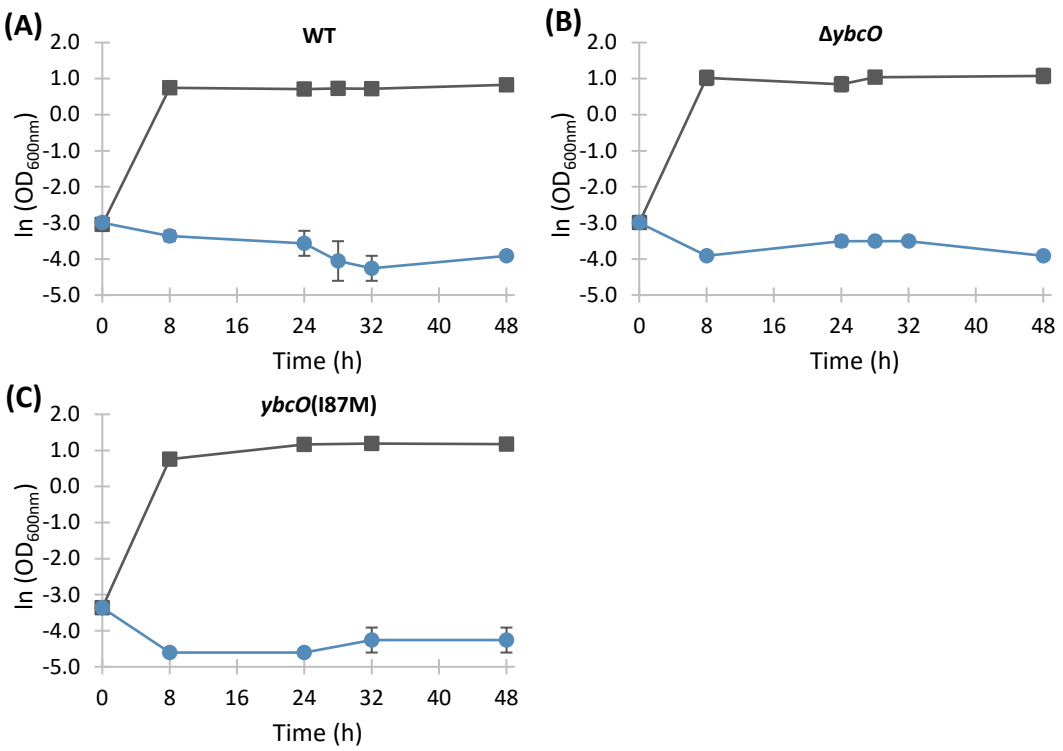

Figure 5.8 - Effect of BMA on the growth of *E. coli* MG1655 *ybcO* mutants. *E. coli* MG1655 WT (A), *E. coli* MG1655 Δ*ybcO* (B) and *E. coli* MG1655 *ybcO*(I87M) (C) were grown in MSX medium in the absence [■] or presence [●] of 20 %(v/v) BMA, in 30 mL vials at 37°C and 250 rpm shaking. BMA was added immediately after inoculation. Means of two replicates are shown and error bars represent standard deviations. Growth data shown in Table 5.3, page 111.

Neither the presence of *ybcO*(I87M) nor the deletion of *ybcO* were beneficial towards BMA tolerance. The mutated gene *ybcO*(I87M) did not confer tolerance to BMA by itself and therefore might not be involved in the mechanism of resistance to BMA. Possibly, the mutation *ybcO*(I87M) occurred only by chance and the isolated strain *E. coli* MG1655 *soxR*(R20H)*ybcO*(I87M) was resistant to BMA only due to mutation in the *soxR* gene. Hence, plasmid-based genetic complementations were not done with the *ybcO*(I87M) mutation. The *ybcO* gene was only further studied by developing new double deletions strains together with the *soxR* gene.

5.1.4 *soxR* and *ybcO* mutants

The genes *soxR* and *ybcO* were further tested by preparing a double KO strain. *E. coli* MG1655 Δ*soxR*Δ*ybcO* was tested in the absence and presence of 20 %(v/v) BMA, added immediately after inoculation (Figure 5.9). The KO strain *E. coli* MG1655

Δ*soxR*Δ*ybcO* was able to grow in the absence of BMA, but did not grow in its presence.

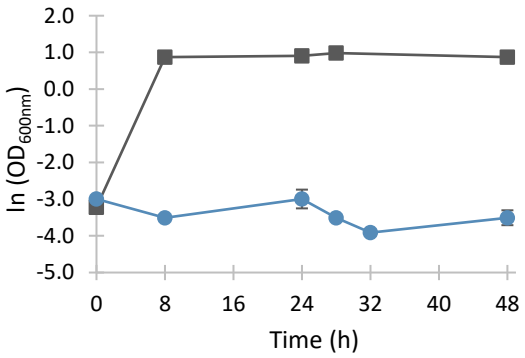

Figure 5.9 - Effect of BMA on the growth of *E. coli* MG1655 *ΔsoxRΔybcO*. *E. coli* MG1655 Δ*soxR*Δ*ybcO* was grown in MSX medium in the absence [■] or presence [●] of 20 %(v/v) BMA, in 30 mL vials at 37°C and 250 rpm. BMA was added immediately after inoculation. Means of two replicates are shown and error bars represent standard deviations. Growth data shown in Table 5.3, page 111.

In addition, *ybcO* was also deleted in the mutant strain with the *soxR* mutation, *E. coli* MG1655 *soxR*(R20H). The resulting strain, *E. coli* MG1655 *soxR*(R20H)Δ*ybcO*, was then grown in the absence and presence of 20 %(v/v) BMA and compared with the mutant *E. coli* MG1655 *soxR*(R20H)*ybcO*(I87M) (Figure 5.10). *E. coli* MG1655 *soxR*(R20H)Δ*ybcO* was capable of growing in the presence of 20 %(v/v) BMA (Figure 5.10 B), reaching an OD_{600nm} of 0.13 ± 0.02 and 0.84 ± 0.11, after 8 and 24 h, respectively. This growth profile was comparable to the growth profile of *E. coli* MG1655 *soxR*(R20H)*ybcO*(I87M), which reached an OD_{600nm} of 0.16 ± 0.02 and 0.98 ± 0.05, after 8 and 24 h of incubation, respectively, and also very comparable to *E. coli* MG1655 *soxR*(R20H), which reached an OD_{600nm} of 0.13 ± 0.01 and 0.80 ± 0.07, after 8 and 24 h of incubation, respectively. A double mutant was also prepared with the Keio collection background, *E. coli* BW25113 Δ*soxR*Δ*ybcO::kan,* which grew in the absence of BMA, but was not able to survive in the presence of 20 %(v/v) BMA (Appendix 11.5, Table 11.5, page 210).

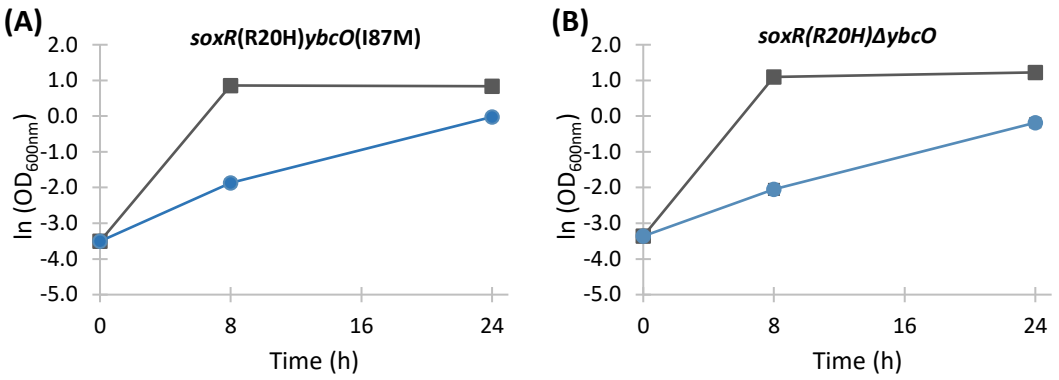

Figure 5.10 - Effect of BMA on the growth of *E. coli* MG1655 *soxR* and *ybcO* mutants. *E. coli* MG1655 *soxR*(R20H)*ybcO*(I87M) (A) and *E. coli* MG1655 *soxR*(R20H)Δ*ybcO* (B) were grown in MSX medium in the absence [■] or presence [●] of 20 %(v/v) BMA, in 30 mL vials at 37°C and 250 rpm. BMA was added immediately after inoculation. Means of two replicates are shown and error bars represent standard deviations. Growth data shown in Table 5.3.

Table 5.3 - Effect of BMA on the OD_{600nm} of *E. coli* MG1655 *ybcO* and *soxR* mutant strains. All strains were grown in MSX medium the absence or presence of 20 %(v/v) BMA, in 30 mL vials at 37°C and 250 rpm. BMA was added immediately after inoculation. Means of two replicates and standard deviations are shown. NG indicates no growth.

	0 %(v/v) BMA		20 %(v/v) BMA	
***E. coli* MG1655 strains**	**OD_{600nm} after 8 h**	**Max OD_{600nm}**	**OD_{600nm} after 8 h**	**Max OD_{600nm}**
WT	2.12 ± 0.08	2.29 ± 0.01	NG	
soxR(R20H)	2.25 ± 0.06	2.58 ± 0.03	0.13 ± 0.01	0.80 ± 0.07
soxR(R20H)*ybcO*(I87M)	2.36 ± 0.04	2.36 ± 0.04	0.16 ± 0.02	0.98 ± 0.05
ybcO(I87M)	2.14 ± 0.12	3.29 ± 0.03	NG	
Δ*ybcO*	3.02 ± 0.24	3.02 ± 0.24	NG	
soxR(R20H)Δ*ybcO*	3.01 ± 0.04	3.41 ± 0.08	0.13 ± 0.02	0.84 ± 0.11
Δ*soxR*Δ*ybcO*	2.45 ± 0.06	2.61 ± 0.07	NG	

In summary, even with the addition of the mutated gene *ybcO*(I87M) or the deletion of *ybcO* in a strain with *soxR*(R20H), the results obtained were the same as the strain with only *soxR*(R20H) by itself. Hence, *ybcO* might not contribute to BMA tolerance.

5.1.5 *soxR* and *acrR* mutants

5.1.5.1 Effect of gene deletions

In section 4.1, it was shown that *E. coli* MG1655 *soxR*(R20H)*acrR*(V29G) and *E. coli* MG1655 *soxR*(R20H)*acrR*(T32fs) were the mutant strains with the highest levels of BMA tolerance. Hence, it was necessary to further study the impact of the combination of *soxR* and *acrR* mutations towards BMA resistance in *E. coli*. Firstly, a double *soxR* and *acrR* KO strain was prepared and grown in the absence or presence of 20 %(v/v) BMA (Figure 5.11).

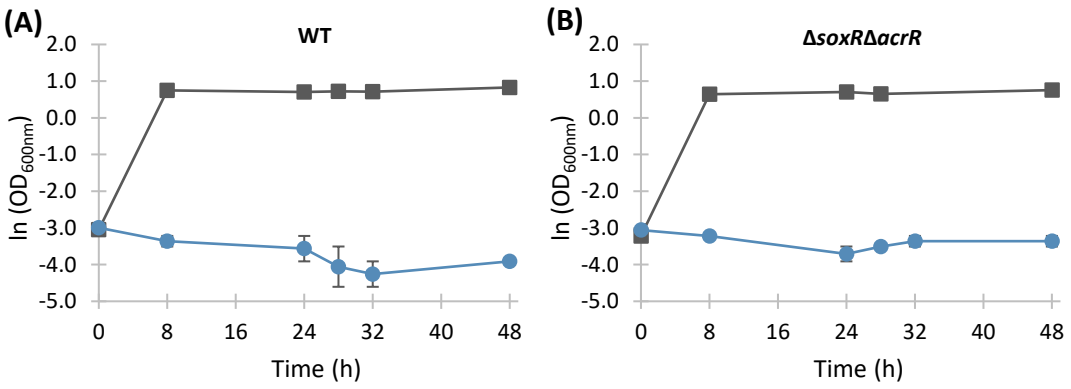

Figure 5.11 - Effect of BMA on the growth of *E. coli* MG1655 Δ*soxR*Δ*acrR*. *E. coli* MG1655 WT (A) and *E. coli* MG1655 Δ*soxR*Δ*acrR* (B) were grown in MSX medium in the absence [■] or presence [●] of 20 %(v/v) BMA, in 30 mL vials at 37°C and 250 rpm shaking. BMA was added immediately after inoculation. Means of two replicates are shown and error bars represent standard deviations. Growth data shown in Table 5.4, page 116.

Although in the absence of BMA *E. coli* MG1655 Δ*soxR*Δ*acrR* could grow, in the presence of 20 %(v/v) BMA it did not grow, like the WT strain (Figure 5.11 B). As *E. coli* MG1655 Δ*soxR* and *E. coli* MG1655 Δ*acrR* did not grow in the presence of BMA, it was not surprising that *E. coli* MG1655 Δ*soxR*Δ*acrR* also could not grow. Nevertheless, a double *soxR* and *acrR* KO also prepared with the Keio collection background, *E. coli* BW25113 Δ*soxR*Δ*acrR::kan,* which was also not able to survive in the presence of 20 %(v/v) BMA, even though it grew in its absence (Appendix 11.5, Table 11.5, page 210).

In addition, *acrR* was also deleted from the *E. coli* MG1655 *soxR*(R20H) mutant, to know if it would lead to a decrease or increase of the levels of tolerance to BMA. The

new KO strain, *E. coli* MG1655 *soxR*(R20H)Δ*acrR,* was then grown in the absence or presence of 20 %(v/v) BMA (Figure 5.12). *E. coli* MG1655 *soxR*(R20H)Δ*acrR* did grow in the absence of BMA, but in its presence was not able to grow.

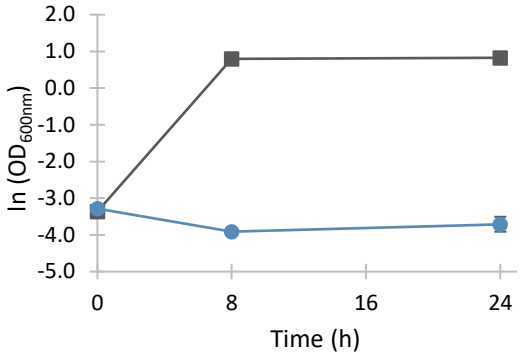

Figure 5.12 - Effect of BMA on the growth of *E. coli* MG1655 *soxR*(R20H)*ΔacrR*. *E. coli* MG1655 *soxR*(R20H)Δ*acrR* was grown in MSX medium in the absence [■] or presence [●] of 20 %(v/v) BMA, in 30 mL vials at 37°C and 250 rpm. BMA was added immediately after inoculation. Means of two replicates are shown and error bars represent standard deviations. Growth data shown in Table 5.4, page 116.

Even with the addition of the beneficial *soxR*(R20H) mutation, *E. coli* did not survive BMA-induced stress with *acrR* deleted from its chromosome. Further studies would be necessary to fully understand how the deletion of *acrR* is negatively affecting tolerance to BMA.

5.1.5.2 Effect of genetic complementations

To further understand the importance of the combination of *soxR*(R20H) plus *acrR*(V29G) or *acrR*(T32fs) mutations towards BMA tolerance, plasmid-based genetic complementations were done in the WT strain and *E. coli* MG1655 Δ*soxR*Δ*acrR*. Neither *E. coli* MG1655 WT nor *E. coli* MG1655 Δ*soxR*Δ*acrR* grew in the presence of 20 %(v/v) BMA (Figure 5.11 A and B). Hence, these strains were transformed with the plasmids pSC101_*soxR*(R20H)_*acrR*(V29G) or pSC101_*soxR*(R20H)_*acrR*(T32fs) to know whether resistance to BMA would be improved. The new strains with the recombinant plasmids, *E. coli* MG1655 Δ*soxR*Δ*acrR* pSC101_*soxR*(R20H)_*acrR*(V29G), *E. coli* MG1655 Δ*soxR*Δ*acrR* pSC101_*soxR*(R20H)_*acrR*(T32fs), *E. coli* MG1655 WT pSC101_*soxR*(R20H)_*acrR*(V29G) and *E. coli* MG1655 Δ*soxR*Δ*acrR* pSC101_*soxR*(R20H)_*acrR*(T32fs), were then grown in the absence or presence of 20

%(v/v) BMA. Additionally, controls with the WT genes or the empty plasmid, *E. coli* MG1655 WT pSC101_*soxR*(WT)_*acrR*(WT) and *E. coli* MG1655 WT pSC101, respectively, were tested in the same way (Figure 5.13, Figure 5.14 and Table 5.4).

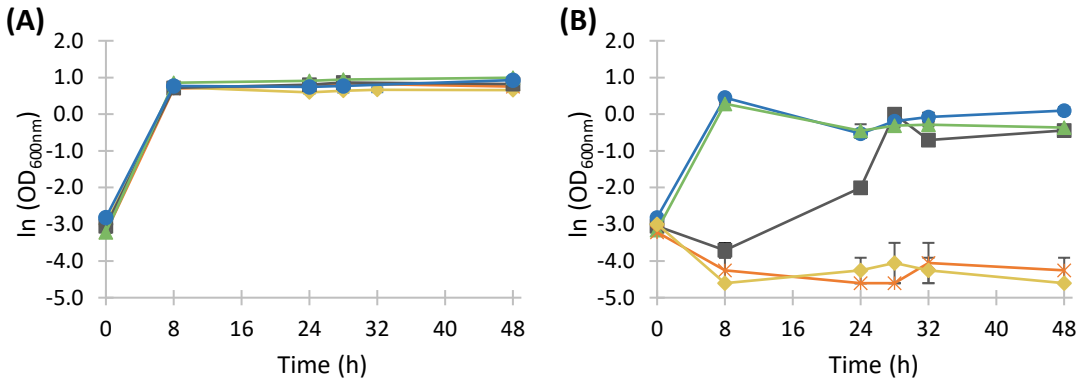

Figure 5.13 - Effect of BMA on the growth of *E. coli* MG1655 strains with chromosomal or plasmid-based *soxR*(R20H) and *acrR*(V29G) mutations. *E. coli* MG1655 *soxR*(R20H)*acrR*(V29G) **[●]**, *E. coli* MG1655 Δ*soxR*Δ*acrR* pSC101_*soxR*(R20H)*acrR*(V29G) **[■]** and *E. coli* MG1655 WT pSC101_*soxR*(R20H)*acrR*(V29G) [▲], *E. coli* MG1655 WT pSC101_soxR(WT)_acrR(WT) [◆] and *E. coli* MG1655 WT pSC101 [✳] were grown in MSX medium with tetracycline (12.5 µg/mL), **either (A) in the absence of BMA or (B)** in the presence of 20 %(v/v) BMA, in 30 mL vials at 37°C and 250 rpm. BMA was added immediately after inoculation. Means of two replicates are shown and error bars represent standard deviations. Growth data shown in Table 5.4, page 116.

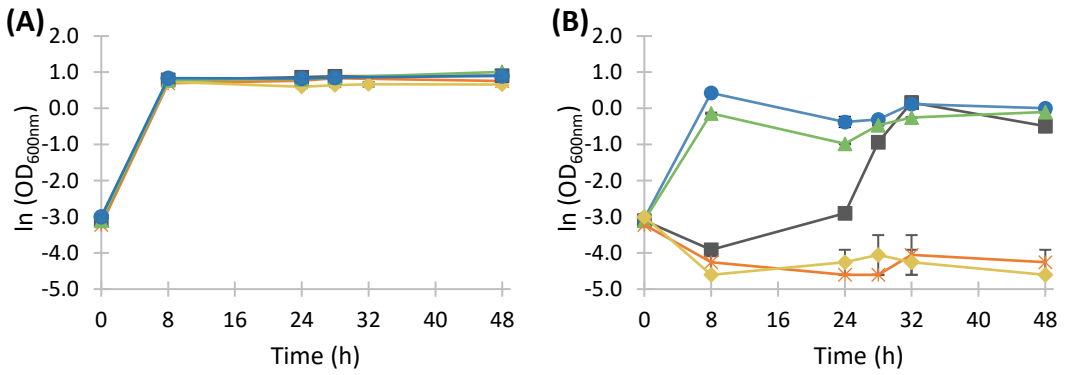

Figure 5.14 - Effect of BMA on the growth of *E. coli* MG1655 strains with chromosomal or plasmid-based *soxR*(R20H) and *acrR*(T32fs) mutations. *E. coli* MG1655 *soxR*(R20H)*acrR*(T32fs) **[●]**, *E. coli* MG1655 Δ*soxR*Δ*acrR* pSC101_*soxR*(R20H)*acrR*(T32fs) **[■]** and *E. coli* MG1655 WT pSC101_*soxR*(R20H)*acrR*(T32fs) [▲], *E. coli* MG1655 WT pSC101_soxR(WT)_acrR(WT) [◆] and *E. coli* MG1655 WT pSC101 [✳] were grown in MSX medium with tetracycline (12.5 µg/mL), **either (A) in the absence of BMA or (B)** in the presence of 20 %(v/v) BMA, in 30 mL vials at 37°C and 250 rpm. BMA was added immediately after inoculation. Means of two replicates are shown and error bars represent standard deviations. Growth data shown in Table 5.4, page 116.

All strains were able to grow in the absence of BMA (Figure 5.13 A and Figure 5.14 A). In the presence of 20 %(v/v) BMA, the control strains *E. coli* MG1655 WT pSC101_*soxR*(WT)_*acrR*(WT) and *E. coli* MG1655 WT pSC101 were not able to grow (Figure 5.13 B). Yet, *E. coli* MG1655 Δ*soxR*Δ*acrR* pSC101_*soxR*(R20H)_*acrR*(V29G)

(Figure 5.13 B), *E. coli* MG1655 WT pSC101_*soxR*(R20H)_*acrR*(V29G) (Figure 5.13 B), *E. coli* MG1655 Δ*soxR*Δ*acrR* pSC101_*soxR*(R20H)_*acrR*(T32fs) (Figure 5.14 B) and *E. coli* MG1655 WT pSC101_*soxR*(R20H)_*acrR*(T32fs) (Figure 5.14 B), were able to grow in the presence of 20 %(v/v) BMA.

However, the tolerance to BMA, as reported by the length of the lag phase, was higher when pSC101_*soxR*(R20H)_*acrR*(V29G) or pSC101_*soxR*(R20H)_*acrR*(T32fs) were added to the WT strain than when they were added to the double KO *E. coli* MG1655 Δ*soxR*Δ*acrR.* In the presence of 20 %(v/v) BMA, both *E. coli* MG1655 WT pSC101_*soxR*(R20H)_*acrR*(V29G) (Figure 5.13 B) and *E. coli* MG1655 WT pSC101_*soxR*(R20H)_*acrR*(T32fs) (Figure 5.14 B) were able to reach high OD_{600nm} after just 8 h, 1.33 ± 0.04 and 0.87 ± 0.02, respectively. Moreover, *E. coli* MG1655 WT pSC101_*soxR*(R20H)_*acrR*(V29G) (Figure 5.13 B) and *E. coli* MG1655 WT pSC101_*soxR*(R20H)_*acrR*(T32fs) (Figure 5.14 B) had growth profiles very similar to the corresponding strains with the mutations in the chromosome, *E. coli* MG1655 *soxR*(R20H)*acrR*(V29G) and *E. coli* MG1655 *soxR*(R20H)*acrR*(T32fs), which after 8 h reached OD_{600nm} of 1.58 ± 0.13 and 1.54 ± 0.10, respectively. Thus, even though the *acrR* and *soxR* WT genes were present in the chromosome, the extra copies of *soxR*(R20H) and *acrR*(V29G) or *acrR*(T32fs) being expressed in *E. coli* MG1655 WT pSC101_*soxR*(R20H)_*acrR*(V29G) and *E. coli* MG1655 WT pSC101_*soxR*(R20H)_*acrR*(T32fs) did confer tolerance to the WT strain, that otherwise would not be able to survive in the presence of 20 %(v/v) BMA.

In contrast, in the presence of 20 %(v/v) BMA, *E. coli* MG1655 Δ*soxR*Δ*acrR* pSC101_*soxR*(R20H)_*acrR*(V29G) (Figure 5.13 B) and *E. coli* MG1655 Δ*soxR*Δ*acrR* pSC101_*soxR*(R20H)_*acrR*(T32fs) (Figure 5.14B) were able to grow to maximum OD_{600nm} of 1.00 ± 0.02 and 1.20 ± 0.21, respectively, reaching similar OD_{600nm} to *E. coli* MG1655 *soxR*(R20H)*acrR*(V29G) and *E. coli* MG1655 *soxR*(R20H)*acrR*(T32fs) after 28 h and 32 h of growth, respectively. Yet, both *E. coli* MG1655 Δ*soxR*Δ*acrR* pSC101_*soxR*(R20H)_*acrR*(V29G) (Figure 5.13 B) and *E. coli* MG1655 Δ*soxR*Δ*acrR* pSC101_*soxR*(R20H)_*acrR*(T32fs) (Figure 5.14 B) had lag phases of at least 8 h.

E. coli MG1655 Δ*soxR* pSC101_*soxR*(R20H) was able to grow in the presence of BMA, with a growth profile similar to *E. coli* MG1655 *soxR*(R20H) (Figure 5.4, section 5.1.1), while both *E. coli* MG1655 Δ*acrR* pSC101_*acrR*(T32fs) and *E. coli* MG1655 Δ*acrR* pSC101_*acrR*(V29G) had lag phases of at least 32 h when grown in the presence of BMA (Figure 5.6 and Figure 5.7, section 5.1.2). Hence, the presence of the *acrR* deletion which results in a short scar sequence in the chromosome, might be affecting the growth in the presence of BMA and preventing *E. coli* MG1655 Δ*acrR* pSC101_*acrR*(T32fs), *E. coli* MG1655 Δ*acrR* pSC101_ *acrR*(V29G), *E. coli* MG1655 Δ*soxR*Δ*acrR* pSC101_*soxR*(R20H)_*acrR*(V29G) and *E. coli* MG1655 Δ*soxR*Δ*acrR* pSC101_*soxR*(R20H)_*acrR*(T32fs) from growing without having long lag phases of at least 8 h. Nevertheless, further studies would be necessary to fully understand if the deletion of *acrR* definitely has a negative effect towards tolerance to BMA in *E. coli*.

Table 5.4 - Effect of BMA on the OD_{600nm} of *E. coli* MG1655 *soxR* and *acrR* mutant strains. All strains were grown in MSX medium in the absence or presence of 20 %(v/v) BMA, in 30 mL vials at 37°C and 250 rpm. BMA was added immediately after inoculation. Means of two replicates and standard deviations are shown. NG indicates no growth.

	0 %(v/v) BMA		20 %(v/v) BMA	
***E. coli* MG1655 strains**	**OD_{600nm} after 8 h**	**Max OD_{600nm}**	**OD_{600nm} after 8 h**	**Max OD_{600nm}**
WT	2.12 ± 0.08	2.29 ± 0.01	NG	
WT pSC101	2.01 ± 0.08	2.31 ± 0.10	NG	
soxR(R20H)*acrR*(V29G)	2.17 ± 0.04	2.54 ± 0.12	1.58 ± 0.13	1.58 ± 0.13
soxR(R20H)*acrR*(T32fs)	2.32 ± 0.07	2.46 ± 0.14	1.54 ± 0.10	1.54 ± 0.10
soxR(R20H)Δ*acrR*	2.22 ± 0.06	2.29 ± 0.05	NG	
Δ*soxR*Δ*acrR*	1.91 ± 0.09	2.13 ± 0.09	NG	
Δ*soxR*Δ*acrR* pSC101_*soxR*(R20H)_*acrR*(V29G)	2.05 ± 0.07	2.37 ± 0.01	0.03 ± 0.01	1.00 ± 0.02
Δ*soxR*Δ*acrR* pSC101_*soxR*(R20H) _*acrR*(T32fs)	2.22 ± 0.08	2.47 ± 0.02	0.02 ± 0.00	1.20 ± 0.21
WT pSC101_*soxR*(R20H)_*acrR*(V29G)	2.36 ± 0.03	2.70 ± 0.07	1.33 ± 0.04	1.33 ± 0.04
WT pSC101_*soxR*(R20H)_*acrR*(T32fs)	2.20 ± 0.12	2.75 ± 0.02	0.87 ± 0.02	0.91 ± 0.03
WT pSC101_*soxR*S(WT)_*acrR*(WT)	2.09 ± 0.01	2.09 ± 0.01	NG	

In summary, except for *ybcO*(I87M), all mutations, *soxR*(R20H), *acrR*(V29G) and *acrR*(T32fs) were able to confer tolerance to BMA by themselves. Yet, the combinations of mutations of *soxR*(R20H) plus *acrR*(V29G) or *acrR*(T32fs) were still the most advantageous, with the highest levels of tolerance towards BMA observed.

Moreover, none of the KO strains were able to grow in the presence of BMA. Additionally, when the recombinant plasmids pSC101_*soxR*(R20H)_*acrR*(V29G), pSC101_*soxR*(R20H)_*acrR*(T32fs) or pSC101_*soxR*(R20H), were supplemented in strains that could not survive BMA, namely *E. coli* MG1655 WT, *E. coli* MG1655 Δ*soxR*Δ*acrR* or *E. coli* MG1655 Δ*soxR,* they were able to restore tolerance to 20 %(v/v) BMA.

5.2 Effect of the antibiotic resistance cassettes on BMA tolerance

To further understand the effect of the *acrR* and *soxR* deletions on the growth of *E. coli* in the presence of BMA, the impact of the antibiotic resistance cassettes was also tested. The KO strains previously tested, *E. coli* MG1655 Δ*soxR, E. coli* MG1655 Δ*acrR* and *E. coli* MG1655 Δ*soxR*Δ*acrR,* did not have an antibiotic resistance cassette, only scar sequences of 102 bp (see Figure 5.1), and did not grow in the presence of 20 %(v/v) BMA. Hence, KO strains with kanamycin and/or chloramphenicol resistance cassettes present in the chromosome replacing either *soxR* or *acrR*, namely *E. coli* MG1655 Δ*soxR::kan, E. coli* MG1655 Δ*soxR::chl*, *E. coli* MG1655 Δ*acrR::kan, E. coli* MG1655 Δ*acrR::chl, E. coli* MG1655 Δ*soxR::kan*Δ*acrR, E. coli* MG1655 Δ*soxR*Δ*acrR::kan*, *E. coli* MG1655 Δ*soxR::kan*Δ*acrR::chl* and *E. coli* MG1655 Δ*soxR::chl*Δ*acrR::kan,* were also tested in the absence or presence of 20 % (v/v) BMA (Figure 5.15, Figure 5.16, and Figure 5.17; Table 11.6, in Appendix 11.5, page 210).

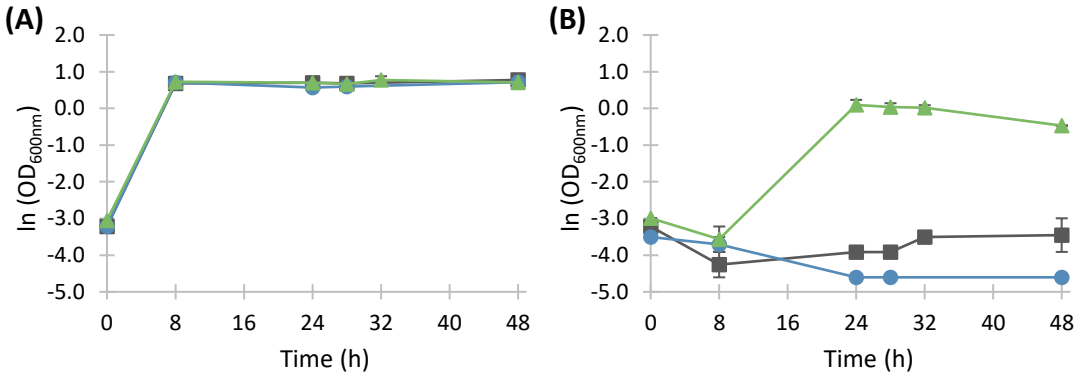

Figure 5.15 - Effect of BMA on the growth of *soxR* deletion strains with different antibiotic resistance cassettes. *E. coli* MG1655 Δ*soxR* **[■]**, *E. coli* MG1655 Δ*soxR::kan* **[●]** and *E. coli* MG1655 Δ*soxR::chl* [▲] were grown in MSX medium in the absence (A) or presence (B) of 20 %(v/v) BMA, in 30 mL vials at 37°C and 250 rpm. BMA was added immediately after inoculation. Means of two replicates are shown and error bars represent standard deviations. Growth data shown in Table 11.6, in Appendix 11.5, page 210.

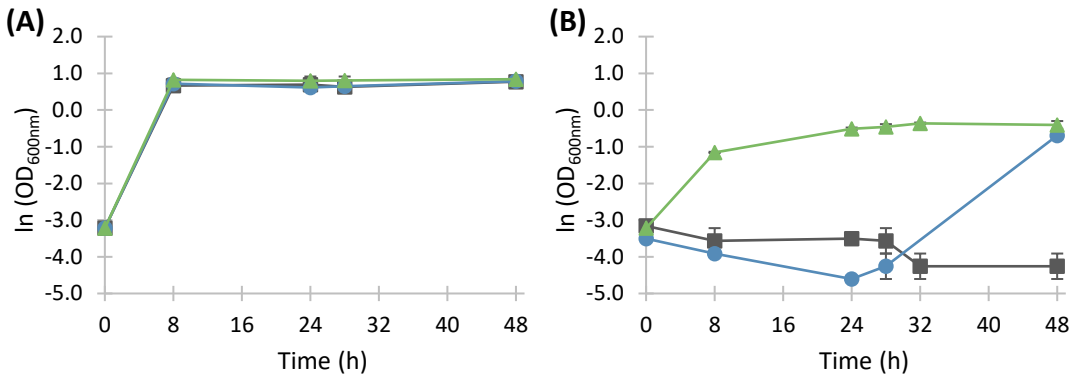

Figure 5.16 - Effect of BMA on the growth of *acrR* deletion strains with different antibiotic resistance cassettes. *E. coli* MG1655 Δ*acrR* **[■]**, *E. coli* MG1655 Δ*acrR::kan* **[●]** and *E. coli* MG1655 Δ*acrR::chl* [▲] were grown in MSX medium in the absence (A) or presence (B) of 20 %(v/v) BMA, in 30 mL vials at 37°C and 250 rpm. BMA was added immediately after inoculation. Means of two replicates are shown and error bars represent standard deviations. Growth data shown in Table 11.6, in Appendix 11.5, page 210

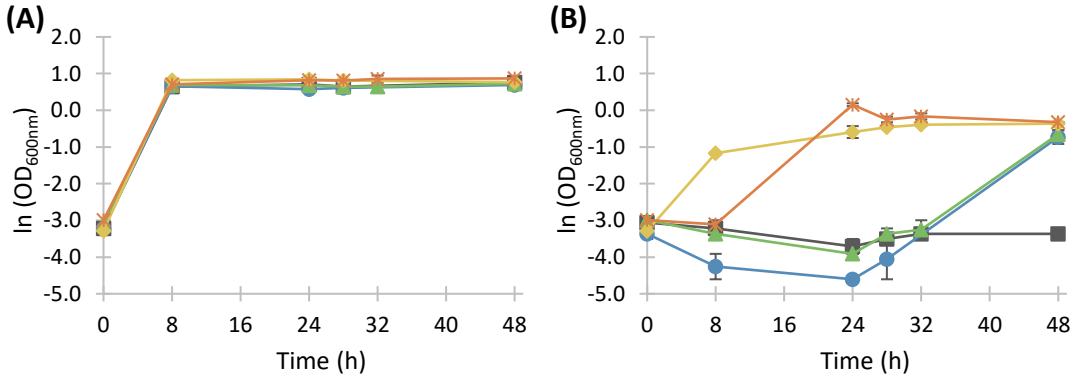

Figure 5.17 - Effect of BMA on the growth of *soxR* and *acrR* double deletion strains with different antibiotic resistance cassettes. *E. coli* MG1655 Δ*soxR*Δ*acrR* **[■]**, *E. coli* MG1655 Δ*soxR::kan*Δ*acrR* **[●]**, *E. coli* MG1655 Δ*soxR*Δ*acrR::kan* [▲], *E. coli* MG1655 Δ*soxR::kan*Δ*acrR::chl* [◆] and *E. coli* MG1655 Δ*soxR::chl*Δ*acrR::kan* [✱] were grown in MSX medium in the absence (A) or presence (B) of 20 %(v/v) BMA, in 30 mL vials at 37°C and 250 rpm. BMA was added immediately after inoculation. Means of two replicates are shown and error bars represent standard deviations. Growth data shown in Table 11.6, in Appendix 11.5, page 210.

All strains could grow in the absence of BMA (Figure 5.15 A, Figure 5.16 A, and Figure 5.17 A), suggesting that the presence of the antibiotic resistance cassettes did not affect the normal growth of the cells. However, in the presence of 20 %(v/v) BMA the KO strains had different behaviours (Figure 5.15 A, Figure 5.16 A, and Figure 5.17 A). The KO strains with only the kanamycin resistance cassette, *E. coli* MG1655 Δ*soxR::kan, E. coli* MG1655 Δ*acrR::kan, E. coli* MG1655 Δ*soxR::kan*Δ*acrR* and *E. coli* MG1655 Δ*soxR*Δ*acrR::kan,* either did not grow or had a lag phase of at least 28 h in the presence of 20 %(v/v) BMA. By contrast, when *acrR* was replaced by the chloramphenicol resistance cassette, *E. coli* MG1655 Δ*acrR::chl* and *E. coli* MG1655

Δ*soxR::kan*Δ*acrR::chl* could grow in the presence of 20 %(v/v) BMA with no apparent lag phase, and when *soxR* was replaced by the chloramphenicol resistance cassette, *E. coli* MG1655 Δ*soxR::chl* and *E. coli* MG1655 Δ*soxR::chl*Δ*acrR::kan* could grow in the presence of 20 %(v/v) BMA after a lag phase of at least 8 h. Thus, the presence of the chloramphenicol resistance cassette conferred tolerance to BMA in *E. coli*.

The antimicrobial mode of action of both kanamycin and chloramphenicol is by inhibiting protein synthesis[268]. Kanamycin binds to the 30S ribosomal subunit and disrupts the peptide elongation[268], whereas chloramphenicol binds to the 50S subunit disrupting the peptidyl transferase activity[269,270]. The chloramphenicol resistance cassette used in this work encodes a chloramphenicol acetyltransferase, which transfers an acetyl group from acetyl-CoA to the C3 hydroxyl group of chloramphenicol, forming the inactive derivative 1-acetyl chloramphenicol[269-271]. In a non-enzymatic step, the acetyl group is transferred from the C3 to C1 positions, and the chloramphenicol acetyltransferase can then catalyse another acetylation on the C3 position, forming the inactive derivative 1,3-diacetyl chloramphenicol. The kanamycin resistance cassette encodes an aminoglycoside 3'-phosphotransferase[272], which catalyses the phosphorylation of the hydroxyl group in the C3 position, using ATP as the phosphate donor, resulting in an inactivated kanamycin(3')-phosphate [273].

In this experiments, no chloramphenicol or kanamycin were added to the medium. Thus, further studies would be needed to understand why the presence of the chloramphenicol acetyltransferase confers resistance to BMA, but the presence of the aminoglycoside 3'-phosphotransferase does not.

Nevertheless, it seems that *acrR* and *soxR* have a clear influence on the tolerance to BMA. To further understand why the mutations found are essential to confer tolerance towards BMA and chemicals in *E. coli*, it was crucial to analyse the resistance mechanisms that are induced in response to BMA stress in the WT strain but also in the mutant strains.

6 Identification of global transcriptional responses to BMA

Modern "omics" technologies, such as genomics, transcriptomics, proteomics or metabolomics, allow a high-throughput, global analysis of cellular processes and functional dynamics in cells and tissues[274]. In particular, transcriptomics studies are extremely useful for the profiling of gene expression at a genome-wide level, through the quantification of mRNA transcripts[274].

Several different studies have been done to understand the transcriptomic responses of wild type *E. coli* strains to different commodity chemicals, such as ethanol, n-butanol, isobutanol and toluene.[88,89,96,100] (see section 1.2 and Table 11.1, in Appendix 11.1, page 194). In general, chemicals can induce several responses in the cells, including changes in the regulation of membrane transporters, membrane structure and fluidity, metabolic flux and induction of responses related to oxidative stress, iron homeostasis, heat shock, osmotic and acid stress, among others [88,89,96,100].

In this study, an RNA sequencing (RNA-seq) analysis, which uses next-generation sequencing, was done to: (1) determine if the mutations found had any effect on the expression of any genes, even in the absence of BMA, and (2) determine which cellular responses were subsequently induced in the presence of BMA in *E. coli* WT and in the mutant strains. With this analysis it was hypothesised that it would be possible to understand the tolerance mechanisms used by the mutants that enables them to survive under BMA stress.

Thus, *E. coli* MG1655 WT, *E. coli* MG1655 *soxR*(R20H), *E. coli* MG1655 *soxR*(R20H)*ybcO*(I87M), *E. coli* MG1655 *soxR*(R20H)*acrR*(V29G) and *E. coli* MG1655 *soxR*(R20H)*acrR*(T32fs) were initially grown in MSX medium under non-stressful conditions and 20 %(v/v) BMA was added during mid-exponential phase, after reaching an OD_{600nm} of approximately 0.3 (as shown in Figure 4.3, section 4.1.2, page 68). Samples for analysis were taken immediately before the addition of 20 %(v/v) BMA, and 1 h after its addition. For the WT strain, in addition to the samples taken before and 1 h after the addition of BMA, an extra control was done to detect basal changes in gene transcripts levels during normal growth, where a sample was also

taken 1 h after reaching an OD_{600nm} of 0.3, but without the addition of BMA. Cultures and subsequent total RNA extraction were done with three biological replicates. Results from RNA-seq analysis were then analysed according to the two different conditions, before and after the addition of BMA.

6.1 Effect of the mutations on the transcriptome of *E. coli* prior to BMA addition

RNA-seq analysis was firstly used to analyse the differentially expressed genes of *E. coli* MG1655 *soxR*(R20H), *E. coli* MG1655 *soxR*(R20H)*ybcO*(I87M), *E. coli* MG1655 *soxR*(R20H)*acrR*(V29G) and *E. coli* MG1655 *soxR*(R20H)*acrR*(T32fs) grown under no stress conditions, before the addition of BMA. The transcripts levels of the mutant strains were individually compared to the WT strain, to determine if the combinations of mutations found in *soxR*, *acrR* and/or *ybcO* altered the expression of any genes, compared to the WT expression levels, *i.e.* if any genes were differentially expressed. The RNA-seq data quality was confirmed by a principle component analysis (PCA) (Figure 11.8, in Appendix 11.6).

All four mutant strains, *E. coli* MG1655 *soxR*(R20H), *E. coli* MG1655 *soxR*(R20H)*ybcO*(I87M), *E. coli* MG1655 *soxR*(R20H)*acrR*(V29G) and *E. coli* MG1655 *soxR*(R20H)*acrR*(T32fs), had over one hundred differentially expressed genes, when compared to the WT strain (Figure 6.1 A). Moreover, all strains had a higher number of down-regulated genes than up-regulated genes. *E. coli* MG1655 *soxR*(R20H) had 444 differentially expressed genes, where 29 % of the genes were up-regulated. *E. coli* MG1655 *soxR*(R20H)*ybcO*(I87M) had the lowest number of differentially expressed genes of all mutants, with a total of 157 genes, 43 % up-regulated and 57 % down-regulated. On the other hand, *E. coli* MG1655 *soxR*(R20H)*acrR*(T32fs) had a total of 441 differentially expressed genes, where 81% of these genes were down-regulated. However, *E. coli* MG1655 *soxR*(R20H)*acrR*(V29G), had a total of 673 differentially expressed genes, corresponding to a 52 % increase compared to the total of differentially expressed genes in *E. coli* MG1655 *soxR*(R20H)*acrR*(T32fs), which has mutations in the same genes as *E. coli* MG1655 *soxR*(R20H)*acrR*(V29G).

This increase of the number of differentially expressed genes in *E. coli* MG1655 *soxR*(R20H)*acrR*(V29G), is mostly linked to an increase in number of down-regulated genes. In *E. coli* MG1655 *soxR*(R20H)*acrR*(V29G), 548 genes were down-regulated, corresponding to 81 % of the total genes, but only 125 genes were up-regulated corresponding to 19 % of the total genes.

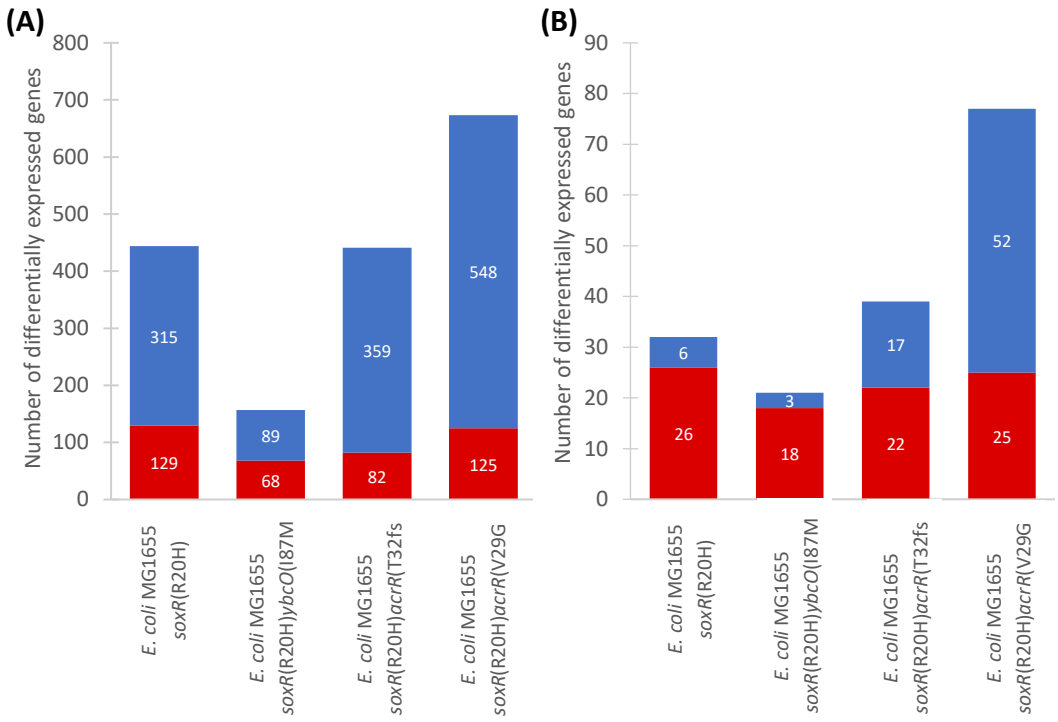

Figure 6.1 - Profile of differentially expressed genes in different *E. coli* mutant strains, compared to the WT strain. *E. coli* MG1655 strains were grown in the absence BMA, in three biological replicates, and a sample for RNA-seq was taken after an OD_{600nm} of approximately 0.3 was reached. RNA sequencing was performed on the Illumina NextSeq500 sequencing platform and the differential expression was obtained using DESeq2. Numbers of up-regulated genes and down-regulated genes are shown in red and blue, respectively. Only genes with a an adjusted p-value ≤ 0.05 and (A) a log2 fold change ≥ 1 or ≤ -1 (i.e. fold change ≥ 2 or ≤ 0.5) or (B) a log2 fold change ≥ 2 or ≤ -2 (i.e. fold change ≥ 4 or ≤ 0.25) were considered as differentially expressed.

Overall, the results from RNA-seq showed that the mutations or combinations of mutations in *soxR*(R20H), *acrR*(V29G), *acrR*(T32fs) and/or *ybcO*(I87M) lead a significant difference in the expression of genes compared to the WT strain. Furthermore, although most of the differentially expressed genes in *E. coli* MG1655 *soxR*(R20H), *E. coli* MG1655 *soxR*(R20H)*ybcO*(I87M), *E. coli* MG1655 *soxR*(R20H)*acrR*(V29G) and *E. coli* MG1655 *soxR*(R20H)*acrR*(T32fs) were down-regulated, in general, the genes that were up-regulated had higher fold

changes than the down-regulated ones (Figure 6.1 B). When considering only higher fold changes (≥ 4 or ≤ 0.25), 81 %, 86 %, 56 % and 33 % of the differentially expressed genes in *E. coli* MG1655 *soxR*(R20H)*, E. coli* MG1655 *soxR*(R20H)*ybcO*(I87M), *E. coli* MG1655 *soxR*(R20H)*acrR*(T32fs) and *E. coli* MG1655 *soxR*(R20H)*acrR*(V29G), respectively, were up-regulated.

6.1.1 Functional enrichment analysis of differentially expressed genes

RNA-seq data was further analysed by doing a functional enrichment analysis. With this functional analysis it was possible to detect which sets of genes were over-represented in one or more strains, based on the gene ontology (GO) terms of the Biological Processes category (Appendix 11.6, Table 11.7, page 212). This way it was possible to determine which key biological processes were induced or repressed in the four *E. coli* mutant strains, compared to the WT strain. Even before the cells were exposed to BMA, different biological responses widely known to be induced or repressed under chemicals stress (see section 1.2), were identified as up or down-regulated by *E. coli* MG1655 *soxR*(R20H), *E. coli* MG1655 *soxR*(R20H)*ybcO*(I87M), *E. coli* MG1655 *soxR*(R20H)*acrR*(V29G) and *E. coli* MG1655 *soxR*(R20H)*acrR*(T32fs), including responses related to iron homeostasis, oxidative stress, membrane transport, cell adhesion (Figure 6.2) and changes in the metabolism (Figure 6.3).

The response to oxidative stress was enriched in all the mutant strains, *E. coli* MG1655 *soxR*(R20H), *E. coli* MG1655 *soxR*(R20H)*ybcO*(I87M), *E. coli* MG1655 *soxR*(R20H)*acrR*(T32fs) and *E. coli* MG1655 *soxR*(R20H)*acrR*(V29G), with over 30 genes identified as up-regulated (Figure 6.2). The transcription factor *soxS* was the most strongly up-regulated gene involved in oxidative stress, with a log2 fold change between 7 and 7.5 across all mutant strains. The transcription factor, *soxR*, which activates the expression of *soxS*, was also slightly up-regulated in all four strains with a log2 fold change around 1. Moreover, other genes which are known to be part of the SoxRS regulon[160], were also highly up-regulated in all the mutant strains, including *pfo* (pyruvate-flavodoxin oxidoreductase), *fumC* (fumarase C), *fpr*

(flavodoxin/ferredoxin NADP$^+$ reductase), *sodA* (superoxide dismutase), *nfo* (endonuclease IV), *ybjC* (uncharacterized) or *zwf* (glucose-6-phosphate dehydrogenase). Hence, the mutated gene *soxR*(R20H) found in all the mutant strains encodes a functional SoxR transcription factor capable of up-regulating the expression of *soxS* and, consequently, the expression of the SoxRS regulon, compared to the WT strain.

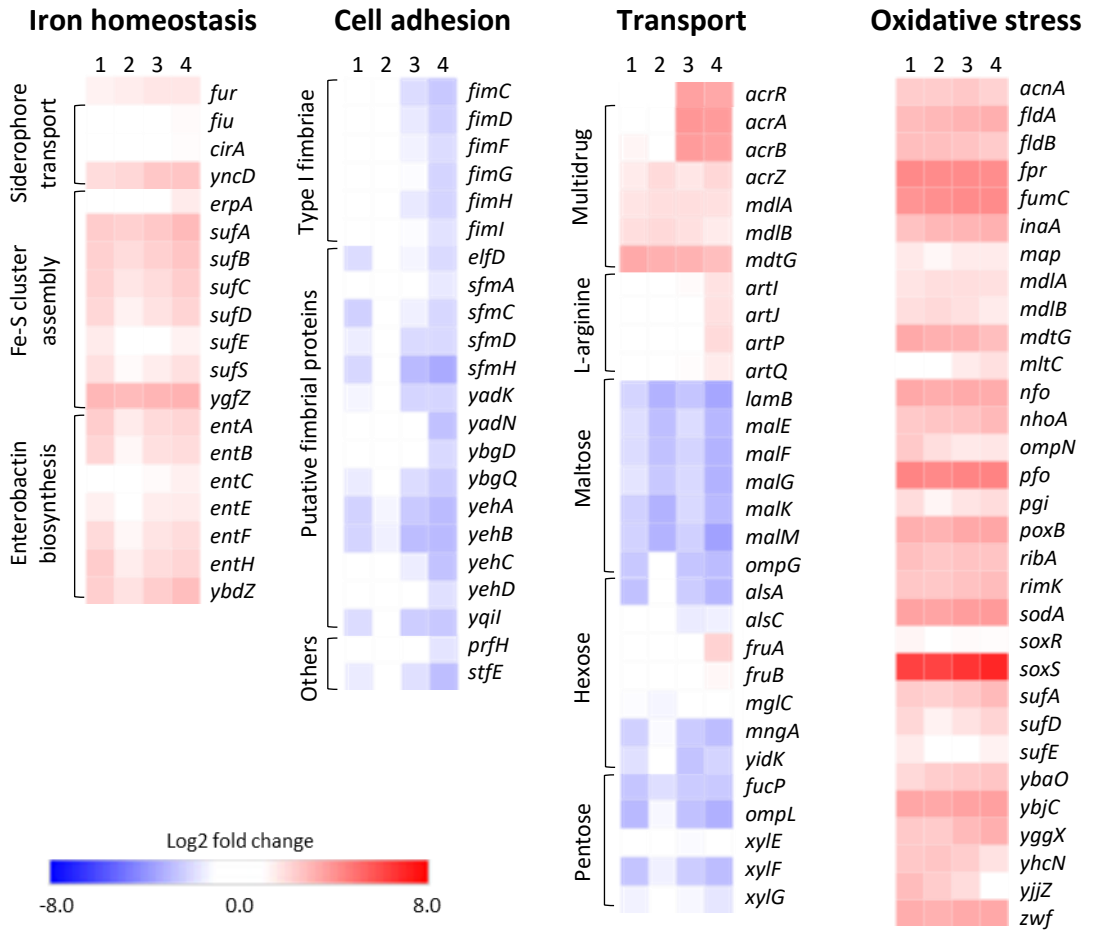

Figure 6.2 - Biological responses induced or repressed in *E. coli* MG16655 mutant strain, compared to the WT strain. Differential expressions for each response in (1) *E. coli* MG1655 *soxR*(R20H), (2) *E. coli* MG1655 *soxR*(R20H)*ybcO*(I87M), (3) *E. coli* MG1655 *soxR*(R20H)*acrR*(T32fs) and (4) *E. coli* MG1655 *soxR*(R20H)*acrR*(V29G) are shown. Heatmaps were generated using the web-based software Morpheus. Heatmaps are shown with a log2 fold change scale, where red and blue indicate up and down-regulated genes, respectively.

Fur, the major iron-dependent regulator that controls iron homeostasis [165,167,169,170], was up-regulated in all the mutant strains, along with other 17 genes involved in iron homeostasis that were also up-regulated in at least two or more mutant strains (Figure 6.2). These genes included the *suf* genes, involved in the assembly of Fe-S clusters, the *ent* genes, involved in the siderophore enterobactin

biosynthesis, or *fiu*, *cirA* and *yncD*, involved in siderophore-mediated iron transport. Furthermore, the iron homeostasis response is closely related to the oxidative stress response, where Fur is positively regulated by SoxRS[157]. However, Fur is known to down-regulate the expression of genes involved in iron uptake when there is excess iron in the cells[165,166].

Several membrane transporters related to multidrug, sugar or amino acid transport, were also induced or repressed in one or more mutant strains (Figure 6.2). The transport related proteins with the highest up-regulation were *acrA* and *acrB* (known to be repressed by *acrR*[79-81]*),* part of the multidrug pump AcrABZ-TolC[64], but were only highly up-regulated in the two mutant strains with mutations in *acrR*, *E. coli* MG1655 *soxR*(R20H)*acrR*(T32fs) and *E. coli* MG1655 *soxR*(R20H)*acrR*(V29G). The log2 fold changes were between 2.9 and 3.4. Yet, *acrB* was also slightly up-regulated in both *E. coli* MG1655 *soxR*(R20H) and *E. coli* MG1655 *soxR*(R20H)*ybcO*(I87M) with a log2 fold change of around 1. Additionally, *acrZ* (known to be activated by SoxS, MarA and Rob[64]) was also up-regulated in all the mutant strains, with log2 fold changes between 1.2 and 1.5. Furthermore, the regulator of the *acrAB* operon, *acrR*, was also up-regulated only in *E. coli* MG1655 *soxR*(R20H)*acrR*(T32fs) and *E. coli* MG1655 *soxR*(R20H)*acrR*(V29G), with log2 fold changes of 2.9 and 2.7, respectively. This suggests that neither *acrR*(T32fs) nor *acrR*(V29G) encoded a functional AcrR protein capable of repressing the expression of the *acr* operon. Consequently, other genes, such as *soxS*, were possibly able to up-regulate the expression of the *acr* genes. Nonetheless, since *E. coli* MG1655 *soxR*(R20H)*acrR*(T32fs) and *E. coli* MG1655 *soxR*(R20H)*acrR*(V29G) were the mutants with the highest level of tolerance towards BMA, the up-regulation of *acrA* and *acrB*, could be one of the crucial mechanisms responsible for the observed phenotype, *i.e.* the multidrug complex AcrABZ-TolC might be pumping BMA out of the cell, and, therefore, increasing the BMA resistance observed in these mutant strains.

Other genes related to multidrug transport were up-regulated in all strains (Figure 6.2), including *mdtG*, associated with resistance to the antibiotic fosfomycin[275], and also part of the SoxRS regulon[276], and *mdlAB*, an ABC transporter proposed to be a multidrug pump[69]. Additionally, transporters involved in transporting sugars were

down-regulated in most mutant strains, including maltose (*mal* genes), xylose (*xyl* genes) or D-allose (*als* genes) transporters. Yet, *fruA* and *fruB*, fructose-specific phosphotransferases[267], were slightly up-regulated in *E. coli* MG1655 *soxR*(R20H)*acrR*(T32fs) and *E. coli* MG1655 *soxR*(R20H)*acrR*(V29G).

Over 20 genes related to cell adhesion were also identified as down-regulated, mostly in *E. coli* MG1655 *soxR*(R20H)*acrR*(T32fs) and *E. coli* MG1655 *soxR*(R20H)*acrR*(V29G) (Figure 6.2). These included *fim* genes, related to the synthesis of type I fimbriae[267], genes part of the *sfmACDHF or yehABCD* operons which encode putative chaperone-usher fimbriae[277].

Apart from the biological responses already mentioned, different biological processes related to cell metabolism were induced or repressed in the mutant strains, when compared to the WT strain (Figure 6.3). However, in this case there were noticeable differences between the mutant strains. For example, genes involved in the biosynthesis of arginine were up-regulated only in *E. coli* MG1655 *soxR*(R20H)*acrR*(T32fs) and *E. coli* MG1655 *soxR*(R20H)*acrR*(V29G), while genes related to histidine biosynthesis were up-regulated only in *E. coli* MG1655 *soxR*(R20H) or *E. coli* MG1655 *soxR*(R20H)*ybcO*(I87M). Genes related to glycolate (*glc* and *gly* operons) or ethanolamine (*eut* operon) catabolism were predominantly down-regulated in *E. coli* MG1655 *soxR*(R20H)*acrR*(T32fs) and *E. coli* MG1655 *soxR*(R20H)*acrR*(V29G), but neither in *E. coli* MG1655 *soxR*(R20H) nor *E. coli* MG1655 *soxR*(R20H)*ybcO*(I87M).

Two different gene ontology terms related to metabolic processes of nitrogen compounds were also identified as down-regulated (Figure 6.3). Genes involved in carnitine metabolism were down-regulated in *E. coli* MG1655 *soxR*(R20H), *E. coli* MG1655 *soxR*(R20H)*acrR*(T32fs) and *E. coli* MG1655 *soxR*(R20H)*acrR*(V29G), but not in *E. coli* MG1655 *soxR*(R20H)*ybcO*(I87M), except for *fixB*, a putative electron transfer flavoprotein, which also had a log2 fold change of -1 in *E. coli* MG1655 *soxR*(R20H)*ybcO*(I87M). Likewise, genes involved in allantoin assimilation pathway were down-regulated only in *E. coli* MG1655 *soxR*(R20H), *E. coli* MG1655

soxR(R20H)*acrR*(T32fs) and *E. coli* MG1655 *soxR*(R20H)*acrR*(V29G), but not in *E. coli* MG1655 *soxR*(R20H)*ybcO*(I87M).

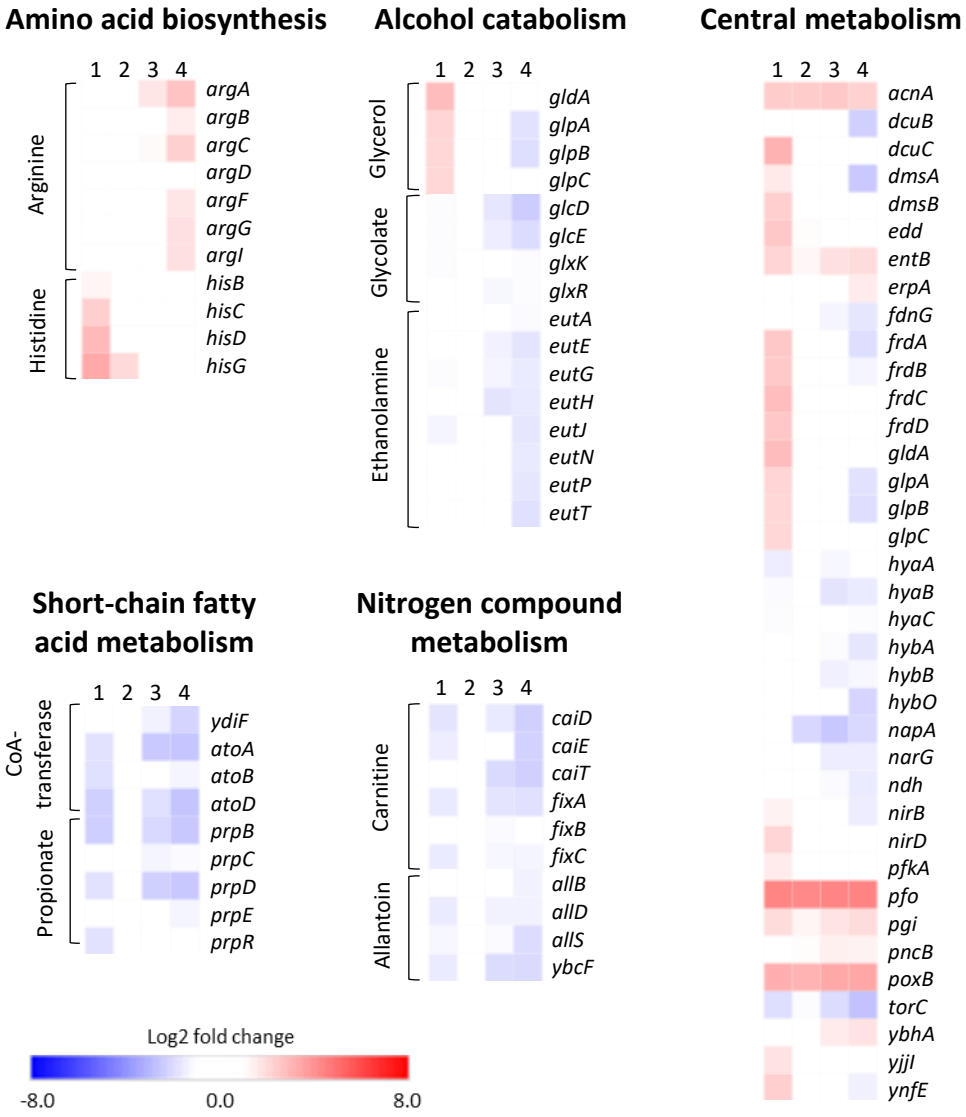

Figure 6.3 - Changes in the metabolism induced or repressed in *E. coli* MG16655 mutant strain, compared to the WT strain. Heatmaps show differential expression detected for each response in (1) *E. coli* MG1655 *soxR*(R20H), (2) *E. coli* MG1655 *soxR*(R20H)*ybcO*(I87M), (3) *E. coli* MG1655 *soxR*(R20H)*acrR*(T32fs) and (4) *E. coli* MG1655 *soxR*(R20H)*acrR*(V29G). Heatmaps were generated using the web-based software Morpheus. Heatmaps are shown with a log2 fold change scale, where red and blue indicate up and down-regulated genes, respectively.

The *prpBCDE* operon, involved in the short-chain fatty acid propionate catabolism, where propionate is converted into pyruvate via the methylcitrate cycle[278], was down-regulated in *E. coli* MG1655 *soxR*(R20H), *E. coli* MG1655 *soxR*(R20H)*acrR*(T32fs) and *E. coli* MG1655 *soxR*(R20H)*acrR*(V29G) (Figure 6.3). Yet, the propionate catabolism positive regulator, *prpR*[279], was only down-regulated in

E. coli MG1655 *soxR*(R20H). The genes *atoB* (thiolase II), *atoA* and *atoD* (acetoacetyl-CoA transferase subunits β and α, respectively), involved in the degradation of short-chain fatty acids[280,281], were also down-regulated only in *E. coli* MG1655 *soxR*(R20H), *E. coli* MG1655 *soxR*(R20H)*acrR*(T32fs) and *E. coli* MG1655 *soxR*(R20H)*acrR*(V29G) (Figure 6.3).

Other genes involved in the central metabolism of the cell, *i.e.* glycolysis, the TCA cycle and/or the respiratory chain, were differentially expressed across the mutant strains (Figure 6.3). Most of these genes were related to anaerobic respiration, including *fdrABCD*, a fumarate reductase responsible for the reduction of fumarate to succinate[240], which was up-regulated in *E. coli* MG1655 *soxR*(R20H). However, *fdrA* and *fdrB* were down-regulated in *E. coli* MG1655 *soxR*(R20H)*acrR*(V29G). The genes *hyaABC* and *hybABO,* part of hydrogenases 1 and 2[240], respectively, were down-regulated in *E. coli* MG1655 *soxR*(R20H), *E. coli* MG1655 *soxR*(R20H)*acrR*(T32fs) and *E. coli* MG1655 *soxR*(R20H)*acrR*(V29G). In addition, *dmsA* and *dmsB*, part of the dimethyl sulfoxide reductase[267], was up-regulated in *E. coli* MG1655 *soxR*(R20H), but *dmsA* was down-regulated in *E. coli* MG1655 *soxR*(R20H)*acrR*(V29G). Lastly, *gldA* and *glpABC*, the glycerol dehydrogenase and the glycerol-3-phosphate dehydrogenase, respectively, also grouped in the glycerol catabolism GO term, were up-regulated in *E. coli* MG1655 *soxR*(R20H), but *glpA* and *glpB* were down-regulated in *E. coli* MG1655 *soxR*(R20H)*acrR*(V29G). Furthermore, as already showed also in Figure 6.2, genes related to oxidative stress which are involved in the metabolism, were up-regulated in all mutant strains, including *acnA* (aconitate hydratase A), *pfo* (pyruvate-flavodoxin oxidoreductase), *pgi* (glucose-6-phosphate isomerase) and *poxB* (pyruvate oxidase).

6.1.2 Commonality of differentially expressed genes

RNA-seq data was further analysed by creating Venn diagrams in order to determine the overlap of differentially expressed genes between the four mutant strains (Figure 6.4). In this way, it was possible to further determine the number of genes that were up-regulated or down-regulated in just one or more mutant strains,

compared to the WT strain. For this analysis only genes with a log2 fold change ≥ 1 or ≤ -1 were considered.

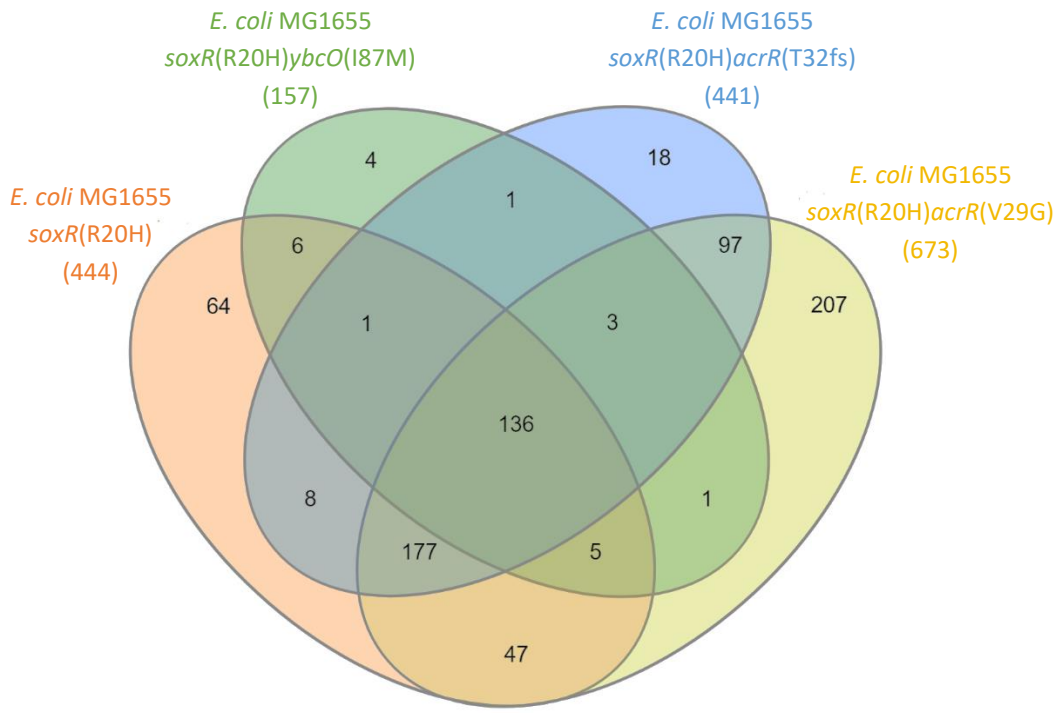

Figure 6.4 - Venn diagram representing the overlap of differentially expressed genes between *E. coli* mutant strains. *E. coli* MG1655 strains were grown in the absence BMA and a sample for RNA-seq was taken after an OD_{600nm} of approximately 0.3 was reached. RNA sequencing was performed on the Illumina NextSeq500 sequencing platform and the differential expression was obtained using DESeq2. Venn diagrams were generated using the InteractiVenn tool[262]. Only genes with a log2 fold change ≥ 1 or ≤ -1 (i.e. fold change ≥ 2 or ≤ 0.5) and an adjusted p-value ≤ 0.05 were considered as differentially expressed.

There were 136 genes that were differentially expressed, either induced or repressed, in all the mutant strains (Figure 6.4). Of these genes, the ones with highest fold change were all up-regulated and included oxidative stress related genes (*soxS*, *pfo*, *fpr*, *fumC*, *sodA*, *ybjC*, *nfo*, *zwf*, *poxB* and *fldA;* see Figure 6.2), *ygfZ* (folate-binding protein, related to Fe-S cluster assembly; Figure 6.2), *nfsA* (nitroreductase A), *yeiI* (putative kinase), *yobH* (uncharacterized protein), *kdgT* (2-keto-3-deoxy-D-gluconate transporter) and *idi* (isopentenyl diphosphate isomerase). Furthermore, *soxS* was the highest up-regulated gene in all strains.

Additionally, 64 genes were differentially expressed only in *E. coli* MG1655 *soxR*(R20H), but only 4 genes were differentially expressed only in *E. coli* MG1655 *soxR*(R20H)*ybcO*(I87M) (Figure 6.4). These 4 genes were the up-regulated *ydeE*

(dipeptide exporter) and the down-regulated *dctA* (C4 dicarboxylate/orotate:H^+ symporter), *mglA* (D-galactose/methyl-galactoside ABC transporter ATP binding subunit) and *yhdW* (putative ABC transporter periplasmic binding protein). However, 6 genes were differentially expressed in both *E. coli* MG1655 *soxR*(R20H) and *E. coli* MG1655 *soxR*(R20H)*ybcO*(I87M), namely the up-regulated *hisG* (ATP phosphoribosyltransferase), *ynfM* (putative arabinose transporter), *feoC* (ferrous iron transport protein), *lpxC* (UDP-3-O-acyl-N-acetylglucosamine deacetylase) and *edd* (phosphogluconate dehydratase) and the down-regulated *mglC* (D-galactose/methyl-galactoside ABC transporter).

Although there was an apparent significant difference in the number of differently expressed genes in *E. coli* MG1655 *soxR*(R20H) and *E. coli* MG1655 *soxR*(R20H)*ybcO*(I87M) when compared to the WT strain, there was not a significant difference in the differently expressed genes when the *E. coli* MG1655 *soxR*(R20H) and *E. coli* MG1655 *soxR*(R20H)*ybcO*(I87M) where compared directly. Before the addition of BMA, there were only 6 differentially expressed genes in *E. coli* MG1655 *soxR*(R20H)*ybcO*(I87M), compared to *E. coli* MG1655 *soxR*(R20H) (Table 6.1). Moreover, these 6 genes had low fold changes. Thus, *E. coli* MG1655 *soxR*(R20H) and *E. coli* MG1655 *soxR*(R20H)*ybcO*(I87M) had similar transcriptome profiles. It seems that the additional mutation *ybcO*(I87M) in *E. coli* MG1655 *soxR*(R20H)*ybcO*(I87M) did not significantly change the expression of any additional genes that were not already being expressed in *E. coli* MG1655 *soxR*(R20H).

Table 6.1 - Differentially expressed genes in *E. coli* MG1655 *soxR*(R20H)*ybcO*(I87M), compared to *E. coli* MG1655 *soxR*(R20H), before BMA addition. Only genes with a log2 fold change ≥ 1 or ≤ -1 (*i.e.* fold change ≥ 2 or ≤ 0.5) and an adjusted p-value ≤ 0.05 were considered as differentially expressed.

Gene	Function	Log2 FC	SE
dinQ	UV inducible membrane toxin	1.2	0.1
azuC	Uncharacterized protein	1.1	0.1
adhE	Alcohol dehydrogenase/aldehyde-ehydrogenase	-1.0	0.1
hisC	Histidinol-phosphate aminotransferase	-1.0	0.1
hisD	Histidinal dehydrogenase/histidinol dehydrogenase	-1.1	0.1
nirD	Nitrite reductase subunit	-1.2	0.2

Regarding the mutant strains with the highest levels of tolerance towards BMA, *E. coli* MG1655 *soxR*(R20H)*acrR*(T32fs) and *E. coli* MG1655 *soxR*(R20H)*acrR*(V29G), there were a total of 97 genes differentially expressed only in both of these strains before BMA addition, when compared to the WT strain. (Figure 6.4). The genes with the highest fold change were *acrA*, *acrB* and *acrR* (see Figure 6.2). However, there were 18 genes differentially expressed only in *E. coli* MG1655 *soxR*(R20H)*acrR*(T32fs) and 207 genes differentially expressed only in *E. coli* MG1655 *soxR*(R20H)*acrR*(V29G).

However, when *E. coli* MG1655 *soxR*(R20H)*acrR*(T32fs) and *E. coli* MG1655 *soxR*(R20H)*acrR*(V29G) were compared directly, there were not significant differences (Table 6.2). There were only 4 genes differentially expressed in *E. coli* MG1655 *soxR*(R20H)*acrR*(V29G) when compared to *E. coli* MG1655 *soxR*(R20H)*acrR*(T32fs). Furthermore, these genes had low fold changes. Therefore, it seems that *E. coli* MG1655 *soxR*(R20H)*acrR*(T32fs) and *E. coli* MG1655 *soxR*(R20H)*acrR*(V29G) had similar transcriptomic profiles and the mutated genes *acrR*(T32fs) and *acrR*(V29G) encode protein that overall induce affect the expression of the same genes.

Table 6.2 - Differentially expressed genes in *E. coli* MG1655 *soxR*(R20H)*acrR*(V29G), compared to *E. coli* MG1655 *soxR*(R20H)*acrR*(T32fs), before BMA addition. Only genes with a log2 fold change ≥ 1 or ≤ -1 (*i.e.* fold change ≥ 2 or ≤ 0.5) and an adjusted p-value ≤ 0.05 were considered as differentially expressed.

Gene	Function	Log2 FC	SE
stpA	DNA-binding transcriptional repressor	1.6	0.1
cspG	Cold shock protein	-1.0	0.1
malM	Maltose regulon periplasmic protein	-1.1	0.1
alaE	L-alanine exporter	-1.4	0.2

In summary, all the different sets of mutations found in the mutant strains lead to the differential expression of hundreds of genes, compared to the WT strain. Most significantly, *soxS* and other oxidative stress genes were highly up-regulated in all mutant strains, suggesting that the presence of *soxR*(R20H) leads to a possible constitutive overexpression of the oxidative stress response. Furthermore, it seems *ybcO*(I87M) did not significantly affect the transcription of any genes, and that *acrR*(T32fs) and *acrR*(V29G) had the same effect on the transcriptome of *E. coli*

MG1655 *soxR*(R20H)*acrR*(T32fs) and *E. coli* MG1655 *soxR*(R20H)*acrR*(V29G). Additionally, *acrA* and *acrB* were highly up-regulated only in the mutant strains with mutations in *acrR*, which had highest resistance to BMA, namely *E. coli* MG1655 *soxR*(R20H)*acrR*(T32fs) and *E. coli* MG1655 *soxR*(R20H)*acrR*(V29G). This suggests that *acrR*(V29G) and *acrR*(T32fs) may encode a non-functional AcrR, incapable of repressing the expression of *acrAB*. Further studies would be necessary to confirm that the mutated AcrR proteins would not bind to the DNA. In addition, *acrZ* was slightly up-regulated in all mutant strains, whereas *tolC* was neither up-regulated nor down-regulated in any of the strains. The outer membrane channel *tolC* is known to be part of several ABC, RND and MFS transporters[282], and constitutively highly expressed in *E. coli*, but it can be further up-regulated by the regulators SoxS, MarA, Rob, PhoPQ, BaeSR, and EvgAS[83,84]. Even though *tolC* was not up-regulated in this work, the up-regulation of *acrA*, *acrB*, and *acrZ*, might suggest that the possible overexpression of AcrABZ-TolC, could be a key factor for BMA resistance in *E. coli*.

6.2 Effect of BMA addition on the transcriptome of *E. coli*

The second part of this RNA-seq study was focused on identifying the biological responses of *E. coli* MG1655 WT and the BMA-tolerant *E. coli* MG1655 mutant strains after BMA exposure. The levels of different mRNAs detected after the addition of BMA were compared with the levels of mRNA detected before the induction, in order to determine the fold changes in each gene induced by the exposure to BMA. All strains were grown under normal conditions and 20 %(v/v) BMA was added during mid-exponential phase, after reaching an OD_{600nm} of approximately 0.3 (as shown in Figure 4.3, section 4.1.2, page 68). Samples were taken before and 1 h after the addition of 20 %(v/v) BMA. With this analysis it was possible to determine not only how BMA affects the WT strain, but also which mechanism of resistance are induced by the mutant strains to allow them to survive in the stressful conditions.

The addition of 20 %(v/v) BMA resulted in the up-regulation or down-regulation of hundreds or even thousands of genes, depending on the strain (Figure 6.5). After the addition of BMA, *E. coli* MG1655 WT up-regulated and down-regulated the

expression of 1641 and 1465 genes, respectively, to a total of 3106 differentially expressed genes, which correspond to about 74 % of all *E. coli* genes (Figure 6.5). The vast majority of genes were induced as a consequence of BMA addition, since only 177 genes were detected as differentially expressed after 1 h of growth when *E. coli* MG1655 WT was grown without BMA addition.

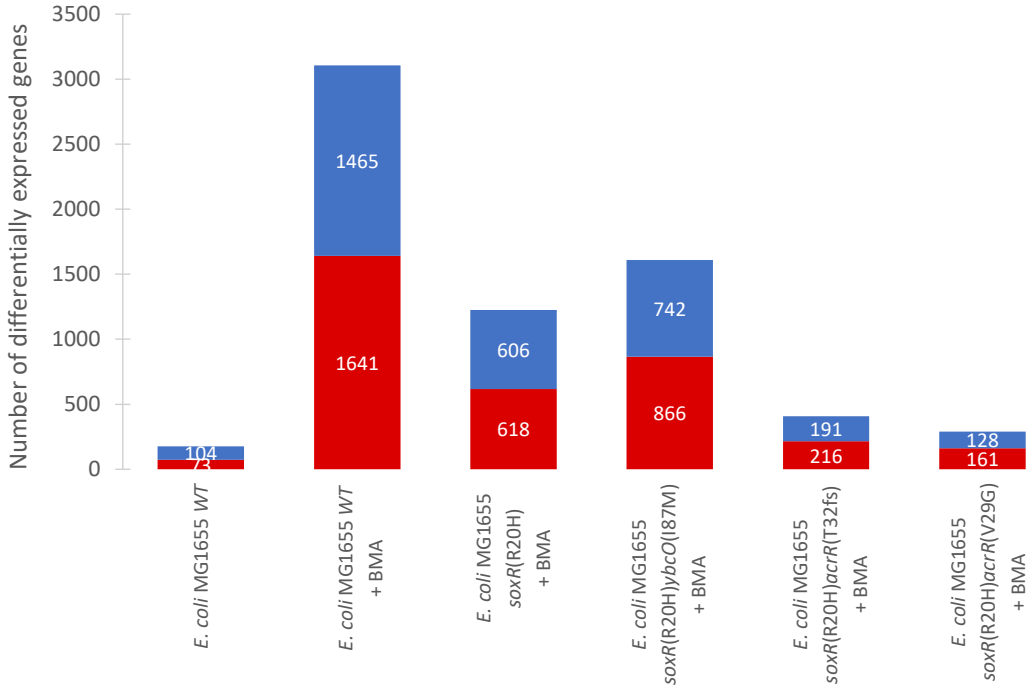

Figure 6.5 - Profile of differentially expressed genes in different *E. coli* mutant strains, after the addition of BMA. BMA was added at a concentration of 20 %(v/v) when *E. coli* MG1655 strains reached an OD_{600nm} of approximately 0.3. Samples for RNA-seq were taken before and 1 h after the addition, with three biological replicates. RNA sequencing was performed on the Illumina NextSeq500 sequencing platform and the differential expression was obtained using DESeq2. Numbers of up-regulated genes and down-regulated genes are shown in red and blue, respectively. Only genes with a log2 fold change ≥ 1 or ≤ -1 (*i.e.* fold change ≥ 2 or ≤ 0.5) and an adjusted p-value ≤ 0.05 were considered as differentially expressed.

E. coli MG1655 *soxR*(R20H) and *E. coli* MG1655 *soxR*(R20H)*ybcO*(I87M) had fewer differentially expressed genes after the addition of BMA than the WT strain. Even so, BMA induced a total of 1224 differentially expressed genes in *E. coli* MG1655 *soxR*(R20H), where 618 genes were up-regulated and 606 were down-regulated, and a total of 1608 differentially expressed genes in *E. coli* MG1655 *soxR*(R20H)*ybcO*(I87M), where 866 genes were up-regulated and 742 were down-regulated (Figure 6.5). By contrast, both *E. coli* MG1655 *soxR*(R20H)*acrR*(T32fs) and *E. coli* MG1655 *soxR*(R20H)*acrR*(V29G) had the lowest number of differentially

expressed genes after the addition of BMA. *E. coli* MG1655 *soxR*(R20H)*acrR*(T32fs) had 216 and 191 genes that were up-regulated and down-regulated, respectively, a total of 407 differentially expressed genes, and *E. coli* MG1655 *soxR*(R20H)*acrR*(V29G) had 161 and 128 genes that were up-regulated and down-regulated, respectively, a total of 289 differentially expressed genes (Figure 6.5).

Thus, it was possible to observe a correlation between the level of tolerance of an *E. coli* strain and the number of differentially expressed genes that were induced after the addition of 20 %(v/v) BMA (Figure 6.5). *E. coli* MG1655 *soxR*(R20H)*acrR*(T32fs) and *E. coli* MG1655 *soxR*(R20H)*acrR*(V29G) were mutant strains with the highest resistance to BMA, whereas *E. coli* MG1655 *soxR*(R20H) and *E. coli* MG1655 *soxR*(R20H)*ybcO*(I87M) had lower levels of resistance and *E. coli* MG1655 WT could not grow in BMA. Hence, it seems that the more tolerant the *E. coli* MG1655 strain is, the smaller number of genes it needs to differentially express to be able to counteract BMA stress, *i.e.* those mutations are "pre-equipping" *E. coli* to deal with subsequent stress.

6.2.1 Functional enrichment analysis of differentially expressed genes

A functional enrichment analysis based on the GO terms of the Biological Processes category, showed there were several biological processes associated with the responses to stress or stimulus induced or repressed across all four mutant strains and WT strain in response to BMA (Figure 6.6, Figure 6.7, Figure 6.8 and Figure 6.9). Although in general, *E. coli* MG1655 *soxR*(R20H)*acrR*(T32fs) and *E. coli* MG1655 *soxR*(R20H)*acrR*(V29G) had fewer number of differentially expressed genes for each biological response.

In response to BMA, 39 genes related to the oxidative stress response were identified as up or down-regulated in some of the mutant strains, but also in the WT strain (Figure 6.6). Some of the down-regulated genes included *fldA* and *fldB* (flavodoxins 1 and 2), *map* (methionine aminopeptidase), *mltC* (membrane-bound lytic murein transglycosylase), *ribA* (guanosine triphosphate cyclohydrolase), *sodA* (superoxide dismutase), the *suf* genes (assembly of Fe-S clusters) and *yggX* (putative

Fe^{2+}-trafficking protein). Moreover, several other genes were up-regulated in all strains, including the WT, such as, *katE* (catalase II), *rclA* (putative pyridine nucleotide-disulfide oxidoreductase), *yfcG* (disulfide reductase), wrbA (NAD(P)H:quinone oxidoreductase) and *yhbO* (protein/nucleic acid deglycase).

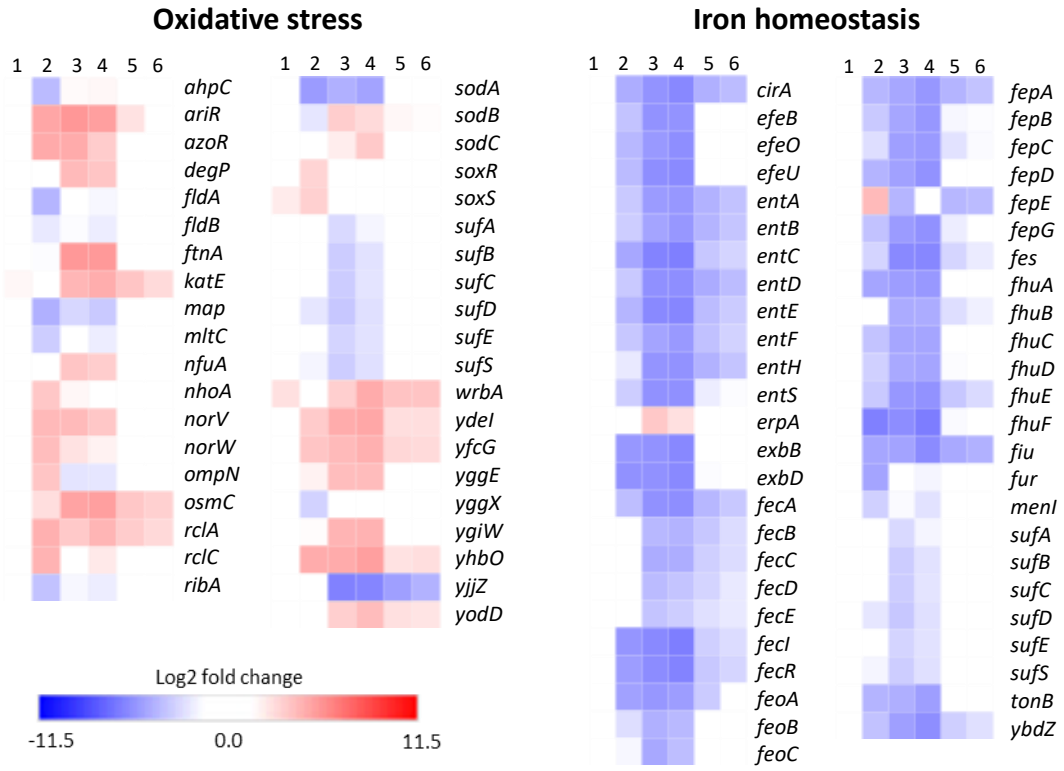

Figure 6.6 - Biological responses related to oxidative stress and iron homeostasis induced or repressed in *E. coli* MG16655 strains, after the addition of BMA. Heatmaps show differential expressions for each response in (1) *E. coli* MG1655 WT with no BMA addition, (2) *E. coli* MG1655 WT with BMA addition, (3) *E. coli* MG1655 *soxR*(R20H) with BMA addition, (4) *E. coli* MG1655 *soxR*(R20H)*ybcO*(I87M) with BMA addition, (5) *E. coli* MG1655 *soxR*(R20H)*acrR*(T32fs) with BMA addition and (6) *E. coli* MG1655 *soxR*(R20H)*acrR*(V29G) with BMA addition. BMA was added at a concentration of 20 %(v/v) when *E. coli* MG1655 strains reached an OD_{600nm} of approximately 0.3. Samples for RNA-seq were taken before and 1 h after the addition. RNA sequencing was performed on the Illumina NextSeq500 sequencing platform and the differential expression was obtained using DESeq2. Heatmaps were generated using the web-based software Morpheus. Heatmaps are shown with a log2 fold change scale, where red and blue indicate up and down-regulated genes, respectively.

Almost 50 genes involved in iron homeostasis were down-regulated in at least one of the strains, after the addition of 20 %(v/v) BMA (Figure 6.6). This included the down-regulated genes involved in ferric ion siderophore-mediated uptake (*e.g. cirA, entS, fecA, fecBCDE, fepA, fepBCDG, fhuA, fhuBCD, fhuE, fhuF, fiu, tonB* and *yncD*), ferrous ion uptake (*e.g.* efeUOB and feoABC) and the siderophore enterobactin

biosynthesis (e.g. *ent* genes, *fes*, and *ybdZ*). Fur, the major regulator know to down-regulate all these iron homeostasis genes in the presence of excess iron[165,166], was in this study down-regulated only in *E. coli* MG1655 WT and *E. coli* MG1655 *soxR*(R20H)*ybcO*(I87M) (Figure 6.6). Additionally, the gene *erpA* (iron-sulfur cluster insertion protein) was up-regulated in *E. coli* MG1655 *soxR*(R20H) and *E. coli* MG1655 *soxR*(R20H)*ybcO*(I87M), while *fepE* (O-antigen length regulator; lipopolysaccharides with long O-antigen chains can positively affect enterobactin-mediated iron uptake[283,284]) was up-regulated in *E. coli* MG1655 WT, but down-regulated in *E. coli* MG1655 *soxR*(R20H), *E. coli* MG1655 *soxR*(R20H)*acrR*(T32fs) and *E. coli* MG1655 *soxR*(R20H)*acrR*(V29G).

Osmotic stress related genes were either up-regulated or down-regulated in the *E. coli* strains tested upon exposure to 20 %(v/v) BMA during mid exponential phase (Figure 6.7). The transcriptional regulator *ompR*, part of the OmpR-EnvZ two-component signal transduction system that responds to osmotic stress[212,214,215], was up-regulated after BMA addition only in *E. coli* MG1655 *soxR*(R20H) and *E. coli* MG1655 *soxR*(R20H)*ybcO*(I87M), while *envZ* was neither up-regulated or down-regulated in any of the strains. Moreover, different genes known to be part of the OmpR regulon[218] were also differentially expressed after BMA exposure. The *csg* genes (curli assembly related proteins; activated by OmpR[218]), were up-regulated in all four mutant strains, except for *csgB*, which was up-regulated in *E. coli* MG1655 *soxR*(R20H) and *E. coli* MG1655 *soxR*(R20H)*ybcO*(I87M), as well as in *E. coli* MG1655 WT. The outer membrane porins, *ompF* (activated by OmpR[218]), *ompC* (activated by OmpR[218]) and *fadL* (repressed by OmpR[219]), were down-regulated. Yet *fadL* was down-regulated in only in *E. coli* MG1655 WT, *E. coli* MG1655 *soxR*(R20H) and *E. coli* MG1655 *soxR*(R20H)*ybcO*(I87M), *ompC* was down-regulated only in the WT strain, whereas *ompF* was down-regulated in the WT strain and the four mutant strains. Other OmpR regulon genes, such as *flhDC* (flagellum regulators; repressed by OmpR[220]) or *malFK* (maltose ABC transporters; repressed by OmpR[218]) were down-regulated, and *galP* (galactose:H^+ MFS symporter; repressed by OmpR[218]) was up-regulated across different strains (Figure 6.7). Other genes known to be osmosensitive but not part of the OmpR regulon[213,218,221-224], were either

up-regulated, such as the *osm* genes (different osmosensitive proteins) or the *tre* genes (osmoprotectant trehalose metabolism), or down-regulated, such as the *pro* genes (glycine betaine ABC transporter).

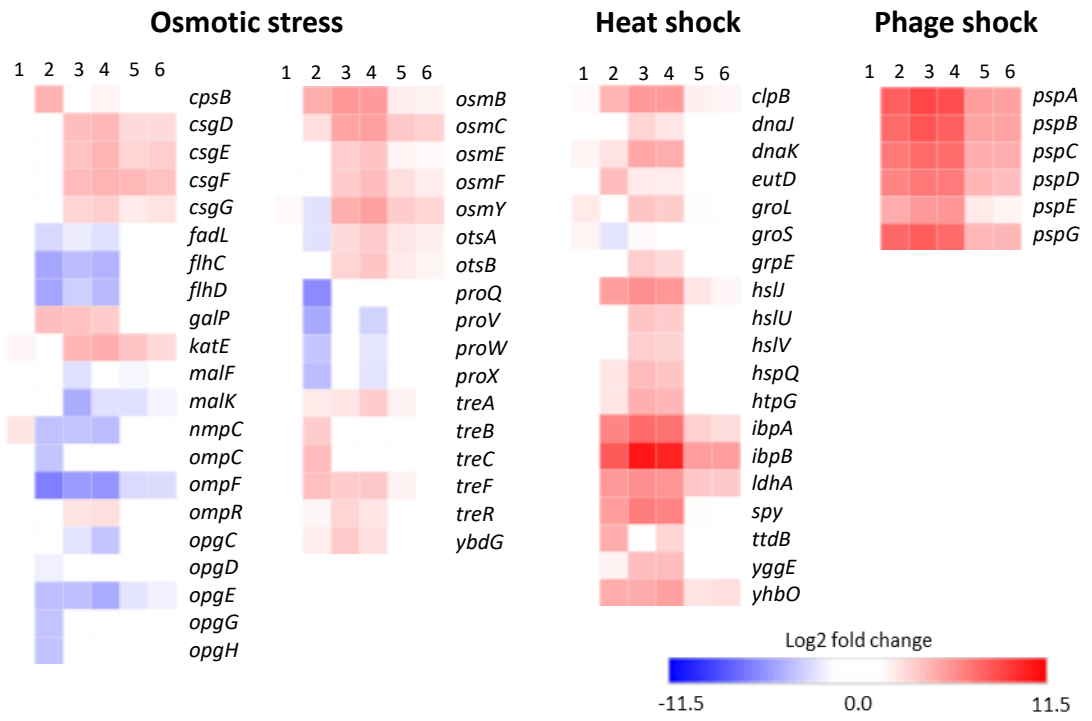

Figure 6.7 - Biological responses related to osmotic stress, heat shock and phage shock induced or repressed in *E. coli* MG16655 strains, after the addition of BMA. Heatmaps show differential expressions for each response in (1) *E. coli* MG1655 WT with no BMA addition, (2) *E. coli* MG1655 WT with BMA addition, (3) *E. coli* MG1655 *soxR*(R20H) with BMA addition, (4) *E. coli* MG1655 *soxR*(R20H)*ybcO*(I87M) with BMA addition, (5) *E. coli* MG1655 *soxR*(R20H)*acrR*(T32fs) with BMA addition and (6) *E. coli* MG1655 *soxR*(R20H)*acrR*(V29G) with BMA addition. BMA was added at a concentration of 20 %(v/v) when *E. coli* MG1655 strains reached an OD_{600nm} of approximately 0.3. Samples for RNA-seq were taken before and 1 h after the addition. RNA sequencing was performed on the Illumina NextSeq500 sequencing platform and the differential expression was obtained using DESeq2. Heatmaps were generated using the web-based software Morpheus. Heatmaps are shown with a log2 fold change scale, where red and blue indicate up and down-regulated genes, respectively.

Another biological response that was up-regulated in all mutant strains, as well as in the WT strain, upon BMA exposure, was the phage shock proteins response, responsible for maintaining the integrity of the membrane under stressful enviroments[121-125]. All *psp* genes, *pspABCDE* and *pspG,* were up-regulated in all strains, with *E. coli* MG1655 WT, *E. coli* MG1655 *soxR*(R20H) and *E. coli* MG1655 *soxR*(R20H)*ybcO*(I87M) having the highest fold changes (Figure 6.7).

Likewise, several heat shock proteins were also highly up-regulated after BMA addition, but the highest expression was observed in *E. coli* MG1655 WT, *E. coli*

MG1655 *soxR*(R20H) and *E. coli* MG1655 *soxR*(R20H)*ybcO*(I87M) (Figure 6.7). Yet, a few heat shock related genes were up-regulated in all mutant strains and the WT strain, namely *ibpA* and *ibpB* (chaperones), *ldhA* (D-lactate dehydrogenase), *yhbO* (protein/nucleic acid deglycase), *clpB* (chaperone) and *hslJ* (lipoprotein). Other widely known chaperones were also up-regulated in *E. coli* MG1655 WT, *E. coli* MG1655 *soxR*(R20H) and *E. coli* MG1655 *soxR*(R20H)*ybcO*(I87M), including *dnaJK*, *spy* or *htpG*. Although the genes *spy* and *dnaK* were also slightly up-regulated in *E. coli* MG1655 *soxR*(R20H)*acrR*(T32fs), and both *dnaJ* and *dnaK* were also slightly up-regulated in the WT control with no BMA added. The chaperonins *groL* and *groS* had different levels of expression across the *E. coli* strains tested. Both of them were up-regulated in the WT control with no BMA added, but *groL* was further up-regulated in *E. coli* MG1655 *soxR*(R20H), *E. coli* MG1655 *soxR*(R20H)*ybcO*(I87M) and *E. coli* MG1655 *soxR*(R20H)*acrR*(T32fs), while *groS* was up-regulated in *E. coli* MG1655 *soxR*(R20H), but down-regulated in *E. coli* MG1655 WT.

Genes associated with the response to starvation were induced in all strains after the addition of BMA, including: *appA* (periplasmic phosphoanhydride phosphatase/multiple inositol-polyphosphate phosphatase), *appY* (DNA-binding transcriptional activator), *phoR* (sensory histidine kinase), *phoU* (phosphate signalling protein), all associated with phosphate starvation[285-287]; *phoQ* (sensory histidine kinase), associated with magnesium starvation[288]; *tauABC* (taurine ABC transporter), associated with sulphur starvation[289] (Figure 6.8). Additionally, *yjiY*, also known as *btsT*, a pyruvate:H^+ symporter involved in pyruvate uptake[290] and related to nutrient limitation[291], was up-regulated in all strains after the addition of BMA. However, *yjiY* was the only gene which had higher fold changes in the most tolerant strains towards BMA, *E. coli* MG1655 *soxR*(R20H)*acrR*(T32fs) and *E. coli* MG1655 *soxR*(R20H)*acrR*(V29G), than in the remaining strains, with log2 fold changes of 3.82 and 2.98, respectively. These findings could suggest that the starvation response was up-regulated as a consequence of the possible reduction of the membrane permeability, obtained with the up-regulation of phage-shock proteins or the down-regulation of membrane porins

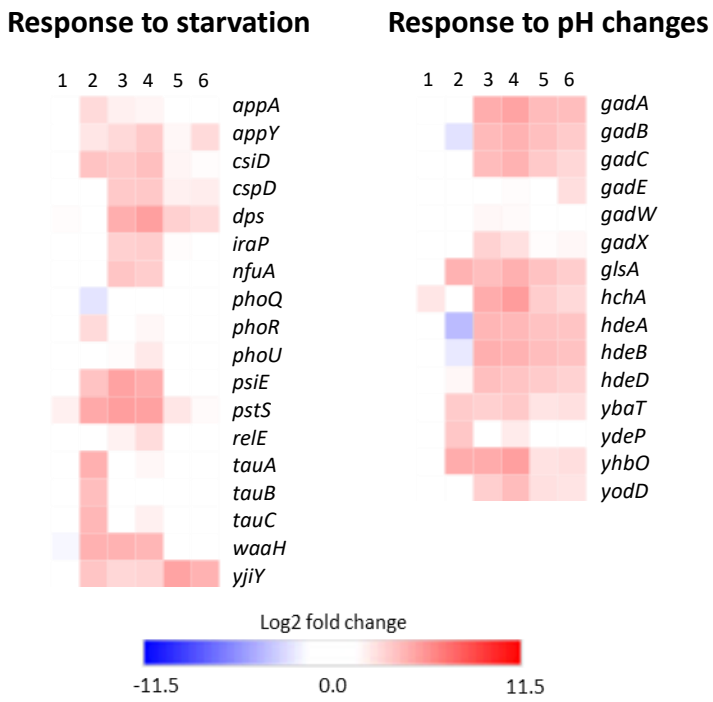

Figure 6.8 - Biological responses related to starvation and pH induced or repressed in *E. coli* MG16655 strains, after the addition of BMA. Heatmaps show differential expressions for each response in (1) *E. coli* MG1655 WT with no BMA addition, (2) *E. coli* MG1655 WT with BMA addition, (3) *E. coli* MG1655 *soxR*(R20H) with BMA addition, (4) *E. coli* MG1655 *soxR*(R20H)*ybcO*(I87M) with BMA addition, (5) *E. coli* MG1655 *soxR*(R20H)*acrR*(T32fs) with BMA addition and (6) *E. coli* MG1655 *soxR*(R20H)*acrR*(V29G) with BMA addition. BMA was added at a concentration of 20 %(v/v) when *E. coli* MG1655 strains reached an OD_{600nm} of approximately 0.3. Samples for RNA-seq were taken before and 1 h after the addition. RNA sequencing was performed on the Illumina NextSeq500 sequencing platform and the differential expression was obtained using DESeq2. Heatmaps were generated using the web-based software Morpheus. Heatmaps are shown with a log2 fold change scale, where red and blue indicate up and down-regulated genes, respectively.

The response to pH changes was also enriched in all strains after the addition of BMA (Figure 6.8). The glutamate decarboxylase system, known as the Gad system, involved in the response to acid stress[46,226,228,229] (see section 1.2.3.6), was up-regulated in all four mutant strains. Yet, only *gadB* (glutamate decarboxylases B), was differentially expressed in the WT strain after BMA addition, but it was down-regulated.

Fifty genes involved in flagellum mobility and chemotaxis were identified as down-regulated after exposure to BMA, mostly in *E. coli* MG1655 WT, *E. coli* MG1655 *soxR*(R20H) and *E. coli* MG1655 *soxR*(R20H)*ybcO*(I87M), but some were also slightly down-regulated in *E. coli* MG1655 *soxR*(R20H)*acrR*(T32fs) and *E. coli* MG1655 *soxR*(R20H)*acrR*(V29G) (Figure 6.9). These genes encoded flagellar transcriptional activators and sigma factors (*e.g. flhDC*, *fliZ* and *fliA*), methyl-accepting chemotaxis

sensor proteins (*e.g. aer*, *tsr*, *tap* and *tar*), motility proteins (*e.g. motAB*), chemotaxis proteins (*e.g*. *cheYZ*), an many other proteins related to flagellar biosynthesis and structure (*fli* and *flg* genes).

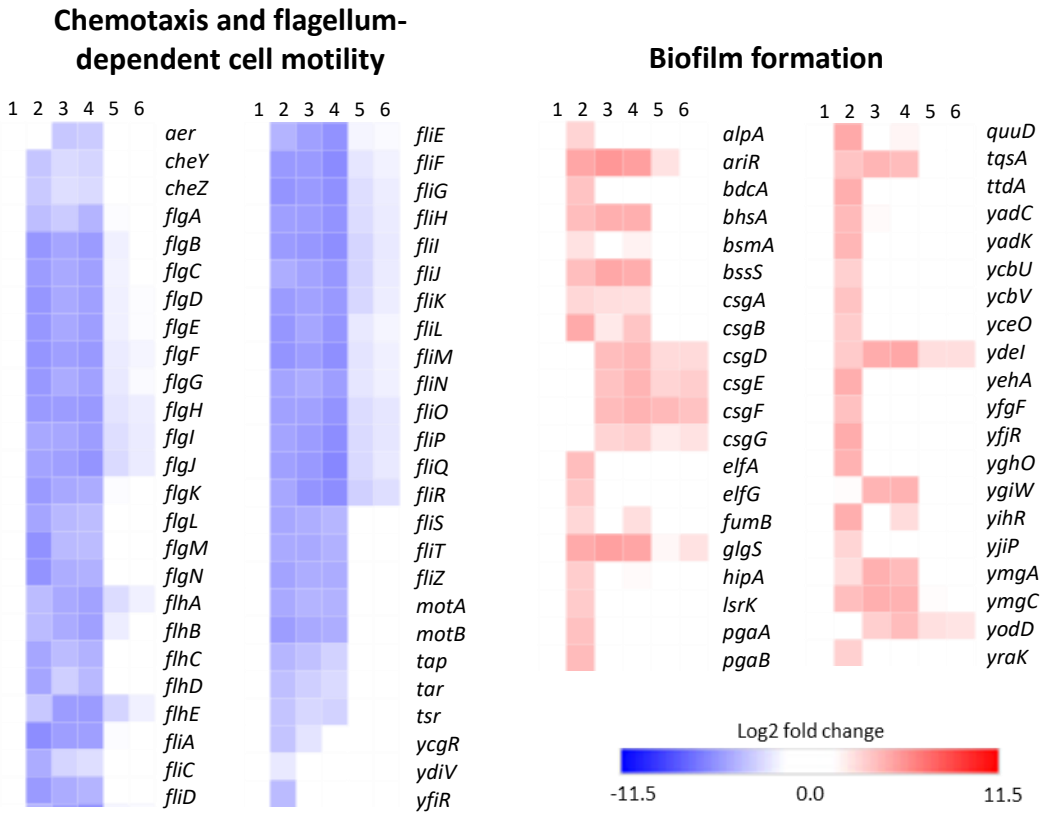

Figure 6.9 - Biological responses related to chemotaxis, flagellum motility and biofilm formation induced or repressed in *E. coli* MG16655 strains, after the addition of BMA. Heatmaps show differential expressions for each response in (1) *E. coli* MG1655 WT with no BMA addition, (2) *E. coli* MG1655 WT with BMA addition, (3) *E. coli* MG1655 *soxR*(R20H) with BMA addition, (4) *E. coli* MG1655 *soxR*(R20H)*ybcO*(I87M) with BMA addition, (5) *E. coli* MG1655 *soxR*(R20H)*acrR*(T32fs) with BMA addition and (6) *E. coli* MG1655 *soxR*(R20H)*acrR*(V29G) with BMA addition. BMA was added at a concentration of 20 %(v/v) when *E. coli* MG1655 strains reached an OD_{600nm} of approximately 0.3. Samples for RNA-seq were taken before and 1 h after the addition. RNA sequencing was performed on the Illumina NextSeq500 sequencing platform and the differential expression was obtained using DESeq2. Heatmaps were generated using the web-based software Morpheus. Heatmaps are shown with a log2 fold change scale, where red and blue indicate up and down-regulated genes, respectively.

Several genes that have been associated with biofilm formation were up-regulated after the addition of BMA, mainly in the WT stain, but also across the mutant strains (Figure 6.9). These included the *csg* genes (curli assembly related proteins; also related associated with osmotic stress and activated by $OmpR^{218}$), *bhsA* (outer membrane protein), *elfAB* (putative fimbrial proteins), *glgS* (surface composition regulator), *ymgAC* (proteins involved in biofilm formation), *yadC* (fimbrial

tip-adhesin), *yadK* (putative fimbrial protein), *ycbUV* (putative fimbrial proteins) and *yodD* (stress-induced protein, also related to acid and oxidative stresses).

Other biological processes were enriched only in *E. coli* MG1655 WT, *E. coli* MG1655 *soxR*(R20H) and/or *E. coli* MG1655 *soxR*(R20H)*ybcO*(I87M), which are summarized in Table 6.3. There were biological responses up-regulated only in the WT strain, such as responses related to cell adhesion (*e.g. csgAB*, curli subunits; *yadCKLMN*, putative fimbrial proteins; *sfmADFH and yehAD,* putative chaperone-usher fimbriae), response to virus (*e.g. casABCDE*, *ygbFT* and *ygcB*, involved in the CRISPR system), and carbohydrate transport, including pentose (*e.g. araEF* and *xylEFG*), galactose (*e.g. ytfQRT*), fructose (*e.g. fruA*, *frvB*, *frwBD* and *fryB*) and hexose transport.

But there were also GO terms down-regulated only in the WT strain, including processes related to membrane biogenesis and organization (*e.g. bamABCDE*, outer membrane protein assembly factors; *lolCD*, lipoprotein release complex; *lptAC*, lipopolysaccharide transport system proteins, and *lptDE*, lipopolysaccharide assembly proteins), cell division, regulation of cell shape and regulation of cellular component biogenesis (Table 6.3). Other sets of genes were down-regulated in the WT strain, but also in some of the mutant strains, such as genes related to branched-chain amino acid transport (*e.g. livFGHKM*, phenylalanine ABC transporter), ribonucleoprotein complex biogenesis (*e.g. rplAEJKW*, 50S ribosomal subunits, and *rpsGIKPS*, 30S ribosomal subunits), organelle assembly and translation (Table 6.3).

Many sets of genes involved in the metabolism of the cells were enriched in one or more *E. coli* strains, after the addition of BMA (Table 6.4). Different processes were only enriched in *E. coli* MG1655 WT, including the induced processes related to lipid metabolism and the repressed processes involved in pigment metabolism and vitamin biosynthesis. Several other processes were enriched in the WT strain, but also in *E. coli* MG1655 *soxR*(R20H) and/or *E. coli* MG1655 *soxR*(R20H)*ybcO*(I87M), including the induced processes related to metabolism of organic hydroxy compounds, nitrogen compounds, organic phosphonate, reactive nitrogen species

and short-chain fatty acids, or the repressed processes related to cofactors metabolism and secondary metabolites biosynthesis. Other GO terms were repressed across most strains, including the ones related to the biosynthesis of carbohydrate derivatives and peptides and the metabolism of nucleic acids. In addition, several biological processes were simultaneously enriched and identified as up-regulated and down-regulated in one or more the strains tested, including processes related to the metabolism of carboxylic acids, carbohydrates, alcohols and sulphur compounds (Table 6.4).

Table 6.3 - Functional enrichment analysis of biological processes GO terms induced or repressed in *E. coli* MG16655 strains, after the addition of BMA. Additional information is shown in Appendix 11.6, Table 11.9, page 213.

	***E. coli* MG1655 strains**					
Biological Process	**WT**	**WT +BMA**	***soxR*(R20H) +BMA**	***soxR*(R20H) *ybcO*(I87M) +BMA**	***soxR*(R20H) *acrR*(V29G) +BMA**	***soxR*(R20H) *acrR*(T32fs) +BMA**
Membrane related processes						
Membrane biogenesis and organization		↓ (18)				
External encapsulating structure organization		↓ (50)				
Cell adhesion		↑ (44)				
Transport						
Sulfur compound transport	↑ (10)					
Phosphate ion transport				↑ (9)		
Modified amino acid transport	↑ (3)				↑ (5)	
Branched-chain amino acid transport		↓ (9)	↓ (6)	↓ (7)		
Carbohydrate transport	↓ (13)	↑ (97)		↑ (38)		
Pentose transport		↑ (7)				
Galactose transport		↑ (7)				
Fructose transport		↑ (6)				
Hexose transport		↑ (16)				
Other cellular processes						
Organelle assembly*		↓ (38)	↓ (29)	↓ (33)		
Cell division		↓ (72)				
Regulation of cell shape		↓ (30)				
Regulation of cellular component biogenesis		↓ (15)				
Ribonucleoprotein complex biogenesis		↓ (57)	↓ (22)	↓ (41)		
Translation		↓ (128)	↓ (59)	↓ (81)		
Response to virus		↑ (12)				
Stress response to metal ion		↑ (6)		↑ (6)		

*Although *E. coli* does not have organelles, this GO term was enriched in the analysis and included genes that encode flagella proteins and ribosomes subunits.

Table 6.4 - Functional enrichment analysis of biological processes GO terms related to the metabolism induced or repressed in *E. coli* MG16655 strains, after the addition of BMA.

	***E. coli* MG1655 strains**					
Metabolic Process	**WT**	**WT +BMA**	***soxR*(R20H) +BMA**	***soxR*(R20H) *ybcO*(I87M) +BMA**	***soxR*(R20H) *acrR*(V29G) +BMA**	***soxR*(R20H) *acrR*(T32fs) +BMA**
Carboxylic acid metabolic process	↑ (24)	↑ (182) ↓ (256)	↑ (87)	↑ (128)	↑ (35)	
Carbohydrate metabolic process		↑ (184) ↓ (151)		↑ (77)		
Carbohydrate derivative biosynthetic process		↓ (148)	↓ (47)	↓ (65)		
Alcohol metabolic process		↑ (22) ↓ (19)	↑ (9) ↓ (8)	↑ (19) ↓ (8)		
Sulfur compound metabolic process	↑ (11)	↑ (11) ↓ (64)	↑ (23) ↓ (28)	↑ (31) ↓ (29)	↑ (12)	↑ (9)
Nitrogen compound metabolic process		↑ (408)	↑ (198)	↑ (271)		
Organic phosphonate metabolic process		↑ (9)		↑ (6)		
Organic hydroxy compound metabolic process		↑ (60)	↑ (28)	↑ (42)		
Ammonium ion metabolic process		↑ (24)		↑ (20)	↓ (8)	
Reactive oxygen species metabolic process			↑ (6)	↑ (6)		
Reactive nitrogen species metabolic process		↑ (15)	↑ (11)	↑ (14)		
Short-chain fatty acid metabolic process		↑ (16)		↑ (10)		
Amino acid metabolic process		↑ (153)				
Histidine biosynthetic process		↑ (9)	↑ (9)	↑ (8)		↑ (6)
Lipid metabolic process		↑ (67)				
Vitamin biosynthetic process		↓ (42)				
Pigment metabolic process		↓ (19)				
Cofactor metabolic process		↓ (137)		↓ (56)		
Peptide biosynthetic process		↓ (138)	↓ (68)	↓ (90)	↓ (15)	↓ (10)
Secondary metabolite biosynthetic process		↓ (12)	↓ (10)	↓ (10)		
Nucleic acid metabolic process		↓ (335)	↓ (102)	↓ (163)	↓ (36)	↓ (11)
Central metabolism						
Electron transport chain		↑ (20) ↓ (20)	↑ (14)			
Anaerobic respiration		↑ (23)	↓ (18)			
Energy derivation by oxidation of organic compounds		↑ (41) ↓ (50)	↑ (20)	↑ (27)		
Nitrogen fixation					↑ (3)	↑ (3)
Proteolysis involved in cellular protein catabolic process			↑ (5)			

Different sets of genes associated with the central metabolism were enriched in *E. coli* MG1655 WT, *E. coli* MG1655 *soxR*(R20H) and/or *E. coli* MG1655 *soxR*(R20H)*ybcO*(I87M), after the addition of BMA. Most of the central metabolism

genes that were differentially expressed after the addition of BMA were related to anaerobic respiration (Table 6.4). For example, the following genes were up-regulated in *E. coli* MG1655 WT: *dmsBC* (dimethyl sulfoxide reductase subunits), *fdnGHI* (formate dehydrogenase N), *hyaABC* (hydrogenase 1), *narGHI* and *narVYZ* (nitrate reductase A and Z, respectively), *nrfB* (periplasmic nitrite reductase penta-heme cytochrome c) and *nrfCD* (putative menaquinol-cytochrome c reductase subunits), *torAC* (menaquinol:trimethylamine N-oxide oxidoreductase I), *torS* (sensory histidine kinase) and *torY* (cytochrome c quinol dehydrogenase). The genes *frdAB* (fumarate reductase subunits), *glpABC* (anaerobic glycerol-3-phosphate dehydrogenase) and *nirD* (nitrite reductase) were down-regulated in *E. coli* MG1655 WT. However, *fdnG*, *narG*, *nrfB*, *nrfC, dmsAB, frdABC, glpABC and nirBD* were down-regulated in *E. coli* MG1655 *soxR*(R20H), but, *hyaAC*, *narIVYZ* were up-regulated in *E. coli* MG1655 *soxR*(R20H). While the genes *hyaAB*, *narIVYZ*, *torC* and *torY* were up-regulated in *E. coli* MG1655 *soxR*(R20H)*ybcO*(I87M). Genes related to aerobic respiration were also up-regulated in *E. coli* MG1655 WT, *E. coli* MG1655 *soxR*(R20H) and *E. coli* MG1655 *soxR*(R20H)*ybcO*(I87M), including *cbdAB* (cytochrome bd-II) and *cydAB* (cytochrome bd-I). But for example, *cyoABCD* (cytochrome bo_3 ubiquinol oxidase subunits) were down-regulated in *E. coli* MG1655 WT.

Furthermore, genes related to the metabolism of reactive oxygen species (*hmp,* nitric oxide dioxygenase; *katE,* catalase; *norV,* reduced flavorubredoxin; *norW,* NADH:flavorubredoxin reductase*; sodB* and *sodC* (Fe and Cu-Zn superoxide dismutases, respectively) or proteolysis (the proteases *clpP, degP, degQ, hslV, lon*) were only enriched as up-regulated in *E. coli* MG1655 *soxR*(R20H) and/or *E. coli* MG1655 *soxR*(R20H)*ybcO*(I87M). Nitrogen fixation related genes, *glnAGL*, were only enriched as up-regulated in *E. coli* MG1655 *soxR*(R20H)*acrR*(T32fs) and *E. coli* MG1655 *soxR*(R20H)*acrR*(V29G).

6.2.2 Commonality of differentially expressed genes

The transcriptomics data was further analysed by determining the overlap of differentially expressed genes between the four mutant strains and the WT strain, to understand which genes were being expressed in one or more strains. A Venn diagram was generated, where only differentially expressed genes with a log2 fold change ≥ 1 or ≤ -1 were considered (Figure 6.10).

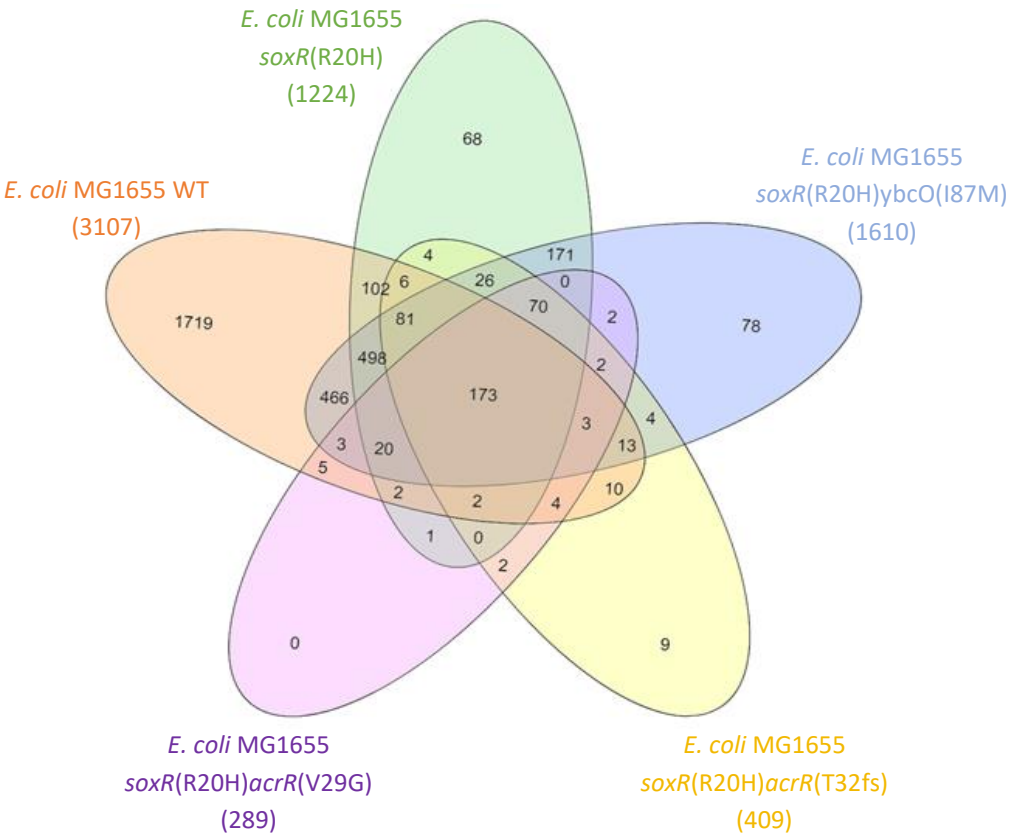

Figure 6.10 - Venn diagram representing the overlap of differentially expressed genes between *E. coli* mutant strains, after the addition of BMA. *E. coli* MG1655 strains were grown in the absence BMA and a sample for RNA-seq was taken after an OD_{600nm} of approximately 0.3 was reached. RNA sequencing was performed on the Illumina NextSeq500 sequencing platform and the differential expression was obtained using DESeq2. Venn diagrams were generated using the InteractiVenn tool[262]. Only genes with a log2 fold change ≥ 1 or ≤ -1 (i.e. fold change ≥ 2 or ≤ 0.5) and an adjusted p-value ≤ 0.05 were considered as differentially expressed.

After the addition of BMA, 173 genes were differentially expressed in all mutant strains and in the WT strain (Figure 6.10). Of these 173 genes, the ones with highest fold change were generally related to phage shock, temperature shock or iron homeostasis, including the up-regulated *pspABCDG* (phage shock proteins; see Figure 6.7), *ibpB* (heat shock chaperone; see Figure 6.7), *yibT* (uncharacterized protein that

has been associated with n-butanol tolerance[292]), and the down-regulated *ybiX* (hydrolase with Fe^{2+}-dependent oxygenase domain), *cirA* (ferric dihyroxybenzoylserine outer membrane transporter; see Figure 6.6), *fiu* (putative iron siderophore outer membrane transporter; see Figure 6.6) and *ymcE* (cold shock protein).

However, there were genes that were differentially expressed in only one of the strains (Figure 6.10). After the BMA addition, there were 1719, 68, 78 and 9 genes differentially expressed only in *E. coli* MG1655 WT, *E. coli* MG1655 *soxR*(R20H), *E. coli* MG1655 *soxR*(R20H)ybcO(I87M) and *E. coli* MG1655 *soxR*(R20H)*acrR*(T32fs), respectively. None of the differentially expressed genes in *E. coli* MG1655 *soxR*(R20H)*acrR*(V29G) were induced or repressed exclusively in this strain.

Furthermore, there were 171 genes differentially expressed only in *E. coli* MG1655 *soxR*(R20H) and *E. coli* MG1655 *soxR*(R20H)ybcO(I87M). Although it seems that there was a significant difference in the number of differentially expressed genes in only *E. coli* MG1655 *soxR*(R20H) or *E. coli* MG1655 *soxR*(R20H)ybcO(I87M), when the strains were compared directly, there were only 29 genes that were differentially expressed in *E. coli* MG1655 *soxR*(R20H)ybcO(I87M) compared to *E. coli* MG1655 *soxR*(R20H) (Table 11.12, Appendix 11.6, page 216). Furthermore, these genes had log2 fold changes between 1.4 and -1.3. Since both strains had over one thousand differentially expressed genes after the BMA addition, it seems that there were no significant differences between the strains and overall *E. coli* MG1655 *soxR*(R20H) and *E. coli* MG1655 *soxR*(R20H)ybcO(I87M) induce or repress the same mechanisms to counteract BMA stress.

By contrast, only 2 genes were differentially expressed both in *E. coli* MG1655 *soxR*(R20H)*acrR*(T32fs) and *E. coli* MG1655 *soxR*(R20H)*acrR*(V29G), namely *hisC* (histidinol-phosphate aminotransferase) and *asnA* (asparagine synthetase A). In addition, the 9 genes only differentially expressed in *E. coli* MG1655 *soxR*(R20H)*acrR*(T32fs) were the up-regulated *metC* (cystathionine β-lyase/L-cysteine desulfhydrase) and the down-regulated *puuE* (4-aminobutyrate aminotransferase), *puuC* (γ-glutamyl-γ-aminobutyraldehyde dehydrogenase), *ibsC* (small toxic protein),

alx (putative membrane-bound redox modulator), *gntK* (D-gluconate kinase), *rcsA* (DNA-binding transcriptional activator), *malM* (maltose regulon periplasmic protein) and *gsiA* (glutathione ABC transporter ATP binding subunit). However, *gsiA* was also slightly up-regulated in the WT control with no chemical. However, all these genes differentially expressed only in *E. coli* MG1655 *soxR*(R20H)*acrR*(T32fs) had low log2 fold changes, always between > -1.5 and <1.1. Furthermore, when *E. coli* MG1655 *soxR*(R20H)*acrR*(T32fs) and *E. coli* MG1655 *soxR*(R20H)*acrR*(V29G) were compared directly, there were no differently expressed genes between these strains after the BMA addition. Thus, it seems that overall *E. coli* MG1655 *soxR*(R20H)*acrR*(T32fs) and *E. coli* MG1655 *soxR*(R20H)*acrR*(V29G) have the same effects on BMA tolerance and affect the expression of the same genes.

Overall, most of the genes that were differentially expressed in *E. coli* MG1655 *soxR*(R20H)*acrR*(T32fs) and *E. coli* MG1655 *soxR*(R20H)*acrR*(V29G) were also differentially expressed in the other mutant strains or in the WT strain (Figure 6.10). Thus, in general, the biggest differences between *E. coli* MG1655 WT, *E. coli* MG1655 *soxR*(R20H), *E. coli* MG1655 *soxR*(R20H)ybcO(I87M) and the most BMA-tolerant strains, *E. coli* MG1655 *soxR*(R20H)*acrR*(T32fs) and *E. coli* MG1655 *soxR*(R20H)*acrR*(V29G), were that the latter had lower number of total differentially expressed genes and generally lower fold changes.

In summary, upon BMA exposure, hundreds or even thousands of genes were differentially expressed across all strains. However, there was a clear pattern between the response observed and the level of BMA resistance of each strain. The WT strain, which could not grow in BMA, had the biggest response to BMA, with over three thousand genes differentially expressed, showing that the cells were over-stressed and employed all the mechanisms available to try to survive. By contrast, the mutant strains had fewer differentially expressed genes in response to BMA, especially *E. coli* MG1655 *soxR*(R20H)*acrR*(T32fs) and *E. coli* MG1655 *soxR*(R20H)*acrR*(V29G), the mutants which had higher levels of BMA tolerance. This suggests that there were several mechanisms in place, including changes in membrane permeability, changes in metabolism and energy consumption, or the induction of the oxidative stress response and membrane transporters, that together

allowed *E. coli* MG1655 *soxR*(R20H)*acrR*(T32fs) and *E. coli* MG1655 *soxR*(R20H)*acrR*(V29G) to have a more focussed response to BMA to enable survival. These findings provided a vast range of chemical tolerance mechanisms that could be further studied and used for strain development.

7 Understanding stress responses induced by BMA

Transcriptomics results showed that the induction of genes related to membrane transport and oxidative stress might be essential for BMA tolerance in *E. coli.* Hence, selected genes were deleted from the mutant strains already resistant to BMA, namely *E. coli* MG1655 *soxR*(R20H) and *E. coli* MG1655 *soxR*(R20H)*acrR*(T32fs), as well as from the WT strain, as a control. In this way it was possible to further know if the presence of these genes is essential for BMA tolerance. KO strains were prepared with the same homologous recombination method described in Figure 5.1 (see section 5.1, page 98).

7.1 Effect of the deletion of the oxidative stress regulator *soxS*

Transcriptomics data showed that the oxidative stress transcription factor *soxS*, along with other genes related to oxidative stress, was highly up-regulated in all four mutant strains tolerant to BMA, *E. coli* MG1655 *soxR*(R20H), *E. coli* MG1655 *soxR*(R20H)*ybcO*(I87M), *E. coli* MG1655 *soxR*(R20H)*acrR*(T32fs) and *E. coli* MG1655 *soxR*(R20H)*acrR*(V29G), compared to the WT strain (Figure 6.2, section 6.1). This differential expression in *soxS*, and the other oxidative stress related genes, was observed in the absence of BMA. Thus, the missense mutation in *soxR* present in all mutant strains activated the expression of the SoxRS regulon, possibly resulting in a constitutive overexpression. Therefore, the up-regulation of *soxS* might be a key factor in BMA resistance in *E. coli*.

Hence, to further test this hypothesis, *soxS* was deleted from *E. coli* MG1655 WT, *E. coli* MG1655 *soxR*(R20H) and one of the double mutants, *E. coli* MG1655 *soxR*(R20H)*acrR*(T32fs). The new strains with *soxS* deletions, *E. coli* MG1655 Δ*soxS*, *E. coli* MG1655 *soxR*(R20H)-Δ*soxS* and *E. coli* MG1655 *soxR*(R20H)*acrR*(T32fs)-Δ*soxS,* were grown in the absence or presence of 20 %(v/v) BMA, along with the original mutants, *E. coli* MG1655 *soxR*(R20H) and *E. coli* MG1655 *soxR*(R20H)*acrR*(T32fs), and the WT strain as controls (Figure 7.1 and Table 7.1).

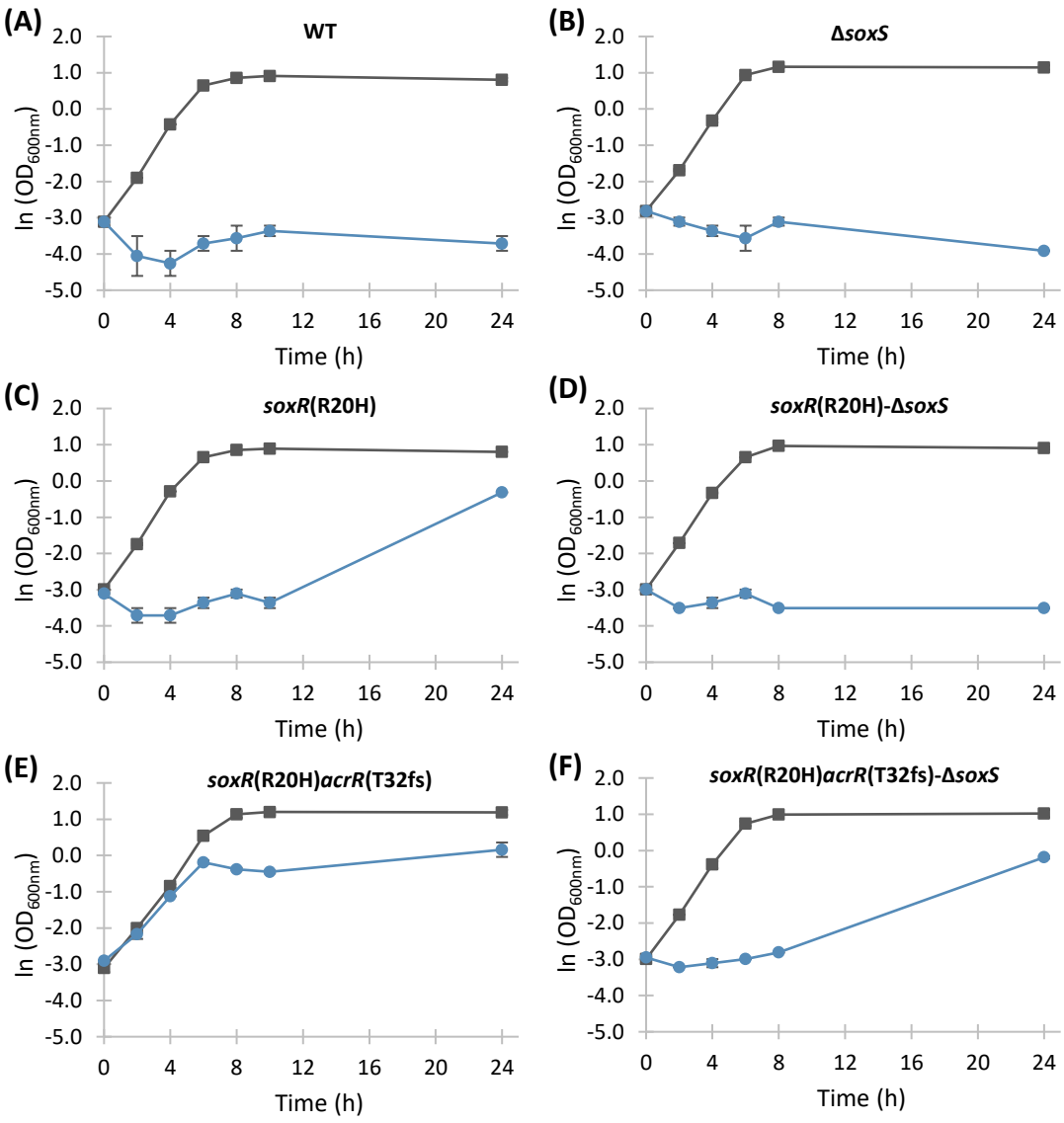

Figure 7.1 - Effect of BMA on the growth of *E. coli* MG1655 stains with *soxS* deletions. *E. coli* MG1655 WT (A), *E. coli* MG1655 Δ*soxS* (B), *E. coli* MG1655 *soxR*(R20H) (C), *E. coli* MG1655 *soxR*(R20H)-Δ*soxS* (D), *E. coli* MG1655 *soxR*(R20H)*acrR*(T32fs) (E) and *E. coli* MG1655 *soxR*(R20H)*acrR*(T32fs)-Δ*soxS* (F) were grown in MSX medium the absence [■] or presence [●] of 20 %(v/v) BMA, added immediately after inoculation. All strains were grown in 30 mL vials at 37°C and 250 rpm shaking. Means of two replicates are shown and error bars represent standard deviations.

In the absence of BMA, *E. coli* MG1655 Δ*soxS*, *E. coli* MG1655 *soxR*(R20H)-Δ*soxS* and *E. coli* MG1655 *soxR*(R20H)*acrR*(T32fs)-Δ*soxS* had the same growth rates as the respective mutant or WT strains without the *soxS* deletion, *i.e. E. coli* MG1655 WT, *E. coli* MG1655 *soxR*(R20H) and *E. coli* MG1655 *soxR*(R20H)*acrR*(T32fs), showing that the *soxR* gene deletion had no effect on normal cell growth. However, in the presence of 20 %(v/v) BMA, neither *E. coli* MG1655 WT nor *E. coli* MG1655 Δ*soxS* could grow (Figure 7.1 A and B). *E. coli* MG1655 *soxR*(R20H)-Δ*soxS* could not grow in the

presence of BMA (Figure 7.1 D), but *E. coli* MG1655 *soxR*(R20H) reached an OD_{600nm} of 0.73 ± 0.00, after 24 h of growth (Figure 7.1 C). By contrast, *E. coli* MG1655 *soxR*(R20H)*acrR*(T32fs)-Δ*soxS* was able to growth to an OD_{600nm} of 0.83 ± 0.0.3 at 24 h, but had a lag phase of at least 8 h (Figure 7.1 E), whereas the corresponding mutant without the *soxS* deletion, *E. coli* MG1655 *soxR*(R20H)*acrR*(T32fs), could grow with no lag phase, reaching an maximum OD of 1.20 ± 0.24 (Figure 7.1 F).

Table 7.1 - Effect of BMA on maximum OD_{600nm} and specific growth rate of *E. coli* MG1655 stains with *soxS* deletions. All strains were grown in MSX medium in the absence or presence of 20 %(v/v) BMA, in 30 mL vials at 37°C and 250 rpm. BMA was added immediately after inoculation. Means of two replicates and standard deviations are shown. All specific growth rates had p-values lower than 0.05. Values with n/a were not possible to determine, due to slow growth. NG: no growth.

	0 %(v/v) BMA		20 %(v/v) BMA	
***E. coli* MG1655 strains**	**Max OD_{600nm}**	**μ (h^{-1})**	**Max OD_{600nm}**	**μ (h^{-1})**
WT	2.50 ± 0.17	0.63 ± 0.03	NG	
Δ*soxS*	3.21 ± 0.10	0.63 ± 0.02	NG	
soxR(R20H)	2.44 ± 0.00	0.62 ± 0.04	0.73 ± 0.00	n/a
soxR(R20H)-Δ*soxS*	2.63 ± 0.03	0.62 ± 0.03	NG	
soxR(R20H)*acrR*(T32fs)	3.34 ± 0.28	0.61 ± 0.02	1.20 ± 0.24	0.49 ± 0.01
soxR(R20H)*acrR*(T32fs)-Δ*soxS*	2.79 ± 0.03	0.63 ± 0.02	0.83 ± 0.0.3	n/a

Thus, the *soxS* deletion had a strong effect on the growth of *E. coli* strains in the presence of 20 %(v/v) BMA, resulting in a significant decline in the capability of the cells to resist BMA stress. It seems that, in general, SoxS must be present and up-regulated in order to obtain *E. coli* strains with tolerance to BMA.

7.2 Effect of the deletion of different membrane transporters

7.2.1 AcrAB deletions

Different membrane transporters were also identified as possibly essential to BMA tolerance in *E. coli*, including the transmembrane fusion protein AcrA and the RND pump AcrB, part of the multidrug export complex AcrABZ-TolC[64]. Transcriptomics data showed that, in the absence of BMA, *acrA* and *acrB* were highly up-regulated, possibly becoming constitutively expressed, only in the mutant strains

with the highest level of tolerance towards BMA, *E. coli* MG1655 *soxR*(R20H)*acrR*(T32fs) and *E. coli* MG1655 *soxR*(R20H)*acrR*(V29G) (Figure 6.2, section 6.1). This indicated that AcrABZ-TolC might be crucial for BMA tolerance, by pumping it out of the cell.

To further understand the importance of the membrane transporter in BMA tolerance, the genes *acrA* and/or *acrB* were deleted from the WT strain and *E. coli* MG1655 *soxR*(R20H)*acrR*(T32fs). The new KO strains, *E. coli* MG1655 Δ*acrA*, *E. coli* MG1655 Δ*acrB*, *E. coli* MG1655 Δ*acrB*, *E. coli* MG1655 *soxR*(R20H)*acrR*(T32fs)-Δ*acrA*, *E. coli* MG1655 *soxR*(R20H)*acrR*(T32fs)-Δ*acrB* and *E. coli* MG1655 *soxR*(R20H)*acrR*(T32fs)-Δ*acrAB*, were grown in the absence or presence of 20 %(v/v) BMA, along with the controls *E. coli* MG1655 WT and *E. coli* MG1655 *soxR*(R20H)*acrR*(T32fs) (Figure 7.2 and Table 7.2).

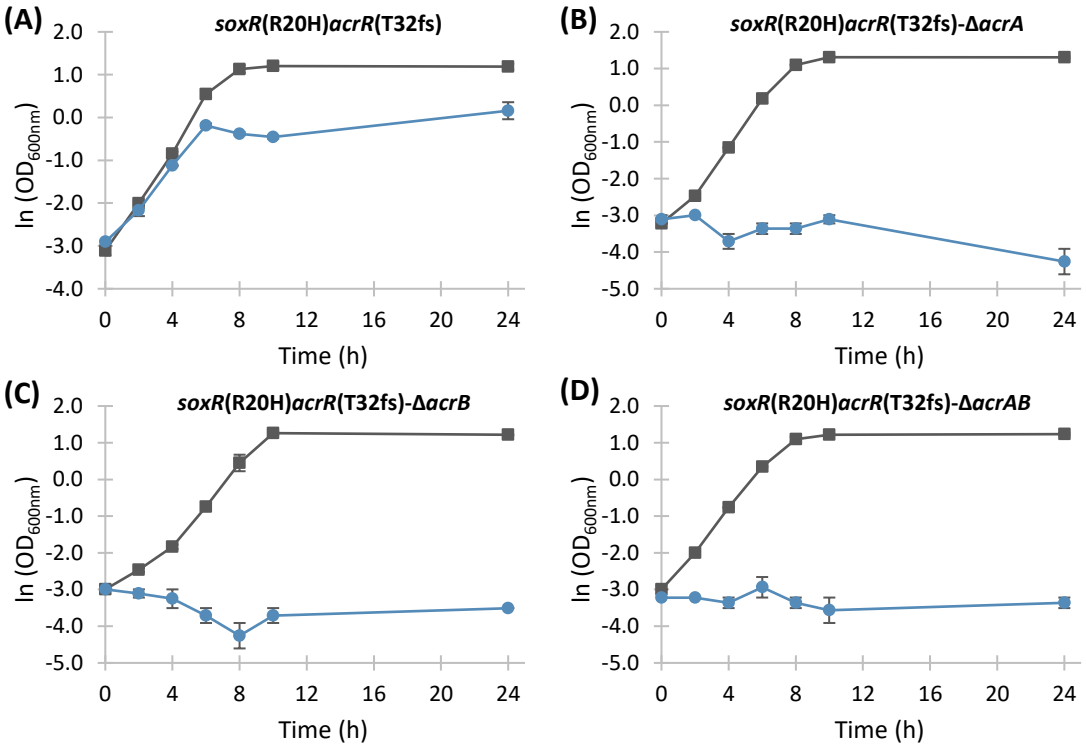

Figure 7.2 - Effect of BMA on the growth of *E. coli* MG1655 stains with *acrA* and/or *acrB* deletions. *E. coli* MG1655 *soxR*(R20H)*acrR*(T32fs) (A), *E. coli* MG1655 *soxR*(R20H)*acrR*(T32fs)-Δ*acrA* (B), *E. coli* MG1655 *soxR*(R20H)*acrR*(T32fs)-Δ*acrB* (C) and *E. coli* MG1655 *soxR*(R20H)*acrR*(T32fs)-Δ*acrAB* (D) were grown in MSX medium in the absence [■] or presence [●] of 20 %(v/v) BMA, added immediately after inoculation. All strains were grown in 30 mL vials at 37°C and 250 rpm shaking. Means of two replicates are shown and error bars represent standard deviations.

Table 7.2 - Effect of BMA on maximum OD_{600nm} and specific growth rate of *E. coli* MG1655 stains with *acrA* and/or *acrB* deletions. All strains were grown in MSX medium in the absence or presence of 20 %(v/v) BMA, in 30 mL vials at 37°C and 250 rpm. BMA was added immediately after inoculation. Means of two replicates and standard deviations are shown. All specific growth rates had p-values lower than 0.05. NG: no growth.

	0 %(v/v) BMA		20 %(v/v) BMA	
***E. coli* MG1655 strains**	**Max OD_{600nm}**	**μ (h^{-1})**	**Max OD_{600nm}**	**μ (h^{-1})**
WT	2.50 ± 0.17	0.63 ± 0.03	NG	
Δ*acrA*	3.14 ± 0.10	0.60 ± 0.00	NG	
Δ*acrB*	3.37 ± 0.03	0.63 ± 0.01	NG	
Δ*acrAB*	3.33 ± 0.09	0.63 ± 0.02	NG	
soxR(R20H)*acrR*(T32fs)	3.34 ± 0.28	0.61 ± 0.02	1.20 ± 0.24	0.49 ± 0.01
soxR(R20H)*acrR*(T32fs)-Δ*acrA*	3.71 ± 0.10	0.60 ± 0.04	NG	
soxR(R20H)*acrR*(T32fs)-Δ*acrB*	3.53 ± 0.16	0.49 ± 0.05	NG	
soxR(R20H)*acrR*(T32fs)-Δ*acrAB*	3.44 ± 0.12	0.56 ± 0.02	NG	

In the presence of 20 %(v/v) BMA, all the strains with *acrA* and/or *acrB* deletions, *E. coli* MG1655 Δ*acrA*, *E. coli* MG1655 Δ*acrB*, *E. coli* MG1655 Δ*acrB, E. coli* MG1655 *soxR*(R20H)*acrR*(T32fs)-Δ*acrA*, *E. coli* MG1655 *soxR*(R20H)*acrR*(T32fs)-Δ*acrB* and *E. coli* MG1655 *soxR*(R20H)*acrR*(T32fs)-Δ*acrAB,* could not grow (Figure 7.2 and Table 7.2). In the absence of BMA all strains with *acrA* and/or *acrB* deletions were able to grow, although *E. coli* MG1655 *soxR*(R20H)*acrR*(T32fs)-Δ*acrB* and *E. coli* MG1655 *soxR*(R20H)*acrR*(T32fs)-Δ*acrAB* had slightly lower growth rates than the *E. coli* MG1655 *soxR*(R20H)*acrR*(T32fs).

Hence, the overexpression of *acrA* and *acrB* was essential for BMA tolerance. Furthermore, in the presence of 20 %(v/v) BMA, *E. coli* MG1655 *soxR*(R20H)*acrR*(T32fs) could not grow if *acrA* or *acrB* were deleted, but could grow, although with a lag phase, when *soxS* was deleted from the chromosome. Thus, the loss of function of *acrA* or *acrB* was more detrimental for BMA resistance than the loss of function of *soxS*. Yet, all three genes, *acrA*, *acrB* and *soxS*, had to be overexpressed in order to achieve the highest level of BMA tolerance. Nevertheless, hundreds of other genes were identified as differentially expressed in the RNA-seq analysis, either before or after the addition of BMA. Thus, many other genes might also be essential for the intricate mechanisms of BMA resistance.

7.2.2 YjiY deletions

After the addition of BMA, YjiY, also known as BtsT, was highly up-regulated in the most tolerant strains towards BMA, *E. coli* MG1655 *soxR*(R20H)*acrR*(T32fs) and *E. coli* MG1655 *soxR*(R20H)*acrR*(V29G), with log2 fold changes of 3.82 and 2.98, respectively, higher than in the less tolerant strains *E. coli* MG1655 *soxR*(R20H) and *E. coli* MG1655 *soxR*(R20H)*ybcO*(I87M) (see Figure 6.8, section 6.2).

YjiY, previously known as putative transporter, has been recently identified as a pyruvate:H^+ symporter involved in pyruvate uptake[290]. It is part of the peptide transporter carbon starvation (CstA) family[293] and it is regulated by the two-component histidine kinase/response regulator system BtsS/BtsR (previously known as YehU/YehT)[291,294]. BtsS/BtsR senses extracellular pyruvate and activates the expression of BtsT, which then imports pyruvate into the cell. BtsT is also regulated by the global regulator cyclic AMP (cAMP) receptor protein (CRP) [295].

To further investigate the potential role of *yjiY* in BMA resistance, this gene was deleted in two strains that were tolerant to BMA, *E. coli* MG1655 *soxR*(R20H) and *E. coli* MG1655 *soxR*(R20H)*acrR*(T32fs), as well as in the WT strains as a control. The new strains, *E. coli* MG1655 Δ*yjiY, E. coli* MG1655 *soxR*(R20H)-Δ*yjiY* and *E. coli* MG1655 *soxR*(R20H)*acrR*(T32fs)-Δ*yjiY* were grown in the absence or presence of 20 %(v/v) BMA (Figure 7.3 and Table 7.3).

Table 7.3 - Effect of BMA on maximum OD_{600nm} and specific growth rate of *E. coli* MG1655 stains with *yjiY* deletions. All strains were grown in MSX medium in the absence or presence of 20 %(v/v) BMA, in 30 mL vials at 37°C and 250 rpm. BMA was added immediately after inoculation. Means of two replicates and standard deviations are shown. All specific growth rates had p-values lower than 0.05. Values with n/a were not possible to determine, due to slow growth. NG: no growth.

	0 %(v/v) BMA		20 %(v/v) BMA	
***E. coli* MG1655 strains**	**Max OD_{600nm}**	**μ (h^{-1})**	**Max OD_{600nm}**	**μ (h^{-1})**
WT	2.50 ± 0.17	0.63 ± 0.03	NG	
Δ*yjiY*	2.72 ± 0.04	0.60 ± 0.01	NG	
soxR(R20H)	2.44 ± 0.00	0.62 ± 0.04	0.73 ± 0.00	n/a
soxR(R20H)-Δ*yjiY*	2.79 ± 0.11	0.57 ± 0.01	0.78 ± 0.01	n/a
soxR(R20H)*acrR*(T32fs)	3.34 ± 0.28	0.61 ± 0.02	1.20 ± 0.24	0.49 ± 0.01
soxR(R20H)*acrR*(T32fs)-Δ*yjiY*	3.20 ± 0.14	0.60 ± 0.01	1.08 ± 0.08	0.49 ± 0.04

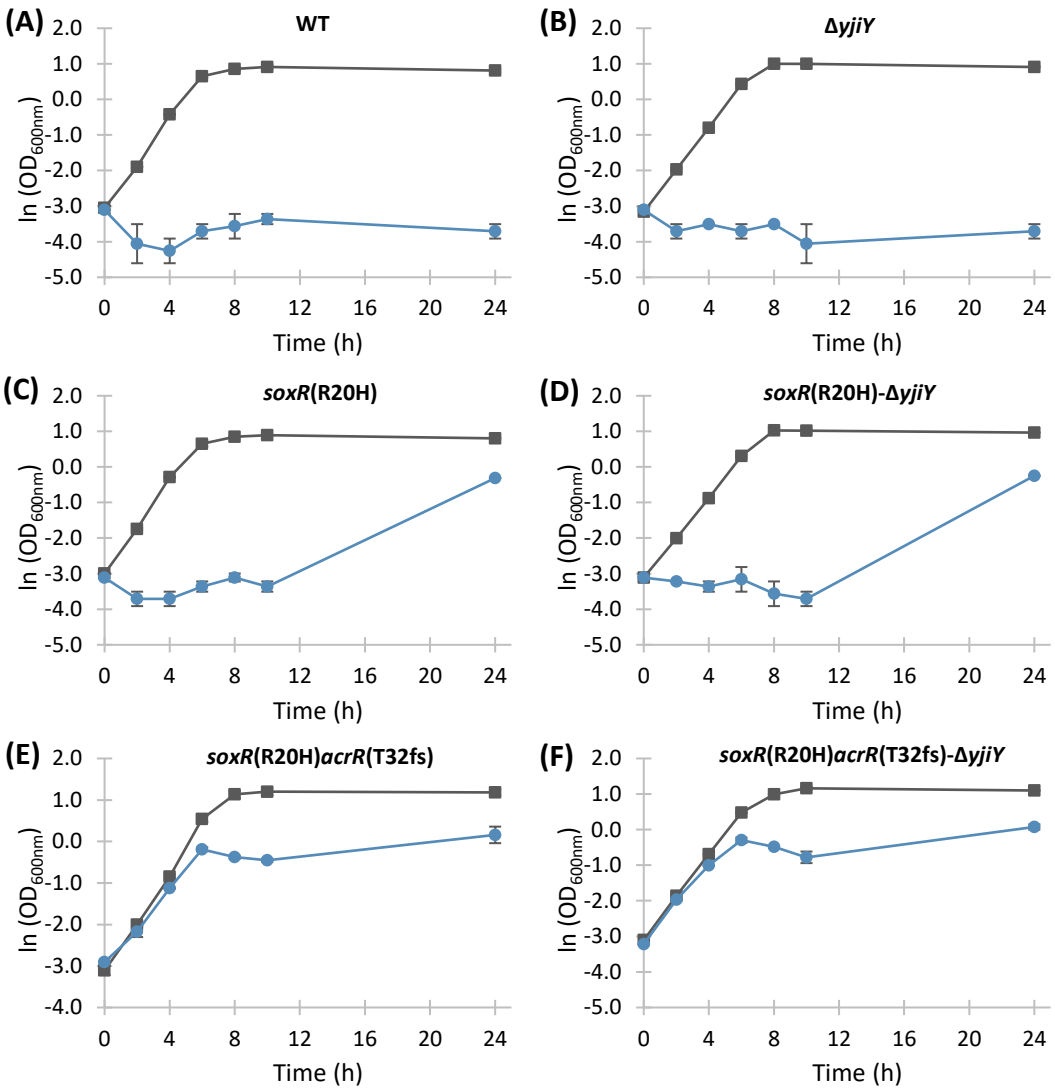

Figure 7.3 - Effect of BMA on the growth of *E. coli* MG1655 stains with *yjiY* deletions. *E. coli* MG1655 WT (A), *E. coli* MG1655 Δ*yjiY* (B), *E. coli* MG1655 *soxR*(R20H) (C), *E. coli* MG1655 *soxR*(R20H)-Δ*yjiY* (D), *E. coli* MG1655 *soxR*(R20H)*acrR*(T32fs) (E) and *E. coli* MG1655 *soxR*(R20H)*acrR*(T32fs)-Δ*yjiY* (F) were grown in MSX medium in the absence [■] or presence [●] of 20 %(v/v) BMA added immediately after inoculation. All strains were grown in 30 mL vials, at 37°C and 250 rpm shaking. Means of two replicates are shown and error bars represent standard deviations.

All strains could grow in the absence of BMA (Figure 7.3), whereas in the presence of 20 %(v/v) BMA, all KO strains with *yjiY* deletion had growth profiles similar to their respective strain without the deletion, reaching similar maximum OD_{600nm} and growth rates. Overall, the deletion of *yjiY* did not have a significant effect on the growth of *E. coli* strains, either in the absence or presence of BMA. Thus, even though *yjiY* was highly up-regulated in *E. coli* MG1655 *soxR*(R20H)*acrR*(T32fs) and *E. coli* MG1655 *soxR*(R20H)*acrR*(V29G) after the addition BMA, its deletion does not seem to result in a BMA resistance decrease. Further experiments would be necessary to fully understand whether YjiY has an impact on BMA tolerance in *E. coli*.

8 Summary of results

The cellular and genetic responses to BMA and other chemicals towards *E. coli* were investigated. Previously isolated BMA-tolerant *E. coli* mutant strains were characterized genotypically and phenotypically, as part of a broader research aimed at developing a sustainable bioprocess for the manufacture of MAE.

- The mutant strains *E. coli* MG1655 *soxR*(R20H)*acrR*(V29G) and *E. coli* MG1655 *soxR*(R20H)*acrR*(T32fs) had higher resistance to 20 %(v/v) BMA than *E. coli* MG1655 *soxR*(R20H) and *E. coli* MG1655 *soxR*(R20H)*ybcO*(I87M).
- The deletion of *soxR* did not confer tolerance to 20 %(v/v) BMA, but when pSC101_*soxR*(R20H) was added to the WT strain or *E. coli* MG1655 Δ*soxR*, the tolerance to 20 %(v/v) BMA was restored, indicating that *soxR*(R20H) encodes a functional protein adapted to confer BMA tolerance.
- The knock-in strains *E. coli* MG1655 *acrR*(V29G) and *E. coli* MG1655 *acrR*(T32fs) could grow in the presence of 20 %(v/v) BMA, but neither the deletion of *acrR* nor the genetic complementations with the plasmids pSC101_*acrR*(V29G) or pSC101_*acrR*(T32fs) conferred tolerance to BMA, showing contradictory results regarding the functionality of the mutated AcrR proteins.
- When pSC101_*soxR*(R20H)_*acrR*(V29G) or pSC101_*soxR*(R20H)_*acrR*(T32fs) were supplemented in *E. coli* MG1655 WT, the tolerance to 20 %(v/v) BMA was restored, confirming how important these genes were for BMA resistance.
- Neither the deletion of *ybcO* nor the presence of *ybcO*(I87M) conferred tolerance to 20 %(v/v) BMA, indicating that this was possibly a bystander mutation.
- The transcription factor *soxS* and other oxidative stress genes were highly up-regulated in all mutant strains, even before BMA addition. The deletion of *soxS* in the mutant strains *E. coli* MG1655 *soxR*(R20H) and *E. coli* MG1655 *soxR*(R20H)*acrR*(T32fs), resulted in a decreased resistance to 20 %(v/v) BMA,

suggesting that the up-regulation of *soxS* and other oxidative stress genes may be essential for BMA tolerance.

- The genes *acrA* and *acrB,* part of the multidrug transporter AcrABZ-TolC, were also highly up-regulated only in *E. coli* MG1655 *soxR*(R20H)*acrR*(T32fs) and *E. coli* MG1655 *soxR*(R20H)*acrR*(V29G), before BMA addition. The deletion of *acrA* and/or *acrB* in *E. coli* MG1655 *soxR*(R20H)*acrR*(T32fs) resulted in no growth in the presence of 20 %(v/v) BMA, indicating that the up-regulation of these genes could be crucial for BMA tolerance.
- After BMA exposure, the strains with the lowest BMA tolerance had higher numbers of differentially expressed genes than the more resistant strains, *E. coli* MG1655 *soxR*(R20H)*acrR*(T32fs) and *E. coli* MG1655 *soxR*(R20H)*acrR*(V29G), suggesting that the latter were more prepared to survive BMA stress.
- Several mechanisms of resistance were induced or repressed in all strains after BMA addition, including responses related to oxidative stress, iron homeostasis, osmotic stress, heat shock , phage shock, starvation, acid stress, biofilm formation and flagella motility.
- Although one candidate transporter protein, *yjiY*, was highly up-regulated in the most BMA tolerant strains, the deletion of this gene in *E. coli* MG1655 *soxR*(R20H) and *E. coli* MG1655 *soxR*(R20H)*acrR*(T32fs) did not affect the resistance to 20 %(v/v) BMA.
- The presence of the chloramphenicol resistance cassette, encoding the chloramphenicol acetyltransferase, conferred tolerance to BMA in any of the *E. coli* MG1655 knock-out strains which had this cassette.
- Of more than 20 chemicals investigated, *E. coli* MG1655 *soxR*(R20H)*acrR*(T32fs) had improved tolerance to BMA, isobutyl methacrylate, n-propyl methacrylate, n-butyl isobutyrate, n-hexane and cyclohexane, compared to the WT strain, indicating that there was a narrow range of cross-tolerance conferred by these mutations.

Overall, upon BMA exposure, thousands of genes were differently expressed in *E. coli* MG1655 WT, but the mutations in *soxR* and *acrR* resulted in pre-equipped

E. coli MG1655 mutants, capable of surviving in the presence of BMA and other chemicals (Figure 8.1). The mutants might have originated in a two-step evolution, where the *soxR* mutation occurred first, but the additional *acrR* mutations lead to a possible constitutive expression of AcrAB, which allowed the cells to be prepared to counteract BMA stress more efficiently.

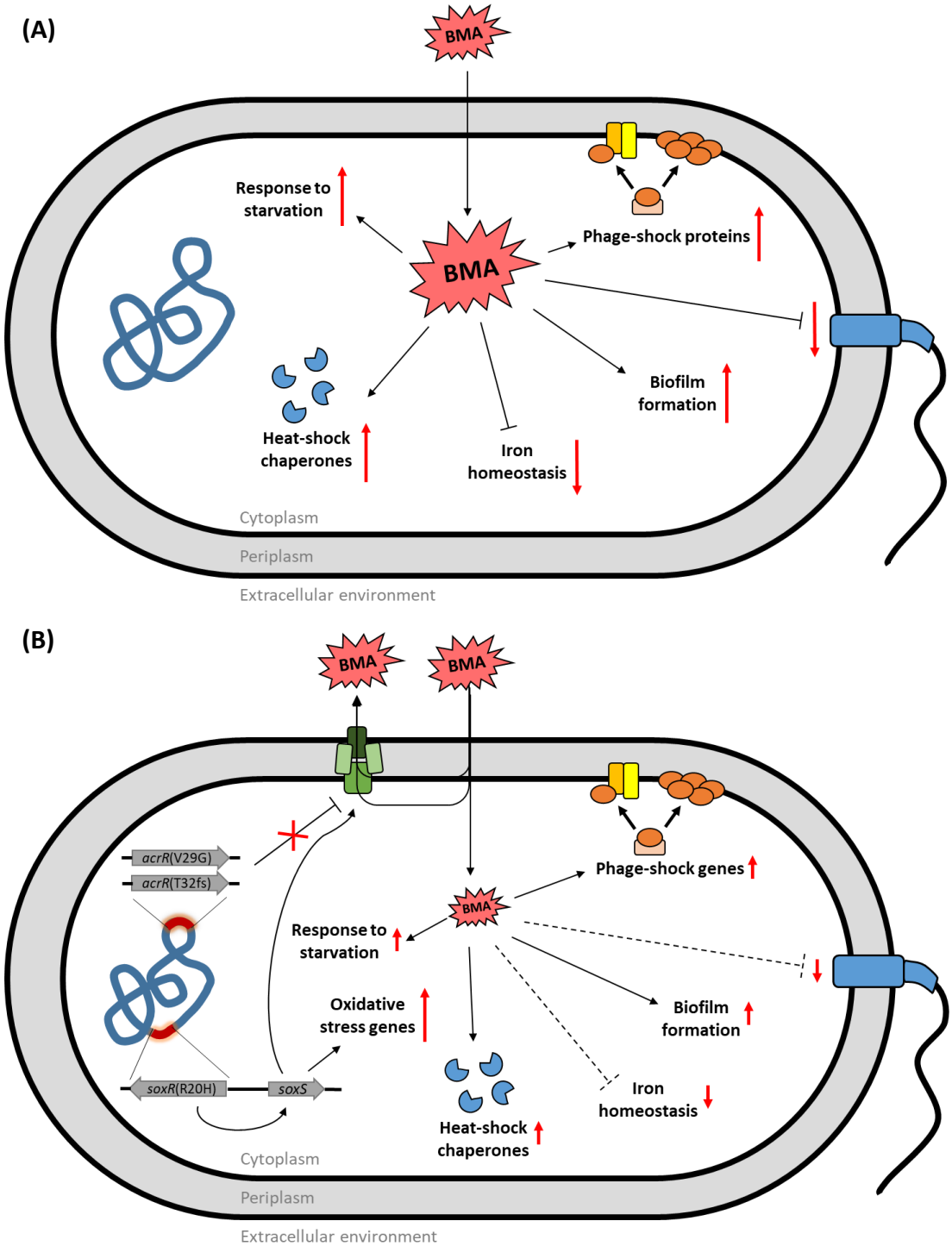

Figure 8.1 - Proposed schematic model of BMA resistance in *E. coli* MG1655. Models represent (A) *E. coli* MG1655 WT and (B) *E. coli* MG1655 *soxR*(R20H)*acrR*(T32fs) or *E. coli* MG1655 *soxR*(R20H)*acrR*(V29G). Arrows indicate induction of genes and black lines with terminal bars indicate repression of genes.

9 Discussion and future work

The mechanisms involved in the tolerance of *E. coli* towards toxic chemicals were investigated by studying four different BMA-resistant mutant strains, *E. coli* MG1655 *soxR*(R20H), *E. coli* MG1655 *soxR*(R20H)*ybcO*(I87M), *E. coli* MG1655 *soxR*(R20H)*acrR*(V29G) and *E. coli* MG1655 *soxR*(R20H)*acrR*(T32fs). The two mutant strains with mutations both in *soxR* and *acrR* were the ones with highest tolerance to BMA. Although other strains with *soxR*(R20H)[246] or *acrR*(V29G)[95,252,253] mutated genes have been previously associated with antibiotics resistance, *E. coli* strains with the combinations of *soxR*(R20H) and *acrR*(V29G) or *acrR*(T32fs) have never been reported.

SoxR is a transcription factor with $[2Fe\text{-}2S]^{+}$ clusters that becomes activated upon exposure to oxidative stress and regulates the oxidative stress response in cells, by activating the expression of dozens of genes part of the SoxRS regulon[33]. The missense mutation R20H found in *soxR* is located in the DNA-binding domain. The genotypic and phenotypic analysis, together with the transcriptomics data, indicated that *soxR*(R20H) encoded a functional transcriptional factor capable of activating the SoxRS regulon and conferring BMA tolerance, above and beyond the WT SoxR. The loss of function of *soxR,* resulting from a gene deletion, did not lead to tolerance to BMA.

In previous studies, the same *soxR*(R20H) mutation has also been found in an *E. coli* strain resistant to fluoroquinolone[246] and an isolate of *Salmonella enterica* serovar Enteritidis resistant to nalidixic acid and ciprofloxacin[248]. Although, it should be noted that these mutants also had mutations in other genes, the *E. coli* mutant had a mutation in *gyrA* (DNA gyrase, also known as topoisomerase II)[246] and the *Salmonella* mutant had two additional mutations in *gyrA*, and also a *soxS*(E52K) mutation[248]. However, it was difficult to compare these studies with the results observed in the present work, has the effect of the *soxR*(R20H) mutations was not studied individually.

All mutant strains with *soxR*(R20H) highly up-regulated the expression of *soxS* and other oxidative stress genes prior to BMA addition, compared to the WT strain. The RNA-seq results obtained in this work with *E. coli* MG1655 *soxR*(R20H), prior to BMA addition, were further compared with a previous SoxRS regulon study[160] (Table 9.1). Out of the 34 genes identified as part of the SoxRS regulon[160], 23 genes were also differently expressed in *E. coli* MG1655 *soxR*(R20H) compared to the WT, prior to BMA addition. Several genes known to be activated by SoxS, such as *nfo*, *zwf*, *fumC*, *fpr* and *pfo*, were highly up-regulated in this work, but only one SoxR target, *soxS*, was differentially expressed (Table 9.1). The transcriptional regulator *rob*, previously identified as repressed by SoxS, was down regulated in the mutants with the *soxR*(R20H) mutation. These results seem to confirm that the *soxR*(R20H) mutation resulted in an induction of the oxidative stress response, by highly up-regulating *soxS* and, consequently, the SoxS regulon. Therefore, the oxidative stress genes, including *soxS,* seemed to be expressed constitutively in the mutant strains. Furthermore, the deletion of *soxS* lead to a clear decrease in the resistance to BMA, showing once more, how important this gene was to BMA resistance.

Table 9.1 - SoxRS regulon of *E. coli* K-12 MG1655 in the presence of paraquat, analysed by RNA-seq and chromatin immunoprecipitation (ChIP), compared to RNA-seq results observed in this study with *E. coli* MG1655 *soxR*(R20H).

			Regulation	
TF	**Gene**	**Function**	**Literature[160]**	**This study (Log2 FC)**
SoxR	*soxS*	transcriptional dual regulator	Activated	7.0
	mgtA	Mg^{2+} importing P-type ATPase	Activated	-
	ahpF	Alkyl hydroperoxide reductase	ND	-
	yhcC	Radical SAM family oxidoreductase	ND	-
SoxR and SoxS	*sodA*	Superoxide dismutase (Mn)	Activated	2.9
	lpxC	UDP-3-O-acyl-N-acetylglucosamine deacetylase	Activated	1.0
	aroF	3-deoxy-7-phosphoheptulonate synthase	Activated/ND*	-
	tyrA	Fused chorismate mutase/prephenate dehydrogenase	Activated/ND*	-
	yjcB	Uncharacterized protein	Activated/ND*	0.5
	yrbL	Protein kinase-like domain-containing protein	Activated	0.6
SoxS	*fur*	Transcriptional dual regulator (iron)	ND	1.1
	nfo	Endonuclease IV	Activated	2.7
	zwf	$NADP^+$-dependent glucose-6-phosphate dehydrogenase	Activated	2.5
	acnA	Aconitate hydratase A	Activated	1.7
	fumC	Fumarase C	Activated	3.5

ribA	GTP cyclohydrolase 2	Activated	2.0
fpr	Flavodoxin/ferredoxin-NADP+ reductase	Activated	4.0
fldA	Flavodoxin 1	Activated	2.0
pfo	Putative pyruvate-flavodoxin oxidoreductase	Activated	4.3
acrA	multidrug efflux pump membrane fusion lipoprotein	ND	-
acrB	multidrug efflux pump RND permease	ND	1.1
acrZ	multidrug efflux pump accessory protein	ND	1.2
mdlB	ABC transporter family protein	Activated	1.4
mdlA	ABC transporter family protein	Activated	1.3
ariR	regulator of acid resistance	ND	-
ymgC	Uncharacterized protein	ND	-
ymgA	putative two-component system connector protein	ND	-
nepI	purine ribonucleoside exporter	Activated	-
nhoA	arylamine N-acetyltransferase	Activated	1.7
nfsA	NADPH-dependent nitroreductase	Activated	2.7
rob	transcriptional dual regulator	Repressed	-1.2
ybaO	DNA-binding transcriptional activator	Activated	1.5
ypeC	Uncharacterized protein	ND	-
ybjC	Uncharacterized protein	Activated	2.8

Genes that were not differentially expressed (log2 fold change ≥ 1 or ≤ -1) are indicated as (-).
ND: Not determined.
*Genes activated by SoxR and regulated (either activated or repressed) by SoxS

Although the R20H mutation in SoxR was beneficial for BMA tolerance, other studies reported that mutations in the DNA binding domain of SoxR, such as Y31H, L36V, I62V, I62N and I73F, result in unstable $[2Fe\text{-}2S]^{+}$ clusters and in a decrease in the ability of SoxR to became activated and bind to the DNA[249,250]. This contradicts the results observed in this work, which suggest that R20H mutation in SoxR facilitates the binding to the DNA and, consequently, the activation of other genes. The ability of the mutated *soxR* to bind to the DNA would definitely be vital to prove in future research. Further work has already been done to determine the affinity of the protein encoded by *soxR*(R20H) to a synthetic oligonucleotide representing a SoxR promoter region, compared to the WT SoxR (Simon Caulton, University of Nottingham; unpublished data). However, neither SoxR WT nor the mutant SoxR can bind to the promoter DNA sequence used. Even though SoxR only activates the transcription of genes when the $[2Fe\text{-}2S]^{+}$ clusters are oxidized, the reduced form of SoxR can also bind to the DNA[161], hence SoxR WT should still bind to the DNA in affinity assays. Therefore, results were inconclusive and the ability of the mutated *soxR* to bind to the promoter region should continue to be explored. Furthermore, it

would be interesting to test if other mutations in the DNA binding domain or even in the dimerization domain of SoxR, could also confer BMA tolerance. SoxR mutations previously found in literature (Y31H, L36V, I62V, I62N and I73F[249,250]) could be tested against BMA stress. In addition, a *soxR* random mutagenesis library done using error-prone PCR could also be tested and pooled in serial solutions in the presence of BMA, to select any other *soxR* mutations beneficial for BMA tolerance.

AcrR is a transcriptional factor that represses the expression of the *acrAB* operon, which encodes proteins for the widely studied RND efflux pump AcrABZ-TolC[82]. The two mutations found in *acrR,* V29G and T32fs, are also located in the DNA binding domain. Prior to BMA exposure, *acrA* and *acrB* were highly up-regulated only in the strains with *acrR* mutations, suggesting that the two mutated *acrR* genes encode a non-functional protein incapable of repressing the transcription of *acrAB*. Subsequent studies have shown that the AcrR with a V29G mutation had a 50-fold lower affinity for the promoter region of *acrAB* than the WT AcrR (Simon Caulton, University of Nottingham; unpublished data). Furthermore, AcrR(T32fs) was insoluble, suggesting that this truncated protein may not even fold correctly and, consequently, could not bind to the DNA (Simon Caulton, University of Nottingham; unpublished data). The structures of the proteins encoded by *acrR*(V29G) and *acrR*(T32fs) could be further studied by computational modelling, to understand the folding of these proteins and what conformational changes possibly occurred, compared to the WT AcrR, that lead to observed phenotype. Additionally, to test if any other mutations in the DNA-binding domain confer tolerance to BMA in *E. coli*, an *acrR* random mutagenesis library could also be constructed and pooled in serial solutions in the presence of BMA.

However, in the present work, the *acrR* deletion did not confer tolerance to 20 %(v/v) BMA, even though strains with *acrR*(V29G) or *acrR*(T32fs) mutations did. Yet, the deletion of *acrR* is known to improve tolerance to ethanol, n-butanol, isobutanol[71] and n-hexane[296]. Therefore, it remains unclear why the deletion of the repressor *acrR* did not confer BMA tolerance. One hypothesis is that the scar sequence resulting from the deletion of *acrR* using the λ red recombination method was possibly negatively affecting the promoter region of *acrAB,* hindering the

transcription of this operon, something that would not have happen in the knock-in *acrR*(V29G) and *acrR*(T32fs) strains, as the scar sequence would be upstream of the *acrR* gene instead of the promoter region. In future work this hypothesis could be tested by deleting the *acrR* gene using scarless chromosomal deletion methods, such as the homing endonuclease I-SceI system[297] or the scarless Cas9 assisted recombineering (no-SCAR) system[298]. In addition, the overexpression of *acrA* and *acrB* was crucial for BMA tolerance, as the deletion of these genes in BMA-resistant strains resulted in the loss of BMA tolerance. Most of the findings in this work suggest that the multidrug transporter AcrABZ-TolC was one of the key mechanisms involved in BMA tolerance, by pumping BMA out of the cells. Future research could aim to confirm that BMA is a substrate for AcrABZ-TolC, by performing efflux and binding assays[299].

The presented work did not provide any evidence regarding the biological function of the uncharacterized protein YbcO, since the mutated gene *ybcO*(I87M) did not seem to influence BMA tolerance. There were no significant differences between the induced and repressed genes of *E. coli* MG1655 *soxR*(R20H) and *E. coli* MG1655 *soxR*(R20H)*ybcO*(I87M), either before or after the addition of BMA, and neither the KO nor KI strains of *ycbO* grew in the presence of BMA. It still remains unclear why one of the mutant strains had this extra mutation and further studies would be needed to determine the function of YbcO. Based on structure homology, YbcO has been predicted to be a nuclease[254]. Further studies could aim to confirm that YbcO encodes a nuclease, by performing a nuclease activity assay[300].

Although SoxR and AcrR and their regulons have a high impact on BMA tolerance, hundreds of other genes were also affected upon BMA exposure, indicating that the response to a toxic chemical in *E. coli* is complex. However, there was a clear correlation between the level of BMA resistance of a given strain and its number of differentially expressed genes after BMA addition. In the WT strain, which did not grow in the presence of BMA, over three thousand genes were differentially expressed, corresponding to about 74 % of the genes in *E. coli* genome, whereas in the most resistant strains (the ones with both the *soxR* and *acrR* mutations), only a few hundred genes were differentially expressed. The vast number of differentially

expressed genes was symptomatic that the WT strain was dying after exposure to BMA and, consequently, was inducing or repressing a wide range of mechanisms to try to resist to BMA and survive. On the other hand, the resistant mutants induced or repressed tolerance mechanisms even before the addition of BMA, which possibly allowed the cells to be more prepared to counteract BMA stress, without the need to recruit as many survival mechanisms after BMA addition.

In general, most of the biological responses expressed in the most BMA-tolerant strains, *E. coli* MG1655 *soxR*(R20H)*acrR*(V29G) and *E. coli* MG1655 *soxR*(R20H)*acrR*(T32fs), were also expressed in the other mutant strains and in the WT strain, and seemed to be highly interconnected and functionally linked. The phage shock genes were highly up-regulated in all mutant strains and WT upon BMA exposure, and are also known to be up-regulated in the presence of other chemicals, such as *n*-hexane and cyclooctane[134]. This could mean that BMA possibly disrupted the structure of the membrane bilayer and membrane proteins such as the phage shock proteins were induced to maintain membrane integrity. The effects of BMA on the membrane integrity could further explored by performing lipidomic analysis and structural studies on membrane fluidity, to determine if there were changes in the *cis-trans* isomerization of unsaturated fatty acids or in the ratio of saturated-to-unsaturated fatty acids. Furthermore, the importance of the phage shock genes in the resistance to BMA in *E. coli* could be tested by deleting these genes from BMA-resistance strains and analysing the resulting phenotype.

The down-regulation of non-specific transport (outer membrane porins) in all mutant strains and in the WT strain upon BMA exposure, could be related to the possible attempt to increase membrane bilayer integrity by up-regulating phage shock proteins. Together, these mechanisms could lead to a reduction of membrane permeability and, consequently, to the induction of the starvation response, which was indeed up-regulated in all mutant strains and also in the WT strain, after the addition of BMA. Hence, the response to starvation could be one of the essential mechanisms that *E. coli* needs to induce in order to survive BMA stress. The starvation-related genes up-regulated in the mutant strains could be deleted from the BMA resistant strains, to know whether the tolerance to BMA would decrease.

Furthermore, the up-regulation of genes related to biofilm formation in all strains after BMA addition (which are also up-regulated in the presence of other chemicals, such as octanoic acdic[101], n-butanol and acetate[100]), could be related to the starvation response, but also act as an additional mechanism of defence, for the cells to avoid contact with BMA. Once again, the importance of the biofilm formation genes could further proved by doing gene deletions in the BMA resistant strains. In addition, future research could also determine if biofilm is actually being formed upon exposure to BMA, by using, for example, microscopy techniques such as scanning electron microscopy[301].

BMA exposure lead to the down-regulation of flagella genes and methyl-accepting chemotaxis sensor proteins in the WT strain and all the mutant strains. Most genes related to flagella assembly and synthesis are also down-regulated in the presence of other chemicals, such as toluene, n-butanol and ethanol[88,96,101], but chemotaxis related genes are up-regulated in the presence of ethanol[96]. The down-regulation of flagella and chemotaxis genes could also be closely related to the up-regulation of biofilm formation genes. Furthermore, it has been hypothesised that, in response to toxic chemicals, flagella genes are down-regulated to save energy[141], which could be directed to other biological processes more important for cell survival. To further understand the involvement of flagella genes in BMA tolerance, the energy metabolism could be studied by performing a metabolomics analysis and the expression of flagella genes before and after BMA addition could be quantified by a proteomics analysis.

The response to pH changes was also up-regulated in all mutant strains after the addition of BMA, and is known to be up-regulated in the presence of other chemicals such as ethanol[96] and octanoic acid[101]. The acid stress response is induced at low intracellular pH levels, which dissipate the transmembrane pH gradient and decrease the electrochemical potential, interfering with energy synthesis or transport processes[40-42]. Therefore, this toxicity effect might be related to other mechanisms that can also affect the membrane. The importance of the acid stress response for conferring BMA tolerance could be further tested by studying the phenotype of

BMA-resistant strains with deletions of the up-regulated genes related to the acid stress response.

Some genes involved in the oxidative stress response were up-regulated after the addition of BMA, while others where down-regulated, and, in addition, there was variability in the expression across the different strains (see Figure 6.6, page 135). Genes related to the oxidative stress response are up-regulated in response to n-butanol, n-cyclohexyl-pyrrolidone, cyclopentanone, dimethyl sulphide, toluene, ethanol, octanoic acid and 1,4-butanediol[88,96,100,101]. However, for example, genes such as *sodA* (manganese containing superoxide dismutase), up-regulated in the presence of ethanol[96], n-butanol[100] and 1,4-butanediol[100], and the *suf* genes (assembly of Fe-S clusters), up-regulated in the presence of n-butanol, cyclopentanone, N,N-dimethylacetamide and dimethyl sulphide[88], were all down-regulated in this study in the presence of BMA, in the WT strain and in the mutants *E. coli* MG1655 *soxR*(R20H) and *E. coli* MG1655 *soxR*(R20H)*ybcO*(I87M). Overall, the iron homeostasis, closely related to the oxidative stress response, was down-regulated in all the strains upon BMA exposure, yet, in other studies some iron homeostasis systems are down-regulated and some are up-regulated in the presence of n-butanol, isobutanol, cyclopentanone, ethanol, toluene and/or 1,4-butanediol [88,89,96,99,100,102]. Hence, there were differences between the findings of this work and literature previously reported on the induction of the oxidative stress and iron homeostasis responses by toxic chemicals. However, transcriptomics data could suggest that the oxidative stress response, and, consequently, the iron homeostasis response, could be induced due to the disruption of the membrane bilayer, which could affect the respiration processes of the cell and, consequently, generate reactive oxygen species[146-148]. Once again, proteomics, metabolomics and lipidomics studies would be useful to further elucidate on the role of the oxidative stress response and iron homeostasis on the resistance to BMA stress, by analysing the changes in the membrane structure, in the energy metabolism and respiration processes and in the expression of oxidative stress related proteins. Nonetheless, the present work shows that several mechanisms could be further studied in more detail, to improve tolerance to BMA and possibly other MAE.

The present work also provided a novel platform to possibly solve BMA toxicity. *E. coli* MG1655 WT could not grow in the presence of 20 %(v/v) BMA, but with the genetic complementations done using the recombinant plasmids pSC101_*soxR*(R20H)_*acrR*(V29G) or pSC101_*soxR*(R20H)_*acrR*(T32fs), the tolerance to 20 %(v/v) BMA was restored. The addition of the plasmids expressing the mutated *soxR* and *acrR* genes could provide a solution to obtain BMA tolerance in an *E. coli* WT strain, and, consequently, significantly improve the production of BMA. In flask cultures, wild type *E. coli* BW25115 transformed with the MAE production pathway (see Figure 1.5, section 1.1.2, page 19) is only capable of producing 0.6 mg/L of BMA after 48 h, which is far below the productivity target of 2 g/L/h of BMA (Graham Eastham, Lucite International, personal communication). In future research, strains with the MAE production pathway could be tested with the plasmids pSC101_*soxR*(R20H)_*acrR*(V29G) or pSC101_*soxR*(R20H)_*acrR*(T32fs) to know if the expression of these mutated genes could improve BMA productivity.

The *E. coli* MG1655 strains with *acrR* and *soxR* mutations or the plasmids pSC101_*soxR*(R20H)_*acrR*(V29G) and pSC101_*soxR*(R20H)_*acrR*(T32fs) could also have the potential to be used in other bioprocesses beyond the production of MAE. *E. coli* MG1655 *soxR*(R20H)*acrR*(T32fs) was able to grow in the presence of 20 %(v/v) n-hexane and 20 %(v/v) cyclohexane, and had improved tolerance compared to the WT strain, which could grow in the presence of 20 %(v/v) n-hexane, although with a lower growth rate, but could not grow in the presence of 20 %(v/v) cyclohexane. This difference in the levels of toxicity in *E. coli* MG1655 WT could be explained by the difference in the log P_{ow} of the chemicals. The log P_{ow} value is the partition coefficient of a chemical in an equimolar mixture of octanol and water[16-20], and, consequently, chemicals with higher log P_{ow} values are more nonpolar and hydrophobic and, thus, more toxic to the cells[16-20]. n-Hexane and cyclohexane have log P_{ow} values of 3.90 and 3.44, therefore n-hexane is less toxic. A previous study has shown that *E. coli* JA300 strains can grow in the presence of n-hexane but not cyclohexane[302]. In another study, mutant strains with *acrR* mutations, namely A41D, M1I, and a 1195 bp insertion sequence (IS5) element, and additional mutations in *marR*, also had improved tolerance to cyclohexane compared to the WT strain *E. coli* JA300, which

did not grow in the presence of cyclohexane[251]. However, in these studies, toxicity tests were done in solid LBGMg agar medium overlaid with a layer of chemicals, which is not comparable to production conditions. In addition, previous studies have associated the overexpression of *soxS* with an increase in cyclohexane tolerance[302,303]. In line with the previous studies, this work showed that there might be a close relation between the tolerance mechanisms regulated by AcrR and SoxR and the levels of toxicity to cyclohexane. Future research could also continue to explore the toxicity limits of *E. coli* MG1655 *soxR*(R20H)*acrR*(T32fs) towards other commodity chemicals which are relevant to industry, such as toluene, styrene, xylenes, octanoic acid, phenol or 1,4-butanediol.

Another surprising discovery was that the presence of the chloramphenicol resistance cassette confers tolerance to BMA. *E. coli* MG1655 KO strains which had the *acrR* or *soxR* genes replaced with a chloramphenicol resistance cassette, encoding the chloramphenicol acetyltransferase, could grow in the presence of 20 %(v/v) BMA, while KO strains with a short scar sequence following the removal of the antibiotic resistance gene could not. This could prove to be an important finding to further develop a BMA production process. Future research should continue to characterize these KO strains to understand why the presence of chloramphenicol resistance cassette affects BMA tolerance and if the phenotype observed is specific to the deletions of *acrR* and *soxR* only. In line with the previous experiments done with the production strain and the recombinant plasmids with BMA resistance, future studies could examine how this KO strains with chloramphenicol resistance could improve BMA production titres.

In summary, the combinations of the mutated genes *soxR*(R20H) plus *acrR*(V29G) or *acrR*(T32fs), never reported in literature before, had improved tolerance to high concentrations of BMA, but also to other commodity chemicals such as isobutyl methacrylate, n-propyl methacrylate, n-butyl isobutyrate, n-hexane and cyclohexane. Furthermore, the over expression of *soxS*, involved in the oxidative stress response, and *acrA* and *acrB*, part of the multidrug pump AcrABZ-TolC, was crucial for the BMA tolerance observed. These mutant strains or the recombinant plasmids with the mutated genes developed in this study could be used as a novel

platform to improve tolerance and, consequently, the productivity yields in the sustainable production of MAE using *E. coli*, and possibly in other processes relevant to industry.

10 References

1 Sardessai, Y. N. & Bhosle, S. Industrial Potential of Organic Solvent Tolerant Bacteria. *Biotechnology Progress* 20, 655-660 (2004).

2 Lucite-International. *Innovation in biotechnology*, <http://www.luciteinternational.com/our-technologies-innovation-130/#biotechnology> (2016).

3 Chang, R. J. & Naqvi, S. *Methyl Methacrylate (MMA) Process Summary*, <https://www.ihs.com/pdf/RW2014-05-toc_183646110917062932.pdf> (2014).

4 Kind, S. *et al.* From zero to hero - production of bio-based nylon from renewable resources using engineered Corynebacterium glutamicum. *Metabolic engineering* 25, 113-123 (2014).

5 Becker, J., Lange, A., Fabarius, J. & Wittmann, C. Top value platform chemicals: bio-based production of organic acids. *Current Opinion in Biotechnology* 36, 168-175 (2015).

6 Eastham Graham, R., Stephens, G. & Yiakoumetti, A. Process For The Biological Production Of Methacrylic Acid And Derivatives Thereof. US patent US 2018/0171368 A1 (2018).

7 Disley, Z. *Towards the bioproduction of methyl methacrylate: solving the problem of product toxicity.* PhD thesis, University of Nottingham (2018).

8 Becker, J. & Wittmann, C. Advanced biotechnology: metabolically engineered cells for the bio-based production of chemicals and fuels, materials, and health-care products. *Angewandte Chemie (International ed. in English)* 54, 3328-3350 (2015).

9 Lucite-International. *Corporate review*, <http://www.luciteinternational.com/wp-content/uploads/lucite-international/assets/292/CorporateReview0811_original.pdf > (2011).

10 Lucite-International. *Our products - monomers*, <http://www.luciteinternational.com/monomers-emea-products-and-applications-our-products-21/> (2016).

11 Harris, B. *Acrylics for the future*, <http://www.ingenia.org.uk/Content/ingenia/issues/issue45/harris.pdf> (2010).

12 Bauer, W. *Methacrylic Acid and Derivatives*. in *Ullmann's Encyclopedia of Industrial Chemistry*, Wiley-VCH Verlag GmbH & Co. KGaA (2000).

13 Joshi, S. S. R. V. V. *Industrial catalytic processes for fine and specialty chemicals*. Ch. 14, 678 (2016).

14 Lucite-International. *Raw materials flow*, <http://www.luciteinternational .com/monomers-emea-manufacturing-raw-materials-flow-20/> (2016).

15 Demain, A. L. The business of biotechnology. *Industrial Biotechnology* 3, 269-283 (2007).

16 Inoue, A. & Horikoshi, K. A Pseudomonas thrives in high concentrations of toluene. *Nature* 338, 264-266 (1989).

17 Luisi, P. L. & Laane, C. Solubilization of enzymes in apolar solvents via reverse micelles. *Trends Biotechnol.* 4, 153-161 (1986).

18 Salter, G. J. & Kell, D. B. Solvent selection for whole cell biotransformations in organic media. *Crit. Rev. Biotechnol.* 15, 139-177 (1995).

19 Inoue, A. & Horikoshi, K. Estimation of solvent-tolerance of bacteria by the solvent parameter log P. *Journal of Fermentation and Bioengineering* 71, 194-196 (1991).

20 Heipieper, H. J., Weber, F. J., Sikkema, J., Keweloh, H. & de Bont, J. A. M. Mechanisms of resistance of whole cells to toxic organic solvents. *Trends in Biotechnology* 12, 409-415 (1994).

21 Ingram, L. O. Mechanism of lysis of Escherichia coli by ethanol and other chaotropic agents. *Journal of Bacteriology* 146, 331-336 (1981).

22 Ingram, L. O. Adaptation of membrane lipids to alcohols. *Journal of Bacteriology* 125, 670-678 (1976).

23 Royce, L. A., Liu, P., Stebbins, M. J., Hanson, B. C. & Jarboe, L. R. The damaging effects of short chain fatty acids on Escherichia coli membranes. *Applied Microbiology and Biotechnology* 97, 8317-8327 (2013).

24 Lennen, R. M. *et al.* Membrane Stresses Induced by Overproduction of Free Fatty Acids in Escherichia coli. *Applied and Environmental Microbiology* 77, 8114-8128 (2011).

25 Hyldgaard, M., Sutherland, D. S., Sundh, M., Mygind, T. & Meyer, R. L. Antimicrobial Mechanism of Monocaprylate. *Applied and Environmental Microbiology* 78, 2957-2965 (2012).

26 Jarboe, L. R., Royce, L. A. & Liu, P. Understanding biocatalyst inhibition by carboxylic acids. *Frontiers in Microbiology* 4, 272 (2013).

27 Watson, H. Biological membranes. *Essays in Biochemistry* 59, 43-69 (2015).

28 Segura, A. *et al.* Solvent tolerance in Gram-negative bacteria. *Curr. Opin. Biotechnol.* 23, 415-421 (2012).

29 Sikkema, J., de Bont, J. A. & Poolman, B. Interactions of cyclic hydrocarbons with biological membranes. *The Journal of biological chemistry* 269, 8022-8028 (1994).

30 Spears, R. J. & Fascione, M. A. Site-selective incorporation and ligation of protein aldehydes. *Organic & Biomolecular Chemistry* 14, 7622-7638 (2016).

31 Agten, S. M., Dawson, P. E. & Hackeng, T. M. Oxime conjugation in protein chemistry: from carbonyl incorporation to nucleophilic catalysis. *Journal of Peptide Science* 22, 271-279 (2016).

32 Tittensor, J. R. & Walker, R. T. The isolation, analysis and chemical reactions of deoxyribonucleic acid [DNA]—III. The chemical reactions of DNA. *European Polymer Journal* 4, 39-54 (1968).

33 Imlay, J. A. Transcription factors that defend bacteria against reactive oxygen species. *Annu. Rev. Microbiol.*, Ahead of Print (2015).

34 Imlay, J. A. Diagnosing oxidative stress in bacteria: not as easy as you might think. *Curr. Opin. Microbiol.* 24, 124-131 (2015).

35 Ezraty, B., Gennaris, A., Barras, F. & Collet, J. F. Oxidative stress, protein damage and repair in bacteria. *Nature reviews. Microbiology* 15, 385-396 (2017).

36 Farr, S. B. & Kogoma, T. Oxidative stress responses in Escherichia coli and Salmonella typhimurium. *Microbiological Reviews* 55, 561-585 (1991).

37 Vaca, C. E., Wilhelm, J. & Harms-Ringdahl, M. Interaction of lipid peroxidation products with DNA. A review. *Mutation Research/Reviews in Genetic Toxicology* 195, 137-149 (1988).

38 Lee, C. & Park, C. Bacterial Responses to Glyoxal and Methylglyoxal: Reactive Electrophilic Species. *International Journal of Molecular Sciences* 18, 169 (2017).

39 Russell, J. B. Another explanation for the toxicity of fermentation acids at low pH: anion accumulation versus uncoupling. *Journal of Applied Bacteriology* 73, 363-370 (1992).

40 Baronofsky, J. J., Schreurs, W. J. A. & Kashket, E. R. Uncoupling by Acetic Acid Limits Growth of and Acetogenesis by Clostridium thermoaceticum. *Applied and Environmental Microbiology* 48, 1134-1139 (1984).

41 Herrero, A. A., Gomez, R. F., Snedecor, B., Tolman, C. J. & Roberts, M. F. Growth inhibition of Clostridium thermocellum by carboxylic acids: A

mechanism based on uncoupling by weak acids. *Applied Microbiology and Biotechnology* 22, 53-62 (1985).

42 Huesemann, M. & Papoutsakis, E. T. Effect of acetoacetate, butyrate, and uncoupling ionophores on growth and product formation of Clostridium acetobutylicum. *Biotechnol. Lett.* 8, 37-42 (1986).

43 Axe, D. D. & Bailey, J. E. Transport of lactate and acetate through the energized cytoplasmic membrane of Escherichia coli. *Biotechnology and Bioengineering* 47, 8-19 (1995).

44 Russell, J. B. & Diez-Gonzalez, F. The Effects of Fermentation Acids on Bacterial Growth. *Advances in Microbial Physiology* 39, 205-234 (1997).

45 Trček, J., Mira, N. P. & Jarboe, L. R. Adaptation and tolerance of bacteria against acetic acid. *Applied Microbiology and Biotechnology* 99, 6215-6229 (2015).

46 Liu, Y., Tang, H., Lin, Z. & Xu, P. Mechanisms of acid tolerance in bacteria and prospects in biotechnology and bioremediation. *Biotechnol. Adv.* 33, 1484-1492 (2015).

47 Stancu, M. M. & Vila, J. Physiological Response of Escherichia coli IBBCt1 to n-Alkanes and Kerosene. *Environmental Forensics* 14, 50-58 (2013).

48 Wang, L., Qiao, N., Sun, F. & Shao, Z. Isolation, gene detection and solvent tolerance of benzene, toluene and xylene degrading bacteria from nearshore surface water and Pacific Ocean sediment. *Extremophiles* 12, 335-342 (2008).

49 Ramos, J. L., Duque, E., Huertas, M. J. & Haïdour, A. Isolation and expansion of the catabolic potential of a Pseudomonas putida strain able to grow in the presence of high concentrations of aromatic hydrocarbons. *Journal of Bacteriology* 177, 3911-3916 (1995).

50 Weber, F. J., Ooijkaas, L. P., Schemen, R. M. W., Hartmans, S. & de Bont, J. A. M. Adaptation of Pseudomonas putida S12 to high concentrations of styrene and other organic solvents. *Appl. Environ. Microbiol.* 59, 3502-3504 (1993).

51 Segura, A., Hurtado, A., Rivera, B. & Lazaroaie, M. M. Isolation of new toluene-tolerant marine strains of bacteria and characterization of their solvent-tolerance properties. *Journal of Applied Microbiology* 104, 1408-1416 (2008).

52 Kanno, M. *et al.* Isolation of Butanol- and Isobutanol-Tolerant Bacteria and Physiological Characterization of Their Butanol Tolerance. *Applied and Environmental Microbiology* 79, 6998-7005 (2013).

53 Zahir, Z., Seed, K. D. & Dennis, J. J. Isolation and characterization of novel organic solvent-tolerant bacteria. *Extremophiles* 10, 129-138 (2006).

54 Boyarskiy, S. & Tullman-Ercek, D. Getting pumped: membrane efflux transporters for enhanced biomolecule production. *Curr. Opin. Chem. Biol.* 28, 15-19 (2015).

55 McMurry, L., Petrucci, R. E. & Levy, S. B. Active efflux of tetracycline encoded by four genetically different tetracycline resistance determinants in Escherichia coli. *Proceedings of the National Academy of Sciences of the United States of America* 77, 3974-3977 (1980).

56 Blair, J. M., Richmond, G. E. & Piddock, L. J. Multidrug efflux pumps in Gram-negative bacteria and their role in antibiotic resistance. *Future Microbiology* 9, 1165-1177 (2014).

57 Wong, K., Ma, J., Rothnie, A., Biggin, P. C. & Kerr, I. D. Towards understanding promiscuity in multidrug efflux pumps. *Trends Biochem. Sci.* 39, 8-16 (2014).

58 Schindler, B. D. & Kaatz, G. W. Multidrug efflux pumps of Gram-positive bacteria. *Drug Resistance Updates* 27, 1-13 (2016).

59 Chitsaz, M. & Brown, Melissa H. The role played by drug efflux pumps in bacterial multidrug resistance. *Essays In Biochemistry* 61, 127-139 (2017).

60 Aono, R., Tsukagoshi, N. & Yamamoto, M. Involvement of outer membrane protein TolC, a possible member of the mar-sox regulon, in maintenance and improvement of organic solvent tolerance of Escherichia coli K-12. *J. Bacteriol.* 180, 938-944 (1998).

61 Mikolosko, J., Bobyk, K., Zgurskaya, H. I. & Ghosh, P. Conformational flexibility in the multidrug efflux system protein AcrA. *Structure (London, England : 1993)* 14, 577-587 (2006).

62 Murakami, S., Nakashima, R., Yamashita, E., Matsumoto, T. & Yamaguchi, A. Crystal structures of a multidrug transporter reveal a functionally rotating mechanism. *Nature* 443, 173-179 (2006).

63 Koronakis, V., Sharff, A., Koronakis, E., Luisi, B. & Hughes, C. Crystal structure of the bacterial membrane protein TolC central to multidrug efflux and protein export. *Nature* 405, 914-919 (2000).

64 Hobbs, E. C., Yin, X., Paul, B. J., Astarita, J. L. & Storz, G. Conserved small protein associates with the multidrug efflux pump AcrB and differentially affects antibiotic resistance. *Proc. Natl. Acad. Sci. U. S. A.* 109, 16696-16701, S16696/16691-S16696/16699 (2012).

65 Rosano, G. L. & Ceccarelli, E. A. Recombinant protein expression in Escherichia coli: advances and challenges. *Front Microbiol* 5, 172 (2014).

66 Wang, Z. *et al.* An allosteric transport mechanism for the AcrAB-TolC multidrug efflux pump. *eLife* 6, e24905 (2017).

67 Seeger, M. A., von Ballmoos, C., Verrey, F. & Pos, K. M. Crucial role of Asp408 in the proton translocation pathway of multidrug transporter AcrB: evidence from site-directed mutagenesis and carbodiimide labeling. *Biochemistry* 48, 5801-5812 (2009).

68 Du, D., Voss, J., Wang, Z., Chiu, W. & Luisi, B. F. The pseudo-atomic structure of an RND-type tripartite multidrug efflux pump. *Biol. Chem.* 396, 1073-1082 (2015).

69 Saier, M. H., Tran, C. V. & Barabote, R. D. TCDB: the Transporter Classification Database for membrane transport protein analyses and information. *Nucleic Acids Research* 34, D181-D186 (2006).

70 Hassan, K. *et al.* An ace up their sleeve: a transcriptomic approach exposes the AceI efflux protein of Acinetobacter baumannii and reveals the drug efflux potential hidden in many microbial pathogens. *Frontiers in Microbiology* 6 (2015).

71 Luhe, A. L., Gerken, H., Tan, L., Wu, J. & Zhao, H. Alcohol tolerance of Escherichia coli acrR and marR regulatory mutants. *J. Mol. Catal. B: Enzym.* 76, 89-93 (2012).

72 Shah, A. A. *et al.* Enhancement of resistance of Escherichia coli by MarA overexpression. *J. Biosci. Bioeng.* 115, 253-258 (2013).

73 White, D. G., Goldman, J. D., Demple, B. & Levy, S. B. Role of the acrAB locus in organic solvent tolerance mediated by expression of marA, soxS, or robA in Escherichia coli. *Journal of Bacteriology* 179, 6122-6126 (1997).

74 Hirakawa, H. *et al.* AcrS/EnvR represses expression of the acrAB multidrug efflux genes in Escherichia coli. *J. Bacteriol.* 190, 6276-6279 (2008).

75 Takrouri, K. *et al.* Progress against Escherichia coli with the Oxazolidinone Class of Antibacterials: Test Case for a General Approach To Improving Whole-Cell Gram-Negative Activity. *ACS Infect. Dis.*, Ahead of Print (2016).

76 Du, D. *et al.* Structure of the AcrAB-TolC multidrug efflux pump. *Nature (London, U. K.)* 509, 512-515 (2014).

77 Du, D., van Veen, H. W. & Luisi, B. F. Assembly and operation of bacterial tripartite multidrug efflux pumps. *Trends Microbiol.* 23, 311-319 (2015).

78 Seeger, M. A. *et al.* Structural Asymmetry of AcrB Trimer Suggests a Peristaltic Pump Mechanism. *Science* 313, 1295-1298 (2006).

79 Ramos, J. L. *et al.* The TetR Family of Transcriptional Repressors. *Microbiology and Molecular Biology Reviews* 69, 326-356 (2005).

80 Li, M. *et al.* Crystal structure of the transcriptional regulator AcrR from Escherichia coli. *J. Mol. Biol.* 374, 591-603 (2007).

81 Su, C.-C., Rutherford, D. J. & Yu, E. W. Characterization of the multidrug efflux regulator AcrR from Escherichia coli. *Biochemical and biophysical research communications* 361, 85-90 (2007).

82 Ma, D., Alberti, M., Lynch, C., Nikaido, H. & Hearst, J. E. The local repressor AcrR plays a modulating role in the regulation of acrAB genes of Escherichia coli by global stress signals. *Molecular Microbiology* 19, 101-112 (1996).

83 Zhang, A., Rosner, J. L. & Martin, R. G. Transcriptional activation by MarA, SoxS and Rob of two tolC promoters using one binding site: a complex promoter configuration for tolC in Escherichia coli. *Mol. Microbiol.* 69, 1450-1455 (2008).

84 Zgurskaya, H. I., Krishnamoorthy, G., Ntreh, A. & Lu, S. Mechanism and Function of the Outer Membrane Channel TolC in Multidrug Resistance and Physiology of Enterobacteria. *Front Microbiol* 2, 189 (2011).

85 Manjasetty, B. A. *et al.* Loop-to-helix transition in the structure of multidrug regulator AcrR at the entrance of the drug-binding cavity. *J. Struct. Biol.* 194, 18-28 (2016).

86 Wilkens, S. Structure and mechanism of ABC transporters. *F1000Prime Reports* 7, 14 (2015).

87 Locher, K. P. Mechanistic diversity in ATP-binding cassette (ABC) transporters. *Nature Structural &Amp; Molecular Biology* 23, 487 (2016).

88 Yung, P. Y. *et al.* Global transcriptomic responses of Escherichia coli K-12 to volatile organic compounds. *Sci. Rep.* 6, 19899 (2016).

89 Brynildsen, M. P. & Liao, J. C. An integrated network approach identifies the isobutanol response network of Escherichia coli. *Molecular Systems Biology* 5 (2009).

90 Zhou, J. *et al.* Identification of membrane proteins associated with phenylpropanoid tolerance and transport in Escherichia coli BL21. *J Proteomics* 113, 15-28 (2015).

91 Lu, M. *et al.* Structures of a Na+-coupled, substrate-bound MATE multidrug transporter. *Proceedings of the National Academy of Sciences* 110, 2099-2104 (2013).

92 Yan, N. Structural Biology of the Major Facilitator Superfamily Transporters. *Annual Review of Biophysics* 44, 257-283 (2015).

93 Tanabe, M. *et al.* The multidrug resistance efflux complex, EmrAB from Escherichia coli forms a dimer in vitro. *Biochemical and Biophysical Research Communications* 380, 338-342 (2009).

94 Tal, N. & Schuldiner, S. A coordinated network of transporters with overlapping specificities provides a robust survival strategy. *Proceedings of the National Academy of Sciences* 106, 9051-9056 (2009).

95 Shuster, Y., Steiner-Mordoch, S., Alon Cudkowicz, N. & Schuldiner, S. A Transporter Interactome Is Essential for the Acquisition of Antimicrobial Resistance to Antibiotics. *PLOS ONE* 11, e0152917 (2016).

96 Cao, H. *et al.* Systems-level understanding of ethanol-induced stresses and adaptation in E. coli. *Sci Rep* 7, 44150 (2017).

97 Fernandez, L. & Hancock, R. E. Adaptive and mutational resistance: role of porins and efflux pumps in drug resistance. *Clinical microbiology reviews* 25, 661-681 (2012).

98 Vollan, H., Tannæs, T., Vriend, G. & Bukholm, G. In Silico Structure and Sequence Analysis of Bacterial Porins and Specific Diffusion Channels for Hydrophilic Molecules: Conservation, Multimericity and Multifunctionality. *International Journal of Molecular Sciences* 17, 599 (2016).

99 Zhang, D.-F., Li, H., Lin, X.-M., Wang, S.-Y. & Peng, X.-X. Characterization of Outer Membrane Proteins of Escherichia Coli in Response to Phenol Stress. *Current Microbiology* 62, 777-783 (2011).

100 Rau, M. H., Calero, P., Lennen, R. M., Long, K. S. & Nielsen, A. T. Genome-wide Escherichia coli stress response and improved tolerance towards industrially relevant chemicals. *Microbial cell factories* 15, 176 (2016).

101 Royce, L. A. *et al.* Transcriptomic Analysis of Carboxylic Acid Challenge in Escherichia coli: Beyond Membrane Damage. *PLOS ONE* 9, e89580 (2014).

102 Roma-Rodrigues, C., Santos, P. M., Benndorf, D., Rapp, E. & Sa-Correia, I. Response of Pseudomonas putida KT2440 to phenol at the level of membrane proteome. *J Proteomics* 73, 1461-1478 (2010).

103 Nikaido, H. Molecular basis of bacterial outer membrane permeability revisited. *Microbiology and molecular biology reviews : MMBR* 67, 593-656 (2003).

104 Murínová, S. & Dercová, K. Response Mechanisms of Bacterial Degraders to Environmental Contaminants on the Level of Cell Walls and Cytoplasmic Membrane. *International Journal of Microbiology* 2014, 873081 (2014).

105 Weber, F. J. & de Bont, J. A. M. Adaptation mechanisms of microorganisms to the toxic effects of organic solvents on membranes. *Biochimica et Biophysica Acta (BBA) - Reviews on Biomembranes* 1286, 225-245 (1996).

106 Sikkema, J., de Bont, J. A. & Poolman, B. Mechanisms of membrane toxicity of hydrocarbons. *Microbiological Reviews* 59, 201-222 (1995).

107 Segura, A., Duque, E., Mosqueda, G., Ramos, J. L. & Junker, F. Multiple responses of Gram-negative bacteria to organic solvents. *Environmental Microbiology* 1, 191-198 (1999).

108 Ramos, J.-L. *et al.* Mechanisms of solvent resistance mediated by interplay of cellular factors in Pseudomonas putida. *FEMS Microbiology Reviews* 39, 555-566 (2015).

109 Zu, T. N. K., Athamneh, A. I. M., Wallace, R. S., Collakova, E. & Senger, R. S. Near-Real-Time Analysis of the Phenotypic Responses of Escherichia coli to 1-Butanol Exposure Using Raman Spectroscopy. *Journal of Bacteriology* 196, 3983-3991 (2014).

110 CLARK, D. P. & BEARD, J. P. Altered Phospholipid Composition in Mutants of Escherichia coli Sensitive or Resistant to Organic Solvents. *Microbiology* 113, 267-274 (1979).

111 Silhavy, T. J., Kahne, D. & Walker, S. The Bacterial Cell Envelope. *Cold Spring Harbor Perspectives in Biology* 2, a000414 (2010).

112 Dombek, K. M. & Ingram, L. O. Effects of ethanol on the Escherichia coli plasma membrane. *Journal of Bacteriology* 157, 233-239 (1984).

113 Carey, V. C. & Ingram, L. O. Lipid composition of Zymomonas mobilis: effects of ethanol and glucose. *Journal of Bacteriology* 154, 1291-1300 (1983).

114 Silveira, M. G., Baumgärtner, M., Rombouts, F. M. & Abee, T. Effect of Adaptation to Ethanol on Cytoplasmic and Membrane Protein Profiles of Oenococcus oeni. *Applied and Environmental Microbiology* 70, 2748-2755 (2004).

115 Taylor, F. R. & Cronan, J. E., Jr. Cyclopropane fatty acid synthase of Escherichia coli. Stabilization, purification, and interaction with phospholipid vesicles. *Biochemistry* 18, 3292-3300 (1979).

116 Cascales, E., Gavioli, M., Sturgis, J. N. & Lloubes, R. Proton motive force drives the interaction of the inner membrane TolA and outer membrane pal proteins in Escherichia coli. *Mol Microbiol* 38, 904-915 (2000).

117 Krojer, T. *et al.* Structural basis for the regulated protease and chaperone function of DegP. *Nature* 453, 885-890 (2008).

118 Strauch, K. L. & Beckwith, J. An Escherichia coli mutation preventing degradation of abnormal periplasmic proteins. *Proc Natl Acad Sci U S A* 85, 1576-1580 (1988).

119 Lacroix, J. M., Loubens, I., Tempête, M., Menichi, B. & Bohin, J. P. The mdoA locus of Escherichia coli consists of an operon under osmotic control. *Molecular Microbiology* 5, 1745-1753 (1991).

120 Brissette, J. L., Russel, M., Weiner, L. & Model, P. Phage shock protein, a stress protein of Escherichia coli. *Proc Natl Acad Sci U S A* 87, 862-866 (1990).

121 Flores-Kim, J. & Darwin, A. J. The Phage Shock Protein Response. *Annual Review of Microbiology* 70, 83-101 (2016).

122 Joly, N. *et al.* Managing membrane stress: the phage shock protein (Psp) response, from molecular mechanisms to physiology. *FEMS Microbiology Reviews* 34, 797-827 (2010).

123 Darwin, A. J. The phage-shock-protein response. *Molecular Microbiology* 57, 621-628 (2005).

124 Rowley, G., Spector, M., Kormanec, J. & Roberts, M. Pushing the envelope: extracytoplasmic stress responses in bacterial pathogens. *Nature reviews. Microbiology* 4, 383-394 (2006).

125 Bury-Mone, S. *et al.* Global analysis of extracytoplasmic stress signaling in Escherichia coli. *PLoS Genet.* 5, No pp. given (2009).

126 Jovanovic, G., Weiner, L. & Model, P. Identification, nucleotide sequence, and characterization of PspF, the transcriptional activator of the Escherichia coli stress-induced psp operon. *J Bacteriol* 178, 1936-1945 (1996).

127 Saori, Y., Erwan, G., Kaye, H. N. & J., D. A. Membrane association of PspA depends on activation of the phage-shock-protein response in Yersinia enterocolitica. *Molecular Microbiology* 78, 429-443 (2010).

128 Saori, Y., A., R. D., Eli, R. & J., D. A. Changes in Psp protein binding partners, localization and behaviour upon activation of the Yersinia enterocolitica phage shock protein response. *Molecular Microbiology* 87, 656-671 (2013).

129 Dworkin, J., Jovanovic, G. & Model, P. The PspA Protein of Escherichia coli Is a Negative Regulator of ς54-Dependent Transcription. *Journal of Bacteriology* 182, 311-319 (2000).

130 Joly, N., Burrows, P. C., Engl, C., Jovanovic, G. & Buck, M. A Lower-Order Oligomer Form of Phage Shock Protein A (PspA) Stably Associates with the Hexameric AAA(+) Transcription Activator Protein PspF for Negative Regulation. *Journal of Molecular Biology* 394, 764-775 (2009).

131 Jovanovic, G., Engl, C. & Buck, M. Physical, functional and conditional interactions between ArcAB and phage shock proteins upon secretin-induced stress in Escherichia coli. *Mol. Microbiol.* 74, 16-28 (2009).

132 Chiou, R. Y. Y., Phillips, R. D., Zhao, P., Doyle, M. P. & Beuchat, L. R. Ethanol-Mediated Variations in Cellular Fatty Acid Composition and Protein Profiles of Two Genotypically Different Strains of Escherichia coli O157:H7. *Applied and Environmental Microbiology* 70, 2204-2210 (2004).

133 He, M.-x. *et al.* Transcriptome profiling of Zymomonas mobilis under ethanol stress. *Biotechnology for Biofuels* 5, 75 (2012).

134 Kobayashi, H., Yamamoto, M. & Aono, R. Appearance of a stress-response protein, phage-shock protein A, in Escherichia coli exposed to hydrophobic organic solvents. *Microbiology* 144, 353-359 (1998).

135 Vrancken, K., Van Mellaert, L. & Anné, J. Characterization of the Streptomyces lividans PspA Response. *Journal of Bacteriology* 190, 3475-3481 (2008).

136 Ron, E. Z. *Bacterial Stress Response*. in *The Prokaryotes: Volume 2: Ecophysiology and Biochemistry*, 1012-1027 Springer New York (2006).

137 Petersohn, A. *et al.* Global Analysis of the General Stress Response ofBacillus subtilis. *Journal of Bacteriology* 183, 5617-5631 (2001).

138 Shimizu, K. Metabolic Regulation of a Bacterial Cell System with Emphasis on Escherichia coli Metabolism. *ISRN Biochemistry* 2013, 47 (2013).

139 Shimizu, K. Regulation Systems of Bacteria such as Escherichia coli in Response to Nutrient Limitation and Environmental Stresses. *Metabolites* 4, 1-35 (2014).

140 Qiao, Y. *et al.* Transcriptomic and proteomic profiling revealed global changes in Streptococcus thermophilus during pH-controlled batch fermentations. *Journal of microbiology (Seoul, Korea)* (2019).

141 Molina-Santiago, C., Udaondo, Z., Gómez-Lozano, M., Molin, S. & Ramos, J.-L. Global transcriptional response of solvent-sensitive and solvent-tolerant Pseudomonas putida strains exposed to toluene. *Environmental Microbiology* 19, 645-658 (2017).

142 Yang, S. *et al.* Systems Biology Analysis of Zymomonas mobilis ZM4 Ethanol Stress Responses. *PLOS ONE* 8, e68886 (2013).

143 Chiang, S. M. & Schellhorn, H. E. Regulators of oxidative stress response genes in Escherichia coli and their functional conservation in bacteria. *Arch. Biochem. Biophys.* 525, 161-169 (2012).

144 Lemire, J., Alhasawi, A., Appanna, V. P., Tharmalingam, S. & Appanna, V. D. Metabolic defence against oxidative stress: the road less travelled so far. *Journal of Applied Microbiology*, n/a-n/a (2017).

145 Frey, H. E. & Pollard, E. C. Ionizing Radiation and Bacteria: Nature of the Effect of Irradiated Medium. *Radiation Research* 28, 668-676 (1966).

146 Murphy, Michael P. How mitochondria produce reactive oxygen species. *Biochemical Journal* 417, 1-13 (2009).

147 Bhattacharyya, A., Chattopadhyay, R., Mitra, S. & Crowe, S. E. Oxidative Stress: An Essential Factor in the Pathogenesis of Gastrointestinal Mucosal Diseases. *Physiological Reviews* 94, 329-354 (2014).

148 Liemburg-Apers, D. C., Willems, P. H. G. M., Koopman, W. J. H. & Grefte, S. Interactions between mitochondrial reactive oxygen species and cellular glucose metabolism. *Archives of Toxicology* 89, 1209-1226 (2015).

149 Gu, M. & Imlay, J. A. The SoxRS response of Escherichia coli is directly activated by redox-cycling drugs rather than by superoxide. *Mol. Microbiol.* 79, 1136-1150 (2011).

150 Fuentes, A. M., Díaz-Mejía, J. J., Maldonado-Rodríguez, R. & Amábile-Cuevas, C. F. Differential activities of the SoxR protein of Escherichia coli: SoxS is not required for gene activation under iron deprivation. *FEMS Microbiology Letters* 201, 271-275 (2001).

151 Li, Z. & Demple, B. SoxS, an activator of superoxide stress genes in Escherichia coli: Purification and interaction with DNA. *Journal of Biological Chemistry* 269, 18371-18377 (1994).

152 Liochev, S. I. & Fridovich, I. Fumarase C, the stable fumarase of Escherichia coli, is controlled by the soxRS regulon. *Proc Natl Acad Sci U S A* 89, 5892-5896 (1992).

153 Greenberg, J. T., Monach, P., Chou, J. H., Josephy, P. D. & Demple, B. Positive control of a global antioxidant defense regulon activated by superoxide-generating agents in Escherichia coli. *Proc. Natl. Acad. Sci. U. S. A.* 87, 6181-6185 (1990).

154 Nakayama, T., Yonekura, S.-I., Yonei, S. & Zhang-Akiyama, Q.-M. Escherichia coli pyruvate:flavodoxin oxidoreductase, YdbK - regulation of expression and biological roles in protection against oxidative stress. *Genes & Genetic Systems* 88, 175-188 (2013).

155 Varghese, S., Tang, Y. & Imlay, J. A. Contrasting sensitivities of Escherichia coli aconitases A and B to oxidation and iron depletion. *J Bacteriol* 185, 221-230 (2003).

156 Rungrassamee, W., Liu, X. & Pomposiello, P. J. Activation of glucose transport under oxidative stress in Escherichia coli. *Archives of Microbiology* 190, 41-49 (2008).

157 Zheng, M., Doan, B., Schneider, T. D. & Storz, G. OxyR and SoxRS regulation of fur. *Journal of Bacteriology* 181, 4639-4643 (1999).

158 Pomposiello, P. J. & Demple, B. Redox-operated genetic switches: the SoxR and OxyR transcription factors. *Trends Biotechnol.* 19, 109-114 (2001).

159 Blanchard, J. L., Wholey, W.-Y., Conlon, E. M. & Pomposiello, P. J. Rapid changes in gene expression dynamics in response to superoxide reveal SoxRS-dependent and independent transcriptional networks. *PLoS One* 2, No pp. given (2007).

160 Seo, S. W., Kim, D., Szubin, R. & Palsson, B. O. Genome-wide Reconstruction of OxyR and SoxRS Transcriptional Regulatory Networks under Oxidative Stress in Escherichia coli K-12 MG1655. *Cell Rep* 12, 1289-1299 (2015).

161 Watanabe, S., Kita, A., Kobayashi, K. & Miki, K. Crystal structure of the [2Fe-2S] oxidative-stress sensor SoxR bound to DNA. *Proc Natl Acad Sci U S A* 105, 4121-4126 (2008).

162 Zheng, M. *et al.* Computation-Directed Identification of OxyR DNA Binding Sites in Escherichia coli. *Journal of Bacteriology* 183, 4571-4579 (2001).

163 Wang, L. *et al.* Structural insights into the recognition of the internal A-rich linker from OxyS sRNA by Escherichia coli Hfq. *Nucleic Acids Research* 43, 2400-2411 (2015).

164 Touati, D. Iron and Oxidative Stress in Bacteria. *Archives of Biochemistry and Biophysics* 373, 1-6 (2000).

165 Andrews, S. C., Robinson, A. K. & Rodríguez-Quiñones, F. Bacterial iron homeostasis. *FEMS Microbiology Reviews* 27, 215-237 (2003).

166 Lau, C. K. Y., Krewulak, K. D. & Vogel, H. J. Bacterial ferrous iron transport: the Feo system. *FEMS Microbiol Rev* 40, 273-298 (2016).

167 Cornelis, P., Wei, Q., Andrews, S. C. & Vinckx, T. Iron homeostasis and management of oxidative stress response in bacteria. *Metallomics* 3, 540-549 (2011).

168 Arosio, P. & Levi, S. Ferritin, iron homeostasis, and oxidative damage. *Free Radical Biology and Medicine* 33, 457-463 (2002).

169 Porcheron, G. & Dozois, C. M. Interplay between iron homeostasis and virulence: Fur and RyhB as major regulators of bacterial pathogenicity. *Vet. Microbiol.* 179, 2-14 (2015).

170 Baichoo, N. & Helmann, J. D. Recognition of DNA by Fur: a Reinterpretation of the Fur Box Consensus Sequence. *Journal of Bacteriology* 184, 5826-5832 (2002).

171 McHugh, J. P. *et al.* Global Iron-dependent Gene Regulation in Escherichia coli: A NEW MECHANISM FOR IRON HOMEOSTASIS. *Journal of Biological Chemistry* 278, 29478-29486 (2003).

172 Troxell, B., Fink, R. C., Porwollik, S., McClelland, M. & Hassan, H. M. The Fur regulon in anaerobically grown Salmonella enterica sv. Typhimurium: identification of new Fur targets. *BMC Microbiology* 11, 236-236 (2011).

173 Pi, H. & Helmann, J. D. Ferrous iron efflux systems in bacteria. *Metallomics* 9, 840-851 (2017).

174 Cunningham, L., Gruer, M. J. & Guest, J. R. Transcriptional regulation of the aconitase genes (acnA and acnB) of Escherichia coli. *Microbiology* 143 (Pt 12), 3795-3805 (1997).

175 Park, S. J. & Gunsalus, R. P. Oxygen, iron, carbon, and superoxide control of the fumarase fumA and fumC genes of Escherichia coli: role of the arcA, fnr, and soxR gene products. *J Bacteriol* 177, 6255-6262 (1995).

176 Tseng, C. P. Regulation of fumarase (fumB) gene expression in Escherichia coli in response to oxygen, iron and heme availability: role of the arcA, fur, and hemA gene products. *FEMS Microbiol Lett* 157, 67-72 (1997).

177 Park, S. J., Chao, G. & Gunsalus, R. P. Aerobic regulation of the sucABCD genes of Escherichia coli, which encode alpha-ketoglutarate dehydrogenase and succinyl coenzyme A synthetase: roles of ArcA, Fnr, and the upstream sdhCDAB promoter. *J Bacteriol* 179, 4138-4142 (1997).

178 Shen, J. & Gunsalus, R. P. Role of multiple ArcA recognition sites in anaerobic regulation of succinate dehydrogenase (sdhCDAB) gene expression in Escherichia coli. *Mol Microbiol* 26, 223-236 (1997).

179 Raven, P. H. *Biology*. (2013).

180 Asakura, T., Adachi, K. & Schwartz, E. Stabilizing effect of various organic solvents on protein. *Journal of Biological Chemistry* 253, 6423-6425 (1978).

181 Whitley, D., Goldberg, S. P. & Jordan, W. D. Heat shock proteins: A review of the molecular chaperones. *Journal of Vascular Surgery* 29, 748-751 (1999).

182 Richter, K., Haslbeck, M. & Buchner, J. The Heat Shock Response: Life on the Verge of Death. *Molecular Cell* 40, 253-266.

183 Verghese, J., Abrams, J., Wang, Y. & Morano, K. A. Biology of the Heat Shock Response and Protein Chaperones: Budding Yeast (Saccharomyces cerevisiae) as a Model System. *Microbiology and molecular biology reviews : MMBR* 76, 115-158 (2012).

184 T Yura, H Nagai, a. & Mori, H. Regulation of the Heat-Shock Response in Bacteria. *Annual Review of Microbiology* 47, 321-350 (1993).

185 Guzzo, J. Biotechnical applications of small heat shock proteins from bacteria. *The International Journal of Biochemistry & Cell Biology* 44, 1698-1705 (2012).

186 Straus, D. B., Walter, W. A. & Gross, C. A. The heat shock response of E. coli is regulated by changes in the concentration of [sigma]32. *Nature* 329, 348-351 (1987).

187 Guisbert, E., Herman, C., Lu, C. Z. & Gross, C. A. A chaperone network controls the heat shock response in E. coli. *Genes & Development* 18, 2812-2821 (2004).

188 Foo, J. L. *et al.* Improving Microbial Biogasoline Production in Escherichia coli Using Tolerance Engineering. *mBio* 5 (2014).

189 Rutherford, B. J. *et al.* Functional genomic study of exogenous n-butanol stress in Escherichia coli. *Appl Environ Microbiol* 76, 1935-1945 (2010).

190 Foo, J. L. *et al.* Improving microbial biogasoline production in Escherichia coli using tolerance engineering. *MBio* 5, e01932 (2014).

191 Blom, A., Harder, W. & Matin, A. Unique and overlapping pollutant stress proteins of Escherichia coli. *Applied and Environmental Microbiology* 58, 331-334 (1992).

192 Mann, M. S., Dragovic, Z., Schirrmacher, G. & Lütke-Eversloh, T. Over-expression of stress protein-encoding genes helps Clostridium acetobutylicum to rapidly adapt to butanol stress. *Biotechnology Letters* 34, 1643-1649 (2012).

193 Bormann, S. *et al.* Engineering Clostridium acetobutylicum for production of kerosene and diesel blendstock precursors. *Metabolic engineering* 25, 124-130 (2014).

194 Kang, H.-J. *et al.* Functional characterization of Hsp33 protein from Bacillus psychrosaccharolyticus; additional function of HSP33 on resistance to solvent stress. *Biochemical and Biophysical Research Communications* 358, 743-750 (2007).

195 Desmond, C., Fitzgerald, G. F., Stanton, C. & Ross, R. P. Improved Stress Tolerance of GroESL-Overproducing Lactococcus lactis and Probiotic Lactobacillus paracasei NFBC 338. *Applied and Environmental Microbiology* 70, 5929-5936 (2004).

196 Anfelt, J., Hallström, B., Nielsen, J., Uhlén, M. & Hudson, E. P. Using Transcriptomics To Improve Butanol Tolerance of Synechocystis sp. Strain PCC 6803. *Applied and Environmental Microbiology* 79, 7419-7427 (2013).

197 Stent, G. S. & Brenner, S. A genetic locus for the regulation of ribonucleic acid synthesis. *Proc Natl Acad Sci U S A* 47, 2005-2014 (1961).

198 Hauryliuk, V., Atkinson, G. C., Murakami, K. S., Tenson, T. & Gerdes, K. Recent functional insights into the role of (p)ppGpp in bacterial physiology. *Nat. Rev. Microbiol.* 13, 298-309 (2015).

199 Gaca, A. O., Colomer-Winter, C. & Lemos, J. A. Many means to a common end: the intricacies of (p)ppGpp metabolism and its control of bacterial homeostasis. *J. Bacteriol.* 197, 1146-1156 (2015).

200 Kalia, D. *et al.* Nucleotide, c-di-GMP, c-di-AMP, cGMP, cAMP, (p)ppGpp signaling in bacteria and implications in pathogenesis. *Chem Soc Rev* 42, 305-341 (2013).

201 Bouveret, E. & Battesti, A. 231-250 (American Society for Microbiology).

202 Potrykus, K. & Cashel, M. (p)ppGpp: Still Magical? *Annual Review of Microbiology* 62, 35-51 (2008).

203 English, B. P. *et al.* Single-molecule investigations of the stringent response machinery in living bacterial cells. *Proceedings of the National Academy of Sciences* 108, E365-E373 (2011).

204 Kishimoto, T. *et al.* Transition from Positive to Neutral in Mutation Fixation along with Continuing Rising Fitness in Thermal Adaptive Evolution. *PLOS Genetics* 6, e1001164 (2010).

205 Minty, J. J. *et al.* Evolution combined with genomic study elucidates genetic bases of isobutanol tolerance in Escherichia coli. *Microbial cell factories* 10, 18 (2011).

206 Horinouchi, T. *et al.* Phenotypic convergence in bacterial adaptive evolution to ethanol stress. *BMC Evolutionary Biology* 15, 180 (2015).

207 Horinouchi, T., Sakai, A., Kotani, H., Tanabe, K. & Furusawa, C. Improvement of isopropanol tolerance of Escherichia coli using adaptive laboratory evolution and omics technologies. *Journal of Biotechnology* 255, 47-56 (2017).

208 Srivatsan, A. & Wang, J. D. Control of bacterial transcription, translation and replication by (p)ppGpp. *Current Opinion in Microbiology* 11, 100-105 (2008).

209 Wu, J. & Xie, J. Magic spot: (p) ppGpp. *J. Cell. Physiol.* 220, 297-302 (2009).

210 Volkers, R. J. *et al.* Chemostat-based proteomic analysis of toluene-affected Pseudomonas putida S12. *Environ Microbiol* 8, 1674-1679 (2006).

211 Eymann, C., Homuth, G., Scharf, C. & Hecker, M. Bacillus subtilis functional genomics: global characterization of the stringent response by proteome and transcriptome analysis. *Journal of Bacteriology* 184, 2500-2520 (2002).

212 Wood, J. M. *Osmotic Stress*. in *Bacterial Stress Responses, Second Edition*, American Society of Microbiology (2011).

213 Wood, J. M. Bacterial osmosensing transporters. *Methods in enzymology* 428, 77-107 (2007).

214 Forst, S. A. & Roberts, D. L. Signal transduction by the EnvZ-OmpR phosphotransfer system in bacteria. *Research in microbiology* 145, 363-373 (1994).

215 Stock, A. M., Robinson, V. L. & Goudreau, P. N. Two-component signal transduction. *Annual review of biochemistry* 69, 183-215 (2000).

216 Foo, Y. H., Gao, Y., Zhang, H. & Kenney, L. J. Cytoplasmic sensing by the inner membrane histidine kinase EnvZ. *Prog. Biophys. Mol. Biol.* 118, 119-129 (2015).

217 Yoshida, T., Cai, S. & Inouye, M. Interaction of EnvZ, a sensory histidine kinase, with phosphorylated OmpR, the cognate response regulator. *Mol Microbiol* 46, 1283-1294 (2002).

218 Seo, S. W. *et al.* Revealing genome-scale transcriptional regulatory landscape of OmpR highlights its expanded regulatory roles under osmotic stress in Escherichia coli K-12 MG1655. *Sci Rep* 7, 2181 (2017).

219 Higashitani, A. *et al.* Osmoregulation of the fatty acid receptor gene fadL in Escherichia coli. *Molecular & general genetics : MGG* 240, 339-347 (1993).

220 Shin, S. & Park, C. Modulation of flagellar expression in Escherichia coli by acetyl phosphate and the osmoregulator OmpR. *J Bacteriol* 177, 4696-4702 (1995).

221 Lennon, C. W. *et al.* Folding Optimization In Vivo Uncovers New Chaperones. *Journal of Molecular Biology* 427, 2983-2994 (2015).

222 Yim, H. H. & Villarejo, M. osmY, a new hyperosmotically inducible gene, encodes a periplasmic protein in Escherichia coli. *J Bacteriol* 174, 3637-3644 (1992).

223 Lesniak, J., Barton, W. A. & Nikolov, D. B. Structural and functional features of the Escherichia coli hydroperoxide resistance protein OsmC. *Protein science : a publication of the Protein Society* 12, 2838-2843 (2003).

224 Gutierrez, C. & Devedjian, J. C. Osmotic induction of gene osmC expression in Escherichia coli K12. *Journal of Molecular Biology* 220, 959-973 (1991).

225 Wang, J. *et al.* Global metabolomic and network analysis of Escherichia coli responses to exogenous biofuels. *J. Proteome Res.* 12, 5302-5312 (2013).

226 Kanjee, U. & Houry, W. A. Mechanisms of acid resistance in Escherichia coli. *Annu. Rev. Microbiol.* 67, 65-81 (2013).

227 Audia, J. P., Webb, C. C. & Foster, J. W. Breaking through the acid barrier: An orchestrated response to proton stress by enteric bacteria. *International Journal of Medical Microbiology* 291, 97-106 (2001).

228 Lund, P., Tramonti, A. & De Biase, D. Coping with low pH: molecular strategies in neutralophilic bacteria. *FEMS Microbiol. Rev.* 38, 1091-1125 (2014).

229 Booth, I. R., Cash, P. & O'Byrne, C. Sensing and adapting to acid stress. *Antonie van Leeuwenhoek* 81, 33-42 (2002).

230 Seputiene, V. *et al.* Molecular characterization of the acid-inducible asr gene of Escherichia coli and its role in acid stress response. *J Bacteriol* 185, 2475-2484 (2003).

231 Chevance, F. F. V. & Hughes, K. T. Coordinating assembly of a bacterial macromolecular machine. *Nat Rev Micro* 6, 455-465 (2008).

232 Minamino, T., Imada, K. & Namba, K. Molecular motors of the bacterial flagella. *Current Opinion in Structural Biology* 18, 693-701 (2008).

233 Terashima, H., Kojima, S. & Homma, M. Chapter 2 Flagellar Motility in Bacteria. *International Review of Cell and Molecular Biology* 270, 39-85 (2008).

234 Van Gerven, N., Waksman, G. & Remaut, H. Pili and flagella: biology, structure, and biotechnological applications. *Prog. Mol. Biol. Transl. Sci.* 103, 21-72 (2011).

235 Paulick, A. & Thormann, K. Bacterial motor tuning. *BIOspektrum* 18, 134-137 (2012).

236 Guttenplan, S. B. & Kearns, D. B. Regulation of flagellar motility during biofilm formation. *FEMS Microbiology Reviews* 37, 849-871 (2013).

237 Belas, R. Biofilms, flagella, and mechanosensing of surfaces by bacteria. *Trends in Microbiology* 22, 517-527 (2014).

238 Volkers, R. J. M. *et al.* TrgI, toluene repressed gene I, a novel gene involved in toluene-tolerance in Pseudomonas putida S12. *Extremophiles* 13, 283-297 (2009).

239 Fu, Y., Yoon, J. M., Jarboe, L. & Shanks, J. V. Metabolic flux analysis of Escherichia coli MG1655 under octanoic acid (C8) stress. *Applied Microbiology and Biotechnology* 99, 4397-4408 (2015).

240 Unden, G. & Bongaerts, J. Alternative respiratory pathways of Escherichia coli: energetics and transcriptional regulation in response to electron acceptors. *Biochimica et Biophysica Acta (BBA) - Bioenergetics* 1320, 217-234 (1997).

241 Poole, R. K. & Cook, G. M. Redundancy of aerobic respiratory chains in bacteria? Routes, reasons and regulation. *Adv Microb Physiol* 43, 165-224 (2000).

242 Borisov, V. B. & Verkhovsky, M. I. Oxygen as acceptor. *EcoSal Plus* 6, 1-32 (2015).

243 Iuchi, S. & Weiner, L. Cellular and molecular physiology of Escherichia coli in the adaptation to aerobic environments. *Journal of biochemistry* 120, 1055-1063 (1996).

244 Myers, K. S. *et al.* Genome-scale Analysis of Escherichia coli FNR Reveals Complex Features of Transcription Factor Binding. *PLOS Genetics* 9, e1003565 (2013).

245 Kobayashi, K., Fujikawa, M. & Kozawa, T. Oxidative stress sensing by the iron-sulfur cluster in the transcription factor, SoxR. *J. Inorg. Biochem.* 133, 87-91 (2014).

246 Koutsolioutsou, A., Pena-Llopis, S. & Demple, B. Constitutive soxR mutations contribute to multiple-antibiotic resistance in clinical Escherichia coli isolates. *Antimicrob. Agents Chemother.* 49, 2746-2752 (2005).

247 Hooper, D. C. & Wolfson, J. S. Mode of action of the new quinolones: new data. *European journal of clinical microbiology & infectious diseases : official publication of the European Society of Clinical Microbiology* 10, 223-231 (1991).

248 O'Regan, E. *et al.* Multiple regulatory pathways associated with high-level ciprofloxacin and multidrug resistance in Salmonella enterica serovar enteritidis: involvement of RamA and other global regulators. *Antimicrob Agents Chemother* 53, 1080-1087 (2009).

249 Chander, M., Raducha-Grace, L. & Demple, B. Transcription-defective soxR mutants of Escherichia coli: Isolation and in vivo characterization. *J. Bacteriol.* 185, 2441-2450 (2003).

250 Chander, M. & Demple, B. Functional Analysis of SoxR Residues Affecting Transduction of Oxidative Stress Signals into Gene Expression. *J. Biol. Chem.* 279, 41603-41610 (2004).

251 Watanabe, R. & Doukyu, N. Contributions of mutations in acrR and marR genes to organic solvent tolerance in Escherichia coli. *AMB Express* 2, 58, 11 pp. (2012).

252 Adler, M., Anjum, M., Andersson, D. I. & Sandegren, L. Combinations of mutations in envZ, ftsI, mrdA, acrB and acrR can cause high-level carbapenem resistance in Escherichia coli. *J Antimicrob Chemother* (2016).

253 Zayed, A. A., Essam, T. M., Hashem, A. G. & El-Tayeb, O. M. 'Supermutators' found amongst highly levofloxacin-resistant E. coli isolates: a rapid protocol for the detection of mutation sites. *Emerging microbes & infections* 4, e4 (2015).

254 Kaur, G. & Subramanian, S. Classification of the treble clef zinc finger: noteworthy lessons for structure and function evolution. *Scientific Reports* 6, 32070 (2016).

255 Ito, A., May, T., Kawata, K. & Okabe, S. Significance of rpoS during maturation of Escherichia coli biofilms. *Biotechnology and Bioengineering* 99, 1462-1471 (2008).

256 Baba, T. *et al.* Construction of Escherichia coli K-12 in-frame, single-gene knockout mutants: the Keio collection. *Mol. Syst. Biol.*, No pp. given (2006).

257 Datsenko, K. A. & Wanner, B. L. One-step inactivation of chromosomal genes in Escherichia coli K-12 using PCR products. *Proc. Natl. Acad. Sci. U. S. A.* 97, 6640-6645 (2000).

258 Lessard, J. C. *Chapter Eleven - Growth Media for E. coli*. in *Methods in Enzymology*, Vol. 533 181-189 Academic Press (2013).

259 Wahbi, L. P., Gokhale, D., Minter, S. & Stephens, G. M. Construction and use of recombinant Escherichia coli strains for the synthesis of toluene cis-glycol. *Enzyme and Microbial Technology* 19, 297-306 (1996).

260 Vishniac, W. & Santer, M. The thiobacilli. *Bacteriological reviews* 21, 195-213 (1957).

261 Bindea, G. *et al.* ClueGO: a Cytoscape plug-in to decipher functionally grouped gene ontology and pathway annotation networks. *Bioinformatics* 25, 1091-1093 (2009).

262 Heberle, H., Meirelles, G. V., da Silva, F. R., Telles, G. P. & Minghim, R. InteractiVenn: a web-based tool for the analysis of sets through Venn diagrams. *BMC Bioinformatics* 16, 169 (2015).

263 Falbe, J., Bahrmann, H. , Lipps, W. , Mayer, D. and Frey, G. D. *Alcohols, Aliphatic. In Ullmann's Encyclopedia of Industrial Chemistry*. in *Ullmann's Encyclopedia of Industrial Chemistry*, (2013).

264 Schmidt, R., Griesbaum, K. , Behr, A. , Biedenkapp, D. , Voges, H. , Garbe, D. , Paetz, C. , Collin, G. , Mayer, D. and Höke, H. *Hydrocarbons. In Ullmann's Encyclopedia of Industrial Chemistry.* in *Ullmann's Encyclopedia of Industrial Chemistry*, 1-74 (2014).

265 Cohen, S. N., Chang, A. C., Boyer, H. W. & Helling, R. B. Construction of biologically functional bacterial plasmids in vitro. *Proceedings of the National Academy of Sciences of the United States of America* 70, 3240-3244 (1973).

266 Cohen, S. N., Miller, C. A., Tucker, W. T., Meacock, P. A. & Gustafsson, P. *Partitioning of the pSC101 Plasmid during Cell Division*. in *Plasmids in Bacteria*, 383-395 Springer US (1985).

267 Keseler, I. M. *et al.* The EcoCyc database: reflecting new knowledge about Escherichia coli K-12. *Nucleic Acids Research* 45, D543-D550 (2016).

268 Das, B. & Patra, S. *Antimicrobials: Meeting the Challenges of Antibiotic Resistance Through Nanotechnology*. in *Nanostructures for Antimicrobial Therapy*, 1-22 Elsevier (2017).

269 Rossolini, G. M., Arena, F. & Giani, T. *Mechanisms of Antibacterial Resistance*. in *Infectious Diseases (Fourth Edition)*, 1181-1196.e1181 Elsevier (2017).

270 Schwarz, S., Kehrenberg, C., Doublet, B. & Cloeckaert, A. Molecular basis of bacterial resistance to chloramphenicol and florfenicol. *FEMS microbiology reviews* 28, 519-542 (2004).

271 Roberts, M. C. & Schwarz, S. *Tetracycline and Chloramphenicol Resistance Mechanisms*. in *Antimicrobial Drug Resistance: Mechanisms of Drug Resistance*, 183-193 Humana Press (2009).

272 Cherepanov, P. & Wackernagel, W. Gene disruption in Escherichia coli: TcR and KmR cassettes with the option of Flp-catalyzed excision of the antibiotic-resistance determinant. *Gene* 158, 9-14 (1995).

273 Wright, G. D. & Thompson, P. R. Aminoglycoside phosphotransferases: proteins, structure, and mechanism. *Front Biosci* 4, D9-21 (1999).

274 Zhang, W., Li, F. & Nie, L. Integrating multiple 'omics' analysis for microbial biology: application and methodologies. *Microbiology* 156, 287-301 (2010).

275 Nishino, K. & Yamaguchi, A. Analysis of a complete library of putative drug transporter genes in Escherichia coli. *J Bacteriol* 183, 5803-5812 (2001).

276 Fabrega, A., Martin, R. G., Rosner, J. L., Tavio, M. M. & Vila, J. Constitutive SoxS expression in a fluoroquinolone-resistant strain with a truncated SoxR protein and identification of a new member of the marA-soxS-rob regulon, mdtG. *Antimicrob. Agents Chemother.* 54, 1218-1225 (2010).

277 Korea, C. G., Badouraly, R., Prevost, M. C., Ghigo, J. M. & Beloin, C. Escherichia coli K-12 possesses multiple cryptic but functional chaperone-usher fimbriae with distinct surface specificities. *Environ Microbiol* 12, 1957-1977 (2010).

278 Brock, M., Maerker, C., Schütz, A., Völker, U. & Buckel, W. Oxidation of propionate to pyruvate in Escherichia coli. *European Journal of Biochemistry* 269, 6184-6194 (2002).

279 Palacios, S. & Escalante-Semerena, J. C. 2-Methylcitrate-dependent activation of the propionate catabolic operon (prpBCDE) of Salmonella enterica by the PrpR protein. *Microbiology* 150, 3877-3887 (2004).

280 Jenkins, L. S. & Nunn, W. D. Genetic and molecular characterization of the genes involved in short-chain fatty acid degradation in Escherichia coli: the ato system. *J Bacteriol* 169, 42-52 (1987).

281 Jimenez-Diaz, L., Caballero, A. & Segura, A. *Regulation of Fatty Acids Degradation in Bacteria*. in *Aerobic Utilization of Hydrocarbons, Oils and Lipids*, 1-20 Springer International Publishing (2017).

282 Vassilis Koronakis, Jeyanthy Eswaran, a. & Hughes, C. Structure and Function of TolC: The Bacterial Exit Duct for Proteins and Drugs. *Annual Review of Biochemistry* 73, 467-489 (2004).

283 Ozenberger, B. A., Nahlik, M. S. & McIntosh, M. A. Genetic organization of multiple fep genes encoding ferric enterobactin transport functions in Escherichia coli. *J Bacteriol* 169, 3638-3646 (1987).

284 Conley, Z. C. *et al.* Sugar and iron: Toward understanding the antibacterial effect of ciclopirox in Escherichia coli. *PLOS ONE* 14, e0210547 (2019).

285 Atlung, T., Knudsen, K., Heerfordt, L. & Brøndsted, L. Effects of sigmaS and the transcriptional activator AppY on induction of the Escherichia coli hya and cbdAB-appA operons in response to carbon and phosphate starvation. *Journal of Bacteriology* 179, 2141-2146 (1997).

286 Makino, K., Shinagawa, H. & Nakata, A. Regulation of the phosphate regulon of Escherichia coli K-12: regulation and role of the regulatory gene phoR. *J Mol Biol* 184, 231-240 (1985).

287 Li, Y. & Zhang, Y. PhoU is a persistence switch involved in persister formation and tolerance to multiple antibiotics and stresses in Escherichia coli. *Antimicrob Agents Chemother* 51, 2092-2099 (2007).

288 Kato, A., Tanabe, H. & Utsumi, R. Molecular characterization of the PhoP-PhoQ two-component system in Escherichia coli K-12: identification of extracellular Mg2+-responsive promoters. *J Bacteriol* 181, 5516-5520 (1999).

289 van der Ploeg, J. R. *et al.* Identification of sulfate starvation-regulated genes in Escherichia coli: a gene cluster involved in the utilization of taurine as a sulfur source. *J Bacteriol* 178, 5438-5446 (1996).

290 Kristoficova, I., Vilhena, C., Behr, S. & Jung, K. BtsT, a Novel and Specific Pyruvate/H(+) Symporter in Escherichia coli. *J Bacteriol* 200 (2018).

291 Behr, S., Fried, L. & Jung, K. Identification of a Novel Nutrient-Sensing Histidine Kinase/Response Regulator Network in Escherichia coli. *Journal of Bacteriology* 196, 2023-2029 (2014).

292 Si, H.-M. *et al.* DNA microarray of global transcription factor mutant reveals membrane-related proteins involved in n-butanol tolerance in Escherichia coli. *Biotechnology for Biofuels* 9, 114 (2016).

293 Saier, M. H., Jr., Reddy, V. S., Tamang, D. G. & Vastermark, A. The transporter classification database. *Nucleic Acids Res* 42, D251-258 (2014).

294 Behr, S. *et al.* Identification of a High-Affinity Pyruvate Receptor in Escherichia coli. *Sci Rep* 7, 1388 (2017).

295 Kraxenberger, T., Fried, L., Behr, S. & Jung, K. First insights into the unexplored two-component system YehU/YehT in Escherichia coli. *J Bacteriol* 194, 4272-4284 (2012).

296 Oh, H. Y., Lee, J. O. & Kim, O. B. Increase of organic solvent tolerance of Escherichia coli by the deletion of two regulator genes, fadR and marR. *Appl. Microbiol. Biotechnol.* 96, 1619-1627 (2012).

297 Sung, B. H., Lee, J. H. & Kim, S. C. *Scarless Chromosomal Gene Knockout Methods*. in *Strain Engineering: Methods and Protocols*, 43-54 Humana Press (2011).

298 Reisch, C. R. & Prather, K. L. J. The no-SCAR (Scarless Cas9 Assisted Recombineering) system for genome editing in Escherichia coli. *Sci. Rep.* 5, 15096 (2015).

299 Blair, J. M. A. & Piddock, L. J. V. How to Measure Export via Bacterial Multidrug Resistance Efflux Pumps. *mBio* 7, e00840-00816 (2016).

300 Sheppard, E. C., Rogers, S., Harmer, N. J. & Chahwan, R. A universal fluorescence-based toolkit for real-time quantification of DNA and RNA nuclease activity. *Sci. Rep.* 9, 8853 (2019).

301 Azeredo, J. *et al.* Critical review on biofilm methods. *Crit. Rev. Microbiol.* 43, 313-351 (2017).

302 Aono, R. Improvement of organic solvent tolerance level of Escherichia coli by overexpression of stress-responsive genes. *Extremophiles* 2, 239-248 (1998).

303 Oethinger, M., Podglajen, I., Kern, W. V. & Levy, S. B. Overexpression of the marA or soxS regulatory gene in clinical topoisomerase mutants of Escherichia coli. *Antimicrobial agents and chemotherapy* 42, 2089-2094 (1998).

304 Sven Brand, C. R. *Monitoring of microbial growth curves by laser nephelometry*, <https://www.bmglabtech.com/fileadmin/06_Support/Download_Documents/Application_Notes/AN125.pdf> (2004).

11 Appendices

11.1 Biological responses to toxic chemicals in bacteria

Table 11.1 - Summary of the most studied biological responses to toxic chemicals in bacteria.

	Gene	Function	Regulation	Chemical	Ref
Transport					
Inorganic ions	*mgtA*	Magnesium-transporting ATPase	Up	B, CP, CHP, NMP, NMS, T	88
	mntH	Divalent metal cation transporter	Up		
	kefBG	Glutathione-regulated potassium-efflux system	Up		
	cusABC	Cation efflux system	Down	B, CP, CHP, NMP, T	88
	phoU	Phosphate-specific transport system protein	Up	I, B, E	89
	pstSCAB	Phosphate ABC transporter components	Up		
Metals	*nikC*	Nickel transport system permease	Up	CHP	88
	rcnAB	Nickel/cobalt efflux system	Up	NMP	88
Peptides	*dtpD*	Dipeptide permease D	Up	CP, CHP	88
	oppABCDF	Oligopeptide ABC transporter	Up	B, CP, NMP, NMS, T	88
				I, B	89
	oppD	Oligopeptide ABC transport system	Up	N, Re, Ru	90
	oppA	Oligopeptide ABC transport system	Down	N, Re, Ru	90
	dppA	Dipeptide ABC transporter component	Up	E	96
	sbmA	Antimicrobial peptide (microcin 17 and 25) transporter	Up	CHP	88
Nutrients	*fruAB*	Fructose phosphotransferase system components	Down	NMP, NMS, CP, DMA, B, T	88
			Up	CHP	88
	gatAB	Galactitol phosphotransferase system components	Up	CHP	88
			Down	NMP, NMS, B	88
	manXYZ	Mannose phosphotransferase system components	Down	NMP, NMS, CP, DMA, B	88
	srlABE	Glucitol/sorbitol phosphotransferase system components	Down	NMP, NMS, CP, DMA, DMS, B, T	88
	malE	Maltose ABC transporter component	Up	E	96
	rbsB	Ribose ABC transporter component	Up		
	mglB	D-galactose/ D-glucose- ABC transporter component	Up		
	tnaB	Tryptophan permease	Down	B, CP, CHP, NMP, NMS, T, DMA, DMS	88
			Up	T	88
Multidrug efflux	*mdtG*	Multidrug efflux pump (MFS family)	Up	CHP	88
	emrB	Multidrug efflux pump (MFS EmrKY-TolC efflux system)	Up	NMS, DMA, DMS, B, T	88
	mdtA	Membrane fusion protein (RND MdtABC efflux system)	Up	NMP	88
	emrKY	Putative multidrug MFS transporter (EmrKY-TolC efflux system)	Up		

	yebQ	Putative MFS transporter (trimethoprim-sensitive [275])	Up		
	dinF	Efflux pump (MATE family)	Up	CP	88
Osmolyte transporters	*potFGHI*	Putrescine ABC transporter permease	Up	B, NMP, T, DMA	88
	mdtIJ	Multidrug/Spermidine efflux pump (SMR family)	Up	NMP, NMS, CP, CHP, DMA, DMS, B	88
OM porins	*ompF*	Outer membrane porin F	Down	O	101
			Down	I, B, E	89
			Down	B, 1,4-B	100
			Up	N, Re, Ru	90
	nmpC	Putative outer membrane porin	Down	O	101
	ompC	Outer membrane porin C	Up	E	96
			Up	O	101
	phoE	Outer membrane phosphoporin protein E	Up	NMP	88
	fadL	Long-chain fatty acid outer membrane porin	Up	P	99
			Up	N, Re, Ru	90
	OmpA	Outer membrane porin A	Up	P	99
Cell envelope biogenesis and related proteins					
Phospholipid accumulation	*mlaD*	OM lipid asymmetry maintenance protein; membrane-anchored ABC family periplasmic binding protein	Up	CP, CHP	88
	mlaF	ABC transporter maintaining OM lipid asymmetry	Up		
Cell envelope integrity	*tolA*	Membrane anchored proteins in TolA-TolQ-TolR complex	Up	NMP, NMS	88
	tolQ		Up		
	tolR		Up		
Cell wall biogenesis	*ldtB*	L,D-transpeptidase linking Lpp to murein	Up	NMP	88
	wzzB	Regulator of length of O-antigen component of lipopolysaccharide chains	Up		
	ugd	UDP-glucose 6-dehydrogenase	Up		
	cfa	Cyclopropane fatty acyl phospholipid synthase	Up	O	101
Envelope stress	*rpoE*	RNA polymerase sigma E factor	Up	E	96
	degP	Serine endoprotease (protease Do), membrane-associated	Up		
	opgG	Osmoregulated periplasmic glucans (OPGs) biosynthesis protein G	Up		
	cpxP	Inhibitor of the cpx response; periplasmic adaptor protein	Down	O	101
Biofilm formation	*ymgA*	RcsB connector protein for regulation of biofilm	Up	O	101
	bhsA	Biofilm, cell surface and signaling protein	Up		
Outer membrane proteins	*ompX*	Outer membrane protein X	Up	O	101
Oxidative stress					
	pqiA	Intermembrane transport protein	Up	B, CP, NMP, NMS	88
	pqiB	Intermembrane transport protein	Up		
	yhcN	Uncharacterized protein	Up	B, CP, CHP, NMP, NMS, T, DMS	88
	mntS	Mn2+ response protein	Up		
	msrB	Methionine sulfoxide reductase B	Up		
	rsxC	SoxR [2Fe-2S] reductase	Up	NMP, NMS	88

	fumC	Fumarase C	Up	E	96
	acnA	Aconitate hydratase A	Up		
	dsbG	Disulphide chaperone-isomerase	Up		
	sodA	Manganese containing superoxide dismutase	Up	B, 1,4-B	100
			Up	E	96
	katE	Catalase II	Up	B, 1,4-B	100
			Up	E	96
	marA	DNA-binding transcriptional dual regulator	Up	O	101
	nuoA-N	NADH:quinone oxidoreductase subunits	Down	E	96
Heat shock response					
	htpG	Molecular chaperone, HSP90 family	Up	CP, CHP	88
	dnaK	Chaperone protein	Up		
	dnaJ	Chaperone protein	Up		
	clpB	Chaperone protein	Up	I, B, E	89
			Up	CP, CHP	88
	groE	GroEL-GroES chaperonin complex	Up	CP, CHP	88
	groS	GroEL-GroES chaperonin complex	Up		
	grpE	Nucleotide exchange factor in the DnaK-DnaJ-GrpE chaperone system	Up	E	96
	spy	ATP-independent periplasmic chaperone	Up	I, B	89
			Up	B	100
Iron homeostasis					
Iron transport	*feoA*	Ferrous iron transport protein A	Up	B, CP, CHP, NMP, T, DMA	88
	feoB	Fe2+ transporter FeoB	Up		
	efeO	Ferrous iron transport system protein	Up	B, NMP, NMS, T	88
			Down	B, 1,4-B, HB	100
	fhuA	Ferrichrome outer membrane transporter/phage receptor	Down	I, B, E	89
	fhuC	Iron(III) hydroxamate ABC transporter ATP binding subunit	Down		
	fhuF	Hydroxamate siderophore iron reductase	Down		
	fecI	RNA polymerase, sigma 19 factor	Down		
Siderophore mediated transport	*exbBD*	Ton complex subunits	Up	B, CP, CHP, NMP, NMS, T, DMA	88
			Down	B, 1,4-B, HB	100
	yncD	Putative TonB-dependent outer membrane receptor	Up	B, NMP, NMS, T, DMA, DMS	88
	tonB	Membrane spanning protein in TonB-ExbB-ExbD transport complex	Up	NMP	88
	fepBD	Ferric enterobactin ABC transporter subunits	Up	NMP, NMS	88
Sulphur immobilization system	*sufA*	Iron-sulfur cluster insertion protein	Up	B, CP, DMA, DMS	88
	sufBCD	SufBC2D Fe-S cluster scaffold complex	Up		
	sufE	Sulfur acceptor for SufS cysteine desulfurase	Up		
	sufS	L-Cysteine desulfurase	Up		
	sufA	Iron-sulfur cluster insertion protein	Up	E	96
	suf genes	Sulphur immobilization system	Up	B, 1,4-B, HB	100
Fe/S cluster system	*hscA*	Iron-sulfur cluster biosynthesis chaperone	Up	B, CP, CHP,	88
	hscB	Co-chaperone for [Fe-S] cluster biosynthesis	Up		

	iscA	Iron-sulfur cluster insertion protein	Up	NMP, NMS, T	
	iscU	Scaffold protein for iron-sulfur cluster assembly	Up		
	iscS	Cysteine desulfurase	Up		
	iscA	Iron-sulfur cluster insertion protein	Up	E	96
	iscX	Accessory iron-sulfur cluster assembly protein	Up		
	isc genes		Up	B, 1,4-B, HB	100
Transcription factor	*iscR*	IscR-2Fe-2S DNA-binding transcriptional repressor	Up	B, CP, CHP, NMP, NMS, T, DMA, DMS	88
Metabolism					
TCA cycle	*sucA*	2-Oxoglutarate decarboxylase, thiamine-requiring	Down	I, B, E	89
	sucB	Dihydrolipoyltrans-succinylase	Down		
	sucC	Succinyl-CoA synthetase subunit β	Down		
	sucD	Succinyl-CoA synthetase subunit α	Down		
	sdhCDAB	Succinate:quinone oxidoreductase subunits	Down	I, B, E	89
Respiration	*nuoA-N*	NADH:quinone oxidoreductase subunits	Down/Up	E	96
	ndh	NADH:quinone oxidoreductase II	Up	I, B	89
	cyoABCD	Cytochrome bo3 ubiquinol oxidase subunits	Down/Up	E	96
			Down	I, B, E	89
	cydAB	Cytochrome bd-I ubiquinol oxidase subunit I and II	Down/Up	E	96
			Up	I, B, E	89
	cbdAB	Cytochrome bd-II oxidase, subunits I and II	Down	NMP, NMS	88
	cyoE	Heme O synthase	Down/Up	E	96
	hyaABCD	hydrogenase 1 subunits	Down	E	96
	hyaCD		Down	NMP, NMS	88
Anaerobic respiration	*frdABCD*	Anaerobic fumarate reductase subunits	Up	E	96
	frdAD		Down	NMP, NMS	88
	torAC	Trimethylamine N-oxide (TMAO) reductase I subunits	Up	E	96
Fermentation	*pflB*	Formate C-acetyltransferase 1, anaerobic; pyruvate formate-lyase 1	Up	E	96
	pta	Phosphate acetyltransferase	Down/Up		
	pcp	Phosphoenolpyruvate carboxylase	Down/Up		
	ackA	Acetate kinase A and propionate kinase 2	Down/Up		
Anaerobic β-oxidation of fatty acids	*fadI*	Beta-ketoacyl-CoA thiolase, anaerobic, subunit	Up	E	96
	fadJ	Enoyl-CoA hydratase/epimerase and isomerase/3-hydroxyacyl-CoA dehydrogenase	Up		
	fadK	Short chain acyl-CoA synthetase, anaerobic	Up		
Aerobic β-oxidation of fatty acid	*fadD*	Fatty acyl-CoA synthetase	Down	E	96
Transcription regulators	*fnr*	DNA-binding transcriptional dual regulator	Up	B	100
	arcA	ArcAB Two-Component Signal Transduction System	Up	HB, F, 1,4-B, A	
Acid stress					
	gadA	Glutamate decarboxylase A	Up	E	96
			Up	O	101
	gadB	Glutamate decarboxylase B	Up	E	96

			Up	O	[101]
	gadE	GadE-RcsB DNA-binding transcriptional activator	Up	E	[96]
			Up	O	[101]
	gadC	L-Glutamate:4-aminobutyrate antiporter	Up	O	[101]
	gadX	DNA-binding transcriptional dual regulator	Up		
	asr	Acid shock protein	Up	I, B, E	[89]
			Up	B	[100]
			Up	E	[96]
	hdeA	Periplasmic acid stress chaperone	Up	O	[101]
	hdeB	Periplasmic acid stress chaperone	Up		
	hdeD	Putative acid-resistance membrane protein	Up		
Other stress-related genes					
Universal stress proteins	*uspA*	Universal stress response regulator	Down	B, CHP, CP, DMA, DMS, NMP, NMS, T	[88]
	uspC	Universal stress protein C	Down	NMS	[88]
	uspD	Universal stress protein D	Down	CHP, NMS	[88]
	uspE	Universal stress protein with a role cellular motility	Up	B, CHP, CP, DMA, DMS, T	[88]
			Down	NMP, NMS	[88]
	uspF	Nucleotide binding filament protein	Up	B, DMA, DMS, T	[88]
			Down	NMP, NMS,	
	uspG	Universal stress protein UP12	Down	B, DMA, NMP, NMS, T	[88]
Methionine biosynthesis	*metA*	Homoserine O-succinyltransferase	Up	E	[96]
Nitrogen regulatory protein	*glnK*	Uridylyl-[GlnK]	Down	B, 1,4-B	[100]
	glnL	Sensory histidine kinase NtrB	Down		
	amtB	Ammonia / ammonium transporter	Down		
Methionine synthase	*metE*	Cobalamin-independent homocysteine transmethylase	Down	B, 1,4-B	[100]
Ornithine carbamoyl-transferase	*argI*	Ornithine carbamoyl-transferase	Down	B, 1,4-B	[100]
Quinolinate synthase complex	*nadA*	Quinolinate synthase	Down	B, 1,4-B	[100]

B, 1-butanol; CHP, N-cyclohexyl-pyrrolidone; CP, cyclopentanone; DMA, N,N-dimethylacetamide; DMS, dimethyl sulphide; NMP, N-cyclohexyl-pyrrolidone; NMS, N-methyl succinimide; T, toluene; E, ethanol; O, octanoic acid; I, isobutanol; 1,4-B, 1,4-butanediol; HB, (S)-beta-hydroxy-gamma-butyrolactone; F, furfural; A, acetate; P, phenol; Re, resveratrol; Ru, rutin; N, naringenin.

11.2 Gene and protein sequences

SoxR WT

Gene sequence (465 bp; NCBI gene ID: 948566)

ATGGAAAAGAAATTACCCCGCATTAAAGCGCTGCTAACCCCCGGCGAAGTGGCGAAACGCAGCGGT
GTGGCGGTATCGGCGCTGCATTTCTATGAAAGTAAAGGGTTGATTACCAGTATCCGTAACAGCGGCAA
TCAGCGGCGATATAAACGTGATGTGTTGCGATATGTTGCAATTATCAAAATTGCTCAGCGTATTGGCA
TTCCGCTGGCGACCATTGGTGAAGCGTTTGGCGTGTTGCCCGAAGGGCATACGTTAAGTGCGAAAGAG
TGGAAACAGCTTTCGTCCCAATGGCGAGAAGAGTTGGATCGGCGCATTCATACCTTAGTGGCGCTGCG
TGACGAACTGGACGGATGTATTGGTTGTGGCTGCCTTTCGCGCAGTGATTGCCCGTTGCGTAACCCGG
GCGACCGCTTAGGAGAAGAAGGTACCGGCGCACGCTTGCTGGAAGATGAACAAAACTAA

Protein sequence (154 aa; NCBI accession number: NP_418487.1)

MEKKLPRIKALLTPGEVAKRSGVAVSALHFYESKGLITSIRNSGNQRRYKRDVLRYVAIIKIAQRI
GIPLATIGEAFGVLPEGHTLSAKEWKQLSSQWREELDRRIHTLVALRDELDGCIGCGCLSRSDCPLRN
PGDRLGEEGTGARLLEDEQN

SoxR(R20H)

Gene sequence (465 bp)

ATGGAAAAGAAATTACCCCGCATTAAAGCGCTGCTAACCCCCGGCGAAGTGGCGAAACACAGCGGT
GTGGCGGTATCGGCGCTGCATTTCTATGAAAGTAAAGGGTTGATTACCAGTATCCGTAACAGCGGCAA
TCAGCGGCGATATAAACGTGATGTGTTGCGATATGTTGCAATTATCAAAATTGCTCAGCGTATTGGCA
TTCCGCTGGCGACCATTGGTGAAGCGTTTGGCGTGTTGCCCGAAGGGCATACGTTAAGTGCGAAAGAG
TGGAAACAGCTTTCGTCCCAATGGCGAGAAGAGTTGGATCGGCGCATTCATACCTTAGTGGCGCTGCG
TGACGAACTGGACGGATGTATTGGTTGTGGCTGCCTTTCGCGCAGTGATTGCCCGTTGCGTAACCCGG
GCGACCGCTTAGGAGAAGAAGGTACCGGCGCACGCTTGCTGGAAGATGAACAAAACTAA

Protein sequence (154 aa)

MEKKLPRIKALLTPGEVAKHSGVAVSALHFYESKGLITSIRNSGNQRRYKRDVLRYVAIIKIAQRI
GIPLATIGEAFGVLPEGHTLSAKEWKQLSSQWREELDRRIHTLVALRDELDGCIGCGCLSRSDCPLRN
PGDRLGEEGTGARLLEDEQN

AcrR WT

Gene sequence (648 bp; NCBI gene ID: 945516)

ATGGCACGAAAAACCAAACAAGAAGCGCAAGAAACGCGCCAACACATCCTCGATGTGGCTCTACGT
CTTTTCTCACAGCAGGGGGTATCATCCACCTCGCTGGGCGAGATTGCAAAAGCAGCTGGCGTTACGCG
CGGTGCAATCTACTGGCATTTTAAAGACAAGTCGGATTTGTTCAGTGAGATCTGGGAACTGTCAGAAT
CCAATATTGGTGAACTAGAGCTTGAGTATCAGGCAAAATTCCCTGGCGATCCACTCTCAGTATTAAGA
GAGATATTAATTCATGTTCTTGAATCCACGGTGACAGAAGAACGGCGTCGATTATTGATGGAGATTAT
ATTCCACAAATGCGAATTTGTCGGAGAAATGGCTGTTGTGCAACAGGCACAACGTAATCTCTGTCTGG
AAAGTTATGACCGTATAGAACAAACGTTAAAACATTGTATTGAAGCGAAAATGTTGCCTGCGGATTTA

ATGACGCGTCGCGCAGCAATTATTATGCGCGGCTATATTTCCGGCCTGATGGAAAACTGGCTCTTTGC
CCCGCAATCTTTTGATCTTAAAAAAGAAGCCCGCGATTACGTTGCCATCTTACTGGAGATGTATCTCC
TGTGCCCCACGCTTCGTAATCCTGCCACTAACGAATAA

Protein sequence (215 aa; NCBI accession number: NP_414997.1)

MARKTKQEAQETRQHILDVALRLFSQQGVSSTSLGEIAKAAGVTRGAIYWHFKDKSDLFSEIWELS
ESNIGELELEYQAKFPGDPLSVLREILIHVLESTVTEERRRLLMEIIFHKCEFVGEMAVVQQAQRNLC
LESYDRIEQTLKHCIEAKMLPADLMTRRAAIIMRGYISGLMENWLFAPQSFDLKKEARDYVAILLEMY
LLCPTLRNPATNE

AcrR(V29G)

Gene sequence (648 bp)

ATGGCACGAAAAACCAAACAAGAAGCGCAAGAAACGCGCCAACACATCCTCGATGTGGCTCTACGT
CTTTTCTCACAGCAGGGGGGATCATCCACCTCGCTGGGCGAGATTGCAAAAGCAGCTGGCGTTACGCG
CGGTGCAATCTACTGGCATTTTAAAGACAAGTCGGATTTGTTCAGTGAGATCTGGGAACTGTCAGAAT
CCAATATTGGTGAACTAGAGCTTGAGTATCAGGCAAAATTCCCTGGCGATCCACTCTCAGTATTAAGA
GAGATATTAATTCATGTTCTTGAATCCACGGTGACAGAAGAACGGCGTCGATTATTGATGGAGATTAT
ATTCCACAAATGCGAATTTGTCGGAGAAATGGCTGTTGTGCAACAGGCACAACGTAATCTCTGTCTGG
AAAGTTATGACCGTATAGAACAAACGTTAAAACATTGTATTGAAGCGAAAATGTTGCCTGCGGATTTA
ATGACGCGTCGCGCAGCAATTATTATGCGCGGCTATATTTCCGGCCTGATGGAAAACTGGCTCTTTGC
CCCGCAATCTTTTGATCTTAAAAAAGAAGCCCGCGATTACGTTGCCATCTTACTGGAGATGTATCTCC
TGTGCCCCACGCTTCGTAATCCTGCCACTAACGAATAA

Protein sequence (215 aa)

MARKTKQEAQETRQHILDVALRLFSQQGGSSTSLGEIAKAAGVTRGAIYWHFKDKSDLFSEIWELS
ESNIGELELEYQAKFPGDPLSVLREILIHVLESTVTEERRRLLMEIIFHKCEFVGEMAVVQQAQRNLC
LESYDRIEQTLKHCIEAKMLPADLMTRRAAIIMRGYISGLMENWLFAPQSFDLKKEARDYVAILLEMY
LLCPTLRNPATNE

AcrR(V29G)

Gene sequence (219 bp)

ATGGCACGAAAAACCAAACAAGAAGCGCAAGAAACGCGCCAACACATCCTCGATGTGGCTCTACGT
CTTTTCTCACAGCAGGGGGTATCATCCCCTCGCTGGGCGAGATTGCAAAAGCAGCTGGCGTTACGCGC
GGTGCAATCTACTGGCATTTTAAAGACAAGTCGGATTTGTTCAGTGAGATCTGGGAACTGTCAGAATC
CAATATTGGTGAACTAG

Protein sequence (72 aa)

MARKTKQEAQETRQHILDVALRLFSQQGVSSPRWARLQKQLALRAVQSTGILKTSRICSVRSGNCQ
NPILVN

YbcO WT

Gene sequence (291 bp; NCBI gene ID: 945147)

ATGGCTGATTTGAGAAAAGCAGCGCGTGGTCGGGAATGCCAGGTAAGAATCCCTGGCGTATGTAAT
GGCAACCCTGAAACGTCTGTACTGGCACATATCCGGCTGACTGGATTGTGCGGCACCGGTACGAAACC
GCCAGACCTGATTGCCACCATTGCATGTTCTGCCTGCCACGACGAAATCGACCGCCGCACGCATTTTG
TTGACGCTGGATATGCAAAAGAATGCGCGCTGGAAGGTATGGCGAGAACACAGGTTATCTGGCTGAAA
GAGGGGGTTATTAAGGCGTGA

Protein sequence (96 aa; NCBI accession number: NP_415081.1)

MADLRKAARGRECQVRIPGVCNGNPETSVLAHIRLTGLCGTGTKPPDLIATIACSACHDEIDRRTH
FVDAGYAKECALEGMARTQVIWLKEGVIKA

YbcO (I87M)

Gene sequence (291 bp)

ATGGCTGATTTGAGAAAAGCAGCGCGTGGTCGGGAATGCCAGGTAAGAATCCCTGGCGTATGTAAT
GGCAACCCTGAAACGTCTGTACTGGCACATATCCGGCTGACTGGATTGTGCGGCACCGGTACGAAACC
GCCAGACCTGATTGCCACCATTGCATGTTCTGCCTGCCACGACGAAATCGACCGCCGCACGCATTTTG
TTGACGCTGGATATGCAAAAGAATGCGCGCTGGAAGGTATGGCGAGAACACAGGTTATGTGGCTGAAA
GAGGGGGTTATTAAGGCGTGA

Protein sequence (96 aa)

MADLRKAARGRECQVRIPGVCNGNPETSVLAHIRLTGLCGTGTKPPDLIATIACSACHDEIDRRTH
FVDAGYAKECALEGMARTQVMWLKEGVIKA

11.3 Plasmid maps

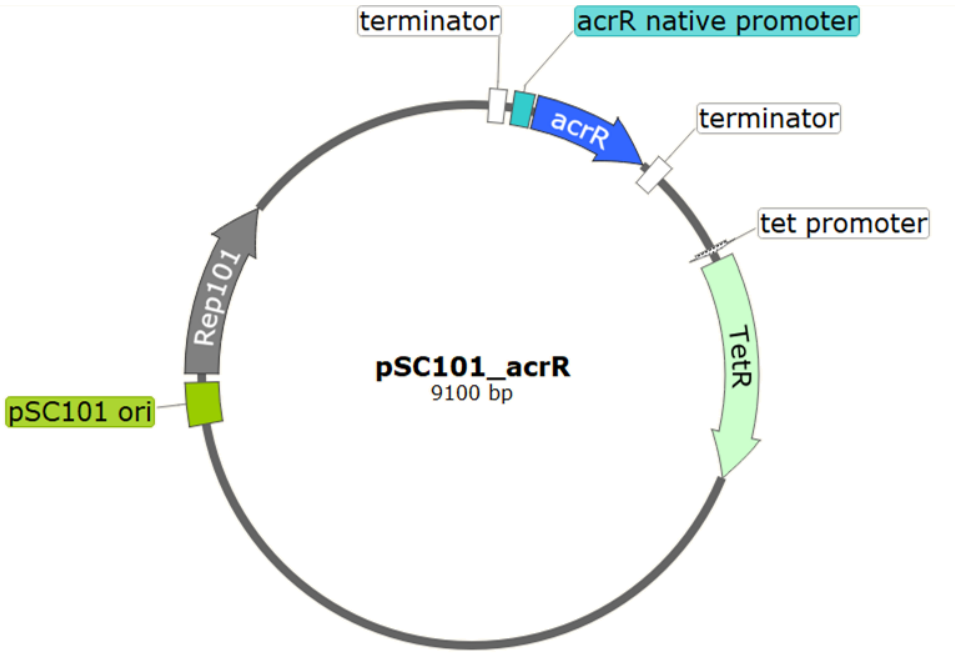

Figure 11.1 – Plasmid map of pSC101-*acrR*(WT).

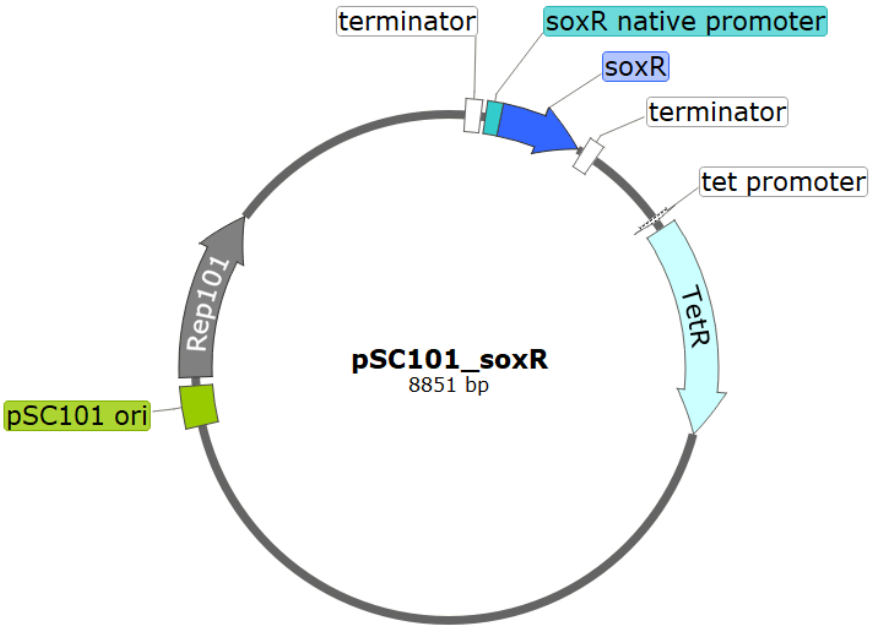

Figure 11.2 - Plasmid map of pSC101-*soxR*(WT).

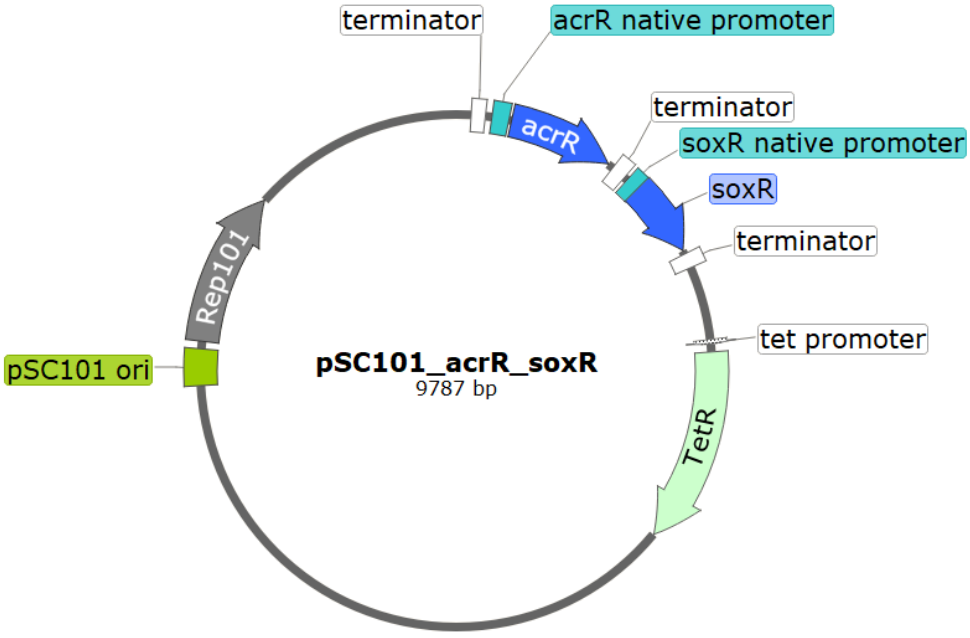

Figure 11.3 - Plasmid map of pSC101-*acrR*(WT)-*soxR*(WT).

11.4 Chemical toxicity tests

Table 11.2 - Effect of different chemicals on maximum OD_{600nm} and specific growth rate of *E. coli* MG1655 WT and *E. coli* MG1655 *soxR*(R20H)*acrR*(T32fs). All strains were grown in MSX medium in the presence of 0.1 to 20 %(v/v) of different chemicals, in 96-well microplates at 37°C and 600 rpm. Chemicals were added immediately after inoculation. Means of six replicates and standard deviations are shown. All specific growth rates had p-values lower than 0.05. Values with n/a were not possible to determine, due to slow growth. NG: no growth.

			***E. coli* MG1655 WT**		***E. coli* MG1655 *soxR*(R20H)*acrR*(T32fs)**	
Chemical	**Log P_{ow}**	**Conc. [%(v/v)]**	**Max OD_{600nm}**	**μ (h^{-1})**	**Max OD_{600nm}**	**μ (h^{-1})**
Control	-	-	1.70 ± 0.05	0.52 ± 0.02	1.73 ± 0.07	0.51 ± 0.01
n-Pentyl methacrylate	3.40	20	1.74 ± 0.04	0.49 ± 0.05	1.63 ± 0.08	0.48 ± 0.05
2-Ethylhexyl methacrylate	4.54	20	1.59 ± 0.11	0.51 ± 0.04	1.61 ± 0.10	0.51 ± 0.05
n-Hexyl methacrylate	3.73	20	1.64 ± 0.07	0.48 ± 0.05	1.57 ± 0.09	0.47 ± 0.04
n-Heptyl methacrylate	4.50	20	1.66 ± 0.04	0.46 ± 0.03	1.75 ± 0.05	0.47 ± 0.02
n-Octyl methacrylate	5.00	20	1.70 ± 0.06	0.52 ± 0.05	1.75 ± 0.06	0.51 ± 0.04
Methyl methacrylate	1.38	0.1	1.57 ± 0.04	0.33 ± 0.01	1.69 ± 0.07	0.30 ± 0.01
		0.5	1.55 ± 0.07	0.34 ± 0.02	1.49 ± 0.09	n/a
		1	NG		NG	
		20	NG		NG	
Ethyl methacrylate	1.94	0.1	0.98 ± 0.06	0.42 ± 0.06	1.02 ± 0.06	0.43 ± 0.04
		0.5	1.02 ± 0.03	0.39 ± 0.05	0.89 ± 0.09	n/a
		1	0.96 ± 0.10	n/a	0.96 ± 0.04	n/a
		20	NG		NG	
n-Propyl methacrylate	2.50	0.1	1.27 ± 0.04	0.32 ± 0.03	1.23 ± 0.08	0.26 ± 0.02
		0.5	1.21 ± 0.06	n/a	1.25 ± 0.02	0.23 ± 0.01
		1	NG		1.21 ± 0.09	n/a
		20	NG		NG	
Isopropyl methacrylate	2.20	0.1	1.01 ± 0.04	0.33 ± 0.03	0.89 ± 0.05	0.28 ± 0.02
		0.5	1.02 ± 0.05	0.35 ± 0.02	0.91 ± 0.06	0.23 ± 0.02
		1	1.09 ± 0.05	0.21 ± 0.01	0.95 ± 0.08	0.24 ± 0.01
		20	NG		NG	
n-Butyl methacrylate	2.88	0.1	1.14 ± 0.07	0.48 ± 0.03	1.40 ± 0.08	0.49 ± 0.04
		0.5	1.17 ± 0.06	0.33 ± 0.02	1.43 ± 0.05	0.45 ± 0.04
		1	1.21 ± 0.07	0.23 ± 0.01	1.43 ± 0.10	0.41 ± 0.01
		20	NG		1.44 ± 0.05	0.40 ± 0.01
Isobutyl methacrylate	2.66	0.1	1.04 ± 0.07	0.34 ± 0.03	1.18 ± 0.04	0.35 ± 0.03
		0.5	1.11 ± 0.06	0.32 ± 0.02	1.25 ± 0.05	0.30 ± 0.02
		1	1.12 ± 0.07	n/a	1.30 ± 0.04	0.31 ± 0.01
		20	1.02 ± 0.09	n/a	1.22 ± 0.03	0.32 ± 0.02
Butanol	0.88	0.5	1.26 ± 0.06	0.26 ± 0.01	1.09 ± 0.07	0.24 ± 0.01
		1	NG		NG	
Isobutanol	0.76	0.5	1.15 ± 0.07	0.27 ± 0.01	0.96 ± 0.05	0.21 ± 0.01

		1	NG		NG	
n-Butyl isobutyrate	2.40	0.1	1.27 ± 0.05	0.46 ± 0.05	1.33 ± 0.06	0.39 ± 0.02
		0.5	1.42 ± 0.06	0.41 ± 0.03	1.39 ± 0.06	0.38 ± 0.03
		1.0	1.47 ± 0.04	0.38 ± 0.02	1.40 ± 0.06	0.37 ± 0.01
		20.0	0.80 ± 0.07	n/a	1.38 ± 0.05	0.39 ± 0.02
n-Butyl isovalerate	2.60	0.1	1.30 ± 0.05	0.44 ± 0.04	1.47 ± 0.07	0.48 ± 0.03
		0.5	1.27 ± 0.05	0.43 ± 0.04	1.39 ± 0.05	0.40 ± 0.03
		1.0	1.30 ± 0.05	0.43 ± 0.04	1.43 ± 0.06	0.42 ± 0.02
		20.0	1.29 ± 0.04	0.42 ± 0.03	1.25 ± 0.03	0.31 ± 0.02
n-Butyl acetate	1.78	0.1	1.15 ± 0.04	0.44 ± 0.03	1.02 ± 0.04	0.29 ± 0.01
		0.5	1.16 ± 0.06	0.37 ± 0.02	1.07 ± 0.02	0.29 ± 0.02
		1.0	NG		NG	
		20.0	NG		NG	
Cyclohexane	3.44	1	1.24 ± 0.11	0.41 ± 0.04	1.31 ± 0.08	0.36 ± 0.01
		5	0.98 ± 0.03	0.17 ± 0.01	1.16 ± 0.06	0.33 ± 0.01
		10	1.06 ± 0.10	0.13 ± 0.01	1.20 ± 0.10	0.35 ± 0.03
		20	0.66 ± 0.10	n/a	1.21 ± 0.06	0.33 ± 0.02
Cyclohexene	2.89	0.5	NG		NG	
		1	NG		NG	
		5	NG		NG	
Ethylcyclohexane	4.56	5	1.65 ± 0.07	0.51 ± 0.05	1.78 ± 0.11	0.51 ± 0.03
		10	1.59 ± 0.07	0.50 ± 0.03	1.66 ± 0.05	0.51 ± 0.04
		20	1.70 ± 0.06	0.52 ± 0.03	1.69 ± 0.08	0.51 ± 0.03
Vinylcyclohexane	3.6	0.5	NG		NG	
		1	NG		NG	
		5	NG		NG	
Cyclooctane	4.45	1	1.34 ± 0.05	0.50 ± 0.05	1.71 ± 0.05	0.48 ± 0.03
		5	NG		1.57 ± 0.09	n/a
Hexane	3.9	1	1.31 ± 0.08	0.45 ± 0.05	1.44 ± 0.07	0.47 ± 0.04
		5	1.43 ± 0.06	0.45 ± 0.04	1.52 ± 0.09	0.45 ± 0.04
		10	1.32 ± 0.10	0.35 ± 0.02	1.44 ± 0.10	0.44 ± 0.04
		20	1.27 ± 0.06	0.33 ± 0.01	1.22 ± 0.06	0.39 ± 0.03
Isohexane	3.2	5	1.56 ± 0.03	0.49 ± 0.05	1.75 ± 0.09	0.53 ± 0.03
		10	1.62 ± 0.08	0.51 ± 0.02	1.70 ± 0.09	0.50 ± 0.08
		20	1.67 ± 0.08	0.49 ± 0.03	1.73 ± 0.09	0.53 ± 0.02
n-Heptane	4.66	5	1.64 ± 0.07	0.50 ± 0.04	1.81 ± 0.06	0.52 ± 0.03
		10	1.56 ± 0.08	0.51 ± 0.04	1.68 ± 0.05	0.51 ± 0.05
		20	1.57 ± 0.05	0.51 ± 0.02	1.72 ± 0.08	0.51 ± 0.01
Ethanol	-0.31	1	0.92 ± 0.06	0.36 ± 0.05	1.04 ± 0.06	0.34 ± 0.03
		5	1.02 ± 0.09	0.17 ± 0.01	0.99 ± 0.05	0.18 ± 0.00
		10	NG		NG	
Isopropanol	0.05	1	1.76 ± 0.07	0.36 ± 0.03	1.69 ± 0.09	0.32 ± 0.02
		5	NG		NG	

Table 11.3 - Effect of alkanes on maximum OD_{600nm} and specific growth rate of *E. coli* MG1655 WT and *E. coli* MG1655 *soxR*(R20H)*acrR*(T32fs). All strains were grown in MSX medium in the presence of 20 %(v/v) alkanes, in 30 mL vials at 37°C and 600 rpm. Chemicals were added immediately after inoculation. Means of two replicates and standard deviations are shown. All specific growth rates had p-values lower than 0.05. Values with n/a were not possible to determine, due to slow growth.

			E. coli MG1655 WT		*E. coli* MG1655 *soxR*(R20H)*acrR*(T32fs)	
Chemical	**Log P_{ow}**	**Conc. [%(v/v)]**	**Max OD_{600nm}**	**μ (h^{-1})**	**Max OD_{600nm}**	**μ (h^{-1})**
Control	-	-	2.75 ± 0.36	0.62 ± 0.03	2.85 ± 0.16	0.60 ± 0.05
Hexane	3.9	20	1.70 ± 0.17	0.29 ± 0.03	2.24 ± 0.03	0.50 ± 0.002
Cyclohexane	3.44	20	0.07 ± 0.00	n/a	1.48 ± 0.02	0.45 ± 0.04
Cyclooctane	4.45	5	0.13 ± 0.01	n/a	0.15 ± 0.01	n/a
Isohexane	3.2	20	1.94 ± 0.09	0.55 ± 0.04	-	-
n-Heptane	4.66	20	2.83 ± 0.05	0.55 ± 0.02	-	-
Ethylcyclohexane	4.56	20	2.72 ± 0.18	0.60 ± 0.03	-	-

Table 11.4 - Chemical properties of esters and their toxicity towards *E. coli* MG1655 strains. *E. coli* MG1655 WT and *E. coli* MG1655 *soxR*(R20H)*acrR*(T32fs) were grown in MSX medium, in the presence 1 %(v/v) of different esters added immediately after inoculation. All strains were grown in 96-well microplates at 37°C and 600 rpm.

Chemical	**Log P_{ow}**	**Boiling point (°C)**	**Vapour pressure (mmHg)**	**WT**				***soxR*(R20H)*acrR*(T32fs)**			
				Concentration [%(v/v)]				**Concentration [%(v/v)]**			
				0.1	**0.5**	**1**	**20**	**0.1**	**0.5**	**1**	**20**
Methyl MA	1.38	101	39	++	++	-	-	++	+	-	-
n-Butyl acetate	1.78	126	12	++	++	-	-	++	++	-	-
Ethyl MA	1.94	117	21	++	++	+	-	++	+	-	-
Isopropyl MA	2.20	125	12*	++	++	+	-	++	++	++	-
n-Butyl isobutyrate	2.40	155	2.6-3.2*	++	++	+	+	++	++	++	++
n-Propyl MA	2.50	141	6.4	++	+	-	-	++	++	+	-
n-Butyl isovalerate	2.60	150	0.8-1.4*	++	++	++	++	++	++	++	++
Isobutyl MA	2.66	155	3.6	++	++	+	-	++	++	++	++
n-Butyl MA	2.88	160	2.1	++	++	+	+	++	++	++	++
n-Pentyl MA	3.40	191*	0.1-0.9*				++				++
n-Hexyl MA	3.73	162	2.3				++				++
n-Heptyl MA	4.50	233*	0.1-0.6*				++				++
2-Ethylhexyl MA	4.54	235*	0.1-0.5*				++				++
n-Octyl MA	5.00	252*	0-0.5*				++				++

Caption: ++, good growth ; + worse growth; -, no growth.
*Predicted value, non-experimental

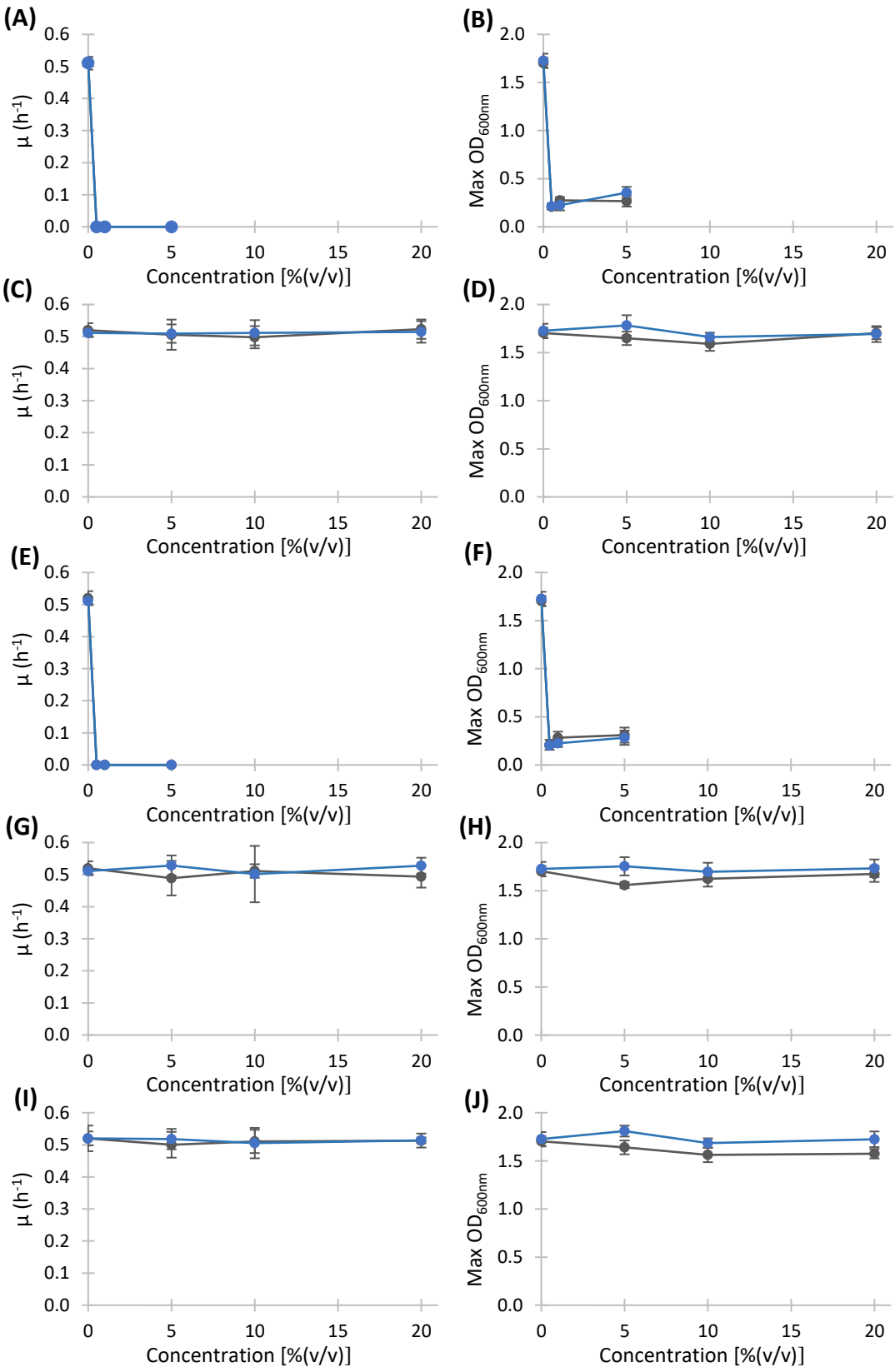

Figure 11.4 - Growth parameters of *E. coli* MG1655 strains when grown at different concentrations of cycloalkanes and cycloalkenes. *E. coli* MG1655 WT (grey bars) and *E. coli* MG1655 *soxR*(R20H)*acrR*(T32fs) (blue bars) were grown in in MSX medium in the presence of cyclohexene (A and B), ethylcyclohexane (C and D), vinylcyclohexane (E and F), isohexane (G and H) and n-heptane (I and J) added immediately after inoculation at

different concentrations. All strains were grown, in 96-well microplates at 37°C and 600 rpm. Means of six replicates are shown and error bars represent standard deviations.

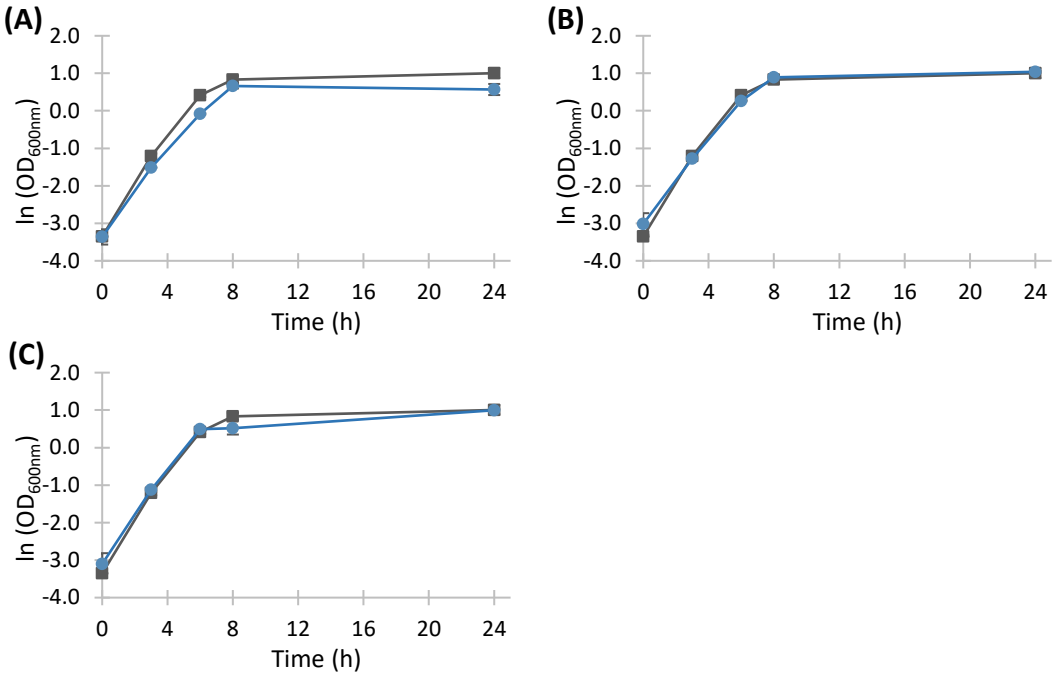

Figure 11.5 - Effect of alkanes on the growth of *E. coli* MG1655 WT. *E. coli* MG1655 WT was grown in MSX medium in the absence [■] or presence [●] of 20 %(v/v) isohexane (A), n-heptane (B) and ethylcyclohexane (C), in 30 mL vials at 37°C and 250 rpm shaking. were added immediately after inoculation. Means of two replicates are shown and error bars are standard deviations. Growth parameters are shown in Appendix 11.4, Table 11.3, page 205.

11.4.1 Development of 96-well microplate growth assays

In order to test the toxicity of different chemicals towards *E. coli*, high-throughput method was developed, where strains were cultured in 96-well microplates and the growth was measured using a microplate nephelometer, namely NEPHELOstar® (BMG Labtech).

Nephelometry is a laser-based method that measures light scattered by the particles suspended in a solution, the higher the concentration of particles the more light will be scattered[304]. Nephelometry is commonly used in solubility screens, immunoprecipitation assays or to monitor polymerization reactions, but it can also be used to measure bacterial growth[304]. It has been shown that with the use of the nephelometer NEPHELOstar® there was a good reproducibility of the growth curves

of *Corynebacterium glutamicum* cultures[304]. Furthermore, up to an OD_{600nm} of 4, there is a good correlation between the OD_{600nm} and the nephelometry units measured.

For these toxicity assays, polypropylene microplates sealed with polypropylene ThermalSeal A™ where used, to ensure the chemicals tested would not react with the plastic material and to avoid evaporation and possible cross-contamination of chemical gas phases between wells. Testes were done to determine the volume of medium (120 – 180 µL) and agitation setting (400 – 800 rpm) that would give the best results. *E. coli* MG1655 WT and *E. coli* MG1655 *soxR*(R20H)*acrR*(T32fs) were grown in the presence or absence of BMA, with six replicates (see methods section 3.2 for further details).

In this experiment, it was expected that *E. coli* MG1655 WT and *E. coli* MG1655 *soxR*(R20H)*acrR*(T32fs) would grow in the absence of BMA. On the other hand, is was expected that *E. coli* MG1655 WT would not grow in the presence of 20 %(v/v) BMA, but that the BMA-tolerant mutant strain *E. coli* MG1655 *soxR*(R20H)*acrR*(T32fs) would. When an agitation of 400 rpm was used, both strains had slow growth in the absence of BMA and could not grow in its presence. By contrast, when agitations of 600 and 800 rpm were used, the expected results were obtained, both strains could grow in the absence of BMA and the WT strain could not grow in the presence of BMA, but the mutant strain did. Yet, in the absence of BMA, *E. coli* MG1655 WT and *E. coli* MG1655 *soxR*(R20H)*acrR*(T32fs) had more comparable growth curves at 600 rpm than at 800 rpm. Furthermore, there was no significant difference between the tested volumes of MSX medium. A medium volume of 120 µL and an agitation of 600 rpm were used for the toxicity tests done in 96-well microplates in this work.

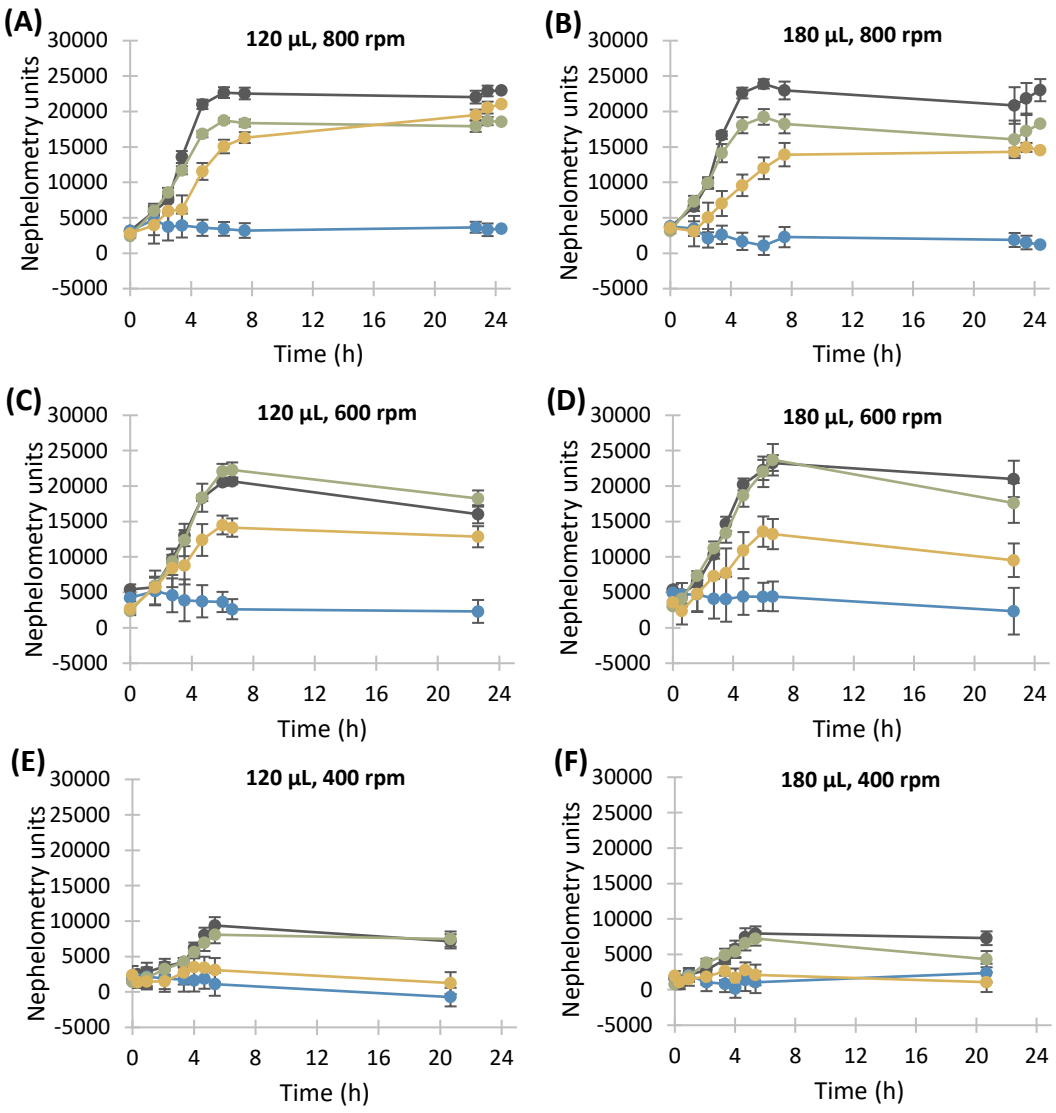

Figure 11.6 - Effect of medium volume and agitation the growth of *E. coli* MG1655 strains in 96-well microplates. *E. coli* MG1655 WT was grown in the absence [●] or presence of 20 %(v/v) BMA [●] and *E. coli* MG1655 *soxR*(R20H)*acrR*(T32fs) was also grown in the absence [●] or presence of 20 %(v/v) BMA [●], added immediately after inoculation. All strains were grown in 96-well microplates in 120 µL (A, C, E) or 180 µL (B, D, F) MSX medium, at 37°C and 800 rpm (A, B), 600 rpm (C, D) or 400 rpm (E, F). Means of six replicates are shown and error bars represent standard deviations.

The optical densities of *E. coli* MG1655 WT and *E. coli* MG1655 *soxR*(R20H)*acrR*(T32fs) cultures were calculated using calibration curves of OD_{600nm} as a function of nephelometry units, as shown in Figure 11.7. *E. coli* MG1655 WT and *E. coli* MG1655 *soxR*(R20H)*acrR*(T32fs) cultures were grown overnight in 10 mL MSX medium, in 50 mL Falcon tubes, and incubated at 37 °C and 250 rpm. From the overnight cultures, different dilutions were prepared in MSX to have samples with OD_{600nm} ranging 0.1 to 2.3. Experiments were done in the with three replicates and nephelometry units were measured.

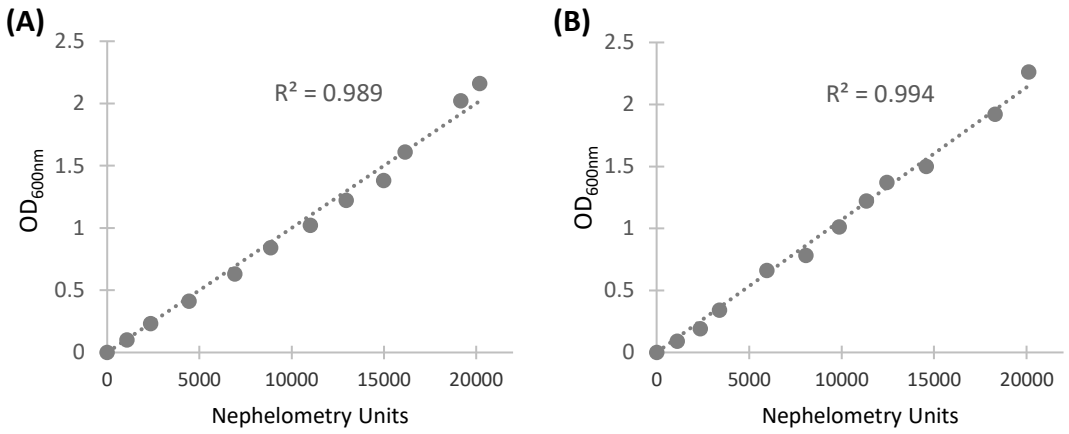

Figure 11.7- Calibration curves of OD_{600nm} versus nephelometry units. Calibrations curves were done for *E. coli* MG1655 WT (A) and *E. coli* MG1655 *soxR*(R20H)*acrR*(T32fs) (B), with 6 replicates.

11.5 Importance of each mutated gene

Table 11.5 - Effect of BMA the on OD_{600nm} after 8 h and 24 h of *E. coli* BW25113 KO strains. All strains were grown in MSX medium in the absence or presence of 20 %(v/v) BMA, in 30 mL vials at 37°C and 250 rpm. BMA was added immediately after inoculation. Means of two replicates and standard deviations are shown. Values with n/a were not possible to determine, due to slow growth or no growth.

	0 %(v/v) BMA		20 %(v/v) BMA	
***E. coli* BW25113**	**OD_{600nm} after 8 h**	**OD_{600nm} after 24 h**	**OD_{600nm} at 8h**	**Max OD_{600nm}**
WT	2.60 ± 0.10	2.51 ± 0.25	NG	
Δ*soxR::kan* (JW4024)	2.38 ± 0.12	2.49 ± 0.06	NG	
Δ*acrR::kan* (JW0453)	2.39 ± 0.15	2.43 ± 0.02	NG	
Δ*ybcO::kan* (JW0537)	2.45 ± 0.11	2.51 ± 0.07	NG	
Δ*ybcO::kan*	3.13 ± 0.25	2.73 ± 0.31	NG	
Δ*soxR*Δ*acrR::kan*	2.30 ± 0.02	2.41 ± 0.01	NG	
Δ*soxR*Δ*ybcO::kan*	2.52 ± 0.03	2.53 ± 0.02	NG	

Table 11.6 - Effect of the antibiotic resistance cassettes on BMA tolerance. All strains were grown in MSX medium in the absence or presence of 20 %(v/v) BMA, in 30 mL vials at 37°C and 250 rpm. BMA was added immediately after inoculation. Means of two replicates and standard deviations are shown. NG indicates no growth.

	0 %(v/v) BMA		20 %(v/v) BMA	
***E. coli* MG1655 strains**	**OD_{600nm} after 8 h**	**Max OD_{600nm}**	**OD_{600nm} after 8 h**	**Max OD_{600nm}**
WT	2.12 ± 0.08	2.29 ± 0.01	NG	
Δ*soxR*	1.99 ± 0.01	2.17 ± 0.01	NG	
Δ*soxR::kan*	2.04 ± 0.12	2.04 ± 0.02	NG	
Δ*soxR::chl*	2.07 ± 0.12	2.18 ± 0.22	0.03 ± 0.01	1.11 ± 0.15
Δ*acrR*	1.95 ± 0.01	2.17 ± 0.19	NG	

Δ*acrR::kan*	2.05 ± 0.01	2.19 ± 0.02	0.02 ± 0.00	0.50 ± 0.02
Δ*acrR::chl*	2.29 ± 0.08	2.32 ± 0.06	0.32 ± 0.01	0.70 ± 0.02
Δ*soxR*Δ*acrR*	1.91 ± 0.09	2.13 ± 0.09	NG	
Δ*soxR::kan*Δ*acrR*	1.92 ± 0.06	2.00 ± 0.10	0.02 ± 0.01	0.49 ± 0.09
Δ*soxR*Δ*acrR::kan*	2.00 ± 0.04	2.07 ± 0.06	0.53 ± 0.06	0.49 ± 0.09
Δ*soxR::kan*Δ*acrR::chl*	2.27 ± 0.04	2.33 ± 0.02	0.31 ± 0.06	0.70 ± 0.01
Δ*soxR::chl*Δ*acrR::kan*	2.03 ± 0.04	2.39 ± 0.05	0.05 ± 0.01	1.17 ± 0.05

11.6 Global transcriptional responses

Complete tables of differentially expressed genes from the RNA-seq analysis were submitted as digital copy and are available from the author upon request.

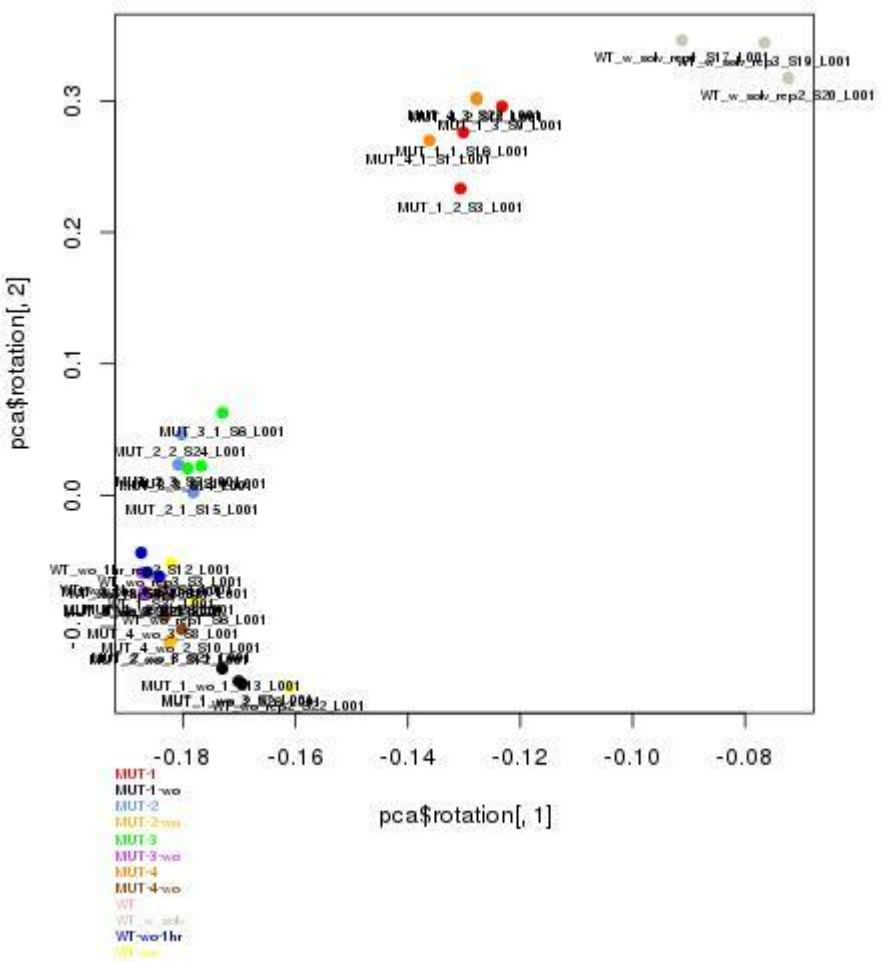

Figure 11.8 – PCA analysis showing the quality of the transcriptomics samples, where each group of samples was compared to each other group of samples. Caption: MUT-1, *E. coli* MG1655 *soxR*(R20H); MUT-2, *E. coli* MG1655 *soxR*(R20H)*acrR*(T32fs); MUT-3, *E. coli* MG1655 *soxR*(R20H)*acrR*(V29G); MUT-4, *E. coli* MG1655 *soxR*(R20H)*ybcO*(I87M); wo, before BMA addition (without).

Table 11.7 - Functional enrichment analysis of biological processes GO terms induced or repressed in *E. coli* MG16655 strains, before the addition of BMA.

Biological Process	*E. coli* MG1655 strains			
	***soxR*(R20H)**	***soxR*(R20H) *ybcO*(I87M)**	***soxR*(R20H) *acrR*(V29G)**	***soxR*(R20H) *acrR*(T32fs)**
Metabolic Process				
Rhs	↓ (5)			
Histidine biosynthetic process	↑ (4)			
Arginine biosynthetic process				↑ (7)
Fructose catabolic process				↑ (2)
Pyruvate metabolic process	↑ (6)	↑ (4)		
NAD metabolic process			↑ (3)	
Fermentation	↑ (5)			↓ (6)
Anaerobic respiration	↑ (12)			↓ (16)
Alcohol metabolic process	↓ (10)		↓ (10)	↓ (19)
Glycerol catabolic process	↑ (4)			
Glycolate catabolic process			↓ (4)	↓ (4)
Ethanolamine catabolic process				↓ (8)
Nitrogen compound metabolic process	↓ (67)		↓ (81)	↓ (121)
Carnitine metabolic process	↓ (5)		↓ (5)	↓ (5)
Allantoin assimilation pathway				↓ (4)
Short-chain fatty acid metabolic process	↓ (8)		↓ (10)	
Propionate metabolic process	↓ (6)		↓ (7)	↓ (7)
Iron related process				
Enterobactin biosynthetic process	↑ (6)	↑ (5)	↑ (8)	↑ (8)
Iron-sulfur cluster assembly	↑ (7)	↑ (6)	↑ (6)	↑ (8)
Siderophore transmembrane transport				↑ (3)
Transport				
L-arginine import into cell				↑ (3)
Carbohydrate transport	↓ (37)	↓ (18)	↓ (34)	↓ (40)
Pentose transport	↓ (4)	↓ (3)	↓ (5)	
Hexose transport		↓ (4)		
Maltose transport	↓ (6)	↓ (5)	↓ (6)	↓ (6)
Response to stimulus				
Response to oxidative stress	↑ (14)	↑ (9)	↑ (11)	↑ (13)
Drug transmembrane transport		↑ (5)	↑ (6)	
Other processes				
Biological adhesion			↓ (16)	↓ (34)

Table 11.8 - Functional enrichment analysis of biological processes GO terms induced or repressed in all *E. coli* MG16655 mutant strains, after the addition of BMA.

	***E. coli* MG1655 strains**					
Biological Process	**WT**	**WT +BMA**	***soxR*(R20H) +BMA**	***soxR*(R20H) *ybcO*(I87M) +BMA**	***soxR*(R20H) *acrR*(V29G) +BMA**	***soxR*(R20H) *acrR*(T32fs) +BMA**
Response to stimulus						
Response to osmotic stress			↑ (10)	↑ (11)	↑ (9)	↑ (7)
Response to pH			↑ (10)	↑ (11)	↑ (8)	↑ (8)
Response to oxidative stress			↑ (32)	↑ (33)	↑ (11)	↑ (11)
Response to starvation		↑ (15)	↑ (14)	↑ (17)	↑ (7)	↑ (6)
Response to heat	↑ (5)		↑ (24)	↑ (25)	↑ (9)	↑ (7)
Phage shock		↑ (6)	↑ (6)	↑ (6)	↑ (6)	↑ (6)
Iron homeostasis process						
Iron chelate transport		↓ (15)	↓ (19)	↓ (18)	↓ (15)	↓ (12)
Siderophore transport			↓ (9)	↓ (9)	↓ (6)	↓ (6)
Enterobactin metabolic process		↓ (10)	↓ (10)	↓ (10)	↓ (9)	↓ (9)
Other processes						
Biofilm formation		↑ (38)	↑ (25)	↑ (27)	↑ (10)	↑ (10)
Chemotaxis		↓ (21)	↓ (19)	↓ (20)	↓ (8)	↓ (6)
Flagellum-dependent cell motility		↓ (40)	↓ (37)	↓ (34)	↓ (22)	↓ (18)

Table 11.9 - Differentially expressed genes of the biological processes GO terms enriched in *E. coli* MG16655 strains, after the addition of BMA.

Biological Process	**Genes**
Membrane related processes	
Membrane biogenesis and organization	*asmA, bamA, bamB, bamC, bamD, bamE, ffh, lolC, lolD, lptA, lptC, lptD, lptE, lpxT, skp, surA, yidC, yidD*
External encapsulating structure organization	*alr, amiA, amiB, amiC, amiD, atpB, bamA, bamB, bamC, bamD, bamE, cpdA, cysE, dacA, dacB, ddlB, fimC, flgJ, ftsI, ftsW, glmU, ispU, lptA, lptC, lptD, lptE, lpxT, mepM, mepS, mltC, mltD, mpl, mraY, mrdA, murA, murB, murC, murD, murE, murF, murG, murI, oppB, pbpG, rlpA, skp, surA, wecA, yafK, ybhC*
Cell adhesion	*csgA, csgB, eaeH, elfA, elfG, focB, pgaC, pgaD, pphA, prfH, sfmA, sfmD, sfmF, sfmH, stfE, yadC, yadK, yadL, yadM, yadN, yaiT, ybgD, ybgO, ycbU, ycbV, ycgI, ycgV, ydeQ, ydeR, ydeS, yeeJ, yehA, yehD, yejO, yfaL, yfcP, yfcQ, yfcR, yfcV, ygiL, ypjA, yqiI, yraH, yraK*
Transport	
Sulfur compound transport	*cysK, cysP, cysU, cysW, gsiA, gsiB, metI, metN, sbp, ydjN*
Phosphate ion transport	*phnC, phnK, phoB, phoR, phoU, pstA, pstB, pstC, pstS*
Modified amino acid transport	*gsiA, osmF, yehW, yehX, yehY*
Branched-chain amino acid transport	*livF, livG, livH, livK, livM, ygaH*
Carbohydrate transport	
Pentose transport	*araE, araF, fucP, ompL, xylE, xylF, xylG*
Galactose transport	*fucP, galP, ompL, yjfF, ytfQ, ytfR, ytfT*
Fructose transport	*fruA, frvB, frwB, frwD, fryB, mngA*
Hexose transport	*araE, fruA, frvB, frwB, frwD, fryB, fucP, galP, mngA, ompL, rhaT, setA, yjfF, ytfQ, ytfR, ytfT*
Other cellular processes	
Organelle assembly	*deaD, flgJ, flgK, flgN, flhA, flhB, flhC, flhD, fliG, fliI, fliK, fliQ, fliR, fliS, fliT, frdA, frdB, frdC, obgE, rhlE, rimM, rimP, rplE, rplK, rplW, rpsG, rpsK, rpsP, rpsS*

Cell division	*amiB, amiC, blr, clpX, dacB, damX, ddlB, dedD, dicA, envC, flhC, ftsA, ftsB, ftsE, ftsH, ftsI, ftsK, ftsL, ftsN, ftsP, ftsQ, ftsW, ftsZ, groS, hflC, hflK, icd, ispU, lolD, mepM, minC, minD, minE, mpl, mraY, mraZ, mrdB, mreB, mukB, mukE, murA, murB, murC, murD, murE, murF, murG, nlpD, nlpI, nrdB, oppB, pal, pbpG, rlmE, rlpA, rng, rseP, sdiA, slmA, sulA, tig, tolA, xerC, ybgF, yfcH, yghB, yihA, yqjK, zapA, zapC, zapD, zipA*
Regulation of cell shape	*alr, dacA, dacB, ddlB, eptC, ftsI, ftsW, glmU, ispU, lpoA, lpoB, mpl, mraY, mrdA, mrdB, mreB, mreC, mreD, murA, murB, murC, murD, murE, murF, murG, murI, oppB, pbpG, rodZ, yafK*
Regulation of cellular component biogenesis	*argR, baeR, deoR, dinJ, flhC, flhD, fliT, minC, minE, mraZ, rsfS, sdiA, slmA, torI, ybjN*
Ribonucleoprotein complex biogenesis	*deaD, obgE, rbfA, rhlE, rho, rimM, rimP, rlmG, rluB, rluC, rplA, rplE, rplJ, rplK, rplW, rpsG, rpsI, rpsK, rpsM, rpsP, rpsS, yciH*
Translation	*accD, acnB, adk, alaS, arfB, argS, asnS, aspS, csrA, cysN, cysS, deaD, def, dnaA, dnaX, efp, epmC, ettA, flhD, fliA, fmt, frr, fusA, glnS, gltX, gluQ, glyQ, glyS, greA, hda, hfq, hisS, hpf, ihfA, ihfB, ileS, infA, infB, infC, lepA, leuS, lysS, metG, nusA, pheS, pheT, prfA, prfB, prfC, prmC, proS, pth, rimP, rnk, rplA, rplB, rplC, rplD, rplE, rplF, rplI, rplJ, rplK, rplL, rplM, rplN, rplO, rplP, rplQ, rplR, rplS, rplT, rplU, rplV, rplW, rplX, rplY, rpmA, rpmB, rpmC, rpmD, rpmE, rpmF, rpmG, rpmH, rpmI, rpmJ, rpsA, rpsB, rpsC, rpsD, rpsE, rpsF, rpsG, rpsH, rpsI, rpsJ, rpsK, rpsL, rpsM, rpsN, rpsO, rpsP, rpsQ, rpsR, rpsS, rpsT, rpsU, rsfS, rsxE, secM, serS, smpB, thrS, thyA, trpS, tsaC, tsf, tufA, tufB, typA, tyrS, uof, valS, yafQ, yeaK, yeiP, yigZ*
Response to virus	*casA, casB, casC, casD, casE, pspA, pspB, pspD, pspG, ygbF, ygbT, ygcB*
Stress response to metal ion	*cusA, cusB, cusC, cusF, ibpB, zntA*

Table 11.10 - Differentially expressed genes in *E. coli* MG1655 *soxR*(R20H)*acrR*(V29G), compared to *E. coli* MG1655 *soxR*(R20H), before BMA addition. Only genes with a log2 fold change ≥ 1 or ≤ -1 (*i.e.* fold change ≥ 2 or ≤ 0.5) and an adjusted p-value ≤ 0.05 were considered as differentially expressed.

Gene	Log2 FC	SE	Gene	Log2 FC	SE	Gene	Log2 FC	SE	Gene	Log2 FC	SE
acrR	3.5	0.1	*yhbS*	-1.1	0.1	*ybjM*	-1.2	0.1	*alaE*	-1.5	0.2
acrA	2.5	0.1	*napA*	-1.1	0.1	*ynfN*	-1.2	0.2	*yhbV*	-1.5	0.1
acrB	2.1	0.1	*ilvM*	-1.1	0.2	*hypB*	-1.2	0.2	*frdA*	-1.6	0.2
mokB	1.3	0.2	*ydjY*	-1.1	0.1	*nikC*	-1.3	0.2	*hybO*	-1.6	0.1
stpA	1.2	0.1	*yqeI*	-1.1	0.2	*cydA*	-1.3	0.1	*hisD*	-1.6	0.1
ndk	1.1	0.1	*aspA*	-1.1	0.2	*yfbS*	-1.3	0.1	*dcuC*	-1.6	0.3
ackA	-1.0	0.1	*gadE*	-1.1	0.2	*ycbJ*	-1.3	0.1	*gldA*	-1.7	0.2
dmsC	-1.0	0.2	*ybcW*	-1.1	0.2	*ydfK*	-1.3	0.1	*feoB*	-1.7	0.2
dcuB	-1.0	0.2	*adhE*	-1.1	0.2	*hypD*	-1.3	0.1	*dmsA*	-1.7	0.2
yjjP	-1.0	0.1	*yliI*	-1.1	0.2	*yfeH*	-1.3	0.1	*glpC*	-1.8	0.2
ysaA	-1.0	0.1	*ravA*	-1.2	0.1	*yqgA*	-1.3	0.1	*frdC*	-1.9	0.2
yjjI	-1.0	0.2	*hisC*	-1.2	0.1	*nirC*	-1.4	0.2	*dmsB*	-2.0	0.2
ynfM	-1.0	0.3	*hcr*	-1.2	0.2	*yaaJ*	-1.4	0.1	*nirB*	-2.1	0.2
focA	-1.0	0.2	*nikB*	-1.2	0.2	*narG*	-1.4	0.1	*nirD*	-2.2	0.2
yjjW	-1.1	0.1	*glpA*	-1.2	0.3	*hisG*	-1.4	0.2	*frdB*	-2.2	0.2
hypC	-1.1	0.2	*ynfE*	-1.2	0.3	*hybA*	-1.5	0.2	*glpB*	-2.2	0.2
appY	-1.1	0.2	*nikD*	-1.2	0.2	*frdD*	-1.5	0.2	*feoC*	-2.3	0.1
fumB	-1.1	0.1	*edd*	-1.2	0.1						

Table 11.11 - Differentially expressed genes in *E. coli* MG1655 *soxR*(R20H)*acrR*(T32fs), compared to *E. coli* MG1655 *soxR*(R20H), before BMA addition. Only genes with a log2 fold change ≥ 1 or ≤ -1 (*i.e.* fold change ≥ 2 or ≤ 0.5) and an adjusted p-value ≤ 0.05 were considered as differentially expressed.

Gene	Log2 FC	SE	Gene	Log2 FC	SE	Gene	Log2 FC	SE	Gene	Log2 FC	SE
acrR	3.3	0.1	*yjgX*	-1.1	0.1	*nikD*	-1.3	0.2	*frdD*	-1.9	0.3
stpA	2.9	0.1	*nrdG*	-1.1	0.2	*yhcA*	-1.3	0.2	*ydhY*	-1.9	0.3
acrA	2.3	0.1	*yjjZ*	-1.1	0.1	*fimD*	-1.3	0.1	*ycbJ*	-1.9	0.1
acrB	1.8	0.1	*leuO*	-1.1	0.2	*fimC*	-1.3	0.1	*yfeH*	-1.9	0.1
hokB	1.6	0.3	*mdtJ*	-1.1	0.1	*yhbS*	-1.3	0.1	*hcr*	-2.0	0.2
thrL	1.6	0.1	*cspF*	-1.1	0.1	*yieE*	-1.4	0.1	*ybfA*	-2.0	0.1
ndk	1.5	0.1	*ydaG*	-1.1	0.2	*ilvX*	-1.4	0.3	*yecH*	-2.0	0.2
yoeI	1.4	0.1	*gntK*	-1.1	0.1	*ybcW*	-1.4	0.2	*nirD*	-2.0	0.2
mokB	1.4	0.3	*adhE*	-1.1	0.2	*yjdQ*	-1.4	0.3	*feoC*	-2.0	0.1
pyrL	1.4	0.1	*nirC*	-1.1	0.2	*fimG*	-1.4	0.1	*yhbV*	-2.0	0.2
argA	1.3	0.1	*nrdD*	-1.1	0.2	*ydjX*	-1.4	0.2	*ybcV*	-2.1	0.4
fruA	1.3	0.3	*yjjW*	-1.1	0.1	*yehD*	-1.4	0.3	*cspG*	-2.1	0.1
lpp	1.3	0.1	*yhcC*	-1.1	0.2	*fumB*	-1.4	0.2	*grcA*	-2.1	0.3
azuC	1.2	0.1	*epd*	-1.1	0.2	*narG*	-1.4	0.1	*ymcE*	-2.1	0.1
argI	1.2	0.1	*zur*	-1.1	0.1	*cpxP*	-1.5	0.1	*abrB*	-2.2	0.1
ilvC	1.2	0.1	*yoeG*	-1.1	0.2	*hypA*	-1.5	0.2	*yaaJ*	-2.2	0.1
metF	1.2	0.1	*arpA*	-1.1	0.2	*pinR*	-1.5	0.2	*yqgA*	-2.2	0.1
leuL	1.2	0.1	*hcp*	-1.1	0.2	*cydA*	-1.5	0.1	*hypB*	-2.2	0.1
fliE	1.2	0.1	*pagP*	-1.2	0.2	*gadE*	-1.5	0.2	*cspB*	-2.2	0.1
metN	1.2	0.1	*ynfF*	-1.2	0.3	*cspH*	-1.5	0.1	*focA*	-2.2	0.2
argC	1.2	0.1	*adiY*	-1.2	0.3	*hypD*	-1.5	0.1	*glpC*	-2.3	0.3
artP	1.1	0.1	*ilvM*	-1.2	0.2	*yehC*	-1.5	0.4	*essQ*	-2.3	0.2
argG	1.1	0.1	*uspE*	-1.2	0.1	*ymgF*	-1.6	0.3	*frdC*	-2.4	0.3
rpsU	1.1	0.1	*nsrR*	-1.2	0.1	*ghoS*	-1.6	0.4	*hisG*	-2.4	0.1
argD	1.1	0.1	*fimI*	-1.2	0.1	*yhbU*	-1.6	0.4	*dmsB*	-2.4	0.2
metK	1.0	0.1	*pinQ*	-1.2	0.2	*ysaA*	-1.6	0.1	*hybO*	-2.4	0.1
yeeE	1.0	0.1	*dmsC*	-1.2	0.3	*ravA*	-1.6	0.1	*ynfN*	-2.5	0.2
argF	1.0	0.1	*lamB*	-1.2	0.1	*yjjI*	-1.6	0.1	*ydfK*	-2.5	0.1
gpt	1.0	0.1	*yohJ*	-1.2	0.2	*nikA*	-1.7	0.3	*bssR*	-2.6	0.3
plaP	1.0	0.1	*fimH*	-1.2	0.1	*yjjP*	-1.7	0.1	*ynfM*	-2.6	0.2
artJ	1.0	0.1	*fimF*	-1.2	0.1	*uspF*	-1.7	0.2	*cspI*	-2.7	0.1
mepH	1.0	0.1	*tqsA*	-1.2	0.1	*hisD*	-1.7	0.1	*nirB*	-2.7	0.2
xanP	1.0	0.1	*ynjE*	-1.2	0.1	*aspA*	-1.7	0.1	*gldA*	-2.8	0.1
dinQ	1.0	0.1	*dtpA*	-1.3	0.1	*hypC*	-1.7	0.2	*yoeA*	-2.8	0.3
fruK	1.0	0.3	*ybaA*	-1.3	0.1	*yliI*	-1.8	0.2	*ynfE*	-2.8	0.3
ghoT	-1.0	0.4	*yqfA*	-1.3	0.1	*pepE*	-1.8	0.1	*raiA*	-2.8	0.2
add	-1.0	0.1	*ydjZ*	-1.3	0.1	*hybA*	-1.8	0.2	*ynfK*	-2.8	0.3
malG	-1.0	0.1	*hisC*	-1.3	0.1	*yfbS*	-1.8	0.1	*frdB*	-3.0	0.2
lpxP	-1.0	0.1	*edd*	-1.3	0.1	*nikC*	-1.8	0.2	*glpB*	-3.1	0.1
gfcA	-1.0	0.1	*uspC*	-1.3	0.1	*yfcZ*	-1.8	0.2	*ttdR*	-3.1	0.1
pmrR	-1.0	0.1	*gnsA*	-1.3	0.1	*rrrQ*	-1.8	0.3	*dmsA*	-3.2	0.1
gfcB	-1.0	0.3	*yadN*	-1.3	0.3	*ydjY*	-1.8	0.1	*glpA*	-3.4	0.2
puuE	-1.0	0.1	*ilvG*	-1.3	0.1	*dcuB*	-1.9	0.2	*feoB*	-3.4	0.1
rzpQ	-1.1	0.4	*aslB*	-1.3	0.1	*ynaE*	-1.9	0.1	*frdA*	-3.5	0.2

yqeC	-1.1	0.3	*yaiV*	-1.3	0.4	*ydfR*	-1.9	0.2	*dcuC*	-3.5	0.3
appY	-1.1	0.2	*yhbT*	-1.3	0.1	*nikB*	-1.9	0.2	*feoA*	-3.6	0.3
insK	-1.1	0.1	*malM*	-1.3	0.1	*ybjM*	-1.9	0.1	*alaE*	-4.1	0.1

Table 11.12 - Differentially expressed genes in *E. coli* MG1655 *soxR*(R20H)*ybcO*(I87M), compared to *E. coli* MG1655 *soxR*(R20H), after BMA addition. Only genes with a log2 fold change ≥ 1 or ≤ -1 (*i.e.* fold change ≥ 2 or ≤ 0.5) and an adjusted p-value ≤ 0.05 were considered as differentially expressed.

Gene	Log2 FC	SE	Gene	Log2 FC	SE	Gene	Log2 FC	SE	Gene	Log2 FC	SE
cysD	1.4	0.2	*allS*	1.0	0.3	*fiu*	-1.0	0.3	*cspF*	-1.1	0.2
cysU	1.4	0.2	*cysW*	1.0	0.2	*carB*	-1.0	0.2	*bioD*	-1.2	0.2
cysP	1.3	0.2	*yahI*	1.0	0.3	*yidD*	-1.1	0.2	*rnpA*	-1.2	0.2
narU	1.2	0.2	*ymgE*	1.0	0.2	*pyrB*	-1.1	0.3	*bioF*	-1.2	0.2
alsA	1.1	0.3	*nanC*	1.0	0.3	*bioC*	-1.1	0.2	*suhB*	-1.2	0.2
ompG	1.1	0.3	*fhuF*	-1.0	0.2	*yqjF*	-1.1	0.2	*ymcE*	-1.2	0.3
uacT	1.1	0.3	*cspA*	-1.0	0.3	*bioB*	-1.1	0.1	*pyrI*	-1.3	0.2
cysN	1.1	0.2									